Eiman Abdel Meguid
Priti L. Mishall
Haley L. Nation
Paul M. Rea   *Editors*

Biomedical Visualisation

Volume 15 – Visualisation in Teaching
of Biomedical and Clinical Subjects: Anatomy,
Advanced Microscopy and Radiology

Springer

Advances in Experimental Medicine and Biology

Volume 1406

Series Editors

Wim E. Crusio, Institut de Neurosciences Cognitives et Intégratives d'Aquitaine, CNRS and University of Bordeaux, Pessac Cedex, France

Haidong Dong, Departments of Urology and Immunology, Mayo Clinic, Rochester, MN, USA

Heinfried H. Radeke, Institute of Pharmacology and Toxicology, Clinic of the Goethe University Frankfurt Main, Frankfurt am Main, Hessen, Germany

Nima Rezaei ⓘD, Research Center for Immunodeficiencies, Children's Medical Center, Tehran University of Medical Sciences, Tehran, Iran

Ortrud Steinlein, Institute of Human Genetics, LMU University Hospital, Munich, Germany

Junjie Xiao, Cardiac Regeneration and Ageing Lab, Institute of Cardiovascular Sciences, School of Life Science, Shanghai University, Shanghai, China

Eiman Abdel Meguid • Priti L. Mishall
Haley L. Nation • Paul M. Rea
Editors

Biomedical Visualisation

Volume 15 – Visualisation in
Teaching of Biomedical and Clinical
Subjects: Anatomy, Advanced
Microscopy and Radiology

Editors
Eiman Abdel Meguid
Queen's University Belfast
Belfast, UK

Priti L. Mishall
Departments of Pathology &
Ophthalmology and Visual Sciences,
Albert Einstein College of Medicine
Bronx, NY, USA

Haley L. Nation
Department of Cell Systems
and Anatomy
UT Health Science Center
at San Antonio
San Antonio, TX, USA

Paul M. Rea 🅾
Anatomy Facility, School of Medicine,
Dentistry and Nursing, College of
Medical, Veterinary and Life Sciences
University of Glasgow
Glasgow, UK

Preface

This book, the 15th volume of the *Biomedical Visualization* series, focuses on scientific visualization. It encapsulates the integration of science and imaging. This volume spans from the microarchitecture of specific proteins to recent advancements in anatomy education, to the clinical application of new technologies and the improvement of patient care. It is the intersection between technology, science, history, creativity, and engineering. This book demonstrates how we can teach and learn in a much more accessible, innovative, and engaging way using technology.

This volume is particularly focused on three main themes: advanced microscopy, anatomy education, and radiology visualization related to patient care. The chapters pertaining to advanced microscopy convey complex biomedical information by visual means. These chapters provide an overview of the principles of microscopy and the unique characteristics of different microscopes; it also provides examples of applications of microscopy that have led to groundbreaking novel discoveries. This volume also delves into the concepts of education. These chapters summarize the recent trends in anatomy education and emphasize the creation and use of existing online tools to support student learning to understand complex data and abstract ideas. Lastly, the radiological visualization segment dives into the history of radiographic imaging, surgical visual instruments, and therapies in medicine and dentistry. This volume highlights the profound effect technology has had on improving patient outcomes and also foreshadows where future advancements might take us.

This volume will be of particular interest to many; the scope of this textbook encompasses medicine, dentistry, allied health professions, biomedical sciences, anatomy education, radiology, and microscopy. Students and researchers who have interests in microscopy and host–pathogen communication will find these chapters useful in expanding their knowledge and understanding microscopies application. Gross anatomy and histology instructors will clearly enjoy the advancements in education explored in these chapters. However, the educational topics discussed are applicable to all higher education staff and across all basic science disciplines such as health care practitioners, ranging from dentists to orthopedists. This volume highlights the clinical importance of advancements in visualization pertaining to patient care. It is our hope that students, educators, researchers, and clinicians reading this book will learn something new, are stimulated to ask

innovative questions, and are inspired to continue the technological advancements pushing science forward.

Belfast, UK   Eiman Abdel Meguid
Bronx, NY   Priti L. Mishall
San Antonio, TX   Haley L. Nation
Glasgow, UK   Paul M. Rea

Contents

About the Editors

Eiman Abdel Meguid   PhD, MBBS, SFHE, is Fellow of the Anatomical Society. She is a medical graduate and Senior Lecturer of Anatomy at Queen's University Belfast (QUB), UK, with expertise in human anatomy, embryology, and neuroanatomy. She is passionate about anatomical sciences education and is keen to actively support the education of her students. Eiman's areas of professional interest include anatomical variation, multimodal teaching strategies, implementing innovative technology, audience response system in teaching, flipped classrooms, and blended learning. She has published widely and presented at many international meetings that included invited talks. She conducts review sessions for clinical trainee revisiting the cadaveric anatomy labs whenever required. She is the Sole Academic Lead for Dental Anatomy Course, Co-lead for Musculoskeletal Unit 2 for the MB BCh BAO, and MSc in Clinical Anatomy Programme. She has multiple publications in high impact journals and was an International Visiting Scholar/Guest Speaker for Weill Cornell Medicine, NY. Dr. Abdel Meguid is the recipient of the Senior Faculty Award for best presentation at the AACA conference, 2022. She has previously acted as a member of the Career Development Committee of the American Association of Clinical Anatomy (AACA), and currently, she is a member of the Educational Affairs Committee of AACA. She is a reviewer for the Clinical Anatomy, BMC Medical Education, and the Anatomical Sciences Education Journals. Through her membership of the Risk Management Group Committee at the Royal College of Surgeons and previous role at the Research Ethics Committee at QUB, she gained lot of experience in reviewing and generating policies for educational and research-related activities. She is involved in peer mentoring as she is passionate about Staff Professional Career Development. Having spent many years teaching as a clinical anatomist, she is well placed to assist in producing resources that would assist the development of student education. The extensive experience she has gained, her international networking, and her interest in tailoring teaching and research have equipped her with the necessary skills.

Priti L. Mishall   MD, MBBS, PGCertME, is Associate Professor in the Departments of Pathology & Ophthalmology and Visual Sciences. She is a medical educator with expertise in human anatomy, embryology, histology, and neuroanatomy. She teaches anatomy to learners in Undergraduate

Medical Education (UME) and Graduate Medical Education (GME). For the UME, she Co-Directs the Anatomy course for the first-year MD program and also Directs the Anatomy course for the MSTP program. She is the Director of the Anatomical Donation Program and is a course faculty member for the second-year Nervous System and Human Behavior course. She is a small group facilitator for the Problem-Based Learning sessions in Pre-clerkship and Transition to Clerkship. Dr. Mishall mentors medical students interested in pursuing projects on creating and evaluating anatomy education learning resources. In the area of GME, she conducts workshops for residents and fellows revisiting cadaver anatomy labs. Her clinical collaborators include Departments of Ophthalmology and Visual Sciences and Rheumatology. She is passionate about participating in faculty development initiatives and is a course faculty at Harvard Macy Institutes' course "Transforming your teaching for the Virtual Environment." She is an active member of the American Association of Clinical Anatomists (AACA) and International Association of Medical Science Educators (IAMSE). She served as the chair of the Education Affairs Committee of AACA and is the member of AACA's Career Development Committee. At Einstein, she implemented various e-learning instructional methods including flipped classrooms, blended and online learning to promote learner interactivity and engagement with the content. Additionally she has expertise in designing and implementing prosection-based anatomy course for preclerkship curriculas. She is a recipient of two teaching awards at Einstein: the Samuel M. Rosen Award for Outstanding Teaching (Pre-Clerkship) and the Harry Eagle Award for Outstanding Teaching (Pre-Clerkship) in recognition for excellence in teaching by students and by peers, respectively.

Haley L. Nation   PhD, is Associate Professor in the Department of Cell Systems and Anatomy at UT Health San Antonio. She is a classically trained anatomist who teaches various basic science disciplines to future health care professionals, including gross anatomy, histology, neuroanatomy, and embryology. Dr. Nation teaches medical, dental, physical therapy, physician assistant, occupational therapy, and master's of anatomy students. She is committed to providing a high quality of education to her students as well as various residents and practicing dentists seeking continuing education. She is invested in the success of the programs she teaches in and the wider academic missions as a whole; she serves on admissions, curriculum, and strategic planning committees and partakes in leadership programs. To help serve the greater anatomical community, she is involved in professional associations and serves on the American Association of Clinical Anatomists (AACA) Educational Affairs Committee (EAC) and Committee on Diversity, Equity, and Inclusion (CDEI). In addition to her educational and service commitments, she also has a particular interest in mentoring graduate students in research projects involving anatomical variations and the creation of new educational tools. Throughout her career she has been devoted to her students, institution, and anatomical community.

Paul M. Rea Paul is Professor of Digital and Anatomical Education at the University of Glasgow. He is Director of Innovation, Engagement and Enterprise within the School of Medicine, Dentistry and Nursing. He is also a Senate Assessor for Student Conduct and Council Member on Senate and coordinates the day-to-day running of the Body Donor Program and is a Licensed Teacher of Anatomy, licensed by the Scottish Parliament. He is qualified with a medical degree (MBChB), an MSc (by research) in craniofacial anatomy/surgery, a PhD in neuroscience, the Diploma in Forensic Medical Science (DipFMS), and an MEd with Merit (Learning and Teaching in Higher Education). He is Senior Fellow of the Higher Education Academy and a Fellow of the Institute of Medical Illustrators (FIMI). Paul has published widely and presented at many national and international meetings, including invited talks. He has been the lead editor for *Biomedical Visualisation* over 13 published volumes and is the founding editor for this book series. This has resulted in almost 90,000 downloads across these volumes, with approximately 400 different authors, across approximately 100 institutions from 19 countries across the globe. He is Associate Editor for the *European Journal of Anatomy* and has reviewed for 25 different journals/publishers. He is the Public Engagement and Outreach lead for anatomy coordinating collaborative projects with the Glasgow Science Centre, NHS, and Royal College of Physicians and Surgeons of Glasgow. Paul is also a STEM ambassador and has visited numerous schools to undertake outreach work.

His research involves a long-standing strategic partnership with the School of Simulation and Visualisation, The Glasgow School of Art. This has led to multi-million-pound investment in creating world-leading 3D digital datasets to be used in undergraduate and postgraduate teaching to enhance learning and assessment. This successful collaboration resulted in the creation of the world's first taught MSc Medical Visualisation and Human Anatomy combining anatomy and digital technologies. The Institute of Medical Illustrators also accredits it. It has created college-wide, industry, multi-institutional, and NHS research linked projects for students.

Advances in Microscopy and Its Applications with Special Reference to Fluorescence Microscope: An Overview

N. B. Pushpa, Apurba Patra, and Kumar Satish Ravi

Abstract

The microscope has revolutionized the understanding of an organism's structural details and cellular functions. With the invention of highly evolved microscopes, the diagnosis and treatment of diseases has gained momentum. Technology has immensely helped demonstrate cellular events like phagocytosis, cell movement, cell division, etc. with enhanced temporal and spatial resolution. One of these advanced inventions is the fluorescent microscope which has enabled scanning through various physiological activities of the cell. A fluorescence microscope uses the property of fluorescence to create an image. In addition to visualizing the structural details of the cells, a fluorescence microscope also aids in witnessing cellular activities. With an immunofluorescence microscope, cellular antigens can be localized. This chapter highlights the basics of microscopy, types of microscopes, principles, and types of fluorescence microscopes, and recent advances in microscopy and its application.

1.1 Introduction

With the recent advances in science, an excellent thirst for looking into the ultrastructure of particles and organisms has emerged. This paved the way for the evolution of a branch of science—"Microscopy," which refers to the observation of minute details of the structure that the naked eye cannot see. Recent microscopes have assured the visualization of particles from nanometers to millimeters in size. The most common type of microscope universally used is the optical microscope. This microscope produces an enlarged image of the sample placed in the focal plane of the lens. The objective piece has a real, magnified picture of the sample set at a defined distance from its front lens. In contrast, the objective of infinite tube-length microscopes is to produce a virtual image of the sample at infinity. Microscopy techniques have revolutionized the field of medicine by giving rise to sub-sepcialties like histology and pathology. Advanced research has been empowering

N. B. Pushpa
Department of Anatomy, JSS Medical College, JSSAHER, Mysore, Karnataka, India

A. Patra
Department of Anatomy, All India Institute of Medical Sciences, Bathinda, Punjab, India

K. S. Ravi (✉)
Department of Anatomy, All India Institute of Medical Sciences, Rishikesh, Uttarakhand, India

super-resolution techniques by enhancing magnification, imaging mode, numerical aperture, spatial resolution, and light wavelength (Abramowitz and Davidson 2007). The older microscopes had limitations in terms of resolution. Depending on the need to visualize different structures and organisms, different types of microscopes have been invented. The invention of sophisticated microscopes has resulted in a better understanding of not only the structural details of the cell but also the physiological activities (The University of Edinburgh 2018).

1.1.1 Magnification

In optics, magnification (×) refers to the size of an image produced relative to the object's size.

Linear magnification refers to the ratio between the image length and the object length measured at the right angle to the optical axis. The term longitudinal magnification is used when the image is enlarged along the optical axis. The image is called inverted when the values of linear magnification are negative. However, angular magnification refers to the ratio of the tangents of the angles formed by an object and its image when measured from a given point in the microscope, i.e., lens or magnifiers. Theoretically, magnification can be infinite, but practically, magnification caused by any optical instrument is limited by its resolving power (Ray 2002; Wayne 2021).

1.1.2 Resolving Power

Resolving power refers to the ability of a microscope to produce precise, distinct images of very closely placed objects. The objective lens's numerical aperture depicts the microscope's ability to delineate the specimen at a fixed distance. The greater the distance between the two points, the greater the resolution will be. The resolution also depends on the property of the light used in the microscope. Hence, if the light of a shorter wavelength is used, then the resolution caused

will be more compared to the light of a greater wavelength (Jonkman et al. 2003).

1.1.3 Parts of Light Microscope (Fig. 1.1)

The essential parts of an optical microscope include stage, slide holder, eyepiece, objective, nosepiece, base, condenser, diaphragm, light source, coarse and fine adjustment, and carrying handle. Objectives and condenser need a special mention also. The objective piece of a microscope can have a single or combination of lenses that face the object and collects light from it. The principal property of objective lenses is magnification. The overall magnification provided will be combined magnification with the eyepiece. For example, an objective with 4× will provide 40 times magnification with a 10× eyepiece. Three or four objectives of different magnifications are fitted into one nosepiece, which can rotate based on the required lens. These objective lenses are color coded for easy selection. Different magnifications available are 4×, 10×, 40×, and 100×. The lowest magnification is 4×, called an objective scanning lens,
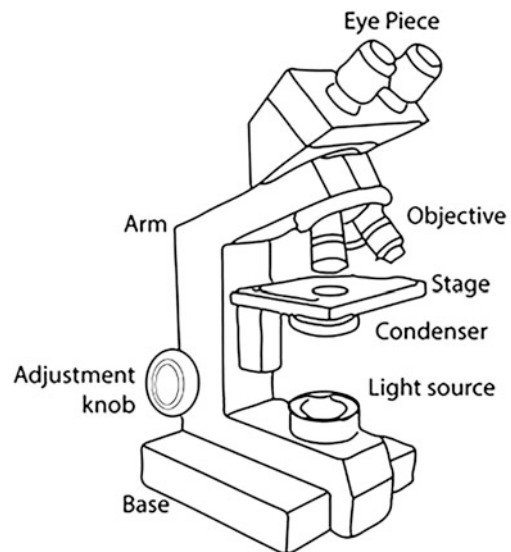
Fig. 1.1 Schematic diagram of Compound microscope showing its parts

while the highest is 100×, called the large objective lens.

The sample is illuminated by gathering light from the source through condenser lenses that are placed over the light source; resulting in a clear, sharp image with optimal magnification. The amount of light entering the condenser can be controlled by the diaphragm. It is suggested to use a condenser for higher magnification rather than for low magnification. Condensers are mainly of three types- chromatic (Abbe), aplanatic, and compound achromatic condensers. The aplanatic condensers are used to correct spherical aberration, while compound achromatic condensers are preferred to rectify both chromatic and spherical aberrations. Although Abbe condensers can be used for magnification of less than 400× only, it is still the most widely used microscope condenser. There are specialized condensers for Phase contrast, dark field, and epifluorescence microscopes. In epifluorescence microscopy, the objective lens functions as both a magnifier and a condenser (Abbe 1874).

1.2 Evolution of Microscope

The idea of constructing a microscope dates back to the thirteenth century and originated with a hand-held lens to magnify objects (Atti 1975). Hence, a simple lens with required magnification, object stand, and adjustment apparatus constituted a light microscope. This was followed by the invention of the primitive form of the compound microscope with two lenses by Dutch eyeglass maker Zacharias Jansen in 1595, which could magnify the specimen by nine times (Van Helden et al. 2010; William 1996). Anton van Leeuwenhoek invented a high magnification microscope, later termed the simple microscope, hence he is referred to as the "Father of Microscopy." The construction of the compound microscope followed this invention. Robert Hooke further embellished the instrument with a stage, light source, and controls for coarse and fine adjustment (Lane 2015). Robert Hooke was the first to use the term "cell" based on their appearance under the microscope. Until the eighteenth

century, microscopes could only magnify up to 50×. Then Carl Zeiss and Ernst Abbe added a substage condenser and improved the lenses, which could provide better magnification and resolution (Abbe 1874).

1.3 Principle of Microscopy

The objective piece of the microscope carries an objective lens that focuses on the object and forms an enlarged image of the object, referred to as a primary image (I1). The resulting magnification is known as primary magnification. This primary image is a magnified, inverted real image, which acts as an object for the eyepiece and is projected up into the focal plane of the eyepiece (Inoué 2006). The eyepiece magnifies the primary image and secondary image (I2) is formed at about 10 inches from it (Fig. 1.2).

1.4 Types

Microscopes are categorized chiefly based on how they interact with the specimen/sample to produce the image. Depending upon the kind of light source used, we have different types of microscopes.

1.4.1 Optical Microscopy

1.4.1.1 Bright Field Microscopy
The basic form of a light microscope. The specimen under observation is illuminated by the light source below and observed from above by the eyepiece. The most significant advantage is its simple technology and easy preparation of the slide used for the study. However, the major drawback is its poor contrast of the specimen and low apparent resolution (Chandler and Roberson 2009).

1.4.1.2 Dark-Field Microscopy
This technique is preferred for ameliorating the contrast of transparent specimens, which are unstained (Abramowitz and Davidson 2007).
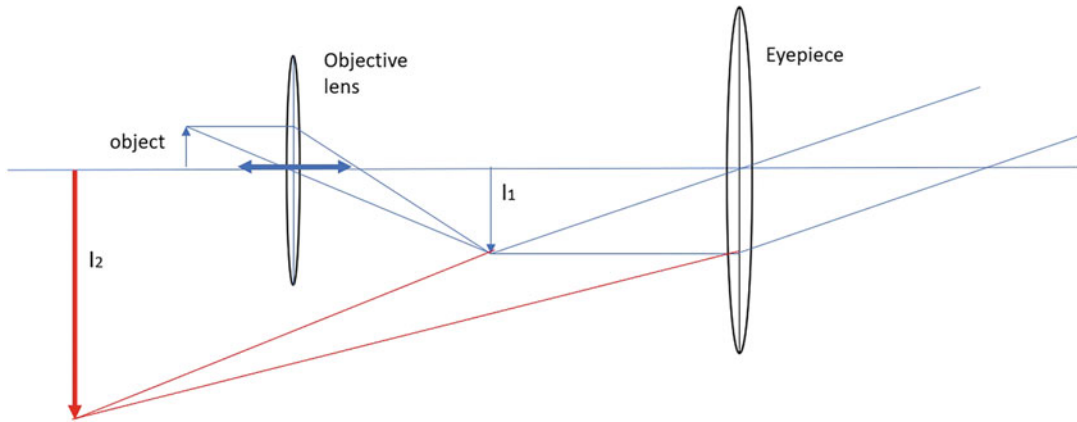
Fig. 1.2 Principle of microscopy showing primary image and secondary image

Darkfield illumination utilizes an aligned light source to limit the amount of transmitted light passing through the image plane. This technique functions by illuminating the structures under observation with intense oblique peripheral light. The central light beam is excluded from approaching the objective lens by the central stopper patch attached to the condenser. Its application is appreciated in the study of extremely tiny and transparent particles. Dark fields can exponentially upgrade the image contrast—particularly of transparent objects. Although this technique requires minimum setup or sample preparation, the limitations of this technique are low apparent resolution and diminished intensity of the final image (Mualla et al. 2018).

1.4.1.3 Oblique Illumination Microscope

This microscope gives a 3D appearance with the use of oblique illumination and also highlights invisible features. The main limitation is the low contrast of various biological samples; the out-of-focus object may result in low apparent resolution. Hoffmann's modulation contrast is a recent advancement in this technique and is used in inverted microscopes for usage in cell culture. The prime limitation in the oblique illumination microscope is identical to those found in bright field microscopy (Chandler and Roberson 2009).

1.4.1.4 Phase Contrast Microscope

This works on the principle that the difference in refractive indices of the media and the object results in phase difference. Hence, an image will be formed because of interference between direct and diffracted light from the object. The greater the phase difference the greater will be the difference in amplitude, and the brighter will be the resulting image. Because of this principle, living cells can be directly observed, hence can visualize the cellular activities under a phase contrast microscope without sacrificing/staining procedure. This enables us to understand ongoing dynamic cellular events in their natural state (Mualla et al. 2018).

1.4.1.5 Interference Microscope

This works on the principle of interference, where a beam of light from the source is split (Mualla et al. 2018).

1.4.1.6 Dispersion Staining Microscopy

It is a set of staining techniques utilized in establishing the identity of an unknown minute particle with the aid of standard particles of known properties. The property utilized here is the "dispersion curve" based on the refractive index of the two particles. The difference in the dispersion curve becomes apparent when they intersect. This technique is mainly employed in detecting asbestos in construction materials. The

novelty of this technique is that it is free from dyes/coloring substances (Bruni et al. 1998).

1.4.1.7 Polarization Microscope

A conventional microscope with a rotating stage has two polarizing elements and balsam. The polarizer is fitted below the condenser, and the analyzer is attached above the objective lens. This microscope is mainly utilized to differentiate between amorphous and crystalline biological specimens (Oldenbourg 2013).

1.4.1.8 Atomic Force Microscope

Offers very high resolution in terms of nanometer fractions, a thousand times more than the regular optical microscope. Here information is obtained by touching/feeling the structure's surface with a mechanical probe (cantilever tip). Currently, this is the only microscope that can provide structural, functional, and mechanical information about the cell at high resolution (Trache and Meininger 2008).

1.4.1.9 Fluorescence Microscope

Tissues are subjected to a fluorescent dye, and ultraviolet light falls on the object. The tissue emits more long-wavelength light and becomes visible against the dark background. Compared to a traditional fluorescence microscope, photon microscopy provides fine resolution of particles/tissue less than 1 mm (Hama et al. 2011).

1.4.1.10 Confocal Microscopy

It uses a focused laser beam that is scanned across the sample to excite fluorescence point by point. To prevent unfocused light from reaching the detector, the emitted light is guided through a pinhole, usually a photomultiplier tube. The image is then compiled in a computer based on the measured fluorescence intensities and the position of the excitation laser. Confocal microscopy provides slightly higher lateral resolution and greatly improves axial resolution/optical sections. Therefore, such microscopy is widely used where the 3D structure of the sample is essential (Pawley 2006).

1.4.2 Electron Microscopy

Here, electrons are used instead of light, and the image is focused on the fluorescent screen by magnetic coils. The resolution provided by the electron microscope is 3–5 angstroms; even the ultrastructure of the cell/object can be visualized. Since it offers a higher resolution, more subtle details of the structure can be studied. In a transmission electron microscope, the images are formed due to the passage of electrons into the object. In a scanning electron microscope, images are formed based on the ability of the object to emit secondary electrons from its surface. The compound microscope had the limitation of lower resolution due to the limited wavelength of light used. This limitation is overcome by electron microscopes, where an electron beam with a much smaller wavelength is used to obtain a higher resolution. A magnetic field is used to obtain electron-optical systems that function much like the glass lenses of a compound microscope. Electron microscopes are basically used to observe and examine ultrastructure. They use specialized digital cameras to create electron micrographs to capture the image (Mualla et al. 2018).

Transmission electron microscopy (TEM) is a traditional form of an electron microscope. In this, a high-voltage electron beam is used to illuminate a very thin slice of the sample/specimen to form an image. The source of the electron beam is usually an electron nozzle with a tungsten filament. The emerging electron beam through the specimen acquires information about the observed specimen and is further magnified by the objective lens. A serial section electron microscope is used to obtain consecutive serial sections of a particular structure. These sections of the 3D volume are exposed to the electron beam, and a complete image of the structure is then obtained (Chandler and Roberson 2009).

Scanning Transmission Electron Microscopy (STEM)—This transmission electron microscope is equipped with a scanning capability. STEM visualizes the details of a structure by detecting electrons scattered through the structure. So, it

can provide a very clear 3D view with high resolution.

Scanning Electron Microscope (SEM)—It uses a scanning probe and a focused electron beam. SEM creates images reflecting their composition and topography. Because a certain amount of energy is lost when the electrons interact with the sample, the image produced in this microscope has a slightly lower resolution compared to TEM. In a reflection electron microscope, the reflected electron beam is detected instead of the secondary/transmitted electrons. This principle is often combined with reflection high energy diffraction (RHEED)/reflection high energy loss spectroscopy (RHELS). Electron microscopes are designed for X-ray spectroscopy and can provide quantitative and qualitative elemental analysis, also called analytical electron microscopes, and are an effective tool for analyzing nanomaterials (Kosasih and Ducati 2018).

1.4.3   Scanning Probe Microscopy

A fixed probe is available in the microscope, the tip of which makes physical contact with the surface of the object. The atomic force microscope (AFM), photonic force microscope, scanning tunneling microscope, and repetition monitoring microscope are various examples of scanning probe microscopes (Mualla et al. 2018).

1.4.4   Ultrasonic Force Microscopy (UFM)

This microscopic method was introduced to improve the image contrast and detail on "flat" regions under study, where AFM images have contrast limitations. AFM-UFM fusion enables near-field acoustic microscopic image generation. The AFM tip enables the detection of ultrasonic waves and overcomes the wavelength limitation encountered in acoustic microscopy. The elastic changes that occur under the AFM tip help create an image with more detail than that produced by AFM. In UFM, local elasticity mapping is enabled in AFM by applying ultrasonic vibrations to a cantilever or sample. In order to quantitatively analyze the UFM results, a force-distance curve measurement is performed with ultrasonic vibration applied to the cantilever base. Then the results are compared with a dynamic model of the cantilever and the tip-sample interaction depending on the finite difference technique (Dinelli et al. 2011).

1.4.5   Ultraviolet Microscopy

In this type, ultraviolet light is used as a source of light. The amount of light absorbed by the object is recorded photographically, and the molecules in the object, like purine, pyrimidine, DNA, etc., are identified. This technique serves two main purposes. The first is the use of shorter wavelength ultraviolet electromagnetic energy to improve image resolution beyond standard optical microscopes. The second application is the increase of contrast when the response of individual samples relative to their surroundings is increased due to the interaction of light with the molecules in the examined sample. One such example is the contrast enhancement of protein crystals that form in salt solutions (Heimann and Urstadt 1990).

1.4.6   Infrared Microscopy

This type of microscopy refers to using infrared waves in the microscope. In a typical microscope configuration, a Fourier transforms infrared (FTIR) spectrometer is combined with an infrared detector and an optical microscope. The infrared detector can be a linear array/2D focal plane array/single point detector. FTIR enables chemical analysis using infrared spectroscopy, then the microscope and point/matrix detector further allow this chemical analysis to be spatially resolved, i.e., performed in different areas of the sample. The technique itself is also called infrared microspectroscopy. An alternative arrangement known as laser direct infrared imaging involves a combination of a tuneable infrared

light source, and a single-point detector mounted on a flying objective. This technique is often used for infrared chemical imaging, where image contrast is due to the response of individual sample regions to specific user-selected IR wavelengths, specific IR absorption bands, and associated molecular resonances. A prime limitation of conventional infrared microspectroscopy is that spatial resolution is limited by diffraction (Pollock and Kazarian 2014).

1.4.7 Photoacoustic Microscopy

This microscopic technique relies on the photoacoustic effect (Bell 1880), which is the generation of ultra-level sound caused by the absorption of light. A focused intensity modulated laser beam is raster scanned across the sample. The generated (ultra) sound is detected using an ultrasonic transducer. Piezoelectric ultrasonic transducers are commonly used in photoacoustic microscopy to analyze the structure (Yao and Wang 2013).

1.4.8 Digital Holographic Microscopy

In DHM, interfering wavefronts arising from a coherent or monochromatic light source are recorded on the sensor. The image created in this way from the recorded hologram is digitally reconstructed by a computer. In addition to the normal image in the bright field, an image with a phase shift is also created. This technique can control both transmission mode and reflection. In transmission mode, the phase-shift image enables a label-free quantitative measurement of the optical thickness of the sample. While in reflection mode, the phase shift image provides a relative distance measurement and thus represents a topographical map of the reflecting surface. Phase shift images of biological cells are very similar to stained cells and have been successfully analyzed by high content analysis software. A unique feature of DHM is its ability to adjust focus even after the final image is recorded, as all focus planes are recorded simultaneously by

the hologram. This feature makes it easier to capture moving objects. Another attractive feature is the DHM's ability to use low-cost optics with software-based optical aberration correction (Rappaz et al. 2014).

1.4.9 Digital (Virtual Microscopy)

Digital pathology is made possible partly with virtual microscopy, in which the glass slides are converted into digital slides that can be viewed and analyzed. This technique is a visual information environment that enables a computer-aided mechanism to manage information generated from a digital slide (Mualla et al. 2018).

1.4.10 Laser Microscopy

In laser microscopy, the laser beam is utilized as an illumination source (Duarte 2016). For example, laser microscopy focused on biological applications uses ultrashort pulse lasers in a variety of techniques referred to as saturation microscopy, nonlinear microscopy, and two-photon excitation microscopy (Thomas and Rudolph 2008).

High-intensity, short-pulse laboratory X-ray lasers are under evaluation. If this technology is successfully developed, it will be possible to obtain enlarged 3D images of basic biological structures in vivo at a particular time. The resolution is limited primarily by the hydrodynamic expansion that occurs when the required number of photons is registered (Solem 1983). Thus, even if a specimen is destroyed by exposure, its configuration may be captured before it explodes (Solem 1982).

1.5 Fluorescence Microscopy

1.5.1 Principle and Mechanism

A fluorescence microscope uses the property of fluorescence with other properties like reflection, scattering, and absorption to produce the image.

Fluorescence is the emission of light by a substance that has absorbed light or electromagnetic radiation (Gill 2010). The objects become visible when absorbed radiation is ultraviolet (UV) rays of the electromagnetic spectrum, and the structure/specimen under study emits visible light; this provides the structure with distinct color to be observed in the presence of UV light. Spectral emission filters are used to separate the illuminating light from emitted fluorescence. The fluorescent structure stops glowing when the radiation source is stopped (Fig. 1.3).

Fluorescence occurs when a particle/atom relaxes from a high to a lower energy state by emitting a photon without altering the electron spin. There is a loss of some energy in this process resulting in photons with less power (Helmchen and Denk 2005). Higher energy rays have a short wavelength, and those with low energy have a long wavelength; as a rule, the emitted rays will have a longer wavelength called Stokes shift. It is also possible for a source to absorb energy at a time and emit a single photon with less energy. This energy difference will assign a different color to the particle than in reality. Hence red light can be utilized to produce green light. This is better achieved with photons having high spatial and temporal density. That is why red light is more preferred as an excitation source over blue light since red light has more penetration to the tissue because of its less scattered nature. Also, the disadvantage of cell damage with high-energy light can be overcome with red light as an excitation source (Zinselmeyer et al. 2009). Image brightness in a fluorescence microscope is directly proportional to the number of photons gathered by the detector during the specific dwell time. Other super-resolution techniques like stimulated emission depletion can overcome the default diffraction limit and produce an image of significant magnification.

In the two-photon fluorescence technique, two photons are simultaneously excited, unlike in the regular fluorescence microscope. Here the wavelength of the utilized light is more than that of emitted light, in contrast to the single photon technique. Often the excitation light is near-infrared rays which can minimize the scattering within the tissue. As two photons are absorbed with each excitation, this technique offers excellent resolution. Hence this is preferred over confocal microscopy with added advantages of decreased photobleaching, deep tissue penetration, clear background, and efficient light detection (Denk et al. 1990).

1.5.2 Epifluorescence Microscopy

Most fluorescence microscopes, particularly those used in the life sciences, have an epifluorescence design, as shown in Fig. 1.3. Light of the excitation-specific wavelength illuminates the sample through an objective lens. The fluorescence emitted by the specimen follows and is focused on the detector, which will need an objective with a higher numerical aperture for greater resolution. Since most of the excitation light passes through the spsecimen, only the reflected excitation light, together with the discharge light, reaches the objective, thus providing a high signal-to-noise ratio. The dichroic beam splitter acts as a wavelength-specific filter, allowing only fluorescent light into the eyepiece or detector, but reflecting back any remaining excitation light toward the source (Sanderson et al. 2014).

1.5.2.1 Light Sources for Fluorescence
Fluorescence microscopy needs intense near monochromatic illumination, which some extended light sources, such as halogen lamps, cannot provide (Huang 2010). Four types of light sources are commonly used, including xenon arc lamps or mercury discharge lamps with a laser, excitation filter, supercontinuum sources, and high-power LEDs. Among them, lasers are the most widely used for more complex fluorescence microscopy techniques, such as total internal
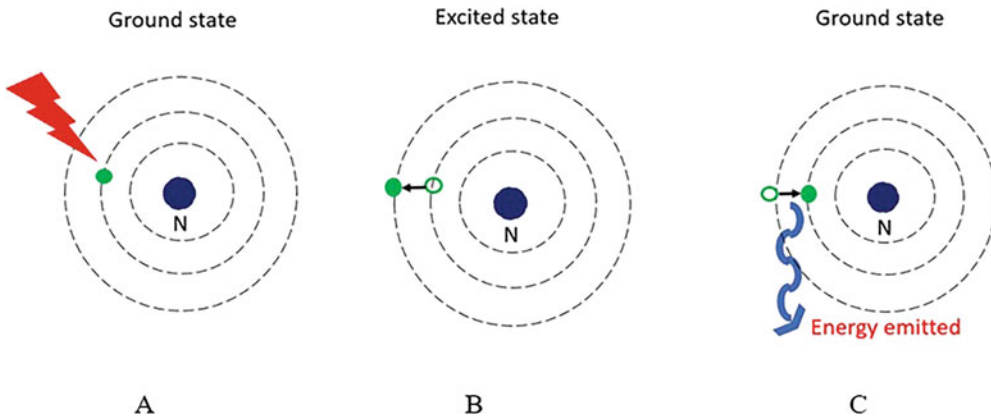
Fig. 1.3 Diagrams showing the basic principle of fluorescence. (**a**) Showing excitation of the photon by light energy, (**b**) Photon in the excited state, (**c**) Photon returning to ground state

reflection fluorescence microscopy and confocal microscopy. In contrast, xenon lamps, mercury lamps, and dichroic excitation filter LEDs are ideally used for wide-angle epifluorescence microscopes. By placing two microlens arrays in the illumination path of a wide-field epifluorescence microscope (Coumans et al. 2012), highly uniform illumination can be achieved.

1.5.2.2 Sample Preparation in Fluorescence Microscopy

The first and foremost criterion for a sample to be suitable for fluorescence microscopy is that it must be fluorescent. There are various methods for creating a fluorescent sample; the main techniques are labeling with fluorescent dyes or, in the case of biological samples, fluorescent protein expression. Alternatively, intrinsic fluorescence or autofluorescence of the sample may also be used. In the life sciences, a fluorescence microscopy is a powerful tool that enables sensitive and specific staining of a sample to detect the distribution of proteins or other molecules of interest. Thus, a variety of techniques are available for fluorescent staining of biological samples of interest (Sanderson et al. 2014).

1.5.3 Fluorophores

Fluorophores/fluorochromes are fluorescent chemicals that can re-emit the light on excitation. They are used as a dye to stain structures, probes, or substrates for specific enzymes. They covalently attach to the macromolecule under observation, thus allowing them to be visible under a fluorescent microscope or spectroscope. Fluorescein is the most widely used fluorophore derived from fluorescein isothiocyanate (FITC). Ideal fluorophores should be more photostable, less pH-sensitive, and brighter, and such qualities are seen in newer-generation fluorophores (Gustafsson et al. 2008). Since fluorophores absorb and emit light, the wavelength of the absorbed light, the efficiency of energy transmission, and the time taken for transmission depend on the nature of the fluorophore and its interaction with the environment. Fluorophores are broadly classified into four groups based on their molecular structure and synthetic methods. They are small organic compounds, proteins and peptides, synthetic oligomers and polymers, and multi-component systems (Tsien and Waggoner 1995; Lakowicz 2006).

1.5.4   Immunofluorescence

Immunofluorescence is a technique in microscopy widely used in microbiology. It uses antibodies labeled with fluorescent dyes to illuminate and study the structure under observation (Lichtman and Conchello 2005). The antibodies help locate the particular particle throughout the sample or identify a specific cell. The region of contact of the antibody on the antigen is called the epitope. The antibodies are either covalently bound to the fluorescent dye or by means of one more antibody, referred to as primary antibody and secondary antibody, respectively (Im et al. 2019). Subsequently, the first method is called direct immunofluorescence, and the second is called indirect immunofluorescence. Immunofluorescence provides an essential advantage of revealing molecules in their indigenous state, decreasing potential distortion of protein structure, localization of the protein, and understanding its function using fluorophore tagging (Mutasim and Adams 2001).

Immunofluorescence is not devoid of disadvantages, the major drawback being photobleaching which results in the loss of activity of the fluorophore (Wäldchen et al. 2015). This can be reduced by limiting the intensity and period of light exposure and utilizing fluorophores of ideal quality, which can resist photobleaching. Other limitations include restriction to a particular cell and lesser penetration of fluorophore into the cells (Im et al. 2019).

1.5.5   Components of Fluorescence Microscope

A fluorescence microscope essentially includes the following components (Fig. 1.4)—

The light source—is usually a mercury vapor lamp/Xenon arc lamp/tungsten halogen lamp. Laser beams in laser scanning microscopes scan the specimen and create an image. Recent light source improvement uses bright, single-wavelength light-emitting diodes (LEDs). Appreciable advantages of LEDs are fast switching without shutters, increased longevity, and tight control of wavelength.

Excitation filter—it ensures the transmission of only light of the required wavelength. Hence, it allows the light reflected by the dichroic mirror to illuminate the specimen. Excitation filter has limited use when monochromatic or laser light is for excitation purposes.

Dichroic beam splitter—since the excitation source is brighter than the emitted light, it is necessary to have filters that can block the bright excitation light. This can be achieved by using filters that separate excitation and cast light. By this arrangement, the specimen's excitation light of a shorter wavelength is reflected, and light of a longer wavelength is transmitted to the detector by the dichroic mirror. Sometimes they can also be used to send short-wavelength light and reflect the light of longer wavelength (Sanderson et al. 2014).

Emission filter—when the light passes through the filters, there is always a threat of decreasing intensity. Also, the image brightness is determined by the light transmitted by the filters. Hence it is always essential to have emission filters that can only block spurious excitation light, thus ensuring a bright image of the specimen.

Filter cube—this is used to align the excitation and emission filters in the light path. It directs light from the excitation source to the specimen and from the specimen to the detector. Hence, the orientation of each element is essential within the filter cube. It is about a one-inch-sized box containing a set of excitation filters, a dichroic filter at 45°, and an emission filter. The set of filters included depends upon the fluorescent dye used. A recent microscope consists of an automated filter changer enabling rapid switching in and switching out filters from the light path (Murphy and Davidson 2012) (Fig. 1.4).

Fig. 1.4 Parts and function of fluorescence microscope
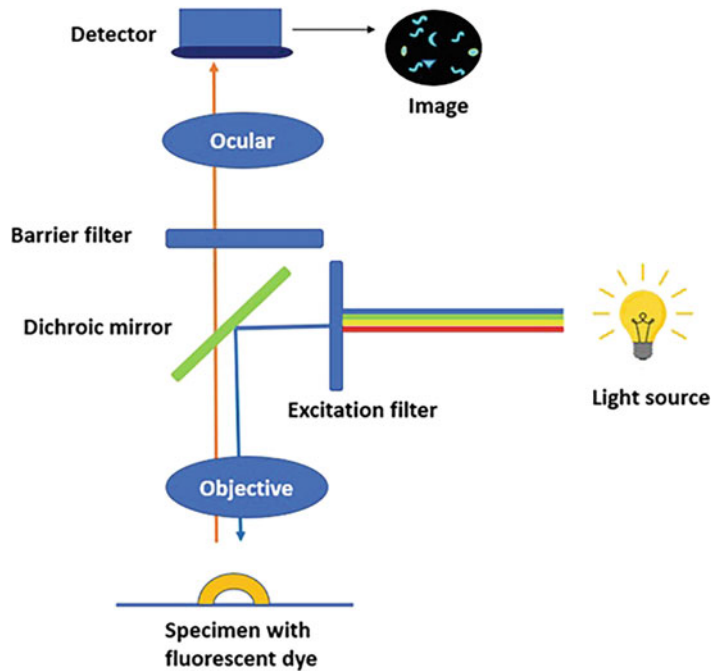
1.6 Types of Fluorescence Microscope

With its widespread application, the fluorescence microscope has become an essential tool for cell biologists. In this microscope, light from the source illuminates the specimen to excite the fluorophore attached. Different types of fluorescence have been listed based on the microscope's ability to cast a particular region or whole of the specimen.

1.6.1 Wide-Field Fluorescence Microscopy

Wide-field fluorescence microscopy is Wide-field microscope is ideally suited for viewing 2D images of the specimen. The most significant advantage of wide-field microscopes is the ability to capture and view an entire specimen at a glance. Conversely, the image obtained in this microscope is of less contrast and spatial orientation owing to diffraction-limited optics and projection of out-of-focus light on the camera's

image plane (Pawley 2006). These limitations can be overcome to a certain extent by the optimal selection of a specimen that falls entirely under the focus and with thin sections and by reducing the numerical aperture of the objective to avoid out-of-focus light. Other advantages of a vast field microscope are cost-effectivity, simplicity, reduced photobleaching/phototoxicity, and flexibility (Sanderson et al. 2014).

1.6.2 Confocal Microscopy

Laser scanning microscopes enable thick specimens and reduce out-of-focus light. In contrast to a wide field fluorescence microscope, the light source is a laser- a bright point source. Other differences are that point source illumination is sequentially scanned, and the emitted light is detected using a photomultiplier tube. Also, the image is compiled pixel by pixel at each point. The optimal magnification of the image depends on the dwell time of the laser spot that remains over the specimen's particular site. The greater the dwell time, the image is formed due to the increased number of photons being captured.

However, dwell time can simultaneously boost the chances of photobleaching. Reduction of focus light is achieved in confocal microscopes by using a pinhole aperture, as it can exclude light that is out of focus. However, this is again at the cost of the reduced intensity of the image obtained, which is in turn due to reduced photons captured at that particular dwell time. The other major drawback of a confocal microscope is reduced tissue penetration, which can be overcome using pulsed, long-wavelength laser excitation sources, and two-photon excitation modes. Two-photon microscopes also concentrate on photobleaching as there is limited use of indicators to produce the image. Also, using more extended wavelength lasers allows for deeper penetration of tissues (Denk et al. 1994; Hama et al. 2011).

1.6.3 Total Internal Reflection Fluorescence Microscopy

The limitations of confocal and two photo microscopes are reduced axial resolution and diffraction-limited approach. This resulted in the invention of a total internal reflection fluorescence (TIRF) microscope (Axelrod 2001). The use of total internal reflection to illuminate tissues was first advocated by Axelrod (Ambrose 1956). Here, a glass substrate is used to direct the emitted light toward the aqueous specimen placed at a shallow angle. This results in total internal reflection because of the difference in the refractive index at the glass water interface. The penetration depth depends on the wavelength of emitted light, the difference in the refractive index, and the angle of incident illumination. The major limitation is that this field can only excite the fluorophores, which are just adjacent to the interface, thus resulting in an optical sectioning effect. This can be addressed by using prism-based TIRF microscopes, as excitation light bypasses the objective lens (Brakenhoff et al. 1986; Mandracchia et al. 2020).

1.7 Applications/Uses of Fluorescence Microscope

The fluorescence microscope is widely employed to study structures in biological samples. It enables the observation of the ultrastructure of the cell. This technique can also be studied for the morphology and even the activities within the cells. With its potential to segregate individual cell proteins with utmost precision in the midst of non-fluorescence materials, it is the most preferred microscopy technique to understand the dynamic behavior of living cells. Hence it can detect as low as 50 molecules/mm^3. Many structures can be traced at once with fluorescent dyes of different colors. This property has led to the widespread usage of fluorescence microscopy in neurobiology, physiology, embryology, oncology, etc. (Masters et al. 1997).

1.8 Recent Trends and Application

With the advancement in technology, many more features have been invented in microscopy, thus extending its applications to different fields. A basic fluorescence microscope is a routine instrument for a cell biologist. A few of the recent inventions include scanning probe microscopy, ultrasonic force microscopy, digital holographic microscopy, photoacoustic microscopy, laser microscopy, etc. The use of a microscope is no longer limited to observing objects invisible to the naked eye. It is widely used in the medical field for In-vitro diagnostics, examining forensic pieces of evidence, 3D imaging, next-generation sequencing of genetic material, digital assisted cell morphology, automated digital pathology, cell sorting, and counting, studying the atomic structure, etc. When closely placed fluorescent objects are viewed under a microscope, there is a greater chance of blur image formation due to bright blur as each object emits an overlapping cone of light. Super-resolution microscopy has helped to overcome the traditional diffraction

limits encountered in optical microscopy (Dani and Huang 2010). Hence the observation of objects which are sparsely spaced can yield a better image, which is the principle behind photoactivated localization microscopy (PALM) (Betzig et al. 2006) and stochastic optical reconstruction microscopy (STORM) (Rust et al. 2006). PALM fluorescence from the individual fluorophore is separated by temporary separation of their emission periods. STORM is a super-resolution variant of the immunofluorescence technique that uses photo sandwich-able fluorescent dyes. Another dynamic approach is the stimulated emission depletion (STED) microscope. Here indicators are separated by reducing the excitation spot size. Although the diffraction limit of microscope optics still exists in this type, the major advantage of the STED microscope is using a simple continuous wavelength laser instead of synchronized pulsed lasers (Hell 2009).

1.9   Conclusion

The science of microscopy is centuries old. Inventions with the ability to visualize clearly and accurately are the key factor that has led to the evolution of different microscopes. Each advancement has led to steady improvement in microscopy, which has revolutionized the field of science, especially medicine. It is indeed microscopy that has resulted in the development of different branches of medicine like histology, pathology, microbiology, etc. Histopathology has enabled the accurate diagnosis of various diseases and timely treatment of the same. Recent microscopes have made possible three-dimensional views of various structures/samples under study. This is aided by updated software and graphics which can record, store and analyze complex data. The future of microscopy depends on the development of technologies that enables the observer to visualize the sample in three dimensions with utmost precision. With the application of artificial intelligence, there is more scope for digitalization and integration by which the observer can witness the whole process happening in the entire biological sample. Also,

novel soft wares have been developed to refrain unwanted signals arising from of focus region of the sample and disclose the in-focus region of interest. This will result in enhanced precision and reliability, thus enabling the observations to be more reproducible and significant. Such advancements will not only spearhead a new era of scientific imaging and fundamentally switch the way that researchers think when observing an organism, tissues, and three-dimensional cell cultures like organoids; they will also optimize and further enhance what is already existing.

References

Abbe E (1874) A contribution to the theory of the microscope and the nature of microscopic vision. Proc Bristol Nat Soc 1:200–261

Abramowitz M, Davidson MW (2007) Introduction to microscopy. Molecular Expressions. Retrieved June 30, 2022

Ambrose EJ (1956) A surface contact microscope for the study of cell movements. Nature 178:1194

Atti Della, Fondazione Giorgio, Ronchi E (1975) Contributi Dell'Istituto Nazionale Di Ottica, vol 30, La Fondazione, p 554

Axelrod D (2001) Total internal reflection fluorescence microscopy in cell biology. Traffic 2:764–774

Bell AG (1880) On the production and reproduction of sound by light. Am J Sci s3-20(118):305–324

Betzig E, Patterson GH, Sougrat R, Lindwasser OW, Olenych S, Bonifacino JS et al (2006) Imaging intracellular fluorescent proteins at nanometer resolution. Science 313:1642–1645

Brakenhoff GJ, Voort HVD, Spronsen EV, Nanninga N (1986) Three-dimensional imaging by confocal scanning fluorescence microscopy a. Ann N Y Acad Sci 483(1):405–415

Bruni M, Cimini F, Costa U (1998) An alternative method of detecting dispersion staining colors for the determination of asbestos fibers in bulk materials. Med Lav 89(3):254–264

Chandler DE, Roberson RW (2009) Bioimaging: current concepts in light and electron microscopy. Jones & Bartlett Publishers

Coumans FAW, Van der Pol E, Terstappen LWMM (2012) Flat-top illumination profile in an epi-fluorescence microscope by dual micro lens arrays. Cytometry A 81(4):324–331

Dani A, Huang B (2010) New resolving power for light microscopy: applications to neurobiology. Curr Opin Neurobiol 20(5):648–652

Denk W, Strickler JH, Webb WW (1990) Two-photon laser scanning fluorescence microscopy. Science (New York, NY) 248(4951):73–76

Denk W, Delaney KR, Gelperin A, Kleinfeld D, Strowbridge BW, Tank DW, Yuste R (1994) Anatomical and functional imaging of neurons using 2-photon laser scanning microscopy. J Neurosci Methods 54(2):151–162

Dinelli F, Albonetti C, Kolosov OV (2011) Ultrasonic force microscopy: detection and imaging of ultra-thin molecular domains. Ultramicroscopy 111(4):267–272

Duarte FJ (2016) Tunable laser microscopy. In: Duarte FJ (ed) Tunable laser applications, 3rd edn. CRC Press, Boca Raton, FL, pp 315–328

Gill H (2010) Evaluating the efficacy of tryptophan fluorescence and absorbance as a selection tool for identifying protein crystals. Acta Crystallogr F66 (Pt 3):364–372

Gustafsson MG, Shao L, Carlton PM, Wang CR, Golubovskaya IN, Cande WZ et al (2008) Three-dimensional resolution doubling in wide-field fluorescence microscopy by structured illumination. Biophys J 94(12):4957–4970

Hama H, Kurokawa H, Kawano H, Ando R, Shimogori T, Noda H, Fukami K, Sakaue-Sawano A, Miyawaki A (2011) Scale: a chemical approach for fluorescence imaging and reconstruction of transparent mouse brain. Nat Neurosci 14:1481–1488

Heimann PA, Urstadt R (1990) Deep ultraviolet microscope. Appl Opt 29(4):495–501

Hell SW (2009) Microscopy and its focal switch. Nat Methods 6:24–32

Helmchen F, Denk W (2005) Deep tissue two-photon microscopy. Nat Methods 2:932–940

Huang B (2010) Super resolution fluorescence microscopy. Annu Rev Biochem 78:993–1016

Im K, Mareninov S, Diaz M, Yong WH (2019) An Introduction to Performing Immunofluorescence Staining. Methods Mol Biol (Clifton, N.J.) 1897:299–311

Inoué S (2006) Foundations of confocal scanned imaging in light microscopy. In: Pawley J (ed) Handbook of biological confocal microscopy. Springer, Boston, MA

Jonkman JEN, Swoger J, Kress H, Rohrbach A, Stelzer EHK (2003) Resolution in optical microscopy. Methods Enzymol 360:416–446

Kosasih FU, Ducati C (2018) Characterizing degradation of perovskite solar cells through in-situ and operando electron microscopy. Nano Energy 47:243–256

Lakowicz JR (2006) Principles of fluorescence spectroscopy (3rd ed.). Springer, p 954. ISBN 978-0-387-31278-1

Lane N (2015) The unseen world: reflections on Leeuwenhoek (1677) 'Concerning little animal'. Philos Trans R Soc Lond B Biol Sci 370(1666): 20140344

Lichtman JW, Conchello JA (2005) Fluorescence microscopy. Nat Meth 2:910–919

Mandracchia B, Hua X, Guo C, Son J, Urner T, Jia S (2020) Fast and accurate sCMOS noise correction for fluorescence microscopy. Nat Commun 11(1):1–12

Masters BR, So PTC, Gratton E (1997) Multiphoton excitation fluorescence microscopy and spectroscopy of in vivo human skin. Biophys J 72(6): 2405–2412. Bibcode:1997BpJ...72.2405M

Mualla F, Aubreville M, Maier A (2018) Microscopy, Chapter 5. In: Maier A, Steidl S, Christlein V et al (eds) Medical imaging systems: an introductory guide [Internet]. Springer, Cham, CH. https://doi.org/10.1007/978-3-319-96520-8_5

Murphy DB, Davidson MW (2012) Fundamentals of light microscopy and electronic imaging. Wiley, Hoboken, NJ

Mutasim DF, Adams BB (2001) Immunofluorescence in dermatology. J Am Acad Dermatol 45:803–822. quiz 22–4

Oldenbourg R (2013) Polarized light microscopy: principles and practice. Cold Spring Harb Protoc 11: pdb.top078600. https://doi.org/10.1101/pdb.top078600

Pawley JB (ed) (2006) Handbook of biological confocal microscopy, 3rd edn. Springer, Berlin. ISBN 0-387-25921-X

Pollock HM, Kazarian GS (2014) Microspectroscopy in the mid-infrared. In: Meyers RA (ed) Encyclopedia of analytical chemistry. Wiley, pp 1–26

Rappaz B, Breton B, Shaffer E, Turcatti G (2014) Digital holographic microscopy: a quantitative label-free microscopy technique for phenotypic screening. Comb Chem High Throughput Screen 17(1):80–88

Ray SF (2002) Applied photographic optics: lenses and optical systems for photography, film, video, electronic and digital imaging. Focal Press, p 40. ISBN 0-240-51540-4

Rust MJ, Bates M, Zhuang X (2006) Sub-diffraction-limit imaging by stochastic optical reconstruction microscopy (STORM). Nat Methods 3:793–795

Sanderson MJ, Smith I, Parker I, Bootman MD (2014) Fluorescence microscopy. Cold Spring Harb Protoc, p pdb.top071795. https://doi.org/10.1101/pdb.top071795

Solem JC (1982) High-intensity x-ray holography: an approach to high-resolution snapshot imaging of biological specimens. Los Alamos National Laboratory Technical Report LA-9508-MS. 83:23581

Solem JC (1983) X-ray imaging on biological specimens. Proc Int Conf Lasers 83:635–640

The University of Edinburgh (2018) What is microscopy?. The University of Edinburgh. Retrieved June 30, 2022

Thomas JL, Rudolph W (2008) Biological microscopy with ultrashort laser pulses. In: Duarte FJ (ed) Tunable laser applications, 2nd edn. CRC Press, Boca Raton, FL, pp 245–280

Trache A, Meininger GA (2008) Atomic force microscopy (AFM). Current protocols in microbiology, Chapter 2. doi:https://doi.org/10.1002/9780471729259.mc02c02s8

Tsien RY Waggoner A (1995) Fluorophores for confocal microscopy. In Pawley JB (ed) Handbook of biological confocal microscopy. Plenum, New York, pp 267–274. ISBN 0-306-44826-2. Retrieved 2008-12-13

Van Helden A, Dupré S; van Gent R (2010) The origins of the telescope. Amsterdam University Press, p 24. ISBN 978-90-6984-615-6. Archived from the original on February 15 2017

Wäldchen S, Lehmann J, Klein T, Van De Linde S, Sauer M (2015) Light-induced cell damage in live-cell super-resolution microscopy. Sci Rep 5(1):1–12

Wayne (2021) Magnification ratio and how to choose the Best macro lens. Retrieved June 30, 2022

William Rosenthal (1996) Spectacles and other vision aids: a history and guide to collecting. Norman Publishing, pp 391–392

Yao J, Wang LV (2013) Photoacoustic microscopy. Laser Photonics Rev 7(5):1–36

Zinselmeyer BH, Dempster J, Wokosin DL, Cannon JJ, Pless R, Parker I, Miller MJ (2009) Chapter 16. Two-photon microscopy and multidimensional analysis of cell dynamics. Methods Enzymol 461:349–378

Visualisation of Host–Pathogen Communication

2

Amy Dumigan, Ricardo Calderon Gonzalez, Brenda Morris, and Joana Sá-Pessoa

Abstract

The core of biomedical science is the use of laboratory techniques to support the **diagnosis** and **treatment** of disease in clinical settings. Despite tremendous advancement in our understanding of medicine in recent years, we are still far from having a complete understanding of human physiology in homeostasis, let alone the pathology of disease states. Indeed medical advances over the last two hundred years would not have been possible without the invention of and **continuous development of visualisation techniques** available to research scientists and clinicians. As we have all learned from the recent COVID pandemic, despite advances in modern medicine we still have much to learn regarding infection biology. Indeed antimicrobial resistant (AMR) bacteria are a global threat to human health, meaning research into bacterial pathogenesis is vital. In this chapter, we will briefly describe the nature of microbes and host immune responses before delving into some of the **visualisation techniques** utilised in the field of **biomedical research** with a focus on **host–pathogen interactions**. We will give a brief overview of commonly used techniques from gold standard **staining** methods, *in situ* hybridisation, microscopy, western blotting, microbial characterisation, to cutting-edge image **flow cytometry** and **mass spectrometry**. Specifically, we will focus on techniques utilised to visualise interactions between the host, our own bodies, and invading organisms including bacteria. We will touch on *in vitro* and *ex vivo* modelling methodology with examples utilised to delineate pathogenicity in disease. A better understanding of bacterial biology, immunology and how these fields interact (host–pathogen communications) in biomedical research is integral to developing novel therapeutic approaches which circumvent the need for antibiotics, an important issue as we enter a post-antibiotic era.

Keywords

Cytometry · Host–pathogen interactions · Bacteria · Immune system

2.1 Introduction

Microorganisms can be found almost anywhere on earth playing an important role in ecosystems, manufacturing industry and human health. They can also be regarded as human pathogens and their fast identification is crucial in the clinical

A. Dumigan (✉) · R. C. Gonzalez · B. Morris · J. Sá-Pessoa
Wellcome-Wolfson Institute for Experimental Medicine, Queen's University Belfast, Belfast, UK
e-mail: a.dumigan@qub.ac.uk; r.calderongonzalez@qub.ac.uk; b.morris04@qub.ac.uk; j.sapessoa@qub.ac.uk

setting. To aid in bacterial identification, traditional techniques based on phenotype have been used routinely for many years. They are based on morphology, cell wall, growth in different media or biochemical properties. More recently the advent of new techniques and their automatization allows the use of sequencing or mass spectrometry for a more reliable species identification. In this chapter, we describe some of the most common tests for bacterial identification from staining to molecular methods.

The major groups of microorganisms studied in microbiology are bacteria, algae, viruses, fungi and protozoa. Each of which are found ubiquitously in nature. Most microbes consist of a single cell and are therefore microscopically ranging from 20 nm viruses to large protozoans around 5 mm or more in diameter. Viruses are tiny acellular entities, on the border between living and non-living, only behaving like living organisms once they gain entry to a living host cell. The most well-studied of these organisms are bacteria. Therefore, we rely on visualisation techniques including but not limited to microscopy to study the interaction of these organisms with our host cells in order to understand pathogenicity of disease with the aim of developing medical interventions for infection.

Most bacteria can be described as having either rod, spherical, or spiral morphology with some also possessing filaments. Bacteria can be motile or non-motile and, unlike eukaryotic cells, bacteria do not have nuclei. Many bacteria are able to absorb nutrients from their environment, and some are also capable of making their own nutrients via processes including photosynthesis and other synthetic processes we will discuss later in this chapter. Herein we will focus on the study of bacterial infection biology, meaning the study of bacterial interaction with mammalian host cells. Although bacteria can interact directly and indirectly with all mammalian cells, we will focus on interaction with the main drivers of host defence, i.e. the immune system.

2.1.1 The Immune System

The immune system is a multi-faceted and complex collaboration of cells acting to protect the host from infection and maintain the health of tissues. The main functions of the immune system are to act as a barrier, recognise pathogens and initiate immune responses to restore homeostasis and the health of the host. Epithelial surfaces provide the initial defences against invading pathogens via mechanical, chemical and microbiological methods. Tight junctions between epithelial cells of the skin and linings of the lungs, gut and urogenital tracts act as a mechanical barrier to the external environment. The presence of mucus and internal commensal flora also prevents the passage and establishment of pathogens across epithelial barriers. The importance of the epithelia becomes apparent when the barrier is breached by wounds, burns or loss of epithelial integrity and leads to an increased risk of infection (Murphy et al. 2008).

The immune system consists of innate and adaptive immune responses which can be influenced by factors such as genetics and the environment (Janeway et al. 2001). All multi-cellular organisms possess innate-like immunity including fungi, plants, insects and higher organisms (Beutler 2004). However, only vertebrates benefit from an adaptive immune system and immunological "memory" (Cooper and Alder 2006). The innate immune response is immediate, consistent and broad acting and activates adaptive immune responses. Conversely, the adaptive immune response is delayed and slow acting upon primary encounter with a pathogen, yet is highly specific and provides immunological memory, allowing a rapid response upon secondary exposure to the same pathogen (Lee and Mazmanian 2010). Cells from both innate and adaptive systems coordinate responses via cell–cell contact or production of cytokines or chemokines (Getz 2005), mounting effective and tightly controlled responses while preventing further damage to tissues. Primary immunodeficiency disorders (PID) are a group of heterogeneous illnesses caused by defects in

immune system function. Patients with PID are much more susceptible to autoimmune disorders, malignancy and recurrent infections (Raje and Dinakar 2015). Indeed, bacteria have evolved strategies to circumvent healthy immune responses for their own benefit.

2.1.2 Innate Immunity

The innate immune system has evolved over millennia to recognise and destroy invading pathogens (Carrington and Alter 2012). Innate immunity provides an immediate response towards foreign antigens. Several factors can affect the efficacy of innate immune response including age, health, genetics and lifestyle. The main function of innate immunity is to detect and eradicate cells expressing non-self-antigen and is the first active line of defence against infection. The innate system is largely dependent on cells of the myeloid lineage. Myeloid-derived cells develop in the bone marrow or specialised tissue-resident cells and include macrophages, dendritic cells (DCs), neutrophils, basophils, eosinophils and natural killer (NK) cells of the lymphoid lineage. These are all specialised cells with individual functions that work together towards the destruction and/or clearance of foreign pathogens and damaged cells (Murphy et al. 2008).

Macrophages are distributed throughout the body and are specialised within tissues, i.e. flattened Küpffer cells of the liver and microglial cells of the central nervous system (CNS) (Beutler 2004). In addition to the clearance of dead cells and debris in tissue homeostasis, macrophages and DCs (together with neutrophils) have numerous roles in innate immunity, activation of adaptive immunity, inflammation, response to damage and tissue repair.

The main role of macrophages is the phagocytosis and destruction of non-self-antigen, dead cells and debris. To elicit effective clearance of pathogens, Macrophages must first recognise them via surface receptors. The type of phagocytosis is dependent upon the target and its location although generally the binding of target antigen to its receptor leads to adherence of the antigen to the macrophage plasma membrane; this stimulates contraction of actin and myosin filaments leading to extension of pseudopods around the non-self-matter. As further receptors engage, the foreign antigen is encapsulated in a vacuole known as a phagosome. Cytoplasmic lysosomes fuse with the phagosome and release their contents, which include reactive oxygen species and nitric oxides, leading to the destruction of the foreign antigen. Degradation of the target reveals new ligands which are processed and presented on the cell surface via major histocompatability complex (MHC) (Underhill and Goodridge 2012).

Without even realising it, our bodies are in a constant flux, our cells are communicating with one another to elicit strategic and tightly controlled responses in order to protect us from a plethora of microscopic particles each day. Our immune system is made up of specialised cells, all interacting with one another directly or indirectly to orchestrate a response to invading pathogens during infection. In the field of host–pathogen interactions, we combine techniques and knowledge from both microbiology and immunology to uncover mechanisms utilised by pathogens to circumvent destruction by immune cells, and ultimately how to prevent that therapeutically. In order to do this we must utilise several techniques to assess all aspects of this interaction.

Interestingly some commensal or "good bacteria" found in our bodies, or in the environment, can become problematic or pathogenic whenever they enter areas of our bodies which are not adapted to their presence. For example, when certain bacteria which are harmless when in the gut, get into the lungs, can lead to pneumonia or into the blood leading to septicaemia. One such example of an opportunistic pathogen is *Klebsiella pneumoniae*.

2.1.3 *Klebsiella Pneumoniae and Antimicrobial Resistance: The Problem*

K. pneumoniae is represented by the "K" in ESKAPE pathogens, the six most significant causes of drug-resistant hospital infections and is recognised by the Centre for Disease Control and Prevention, World Health Organisation, and the European Union as a significant threat to global health due to the increasing rates of antimicrobial resistance (Rice 2008; WHO 2014).

A report published in 2022 has shown that, globally, greater than 600,000 deaths were associated with, and approximately 200,000 deaths were attributable to *K. pneumoniae* in 2019 (Murray et al. 2022). *K. pneumoniae* is intrinsically resistant to ampicillin, but extended spectrum beta-lactamase genes, resistance genes against carbapenemases and most recently colistin have now also been reported, leaving ever-reducing therapeutic options (Petrosillo et al. 2019; Aris et al. 2020).

Globally, the third highest mortality rates due to multi-drug resistant infections are either associated with or attributable to *K. pneumoniae* (Murray et al. 2022). Between 2014 and 2017 the total number of bacteraemia cases caused by Klebsiella species in England increased by 12% and Northern Ireland had the highest rates (Public Health England 2020). Trends for 2011–2015 show increasing resistance to third-generation cephalosporins, fluoroquinolones, aminoglycosides, and extended spectrum beta-lactams in England, while at the minute resistance to carbapenems remains relatively uncommon (Public Health England 2020). *K. pneumoniae* has been described as a "canary in the coalmine" as several antibiotic resistance genes have been first identified in Klebsiella species (Holt et al. 2015; Wyres et al. 2020). As a promiscuous donor and recipient of plasmids containing antimicrobial resistance (AMR) genes, *K. pneumoniae*, and other Gram-negative bacterial species are accumulating AMR genes, further

reducing the resources there are to treat these infections (Holt et al. 2015; Wyres et al. 2020).

With the seemingly exponential rise in AMR bacterial species worldwide, it has never been more important to understand the host–pathogen interactions of bacteria versus the host. Indeed the need for the development of effective immunotherapeutics which reduce or eradicate dependency on antibiotics is incredibly important. Without this, we are facing a post-antibiotic era. Using both gold standard and cutting-edge techniques we can uncover the pathogenesis of disease and develop novel therapeutics. Visualisation of interactions is an integral aspect of research and spans from simple staining to mass spectrometry, flow cytometry, and CYTOF technologies.

2.1.4 *In Situ* Visualisation of Host–Pathogen Communications

Using fluorescent microscopy, immunohistochemistry, mass spectrometry and fluorescent in situ hybridisation techniques we can ascertain an abundance of information regarding bacterial infection and host responses. Herein we will describe the applications of each method.

2.1.4.1 Microscopy

Lenses have been used to start fires and correct vision since around the year 1300. However, it was not until 300 years later that the Dutch and Italian spectacle makers combined lenses to visualise far-away objects, a discovery that led to the first microscope. The visualisation of cells as we now know then was not until Antoni van Leeuwenhoek, a Dutch fabric merchant utilised rudimentary microscopes to identify motile or "animate" particles (now knowns as cells) from "inanimate" ones, namely sperm, bacteria, and protozoa (Shapiro 2003). The term "cells" was not used until the mid-1800s, when the development of condensers and the utilisation of multiple lenses improved resolution and allowed

identification of fine cellular structures could be differentiated from artefacts (Shapiro 2018). By the late 1800s Louis Pasteur, Robert Koch and others developed the cell theory, combining their work visualising the metabolic diversity and pathological potential of microorganisms. Indeed, Rudolf Virchow embodied the efforts of many pathologists to understand disease at a molecular level with his quote "*Omnis cellula e cellula*" (Schultz 2008).

2.1.4.2 Stains and Dyes

Visualisation of the intricate cellular structures, morphology and cell-to-cell interactions of tissues and cells was impossible until the development of staining techniques. Indeed, it was not until around the 1860s that it was determined that different coloured organic dyes had chemical affinities that could bind to a variety of cellular components with varying degrees of intensity. This work was led by Paul Ehrlich during his medical education (Kahr et al. 1998). He discovered that the use of synthetic dyes could stain specimens and allow visualisation of different cellular components and thus allowed identification of different cell subsets within a mixed sample. In 1882, Ehrlich joined forces with Robert Koch to develop a stain to detect *Mycobacterium tuberculosis* (*Mtb*), a process which was further developed by others to result in the e Ziehl–Neelsen (ZN) stain, which remains a gold standard technique to detect *Mtb* (Shapiro 2018).

Most cells and microorganisms lack colour and contrast and are impossible to observe or properly characterise morphology under the microscope without the use of staining. In clinical settings, a specimen can be prepared as a wet mount (drop of liquid on a slide or smear of a tissue in a drop of liquid such as water) or fixated (attached cells to a slide). Fixation can involve heat or use of chemical fixatives (methanol, formaldehyde, ethanol and glutaraldehyde being the most common), killing the microorganisms in the specimen while preserving their integrity. After fixing, cells are usually stained to apply colour and facilitate visualisation (Howat and Wilson 2014).

Staining can be done using simple stains that colour all the specimens regardless of only one type of organism being present. If the coloured ion (chromophore) is positively charged it is a basic dye and binds negatively charged components such as cell walls (positive stain). Examples include crystal violet, malachite green, methylene blue and safranin. If the chromophore is negative, the stain is acidic and tends to be repelled by negatively charged cell walls of microbes (negative stain). Examples include eosin and rose Bengal (Franco-Duarte et al. 2019).

Differential staining on the other hand involves the use of multiple stains giving different colours based on the interaction with the dye and the microorganism's physio-chemical properties. The most common example of this type of stain is Gram staining. In Gram staining, first crystal violet is applied followed by iodine to fix the dye and ethanol wash (at this point Gram-negative bacteria lose the colour while Gram-positive remain blue or purple). As a counterstain safranin is used which stains Gram-negative bacteria red. Another example is the acid-fast technique that allows to distinguish acid-fast bacteria such as *Mycobacterium*. Cells are stained with carbolfuchsin (red) using a lipid solvent and washed with a dilute acid-alcohol solution which will be washed away from non-acid-fast bacteria that take up methylene blue afterward. Other stains allow identification of bacterial structures such as flagella (using metals) or spores (using malachite green) (Chauhan and Jindal 2020). Examples are depicted in Table 2.1.

2.1.5 Biochemical Tests

Different bacteria have different biochemical requirements, and these have been used traditionally in the clinic for the classification of bacteria (sometimes up to species level). They rely on

Table 2.1 Examples of commonly used stains to determine physio-chemical characteristics of microorganisms

	Stain type	Dyes	Purpose
Simple stains	Basic	Methylene blue, crystal violet, malachite green, safranin.	Stain negatively charged structures
	Acidic	Eosin, rose Bengal, congo red.	Stain positively charged structures.
	Negative	India ink, nigrosine.	Stains background, not sample.
Differential stains	Gram	Uses crystal violet, Gram's iodine, ethanol and safranin.	Distinguishes cells by their cell wall (Gram-positive are purple, Gram-negative are pink).
	Acid-fast	Basic fuchsin, acid-alcohol and methylene blue.	Distinguishes acid-fast bacteria such as Mycobacterium (red) from non-acid fast cells (blue).
	Endospore	Heat with malachite green and counterstain with safranin.	Endospores appear green while other structures are red.
	Capsule	Negative staining using India ink that stains the background and capsule stays clear if a counterstaining is used to stain the cell	Capsules appear clear or halos while background is dark.

their carbon or metabolic usage capabilities and can be done in test tubes or using commercially available kits that allow to screen for a panel of biochemical reactions and their comparison to a database (Biolog using multiwell plates with the main carbon and nitrogen metabolites for growth, API-20A system using dry powder substrates or VITEK automated broth analysis for instance).

Common biochemical tests include:

- Catalase test (detects catalase, an enzyme that catalyses the release of oxygen from hydrogen peroxide present in most aerobic or facultative anaerobic bacteria such as *Staphylococcus*)
- Coagulase test (used to differentiate *Staphylococcus aureus* from coagulase-negative *Staphylococci* by inoculation with plasma)
- Oxidase test (detects the presence of cytochrome oxidase in *Pseudomonas* and *Vibrio*, which is absent in *Escherichia coli*, *Klebsiella* or *Salmonella*)
- Indole test (detects the ability to degrade tryptophan and is used to distinguish *Enterobacteriaceae* such as *E. coli* that is positive from *Klebsiella* that is negative)
- Citrate test (ability to use citrate as the only carbon source, distinguishes citrate-positive *Klebsiella* from *E. coli*)
- Urease test (detects the ability to degrade urea and produce ammonia and can distinguish urease-positive *Proteus* from urease-negative *E. coli* for instance) (Fig. 2.1)

Other tests based on biochemical properties could be the identification of bacteria based on their lipid composition using FAME (fatty acid methyl ester) or PFLA (phospholipid-derived fatty acids) analysis or the identification of bacteria based on their unique mass spectrum using MALDI-TOF) (Chauhan and Jindal 2020).

2.2 Selective and Differential Media

Another method commonly used to identify bacterial species is the use of selective media. This is when the growth medium is either supplemented with growth factors which are beneficial to the health of the bacteria of interest or includes growth inhibitors which will remove extraneous species. This method allows the identification of closely related microorganisms.

Media may be supplemented with antibiotics which allows only microorganisms resistant to that antibiotic to grow. Examples of differential media include those that have indicators or nutrients that allow a certain biochemical characteristic of a microbe to become apparent (in citrate agar *K. pneumoniae* appears as yellow colonies because they metabolise citrate while *E. coli* appears as blue colonies). Table 2.2 depicts examples of common media.
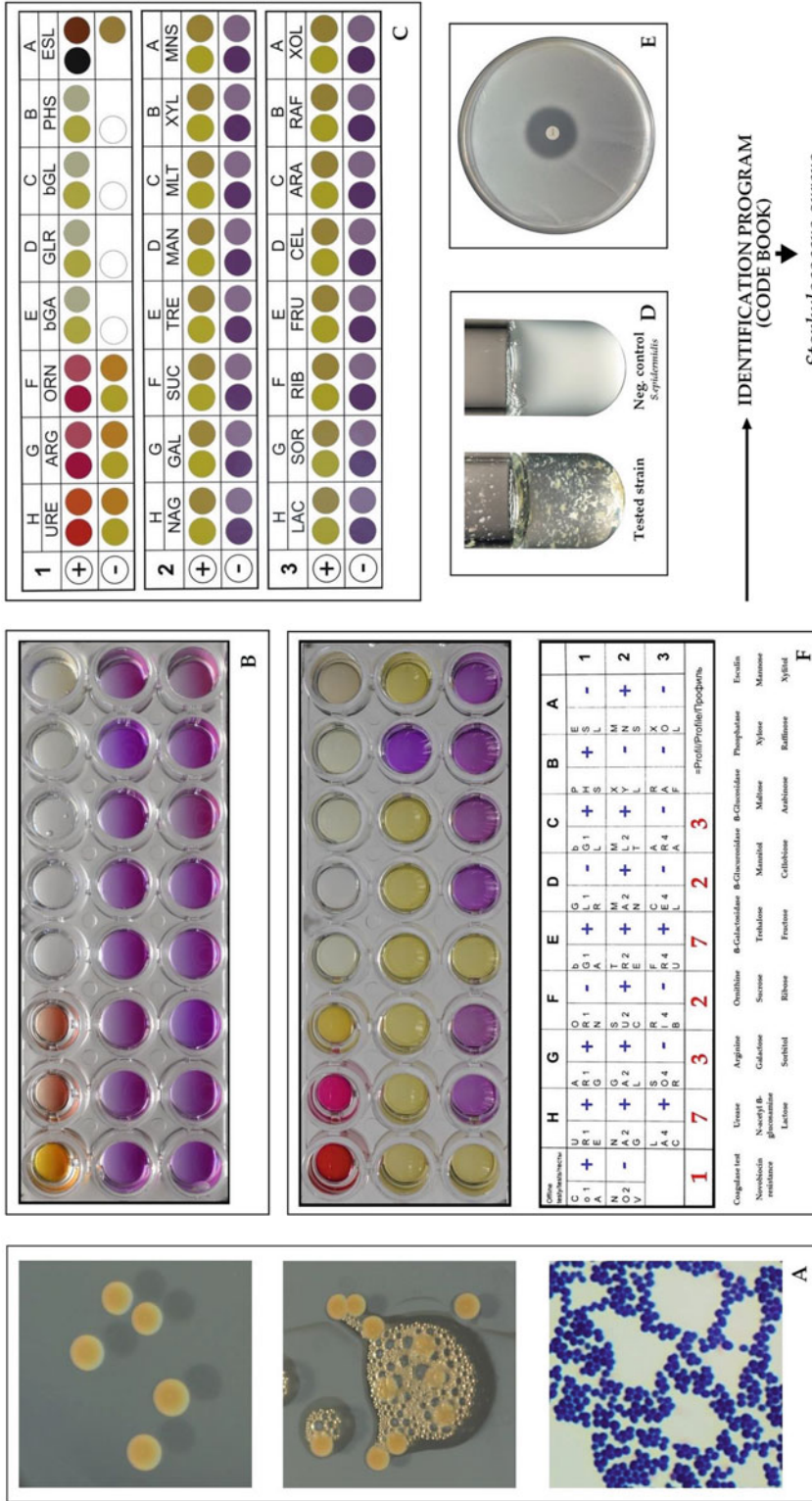
Fig. 2.1 Identification of *Staphylococcus aureus* based on phenotypic and biochemical tests. (**a**) Colonies showing pigmented smooth colonies, catalase-positive and Gram-positive cocci. (**b**) Biochemical test strips. (**c**) Identification of the biochemical test. (**d**) Coagulase test. (**e**) Test of resistance to the antibiotic novobiocin. This file is licensed under the Creative Commons Attribution-Share Alike 4.0 International license. https://creativecommons.org/licenses/by-sa/4.0/legalcode

Table 2.2 Examples of selective and differential growth media commonly used to identify microorganisms

Type	Media name	Types of organisms distinguished
Selective	YM	Yeast and mold
	MacConkey Agar	Gram-negative bacteria
	Mannitol Salt Agar	Gram-positive bacteria
Differential	Blood agar	Becomes transparent in hemolytic strains such as *Streptococcus pyogenes*
	MacConkey	Lactose fermentation
	X-gal plates	Lac operon mutants

2.3 Molecular Methods

Not all microorganisms are culturable in laboratory conditions and standard culturing and biochemical tests are time-consuming. Molecular techniques are more advantageous since they are rapid, more sensitive and more specific, allowing as well to identify strains that are difficult to culture. They include 16S sequencing, RT-PCR, random amplified polymorphism deoxyribonucleic acid (RAPD), restriction fragment length polymorphism (RFLP), whole-genome sequencing (WGS) sequencing and MALDI-TOF (Franco-Duarte et al. 2019).

16S rRNA PCR is one of the most commonly used molecular methods. It relies on the fact that this rRNA is highly conserved amongst bacteria but has variability regions that can be used to identify specific species. It involves the PCR amplification of the 16S rRNA gene, sequencing and comparison to a database. It can be applied to a variety of samples but involves pre-processing as some samples can have compounds that inhibit the PCR reaction. RAPD-PCR on the other hand involves the amplification of random sequences in template bacterial DNA using short primer sequences, resulting in a profile for identification that can be compared to a database. It has the advantage of allowing the identification of bacteria that have not been sequenced and requires no previous DNA isolation. RFLP uses restriction enzymes that can cut PCR products into different fragments generating a unique pattern. WGS has become more affordable and can be useful both in bacterial genotyping but also in antimicrobial resistance allowing to investigate clinical outbreaks. In MALDI-TOF MS, the proteins of a bacterial species are analysed by creating a mass:charge ratio pattern that can be compared to a library of strains (Adzitey et al. 2013).

2.4 Haematoxylin and Eosin

Ehrlich experimented with acidic (able to stain cell cytoplasm) and basic (nucleic) dyes. One such dye was developed from logwood (*Hematoxylon campechianum*) extract, discovered by Spanish explorers in 1502 (Kahr et al. 1998), leading to the development of Haematoxylin and Eosin (H&E) staining technique. H&E staining, arguably first utilised nearly 200 years ago in 1830 (von Waldeyer 1863), though nearly 200 years old, is still considered the gold standard staining technique used by pathologists and researchers globally today. Indeed, millions of microscopy slides are prepared daily to be viewed by pathologists for clinical diagnosis (Titford 2005). When bacteria are present in large numbers, in an abscess for example, they appear as blue-grey granular mass using H&E stain. Often in research, when identifying differences in pathogenicity of bacterial strains, it is more informative to assess host responses using H&E staining.

To better understand how *K. pneumoniae* interacts with immune response, Dumiganb et al. developed a novel whole lung *ex vivo* infection model using porcine lungs. Histological analysis of porcine tissues utilised in a whole lung *ex vivo* lung perfusion model of infection (Dumigan et al. 2019) was carried out based on parameters of acute respiratory distress syndrome (ARDS) in animal models as defined by the American Thoracic Society. Pathogenic hallmarks of lung injury include the thickening of alveolar septa and infiltration of proteinaceous
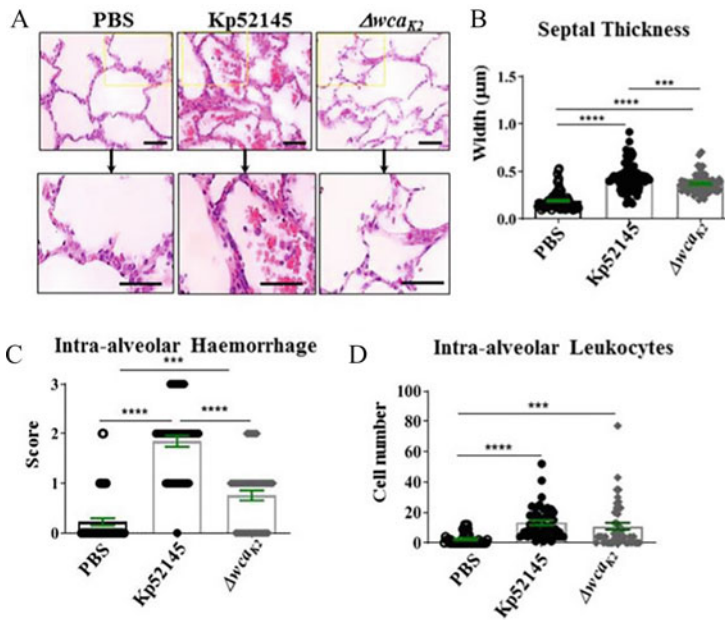
Fig. 2.2 Porcine EVLP model recapitulates clinical hallmarks of *K. pneumoniae*-induced pneumonia. (**a**) Haematoxylin and eosin staining of porcine lung samples (magnification, ×400) from lungs mock-infected (PBS) or infected with Kp52145 and strain 52145-Δ*wca*$_{K2}$. (**b**) Alveolar septal thickness was measured using ImageJ software. Each dot represents an average of three alveolar thicknesses per image, corresponding to three sections per lung across three experimental replicates from lungs mock-infected (PBS) or infected with Kp52145 and strain 52145-Δ*wca*$_{K2}$. (**c**) Intra-alveolar haemorrhage was scored per image whereby 0, 1, 2, and 3 represent none, mild, moderate, and severe levels of red blood corpuscles within the alveolar space from lungs mock-infected (PBS) or infected with Kp52145 and strain 52145-Δ*wca*$_{K2}$. (**d**) Number of nucleated cells evident in the alveolar space per image from lungs mock-infected (PBS) or infected with Kp52145 and strain 52145-Δ*wca*$_{K2}$. Statistical analysis was carried out using one-way ANOVA with Bonferroni correction. Error bars indicate SEM. (Dumigan et al. 2019). Image shared with permission of corresponding author Prof Jose Bengoechea

debris, red blood cells (haemorrhage), and immune cells, including neutrophils, into the alveolar space (neutrophilic alveolitis) (Matute-Bello et al. 2011). Analysis of lung sections stained with H&E revealed signs of injury in the lungs infected with the opportunistic pathogen *Klebsiella pneumoniae*, although injury was more severe in those lungs infected with the non-attenuated clinical strain Kp52145 (Fig. 2.2a). This was further confirmed by analysis of alveolar septal thickness (Fig. 2.2b). Infection with an attenuated mutant strain lacking polysaccharide capsule (a major virulence factor of *Klebsiella pneumoniae*) induced significantly enhanced alveolar septal thickening compared to that of PBS controls; however, this damage was significantly reduced compared to that of Kp52145-infected lungs (Fig. 2.2b).

Using scoring, we can glean further quantitative information from histology. The presence of intra-alveolar haemorrhage was assigned a score of 0, 1, 2, or 3 based on a semiquantitative assessment of none, mild, moderate, or severe. Scoring confirmed significantly enhanced haemorrhage in lungs infected with Kp52145 compared to that in the PBS-mock-infected lungs and the lungs infected with the cps mutant (Fig. 2.2c). Haemorrhage was accompanied by the presence of inflammatory immune cells within the alveolar space. The number of nucleated cells in the alveolar space was quantified, and it was significantly higher in the lungs infected with Kp52145 than in

those infected with the cps mutant or PBS-mock infected (Fig. 2.2d).

In terms of methodology in this model, tissue sections (×1 cm ^{3}) were collected from the cranial, middle, and caudal lobes of each lung fixed in 10 ml 10% formalin. After a minimum of 48 h at room temperature, samples were processed for paraffin embedding, sectioning, and haematoxylin and eosin staining. Samples were imaged using a DM5500 Leica vertical microscope at a magnification of ×200. Alveolar septal oedema was quantified by measuring the alveolar septal thickness with ImageJ software, whereby three measurements of the thickest septa were acquired per image and averaged, and 30 images were acquired, whereby 10 images were acquired per section and 3 sections per lung. Alveolar septa adjacent to a blood vessel or airway were excluded due to normal thickening resulting from collagen deposition. Intra-alveolar haemorrhage and the presence of intra-alveolar mononuclear cells and proteinaceous debris were also recorded. Histological scores were assigned based on parameters described previously (Matute-Bello et al. 2011). Haemorrhage was scored as follows: 0, none; 1, mild; 2, moderate; and 3, severe. Proteinaceous debris scored as follows: 0, none; 1, protein present; and 2, abundant presence of protein in alveolar spaces. The number of nucleated cells within the alveolar space was counted and presented as intra-alveolar leukocytes. Five images were scored per section, with three sections per lung at a magnification of ×400 (Dumigan et al. 2019).

The use of H&E staining in this model allowed us to determine that each of the major hallmarks of human disease was reproducible in our porcine model of disease. In addition, we were able to determine that the model was sensitive enough to test alternative bacterial strains and therefore draw conclusions for further research (Dumigan et al. 2019).

2.5 Fluorescence Microscopy

Microscopy is an important tool in following host–pathogen interactions. It allows the visualisation of the complex interactions between host and pathogen and ascertains how the subcellular localisation could be important in shaping those interactions. It has been evolving since the seventeenth century and now besides allowing us to observe fixed or frozen tissues it allows even to observe at the molecular level.

Fluorescence microscopy takes advantage of the fact that many compounds or proteins have fluorescence properties allowing for visualisation by tagging single molecules with these fluorophores. Another option is immunolabeling whereby a protein is tagged with an antibody molecule and a cognate fluorescent antigen. The advent of confocal microscopy which allows high-resolution and contrast images has improved visualisation. Furthermore, super-resolution approaches such as stimulated emission depletion microscopy (STED) or super-resolution structured illumination microscopy (SR-SIM) have allowed to observe immune responses at the molecular level (Wen et al. 2020).

2.6 Fluorescence In Situ Hybridisation (FISH)

Starting with the first in situ hybridisation (ISH) experiments in 1969 and the first uses of non-radioisotopic probes in the mid-1970 s to the current implementation of microfluidics (Huber et al. 2018), FISH has become a common technique used both on research and clinical diagnostics.

The basic principle of this method is the ISH of a known-sequence probe with a specific sequence inside the cells. Both probe and target can be either RNA or DNA. Multiple uses of FISH technique have been described (Volpi and Bridger 2008), but the processing steps are the same for all of them, and independently that the target is a cytological, histological or a whole-mount preparation (Young et al. 2020).

The first step for a FISH experiment is the design of the probes to use. Regardless of any other aspect, they need to be complementary to the target sequence we want to detect. Their size can vary, as well as the fluorescent molecule that

they have attached and that will allow their detection. Larger probes, between 500 and 1500 bases, are useful when high sensitivity is required (also being less expensive), while shorter ones offer high specificity. That is the case of the Stellaris™ probes, with just a few dozens of nucleotides length, which allow the detection of individual molecules of mRNA (Orjalo et al. 2011).

Once we have the appropriate probes, we can perform the ISH (usually after fixation and permeabilisation steps, to preserve the cellular/histological structure and facilitate the entry of the probes into the cells). For this, optimal conditions have to be assured, paying attention to several factors such as temperature, time, pH, salt concentration, etc. One critical factor is the addition of formamide. The melting temperature (T_m) of DNA is defined as the temperature at which half of the DNA strands are present as single strands. DNA denaturalisation is required prior to the hybridisation with the probes, and as this is usually obtained at high temperatures, there is the risk of damaging the cell/tissue structure. The use of formamide reduces the T_m (McConaughy et al. 1969), linearly by 2.4–2.9 °C per mole of formamide (Blake and Delcourt 1996). Once the hybridisation has been done, several washes in order to reduce the background signal both from the unbound probes and autofluorescence or light scatter caused by the tissue (Richardson and Lichtman 2015). With the samples prepared and mounted, all that remains is visualising the samples in a fluorescence microscopy and, if required, performing quantitative analysis.

2.7 Flow Cytometry

It was in the 1880s when the term "cytometer" appeared, used to describe a device which could count the number of cells in a particular volume. At this time leukaemia and anaemia could be identified, and although the cause was unclear, it was understood that changes in cell morphology and number over time could indicate the clinical outcome of the patient. Though a cytometer describes the device, "cytometry" is the process.

As the cells analysed at this time often came from human blood "haem", an easily obtained sample, led to the birth of "haemocytometer". Microscopy remained the main instrument to assess cell number and morphology until the 1950s and "flow cytometry" would not come around until the 1970s (Harris 1999; Shapiro 2018). In 1953 the first flow cytometer was disclosed, using the Coulter Principle to assess cell numbers in a suspension. The first cell sorter using a similar principle with addition of droplet-based methods for subsequent cell purification arrived in 1965 (Fulwyler 1965). Flow cytometry, as we know it today, could not have come about without the use and development of synthetic dyes to stain samples. This was an essential step as light scattering and absorption by cells is insufficient to allow visual discrimination of internal structures.

In 1968 absorption-based methods for flow cytometry using fluorescent antibodies emerged, a pivotal development meaning specific cell types could be identified in a given population. Cell sorting and flow cytometry rapidly became popular, especially with the development of monoclonal antibodies (Köhler and Milstein 1975).

Over the last 70 years flow cytometry and cell sorting platforms have benefited immensely from developments in hardware and reagents. Developments in device design have reduced device size, costs, and improved flexibility and ergonomics. Flow cytometry allows multi-parametric cell analysis; it can be used to determine the quantity of a given cell type, cell sorting and analysis of biomarker expression. Presently, a standard flow cytometer combines fluidics, optics and software to detect particles using fluorescence and morphological characteristics – namely size and granularity. It is a statistically powerful technique used to characterise heterogeneous populations from a single-cell suspension. This single-cell suspension can be whole blood, or adherent cell lines or solid tissue which has been dissociated to a single-cell suspension. For solid tissues, this can be done by homogenising using a handheld homogeniser (much like a small blender), or with mechanical force aided by digestive enzymes. Tissue suspensions often

require filtering using cell strainers or nylon mesh.

The fluidics system allows the single-cell suspension to be aligned in an orderly stream via hydrodynamic or acoustic focusing. This means that when a single-cell suspension is passed through the flow cell, the cells are focused into a central core stream that is surrounded by an outer sheath of higher pressured fluid. As the cell suspension is passed through the flow cell it intercepts laser beams, they scatter the light and emit fluorescence, which is picked up by detectors and presented on screen as a dot. The position of the dot on the flow plot will indicate the marker expression on a given cell.

We know from previous research mentioned earlier, that immune cells are specialised, meaning they each express markers of their lineage. Antibodies are raised against these antigens and labelled with a fluorescent tag. Depending on the number of lasers a cytometer possesses, we can look at several parameters at once to delineate a particular cell type and assess a given line of investigation. Cell suspensions are generally prepared by first staining markers on their cell surface (for instance Ly6C is a marker for cells of the myeloid lineage, including macrophages and DCs, but not neutrophils). After cell surface markers have been stained with antibodies tagged with fluorophores, cells are then fixed and permeabilised in order to stain intracellular components such interferon-gamma (IFNg) a proinflammatory cytokine. Before washing and analysis using a flow cytometer (Fig. 2.3).

We used this technique to assess the number and activation status of NK cells between wild type (WT) and genetically modified mice lacking receptors for Type I IFNs (IFNAR$^{-/-}$), as shown in Fig. 2.3. Type I IFN signalling induces NK cell accumulation and activation in lungs during *K. pneumoniae* infection (Ivin et al. 2017).

Flow cytometry is an incredibly useful tool employed by research and clinical labs globally and is only set to become a more powerful tool in the future.

2.8   Imaging Flow Cytometry (IFC)

Imaging flow cytometry (IFC) is a relatively new technology combining the conventional benefits of non-imaging flow cytometry to identify, i.e. analyse and quantify single cells in a heterogenous population, with additional imaging IFC, we can determine the size, shape, and structure of a cell. This has inherent benefits as morphological evidence can help determine the stage and progression of disease, improving biomedical research and clinical decisions to design personalised patient treatment strategies (Lei et al. 2018). IFC has rapidly become an established cytometric analysis tool in a wide range of biological research including, but not limited to, microbiology, immunology, and stem cell biology (Lei et al. 2018; Goda et al. 2019). This technique provides spatially registered, morphological, and quantitative data for each, and every event captured, meaning each cell can be characterised in detail providing an image of each cell as well as cytometric evaluation within pure or heterogenous populations. IFC is effective for the detection of cell death, DNA damage/repair, quantification of specific proteins, and peptides. It can also be combined with fluorescent in situ hybridisation. In addition, computational biology can also be utilised in combination with IFC (Eulenberg et al. 2017). This detailed analysis provided by IFC allows us to better understand cell-to-cell interactions in a physiologically relevant setting. Indeed, this technology has a plethora of potential clinical uses including stage and progression of blood-born cancers and the identification of infectious diseases (Goda et al. 2019). Significant expansion of IFC capabilities is expected in the next decade or so, especially with the emergence of microfluidics and its integration into IFC systems. Microfluidics rather than traditional capillary-based flow cytometry provides greater versatility in terms of multiplexing and automation, thus providing greater scope for the preparation, analysis and manipulation of cells (Goda et al. 2019).
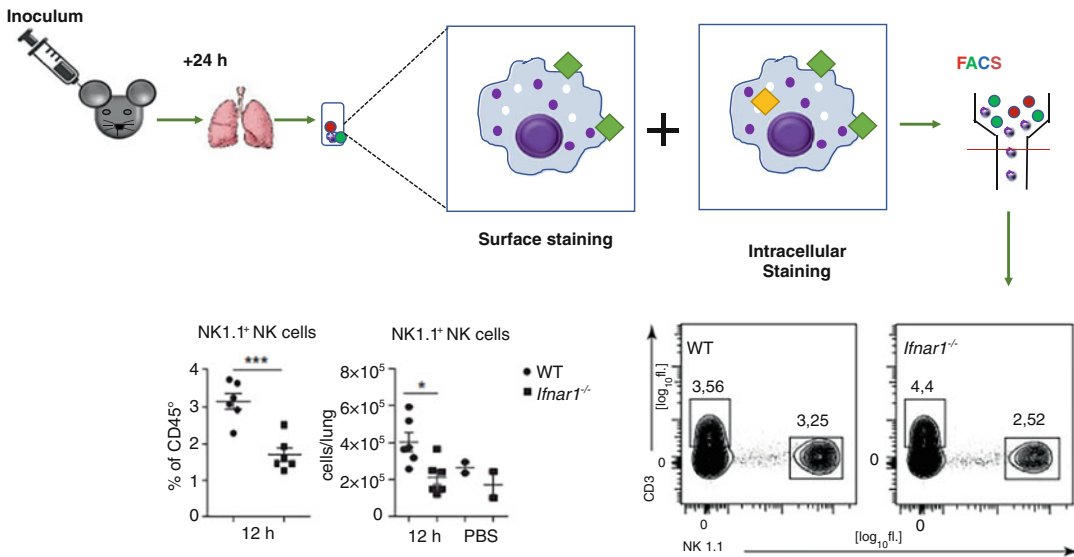
Fig. 2.3 Schematic representation of flow cytometry analysis of murine tissues. Mice were infected with *K. pneumoniae* or PBS controls, at end of infection, lungs are harvested and homogenised before red cells are removed and cell suspension stained with surface expressed markers (blue squares), cells were then fixed and permeabilised before intracellular targets are stained (orange square) followed by analysis by flow cytometry. Shown here are flow plots depicting number of NK cells within WT and IFNAR−/− animals from Ivin et al. (2017). Image included with permission from corresponding author Prof Jose Bengoechea

2.9   ELISAs

Infections can lead to an imbalance of the host immune response and therefore it is important to use immunoassays to determine to what extent that imbalance is affecting the clinical outcomes.

Enzyme-linked immunosorbent assay (ELISA) is a sensitive immunoassay used to detect antibodies, antigens, proteins, glycoproteins and hormones. It is a microwell plate-based method that relies on the binding of an antigen to a target antibody generating a detectable signal, either chemiluminescent, fluorescent or colorimetric.

In *Klebsiella pneumoniae* infection research our laboratory has used this method to detect a natural block of the immune system upon infection. This pathogen dampens the activation of inflammatory responses by inhibiting the activation of the NF-κB pathway and reducing levels of IL-8 released by the immune system (Tomás et al. 2015).

2.10   Western Blotting

Western blotting or immunoblotting was introduced by Towbin in 1979 and is used to separate and identify proteins (Kurien and Scofield 2015). The technique involves gel electrophoresis that separates a mixture of proteins based on molecular weight which is then transferred to a membrane incubated with antibodies specific to the protein of interest. To prepare samples for running on a gel, cells and tissues are lysed to release the proteins of interest and solubilised so they can be migrated individually on the gel. Antibodies recognise a small portion of the protein of interest (the epitope) proteins need to be denatured (unfolded) to allow binding. An anionic detergent and heat are applied for denaturing the proteins. Blocking the membrane prevents the non-specific background binding of the antibodies. To visualise the protein of interest, a primary protein-specific antibody is applied followed by a secondary antibody for detection and visualisation. Immunoblotting is routinely

used in the lab to detect immune responses to bacterial infection by probing common proteins in signalling pathways affected by the pathogen (Wen et al. 2020).

2.11 Visualisation of Bacterial Factors

Bacteria range in size from 0.5 to 5 micrometres (μm). One such example is *Klebsiella pneumoniae*, a Gram-negative encapsulated bacteria approximately 3 μm in length. *K. pneumoniae* are phagocytosed and can survive within macrophages in specialised vacuoles called *Klebsiella*-containing vacuoles (KCV). The size obviously poses difficulty visualising bacteria, and when trying to unravel the complex host–pathogen interactions, even more so.

In this section, we will describe techniques utilised in microbiology research to analyse facets of bacterial function and growth.

2.12 Spectrophotometry

Spectrophotometry is the use of light to measure the turbidity of a solution. A calibration curve of known bacterial number will correspond to a given % Transmission of light, providing a measurement tool that greatly increases the speed at which bacterial number can be established. This is used extensively in microbiology laboratories to equilibrate bacterial numbers used in experiments to ensure valid results. Using *K. pneumoniae* as an example, at an optical density (OD) of 1, there are 5×10^8 bacterial cells/ml.

2.13 Bioscreen

This same principle can be used to determine bacterial growth over time. The generation or doubling time of a given bacterial species can vary widely, again using *K. pneumoniae* as an example, doubling time is approximately 20 min. Population growth consists of 4 phases: lag phase, exponential phase, stationary phase and decline phase. These phases can be determined by taking samples of bacterial cultures every 20 min and measuring the optical density. This process can be automated using a piece of equipment that can read OD at specific time intervals, the Bioscreen CTM Automated Microbial Growth Analyzer (MTX Lab Systems, Vienna, VA, USA) for example. This method can be used to differentiate the ability of bacteria to grow in different conditions. Figure 2.2 shows the growth kinetics of *K. pneumoniae* in chemically defined media supplemented with glucose, and a strain of *K. pneumoniae* that has a metabolic growth defect.

2.14 Plating

Another means of visualising population growth of bacteria is counting of colony-forming units (CFU) (Fig. 2.4a). Each CFU is assumed to have grown from a single bacteria cell. In order to be able to count the number, a sample is taken from a bacterial culture every 20 min and serially diluted. A given volume of the dilution is spotted onto an LB agar (nutrient-rich, solid growth medium) and spread evenly over the agar and the bacteria are allowed to grow.

Bacterial species can be "visualised" using selective agar. *K. pneumoniae* can metabolise citrate. Simmons citrate agar's sole nutrient source is citrate and can therefore act as a selective media (Fig. 2.4a). Citrate can be metabolised by many bacteria by myo-inositol is selective for *Klebsiella* species. Citrate- myo-inositol agar is used during gut colonisation infection experiments with *K. pneumoniae* so only this bacterium grows and the ability to colonise the gut can be determined (Fig. 2.4b).

2.15 String Test

Infections caused by *K. pneumoniae* can be very broadly divided into classical (cKp) and hypervirulent (hvKp) sources, where cKP has been more associated with hospital-acquired infections and hvKp with community-acquired infections
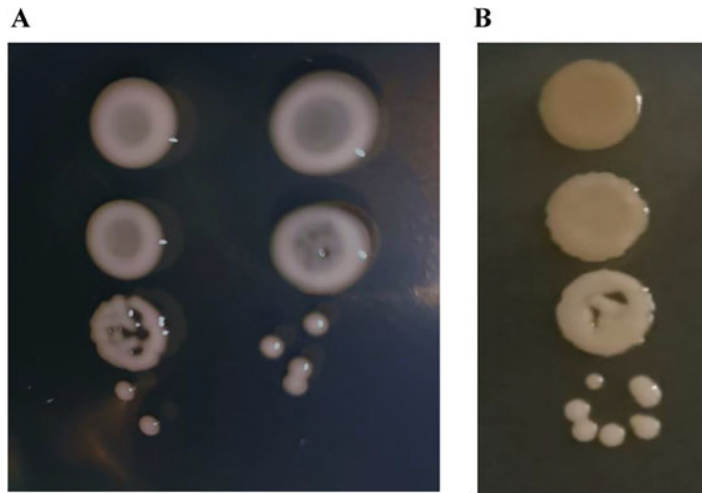
Fig. 2.4 *K. pneumoniae* can be quantified by counting colony-forming units (CFU). As there are too many when concentrated, serial dilutions are performed. (**a**) Image of 1/10 serial dilution of *K. pneumoniae* 5×10^8 initial suspension. At 10^{-6}, the CFU can be counted (4) in 10 uL and the total number of CFU/mL calculated. (**b**) The total CFU/mL can be calculated to determine the survival of *K. pneumoniae* within macrophage by quantifying the number of bacteria harvested from macrophages at specific timepoints. (**b**) Representative serial dilution from 10^{-1} to 10^{-4} of *K. pneumoniae* after 60 min contact with macrophages

(Wyres et al. 2020). Hypervirulent *K. pneumoniae* was initially described from an isolated strain in the mid-1980s in Taiwan (Catalán-Nájera et al. 2017). The most characterised virulence factors of *K. pneumoniae* are the capsule, lipopolysaccharide, O-antigen and siderophores as well as outer membrane proteins, porins and Type1 and 3 fimbriae (Lawlor et al. 2005; Paczosa and Mecsas 2016; Bruchmann et al. 2021). Lipopolysaccharide (LPS) capsule is one of the major constituents of the membrane of Gram-negative bacteria and is typically composed of an outer O-antigen, an oligosaccharide core and inner lipid A molecule (Mills et al. 2017; Bartholomew et al. 2019). One of the key virulence factors for *K. pneumoniae* infection is the characteristic capsule and, as previously described, this can result in a hypermucoviscous phenotype (Paczosa and Mecsas 2016). There are at least 77 recognised capsular types, designated as K1 or K2 for example, with at least 1345 distinct K-types that have been identified through genome sequencing (Wyres and Holt 2016). As a capsulated bacterium, *K. pneumoniae* appears mucoid when grown on nutrient agar but the hypermucoviscous designation is only given to those strains that can produce an elongated filament of ≥5 mm upon stretching with an inoculation loop from an agar plate- the string test (Fang et al. 2004).

The string test is essentially a very simple technique whereby we can quantify the hypermucoviscosity of a given bacterial culture. A loop was used to lift a portion of a single colony approximately 2 mm in diameter from a fresh LB agar plate. The formation of viscous strings >5 mm in length indicates a positive string test (Fang et al. 2004).

2.16 Mass Spectrometry

Since the invention of modern mass spectrometers in 1913 by electron discoverer and Nobel Laureate in Physics Joseph John Thomson (R. 1914), mass spectrometry has become a valuable tool for biological research. Mass spectrometry is an analytical technique used to identify chemical components by measuring mass-to-charge ratio of ions. The results of this

Fig. 2.5 Schematic diagram of a spectrometer
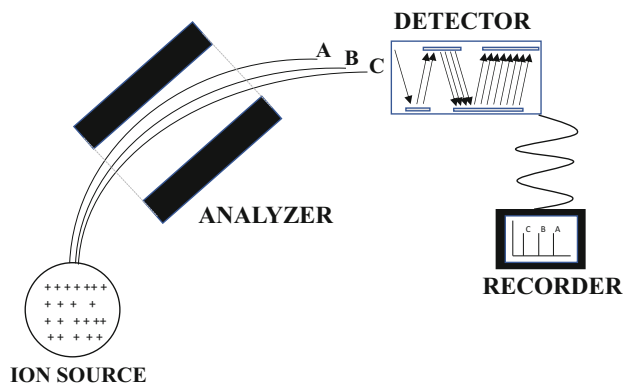
technique are presented as mass spectrums, a plot of intensity as a function of mass-to-charge ratio. These plots are used to determine the elemental or isotopic nature, the masses of particles or molecules within a given sample. Both pure and complex mixtures, gaseous, solid or liquids can be analysed in this procedure.

Mass spectrometers have four main components (Mellon 2003): an ion source, a mass analyser, a detector and a recorder device (Fig. 2.5). First, samples need to be ionised by the ion source, with different techniques being used and determining which kind of samples can be analysed. One of the most used for the study of biomolecules is matrix-assisted laser desorption/ionisation (MALDI), coined for the first time in 1985 (Karas et al. 1985). It consists of the use of a pulse laser to irradiate the sample, which is mixed with a suitable matrix material (DHB, sinapic acid, ferulic acid, etc.) and applied to a metal plate. The application of the laser triggers the ablation and desorption of the sample, and its ionisation by protonation or deprotonation, after which it is accelerated into the analyser.

Another commonly used way to produce ions is electrospray ionisation (ESI), where a high voltage is applied to the sample, which is solved in a mix of water, volatile organic compounds (like methanol or acetonitrile) and some reagent to increase conductivity (like acetic acid). This, coupled with the use of a heated inert gas (i.e. nitrogen) and the high temperature of the ESI source, cause the nebulisation of charged droplets that are ejected and accelerated into the mass analyser (Bruins 1998).

After ionisation, sample's ions are accelerated into the mass analyser. Again, several analysers can be used, but the most common ones for the study of molecules of biological interest are Time-of-flight (TOF) mass analysers. They are based on the fact that ions accelerated in an electric field of constant and known voltage and length (all englobed under a constant K, called calibrating factor), the time they take to reach the detector (t) is related to their mass-to-charge ratio (m/z) according to the following equation (El-Aneed et al. 2009):

$$\frac{m}{z} = Kt^2$$

This way, the time that each of the ionised atoms and molecules of the samples takes to reach the detector is recorded. The most common detector is an electron multiplier, which amplifies the signals received that is recorded and represented most commonly in the form of a mass spectrum (Fig. 2.6). This is usually compared to a library of known mass spectra, which allows the identification of the compound present in the sample.

2.17 Application in Microbiology

Mass spectrometry has become an important tool in both microbiology research and clinical diagnostics, being a fast and accurate method
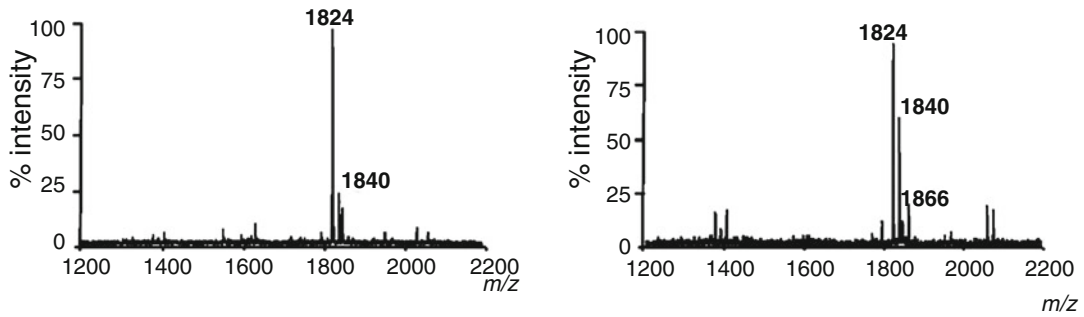
Fig. 2.6 Mass spectra obtained of lipid A extracted from *Klebsiella pneumoniae* strain Kp52145 grown in LB (left) and recovered from lungs of infected C57BL/6 mice (right). Figures obtained from Llobet et al. (2015)

that does not require specialised training and being less expensive than other routine methods (despite having an initial high cost in equipment) (Singhal et al. 2015).

MALDI and ESI mass spectrometry has been recently used for the rapid identification and classification of bacteria and other microorganisms (Sauer and Kliem 2010). Colonies from clinical isolates can be analysed by MALDI-TOF to obtain spectral fingerprints that are compared to those stored in databases provided by the mass spectrometer supplier (Croxatto et al. 2012). Also, direct identification from urine or blood samples can be performed, although this requires some previous processing to concentrate the microorganism, as well as eliminating other compounds present in these fluids that would suppose a too complex mix to be analysed by mass spectrometry.

It has also become a powerful proteomics tool to study host–pathogen interactions (Sukumaran et al. 2021). During an infection, mass spectrometry can be used to analyse the protein composition of different compartments, as cell proteome changes during *Salmonella* infection (Selkrig et al. 2020), different proteome expression in neutrophils from two mice strains infected with *Pseudomonas aeruginosa* (Kugadas et al. 2019), analysis of exosomes released from human macrophages after *Mycobacterium tuberculosis* infection (Diaz et al. 2016), or the characterisation of post-translational modification after viral infections (Kulej et al. 2015). Also, protein-protein interaction can be analysed by

the combination of affinity purification and mass spectrometry (AP-MS) (Morris et al. 2014); this has been recently used in the search of therapeutic target against SARS-CoV-2 infection (Gordon et al. 2020).

Not only proteins can be analysed in mass cytometry. MALDI-TOF can be used for the analysis of nucleic acids, which has been applied to the discovery of single-nucleotide polymorphisms (Stanssens et al. 2004) and epidemiological studies (Ecker et al. 2009).

Genetic analysis of environmental strains and human isolates has distinguished four phylogroups and determined that they should be designated as distinct species: *Klebsiella pneumoniae* (Kp1), *Klebsiella quasipneumoniae* subspecies *quasipneumoniae* (Kp2), *Klebsiella quasipneumoniae* subspecies *similipneumoniae* (Kp4) and *Klebsiella variicola* (Kp3) (Brisse and Verhoef 2001; Rosenblueth et al. 2004; Holt et al. 2015). Recent taxonomic updates and matrix-assisted laser desorption ionisation time of flight (MALDI-TOF) mass spectrometry (MS) has further identified *K. pneumoniae* phylogroups Kp5 and Kp6. Together these are recognised as the *K. pneumoniae* complex (KPC) (Rodrigues et al. 2018). Although all KPC species can cause human infections, *K. pneumoniae* is the strain most isolated from patients (Holt et al. 2015).

Finally, mass spectrometry has been also used to decipher the structure of bacterial lipopolysaccharides. In *Klebsiella pneumoniae*, it has been shown that it modifies lipid A structure in a

tissue-dependent manner (Fig. 2.6) (Llobet et al. 2015). It has been also described how two acyltransferases, LpxL1 and LpxL2, catalyse the addition of laurate and myristate, respectively and have an important role in *Klebsiella* virulence (Mills et al. 2017).

2.18 Closing Statement

In this chapter, we have given a brief overview of the importance of the study of microorganisms and of our own body's defence against infection via specialised cells of the immune system. It is important to remember that we have evolved to have a largely symbiotic relationship with microorganisms in that we have "good bactieria" in our guts which aid digestion. However, when infected with pathogenic bacteria or with normally commensal bacteria in a compartment of the body ill-adapted to the presence of specific bacteria, the example we have provided is that of the opportunistic pathogen *Klebsiella pneumoniea*, we begin to see morbidity and mortality. Therefore, the field of host–pathogen communication is the study of how bacteria and host interact in order to understand the pathogenicity of disease and develop novel effective treatments.

Visualisation of intricate cellular structure, morphology and cell-to-cell interactions is an essential aspect to the study of host–pathogen interactions. Continued development of visualisation techniques and advances in technology available to biomedical researchers and clinicians is integral for the continued progress of medicine. We have covered the development of microscopy and the use of standardised staining and dye protocols which have been around for over a century and are still used today. One such stain is H&E used by pathologists and researchers worldwide. The use of FISH to visualise gene expression *in situ*. The basis of flow cytometry as a highly useful tool in understanding immune cells and the development of cutting-edge imaging f1ow cytometry and mass spectrometry. The use of these technologies in conjunction with standard protein immunoblotting has helped researchers not only determine

cell activation and recruitment but also to delineate cell signalling processes involved. The use of plating techniques allows us to decipher bacterial loads *in vitro* and *in vitro*. Also the use of simple string tests and selective media to characterise bacterial strains are all used in combination. Indeed as researchers we depend on the versatility of techniques available in order to investigate biological questions; this is key as there is not one perfect technique but rather a combination must be used to fully elucidate mechanisms at play. Clinicians also routinely utilise plating, microscopy and flow cytometry to diagnose patients and develop effective treatment plans. Combining proteomics, cell surface expression and intracellular staining We know that *K. p* subverts inflammation and via the use of the techniques described herein, we can observe how *K.p* influences innate immune cells to evade the immune response and promote its own survival. This is very important work as with continued rise of AMR in several bacterial pathogens worldwide (WHO 2014), understanding of host–pathogen interactions is key to developing effective therapeutic interventions.

References

Adzitey F, Huda N, Ali GR (2013) Molecular techniques for detecting and typing of bacteria, advantages and application to foodborne pathogens isolated from ducks. 3 Biotech 3(2):97–107. https://doi.org/10.1007/s13205-012-0074-4

Aris P, Robatjazi S, Nikkhahi F, Amin Marashi SM (2020) Molecular mechanisms and prevalence of colistin resistance of Klebsiella pneumoniae in the Middle East region: A review over the last 5 years. J Glob Antimicrob Resist 22:625–630. https://doi.org/10.1016/j.jgar.2020.06.009

Bartholomew TL, Kidd TJ, Pessoa JS, Conde Álvarez R, Bengoechea JA (2019) 2-Hydroxylation of acinetobacter baumannii lipid a contributes to virulence. Infect Immun 87(4):e00066-19. https://doi.org/10.1128/IAI.00066-19

Beutler B (2004) Innate immunity: an overview. Mol Immunol 40(12):845–859

Blake RD, Delcourt SG (1996) Thermodynamic effects of formamide on DNA stability. Nucleic Acids Res 24(11):2095–2103. https://doi.org/10.1093/nar/24.11.2095

Brisse S, Verhoef J (2001) Phylogenetic diversity of Klebsiella pneumoniae and Klebsiella oxytoca clinical isolates revealed by randomly amplified polymorphic DNA, gyrA and parC genes sequencing and automated ribotyping. Int J Syst Evol Microbiol 51(3):915–924. https://doi.org/10.1099/00207713-51-3-915

Bruchmann S, Feltwell T, Parkhill J, Short FL (2021) Identifying virulence determinants of multidrug-resistant Klebsiella pneumoniae in Galleria mellonella. Pathog Dis 79(3):1–15. https://doi.org/10.1093/femspd/ftab009

Bruins AP (1998) Mechanistic aspects of electrospray ionization. J Chromatogr A 794:345–357. https://doi.org/10.1016/S0021-9673(97)01110-2

Carrington M, Alter G (2012) Innate immune control of HIV. Cold Spring Harb Perspect Med 2(7):a007070. https://doi.org/10.1101/cshperspect.a007070

Catalán-Nájera JC, Garza-Ramos U, Barrios-Camacho H (2017) Hypervirulence and hypermucoviscosity: two different but complementary Klebsiella spp. phenotypes? Virulence 8(7):1111–1123. https://doi.org/10.1080/21505594.2017.1317412

Chauhan A, Jindal T (2020) Microbiological methods for environment food and pharmaceutical analysis. In: Biochemical and molecular methods for bacterial identification. Springer International Publishing, Cham, pp 425–468

Cooper MD, Alder MN (2006) The evolution of adaptive immune systems. Cell 124(4):815–822. https://doi.org/10.1016/j.cell.2006.02.001

Croxatto A, Prod'hom G, Greub G (2012) Applications of MALDI-TOF mass spectrometry in clinical diagnostic microbiology. FEMS Microbiol Rev 36:380–407. https://doi.org/10.1111/j.1574-6976.2011.00298

Diaz G, Wolfe LM, Kruh-Garcia NA, Dobos KM (2016) Changes in the membrane-associated proteins of exosomes released from human macrophages after mycobacterium tuberculosis infection. Sci Rep 6: 37975. https://doi.org/10.1038/srep37975

Dumigan A, Fitzgerald M, Santos JSG, Hamid U, O'Kane CM, McAuley DF, Bengoechea JA (2019) A porcine Ex Vivo lung perfusion model to investigate bacterial pathogenesis. MBio 10(6):e02802-19. https://doi.org/10.1128/mBio.02802-19

Ecker DJ, Massire C, Blyn LB et al (2009) Molecular genotyping of microbes by multilocus PCR and mass spectrometry: a new tool for hospital infection control and public health surveillance. In: Methods in molecular biology (Clifton, N.J.). Humana, Totowa, NJ, pp 71–87

El-Aneed A, Cohen A, Banoub J (2009) Mass spectrometry, review of the basics: electrospray, MALDI, and commonly used mass analyzers. Appl Spectrosc Rev 44:210–230. https://doi.org/10.1080/05704920902717872

Eulenberg P, Köhler N, Blasi T, Filby A, Carpenter AE, Rees P, Theis FJ, Wolf FA (2017) Reconstructing cell cycle and disease progression using deep learning. Nat Commun 8:463

Fang C-T, Chuang Y-P, Shun C-T, Chang S-C, Wang J-T (2004) A novel virulence gene in Klebsiella pneumoniae strains causing primary liver abscess and septic metastatic complications. J Exp Med 199(5): 697–705. https://doi.org/10.1084/jem.20030857

Franco-Duarte R, Černáková L, Kadam S et al (2019) Advances in chemical and biological methods to identify microorganisms—from past to present. Microorganisms 7(5):130. https://doi.org/10.3390/microorganisms7050130

Fulwyler MJ (1965) Science 150:910–911

Getz GS (2005) Thematic review series: the immune system and atherogenesis. bridging the innate and adaptive immune systems. J Lipid Res 46(4):619–622. https://doi.org/10.1194/jlr.E500002-JLR200

Goda K, Filby A, Nitta N (2019 May) In flow cytometry, image is everything. Cytometry A 95(5):475–477. https://doi.org/10.1002/cyto.a.23778

Gordon DE, Jang GM, Bouhaddou M et al (2020) A SARS-CoV-2 protein interaction map reveals targets for drug repurposing. Nature 583:459–468. https://doi.org/10.1038/s41586-020-2286-9

Harris H (1999) The birth of the cell. Yale University Press, New Haven, CT

Holt KE, Wertheim H, Zadoks RN, Baker S et al (2015) Genomic analysis of diversity, population structure, virulence, and antimicrobial resistance in Klebsiella pneumoniae, an urgent threat to public health. Proc Natl Acad Sci U S A 112:E3574–E3581. https://doi.org/10.1073/pnas.1501049112

Howat WJ, Wilson BA (2014) Tissue fixation and the effect of molecular fixatives on downstream staining procedures. Methods 70(1):12–19. https://doi.org/10.1016/j.ymeth.2014.01.022

Huber D, Von Voithenberg LV, Kaigala GV (2018) Fluorescence in situ hybridization (FISH): history limitations and what to expect from micro-scale FISH? Micro Nano Eng 1:15–24. https://doi.org/10.1016/j.mne.2018.10.006

Ivin M, Dumigan A, de Vasconcelos FN, Ebner F, Borroni M, Kavirayani A, Przybyszewska KN, Ingram RJ, Lienenklaus S, Kalinke U, Stoiber D, Bengoechea JA, Kovarik P (2017) Natural killer cell-intrinsic type I IFN signaling controls Klebsiella pneumoniae growth during lung infection. PLoS Pathog 13(11):e1006696. https://doi.org/10.1371/journal.ppat.1006696

Janeway CA Jr, Travers P, Walport M (2001) Immunobiology, 5th edn. Garland Science, New York

Karas M, Bachmann D, Hillenkamp F (1985) Influence of the wavelength in high-irradiance ultraviolet laser desorption mass spectrometry of organic molecules. Anal Chem 57(14):2935–2939. https://doi.org/10.1021/ac00291a042

Kahr B, Lovell S, Subramony JA (1998) The progress of logwood extract. Chirality 10:66/77

Köhler G, Milstein C (1975) Continuous cultures of fused cells secreting antibody of predefined specificity. Nature 256(5517):495–497. https://doi.org/10.1038/256495a0

Kugadas A, Geddes-McAlister J, Guy E et al (2019) Frontline science: Employing enzymatic treatment options for management of ocular biofilm-based infections. J Leukoc Biol 105:1099–1110. https://doi.org/10.1002/JLB.4HI0918-364RR

Kulej K, Avgousti DC, Weitzman MD, Garcia BA (2015) Characterization of histone post-translational modifications during virus infection using mass spectrometry-based proteomics. Methods 90:8–20. https://doi.org/10.1016/j.ymeth.2015.06.008

Kurien BT, Scofield RH (2015) Western blotting: an introduction. In: Western blotting. Methods and protocols. Springer, New York, pp 17–30

Lawlor MS, Hsu J, Rick PD, Miller VL (2005) Identification of Klebsiella pneumoniae virulence determinants using an intranasal infection model. Mol Microbiol 58(4):1054–1073. https://doi.org/10.1111/j.1365-2958.2005.04918.x

Lee YK, Mazmanian SK (2010) Has the microbiota played a critical role in the evolution of the adaptive immune system? Science (New York, N.Y.) 330(6012): 1768–1773. https://doi.org/10.1126/science.1195568

Lei C, Kobayashi H, Wu Y, Li M, Isozaki A, Yasumoto A, Mikami H, Ito T, Nitta N, Sugimura T, Yamada M, Yatomi Y, Di Carlo D, Ozeki Y, Goda K (2018 Jul) High-throughput imaging flow cytometry by optofluidic time-stretch microscopy. Nat Protoc 13(7):1603–1631. https://doi.org/10.1038/s41596-018-0008-7

Llobet E, Martínez-Moliner V, Moranta D et al (2015) Deciphering tissue-induced Klebsiella pneumoniae lipid A structure. Proc Natl Acad Sci 112:E6369–E6378. https://doi.org/10.1073/pnas.1508820112

Matute-Bello G, Downey G, Moore BB, Groshong SD, Matthay MA, Slutsky AS, Kuebler WM, Acute Lung Injury in Animals Study Group (2011) An official American Thoracic Society workshop report: features and measurements of experimental acute lung injury in animals. Am J Respir Cell Mol Biol 44:725–738. https://doi.org/10.1165/rcmb.2009-0210ST

McConaughy BL, Laird C, McCarthy BJ (1969) Nucleic acid reassociation in formamide. Biochemistry 8(8):3289–3295. https://doi.org/10.1021/bi00836a024

Mellon FA (2003) Mass spectrometry | Principles and instrumentation. In: Encyclopedia of food sciences and nutrition. Elsevier, pp 3739–3749

Mills G, Dumigan A, Kidd T et al (2017) Identification and characterization of two klebsiella pneumoniae lpxL lipid A late acyltransferases and their role in virulence. Infect Immun 85:e00068-17. https://doi.org/10.1128/IAI.00068-17

Morris JH, Knudsen GM, Verschueren E et al (2014) Affinity purification–mass spectrometry and network analysis to understand protein-protein interactions. Nat Protoc 9:2539–2554. https://doi.org/10.1038/nprot.2014.164

Murphy K, Travers P, Walport MJ (2008) Janeway's immunobiology, 7th edn. Garland Science, New York

Murray CJL et al (2022) Articles global burden of bacterial antimicrobial resistance in 2019: a systematic analysis. Lancet 6736(21):1–27. https://doi.org/10.1016/S0140-6736(21)02724-0

Orjalo A, Johansson HE, Ruth JL (2011) Stellaris™ fluorescence in situ hybridization (FISH) probes: a powerful tool for mRNA detection. Nat Methods 8(10):i–ii. https://doi.org/10.1038/nmeth.f.349

Paczosa MK, Mecsas J (2016) Klebsiella pneumoniae: going on the offense with a strong defense. Microbiol Mol Biol Rev 80(3):629–661. https://doi.org/10.1128/MMBR.00078-15

Petrosillo N, Taglietti F, Granata G (2019) Treatment options for colistin resistant klebsiella pneumoniae: present and future. J Clin Med 8(7):937. https://doi.org/10.3390/jcm8070934

Public Health England (2020) Laboratory surveillance of Klebsiella spp. bacteraemia in England, Wales and Northern Ireland: 2018. Health Protection Report 14(1):1–19

R. W (1914) Rays of positive electricity and their application to chemical analysis. Nature 92:549–550. https://doi.org/10.1038/092549a0

Raje N, Dinakar C (2015) Overview of immunodeficiency disorders. Immunol Allergy Clin North Am 35(4): 599–623. https://doi.org/10.1016/j.iac.2015.07.001

Rice LB (2008) Federal funding for the study of antimicrobial resistance in nosocomial pathogens: no ESKAPE. J Infect Dis 197(8):1079–1081. https://doi.org/10.1086/533452

Richardson DS, Lichtman JW (2015) Clarifying tissue clearing. Cell 162(2):246–257. https://doi.org/10.1016/j.cell.2015.06.067

Rodrigues C, Passet V, Rakotondrasoa A, Brisse S (2018) Identification of klebsiella pneumoniae, klebsiella quasipneumoniae, klebsiella variicola and related phylogroups by MALDI-TOF mass spectrometry. Front Microbiol 9(DEC):1–7. https://doi.org/10.3389/fmicb.2018.03000

Rosenblueth M, Martínez L, Silva J, Martínez-Romero E (2004) Klebsiella variicola, a novel species with clinical and plant-associated isolates. Syst Appl Microbiol 27(1):27–35. https://doi.org/10.1078/0723-2020-00261

Sauer S, Kliem M (2010) Mass spectrometry tools for the classification and identification of bacteria. Nat Rev Microbiol 8:74–82. https://doi.org/10.1038/nrmicro2243

Schultz M (2008) Rudolf Virchow. Emerg Infect Dis 14(9):1480–1481. https://doi.org/10.3201/eid1409.086672

Selkrig J, Li N, Hausmann A et al (2020) Spatiotemporal proteomics uncovers cathepsin-dependent macrophage cell death during Salmonella infection. Nat Microbiol 5: 1119–1133. https://doi.org/10.1038/s41564-020-0736-7

Shapiro HM (2003) Practical flow cytometry, 4th edn. Wiley-Liss, Hoboken, NJ

Shapiro HM (2018) Flow cytometry: the glass is half full. Methods Mol Biol 1678:1–10. https://doi.org/10.1007/978-1-4939-7346-0_1

Singhal N, Kumar M, Kanaujia PK, Virdi JS (2015) MALDI-TOF mass spectrometry: an emerging technology for microbial identification and diagnosis. Front Microbiol 6:791. https://doi.org/10.3389/fmicb.2015.00791

Stanssens P, Zabeau M, Meersseman G et al (2004) High-throughput MALDI-TOF discovery of genomic sequence polymorphisms. Genome Res 14:126–133. https://doi.org/10.1101/gr.1692304

Sukumaran A, Woroszchuk E, Ross T, Geddes-McAlister J (2021) Proteomics of host–bacterial interactions: new insights from dual perspectives. Can J Microbiol 67:213–225. https://doi.org/10.1139/cjm-2020-0324

Titford M (2005) The long history of hematoxylin. Biotech Histochem 80(2):73–78. https://doi.org/10.1080/10520290500138372

Tomás A, Lery L, Regueiro V, Pérez-Gutiérrez C, Martínez V, Moranta D, Llobet E, González-Nicolau M, Insua JL, Tomas JM, Sansonetti PJ, Tournebize R, Bengoechea JA (2015) Functional genomic screen identifies klebsiella pneumoniae factors implicated in blocking nuclear factor κB (NF-κB) signaling. J Biol Chem 290(27):16678–16697. https://doi.org/10.1074/jbc.M114.621292

Underhill DM, Goodridge HS (2012) Information processing during phagocytosis. Nat Rev Immunol 12(7):492–502. https://doi.org/10.1038/nri3244

Volpi EV, Bridger JM (2008) FISH glossary: an overview of the fluorescence in situ hybridization technique. BioTechniques 45(4):385–409. https://doi.org/10.2144/000112811

von Waldeyer W (1863) Untersuchungen u¨ber den Ursprung und den Verlauf des Axsencylinders bei Wirbellosen und Wirbelthieren sowie u¨ber dessen Endverhalten in der quergestreiften Muskelfaser. Henle Pfeifer's Z Rat Med 20:193/256

Wen L, Fan Z, Mikulski Z, Ley K (2020) Imaging of the immune system - towards a subcellular and molecular understanding. J Cell Sci 133(5):jcs234922. https://doi.org/10.1242/jcs.234922

WHO (2014) Antimicrobial resistance. Bull World Health Organ 61(3):383–394. https://doi.org/10.1007/s13312-014-0374-3

Wyres KL, Holt KE (2016) Klebsiella pneumoniae population genomics and antimicrobial-resistant clones. Trends Microbiol 24(12):944–956. https://doi.org/10.1016/j.tim.2016.09.007

Wyres KL, Lam MMC, Holt KE (2020) Population genomics of Klebsiella pneumoniae. Nat Microbiol 18. https://doi.org/10.1038/s41579-019-0315-1

Young AP, Jackson DJ, Wyeth RC (2020) A technical review and guide to RNA fluorescence in situ hybridization. PeerJ 8:e8806. https://doi.org/10.7717/peerj.8806

A Review of Pathology and Analysis of Approaches to Easing Kidney Disease Impact: Host–Pathogen Communication and Biomedical Visualization Perspective

Advanced Microscopy and Visualization of Host-Pathogen Communication

Kacper Pizon, Savita Hampal, Kamila Orzechowska, and Shahid Nazir Muhammad

Abstract

Introduction: In addition to affecting the upper respiratory tract, severe acute respiratory syndrome-coronavirus (SARS-CoV) and SARS-CoV-2) can target kidneys resulting in disease impact. There is a lack of effective treatment for SARs-CoV and SARS-CoV-2, and so one approach could be to consider to lower the probable risk and onset of disease amongst immunocompromised and immunosuppressed individuals and patients. Angiotensin Converting Enzyme 2 (ACE2) has a promising impact including acting against SARs-CoV and SARS-CoV-2 symptoms. Current literature states that ACE2 is expressed across several physiological systems, including the lungs,
cardiovascular, gut, kidneys, and central nervous, and across endothelia. **Aims:** This chapter seeks to investigate causes and potential mechanisms during SARS infection (CoV-2), renal interaction, and the effects of acute kidney Injury (AKI). **Objectives:** This chapter will provide an overview of microscopy and visualization of host–pathogen communication and principles of ACE2 in the context of immunology and impact on renal pathophysiology. **Design:** This chapter focuses to provide basic principles of ACE2 and the analysis and effect of immunology and pathological components important in relation to SARs infection. **Discussion:** There has been a surge in literature surrounding mechanisms attributing to SARS-CoV and SARS-CoV-2 action on immune response to pathogens. There is an advantage to implementing ACE2 treatment to improve immune response against infection. **Conclusion:** ACE2 may provide appropriate strategies for the management of symptoms that relate to SARS-CoV and SARS-CoV-2 in most immunocompromised or immunosuppressed patients. Visualization of ACE2 action can be achieved through microscopy to understand host–pathogen communication.

K. Pizon · S. Hampal · K. Orzechowska
Department of Life Sciences, Coventry University, Coventry, England, UK

The Renal Patient Support Group (RPSG), Coventry, England, UK

S. N. Muhammad (✉)
Department of Health, and Life Sciences, Coventry University, Coventry, England, UK

University Hospitals Bristol NHS Foundation Trust, Bristol, England, UK
e-mail: ad9152@coventry.ac.uk

3.1 Introduction: Discovery of Coronaviruses

Since December 2019, the severe acute respiratory syndrome Coronavirus 2 (SARS-CoV-2) spread worldwide causing COVID, to be problematic and implicating health risks across the globe (Gheblawi et al. 2020). Coronaviruses can affect multiple organs in humans, including kidneys, increasing mortality, especially in those who are immunosuppressed and/or immunocompromised. Moreover, the lack of treatment has forced biomedical and pharmaceutical industries to investigate and develop treatments to prevent the exaceberation of COVID-19 in the general population (Gheblawi et al. 2020). There is a lack of effective treatment for SARS-CoV and the more recent SARS-CoV-2, and so one approach could be to consider to lower probable risk and onset of disease amongst immunocompromised and immunosuppressed individuals and patients (Gheblawi et al. 2020; Guo et al. 2020a, b). The research surrounding COVID-19 has been progressive; it is important to reduce disease mortality at the epidemiological and population level. However, the understanding of the structure, and pathology of Coronaviruses, especially surrounding host–pathogen communication, and visualization, requires investigation.

3.2 Aims and Objectives

This chapter seeks to investigate the causes and potential mechanisms of severe acute respiratory syndrome (SARS) infection (CoV-2), renal interaction, and the effects of acute kidney injury (AKI). This chapter also provides a review of the pathology and analysis of approaches to easing kidney disease impact by exploring host–pathogen communication, providing a biomedical visualization perspective, and highlighting the principles of Angiotensin Converting Enzyme 2 (ACE2) in the context of immunology and infection to understand the impact on kidney disease.

3.3 Biomedical Classification

Coronaviruses are more recent discoveries than adenoviruses; both fall under the same category, but adenoviruses have more taxonomy investigated (Wang et al. 2020; Beyerstedt et al. 2021). The first Coronavirus strain (B814) was discovered in 1965 by scientists Tyrrell and Bynoe, where biomedical specimens were collected from the respiratory tract of a patient with a common cold (Mahase 2020). Thereafter, Hamre and Procknow were then able to grow isolated virus strains, including B814 and 229E, which improved early biomedical visualization in the context of extraordinary viruses (Mahase 2020).

Linked to early biomedical visualization of common cold and COVID were isolates to virus strains associated with avian bronchitis and mice hepatitis; these were originally explored by Almeida and Tyrrell in 1967 (Mahase 2020). The same year at the National Institute of Health in Bethesda, six additional viruses with morphological similarities were isolated and grown in organ cultures, instead of the usual cell monolayer culture (Mahase 2020). In 1968, a more in-depth investigation of viruses using electron microscopy revealed comparable properties between them, for example, size, lipid layer, and the presence of surface spikes (i.e., protein), which resemble similar structures to the Adenovirus (Lupala et al. 2022). Figure 3.1 provides an overview of the progression and discovery of novel subgroups of viruses/coronaviruses.

Based on taxonomy and pathological features, a team of eight virologists decided to classify them as Coronaviruses, due to their characteristic appearance (Mahase 2020; Beyerstedt et al. 2021). Ongoing research and microscopy advances surrounding Coronaviruses provided greater knowledge of viral structure and function,
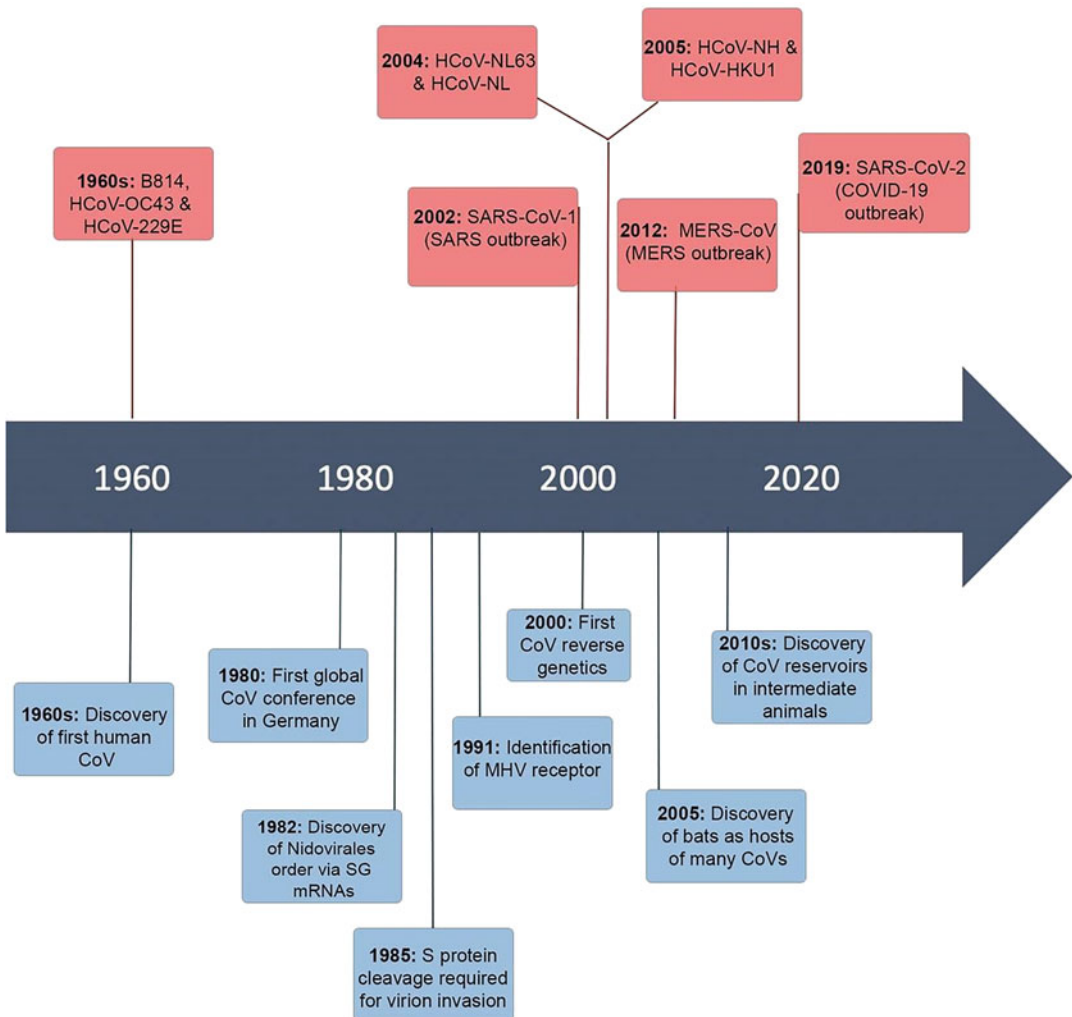
Fig. 3.1 The progression and discovery of novel subgroup of viruses/coronaviruses. *HCoV* human coronavirus, *MERS* middle east respiratory syndrome, *SARS* severe acute respiratory syndrome (Abdul-Fattah et al. 2021)

to discover therapeutic possibilities surrounding unpredictable outbreaks. Advanced microscopy and visualization are pertinent throughout scientific practices and more so in exploring links to COVID-19 virus and the pandemic (Song et al. 2019).

Regarding pharmaceutics, Angiotensin-Converting Enzyme 2 (ACE2) has diverse interplay, as SARS-CoV-2 impounds respiratory health and the implications prompt symptoms that have been highlighted in the literature relating to the COVID-19 pandemic. The implications on health and disease have become more obvious following the SARS outbreak in Wuhan province, China in 2003 (Mahase 2020; Gheblawi et al. 2020). In the next section, an analysis of Coronaviruses in correlation with renal health, and novel therapeutic strategies relating to preventing cardiovascular disease (CVD) and COVID-19 symptoms are considered.

3.4 The Renal Health and COVID-19 Correlation

It has been highlighted that the first pandemic caused by Coronavirus SARS-CoV occurred in 2002–2003, in Asia, wherein 8096 patients evaluated positive for the virus and as a result, 774 deaths had been documented (Sama et al. 2020). Despite common acute respiratory failure caused by diffuse alveolar damage, multi-organ failure was also noticeable wherein there were cases of severe diarrhea, hepatic failure, and Acute Kidney Injury (AKI). It was in 2005, an investigatory team from Hong Kong, retrospectively highlighted that 536 SARS cases (6.7%) developed AKI (Chu et al. 2005). Moreover, the mortality amongst this group was 91.7%, which is significantly higher than patients without any symptoms of AKI, which is 8.8% (Chu et al. 2005).

Gheblawi et al. (2020) and Guo et al. (2020b) also emphasized the importance of AKI in the context of SARS and Middle East Respiratory Coronavirus (MERS-CoV). MERS-CoV induced two epidemics; one in 2012 surrounding countries in the Middle East and one in 2015 in South Korea (Gheblawi et al. 2020; Guo et al. 2020a). The MERS-CoV devastated the lives of 2562 people resulting in 881 deaths. To determine possible nephrological complications associated with MERS-CoV, investigators from South Korea examined 30 patients by monitoring vital signs, bacterial culture of body fluids and virus through polymerase chain reaction investigations. Within a testing group, proteinuria occurred in 40% of cases, haematuria in 63.3% and AKI developed in 26.7% of patients, mostly in the elderly (Gheblawi et al. 2020; Guo et al. 2020b).

The current outbreak of SARS-CoV-2, which originated from Wuhan province, China, spread worldwide threatening life. Within the period of September 1, 2020, to August 31, 2021, 5,642,190 cases of COVID-19 were detected in England, wherein 94,815 cases led to death (UKHSA 2022). Despite being uncommon, renal complications have been correlated to pathophysiology detrimented by the effects of COVID-19 infection, mainly because of AKI (Gheblawi et al. 2020). Moreover, the risk for individuals who are prone to renal insufficiency to contract COVID-19 is higher, and thus interventions have been required to preclude further renal complications and CVD (Huang et al. 2020). The next section provides an in-depth overview of renal health and ACE2 at the microscopic level.

3.5 Renal Cells and COVID-19

Ribonucleic Acid (RNA) sequencing database assessment had demonstrated high expression of ACE2 and transmembrane protease serine 2 (TMPRSS2) in proximal tubular cells and podocytes, which might indicate a higher affinity for SARS-CoV2 (Murray et al. 2020). Microscopically, the presence of ACE2 within proximal tubular cells might indicate direct interaction with Coronavirus, which subsequently reflects kidney damage. However, it does not exclude the possible ischemic damage to the proximal tubular cells from hemodynamic alterations, informing that the knowledge surrounding direct interactions is vague and unspecified (Yang et al. 2017; Henry and Lippi 2020).

Immunobiology data indicate that lower expression of ACE2 correlates with a severe effect of disease owing to the downregulation of ACE2, which leads to a reduced anti-inflammatory effect (Murray et al. 2020). The severity of the illness increases with the lower expression of ACE2 receptors, which might again contradict the correlation among a direct interaction between SARS-CoV-2 and renal cells (Yang et al. 2017; Henry and Lippi 2020). Figure 3.2 provides an overview of ACE2 receptor expression in human organs.

Several investigations present the theory of SARS-CoV-2 tropism, which leads to viral infection of proximal tubular cells (Brake et al. 2020; Yang et al. 2017; Henry and Lippi 2020). The argument is based on the presence of viral particles within urine detected from COVID-19 patients, especially within the second and third

The expression of ACE2 in different organs
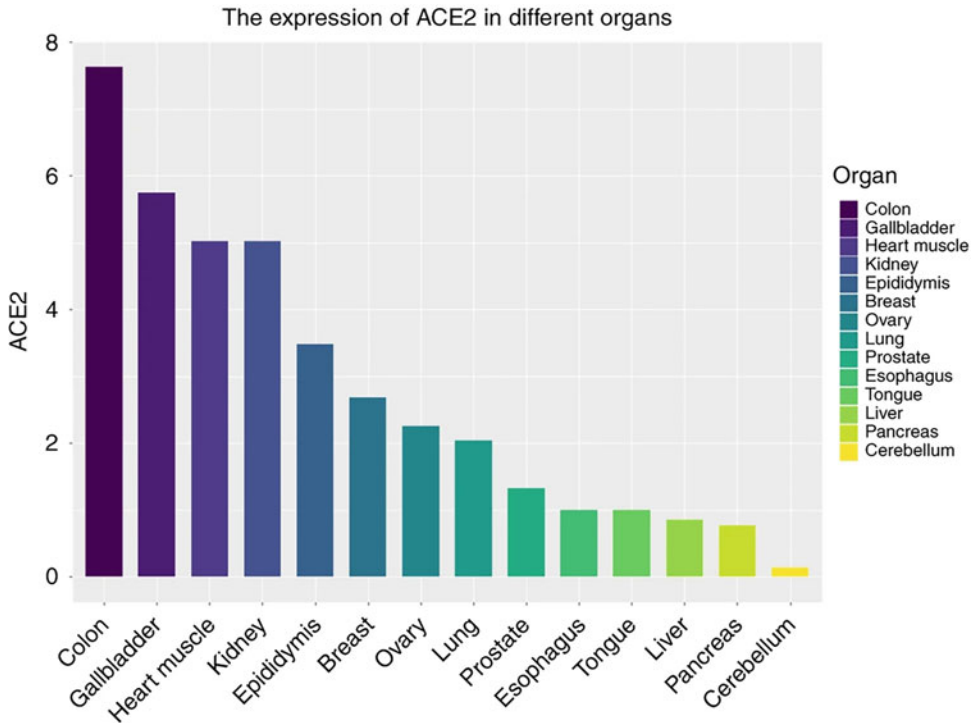
Fig. 3.2 Provides an overview of ACE2 receptor expression in human organs. As the kidney presents a higher level of ACE2 than the lungs, it leads to speculation of possible direct infection of HCoV-SARS-19 within kidney cells (Xu et al. 2020)

week of infection, and when the shedding of SARS-CoV-2 occurs (Guruprasad 2021b). However, histological examination negates the presence of active immune-mediated glomerulonephritis due to the absence of common indicators like electron-dense deposits and mild proteinuria (Baral et al. 2020). Moreover, the number of viral particles differs among several findings due to the lack of standardized sample collection and appropriate PCR assays conducted. Data highlight either little or no detection, and others present a high number of viral particles, which leads to inconsistent data (V'kovski et al. 2021).

A novel infection route was identified for SARS-CoV-2, which was the spike protein attachment to transmembrane glycoprotein CD147 (Guruprasad 2021a). As CD147 is expressed in various cells all around the body, including blood cells and proximal tubules of the kidney, the possible viral entry might affect the cell cycle, which affects inflammatory responses and further development of several diseases (Guruprasad 2021b). Due to the novelty of initial data across the literature, the idea of direct infection within the renal cells is still speculative (Murray et al. 2020; Wang et al. 2020). The next section provides more depth surrounding the analysis of COVID-19 in the context of taxonomy and genera, accordingly.

3.6 Biomedical Visualization and Analysis of COVID-19

The Coronavirus is divided into four genera: (1) Alpha-Coronavirus (HCoV-229E, HCoV-NL63), (2) Beta-Coronavirus (HCoV-OC43, HCoVHKU1, SARS-CoV, MERS-CoV, SARS-CoV2), which originate from bats,

(3) Gamma-Coronavirus, and (4) Delta-Coronavirus can be transmitted from types of birds and swine gene pools (Dhama et al. 2021). A SARS-CoV-2 virion contains an unsegmented, single-stranded, positive-sense RNA genome of around 30 kb, which encodes crucial viral protein used to create progeny viruses and the four essential structural proteins, called membrane (M), envelope (E), nucleocapsid (N), and spike (S) (V'kovski et al. 2021). As far as airborne viruses are concerned, SARS-CoV-2 is transmitted between humans due to the entering of viral particles into the upper respiratory tract (Dhama et al. 2021). The viral entry occurs by the binding of the spike glycoproteins, which are homotrimers present on the surface of the Coronavirus to the ACE2 receptor (Guruprasad 2021a).

The spike proteins are cleaved by host proteases into subunits: S1 subunit for receptor binding and S2 subunit for membrane fusion (Guruprasad 2021b). Microscopically, the infected cells are forced to translate the proteins required for generating the virus's progeny (Mehrbod et al. 2021). The next section provides context surrounding the renin–angiotensin–aldosterone system (RAAS) pathway and the role of ACE2 during COVID-19.

3.7 The Cytokine Storm Perspective and Understanding Renin–Angiotensin–Aldosterone System (RAAS) Pathway and Role of ACE2 During COVID-19

The RAAS is a multi-hormonal regulator of blood volume and systemic vascular resistance. Angiotensinogen is cleaved by renin forming inactive decapeptide Angiotensin I (Ang I), which is next converted by angiotensin-converting enzyme (ACE) into active octapeptide Angiotensin II (Ang II). The binding of Ang II with adequate angiotensin receptor (AT1 or AT2) leads to hypertension, inflammation, and multi-organ failure (Beyerstedt et al. 2021). Works by

Gheblawi et al. (2020), Guo et al. (2020a) highlight common and potent antiviral drugs, however, before these, ACE2 had been available to prompt blood flow between renal afferent and efferent arterioles, thus oxygenating cells throughout general physiology.

ACE2 performs a more protective role by degrading Ang II to active peptide, Ang 1–7 through cleavage of the carboxy-terminal phenylalanine in Ang II (Povlsen et al. 2020). Products of ACE2 action binds with Mitochondrial Assembly Protein-1 (MAP-1) receptor leading to vasodilation, vaso-protection, and cardio-protection, showing regulatory roles of both receptors (Povlsen et al. 2020). However, ACE2 receptors are inhibited during SARS-CoV-2, which downregulates protective action and leads to severe development of COVID-19 by hypercoagulation and microangiopathy. The infected cells are forced to translate proteins required for generating the virus's progeny, which also provokes immune action (Povlsen et al. 2020; Lupala et al. 2022) (Fig. 3.3).

Innate immune cells and macrophages are involved to present viral antigens to T-Helper (TH) cells, which release interleukin-12 to trigger the TH1 cells (Povlsen et al. 2020). Subsequently, TH1 stimulate B cells to produce antigen-specific antibodies and T-Killer cells (CD8+ and TK) to target cells containing viral antigen (Gheblawi et al. 2020). Using the Nuclear Factor kappa-light-chain-enhancer of activated B cells (NF-kB) signaling pathway, Pro-T-cell activate inflammatory cytokine production, secreting chemokine, and cytokines such as IL-8, TNF-α, IL-6, IL-1β, CCL-2 (C-C Motif Chemokine Ligand 2), -3, -5 (Sama et al. 2020; Song et al. 2019; UKHSA 2022).

Accumulation of immune proteins creates a cytokine storm, which leads to tissue damage, resulting in multi-organ failure and death (Gheblawi et al. 2020; Wang et al. 2020). The limitations related to post-mortem examinations of renal cells demonstrate evidence of AKI (Gheblawi et al. 2020; Guo et al. 2020a, b). At the same time, early COVID-19 cases have presented involvement, mainly IL-6 which, induces renal endothelial cells to prompt
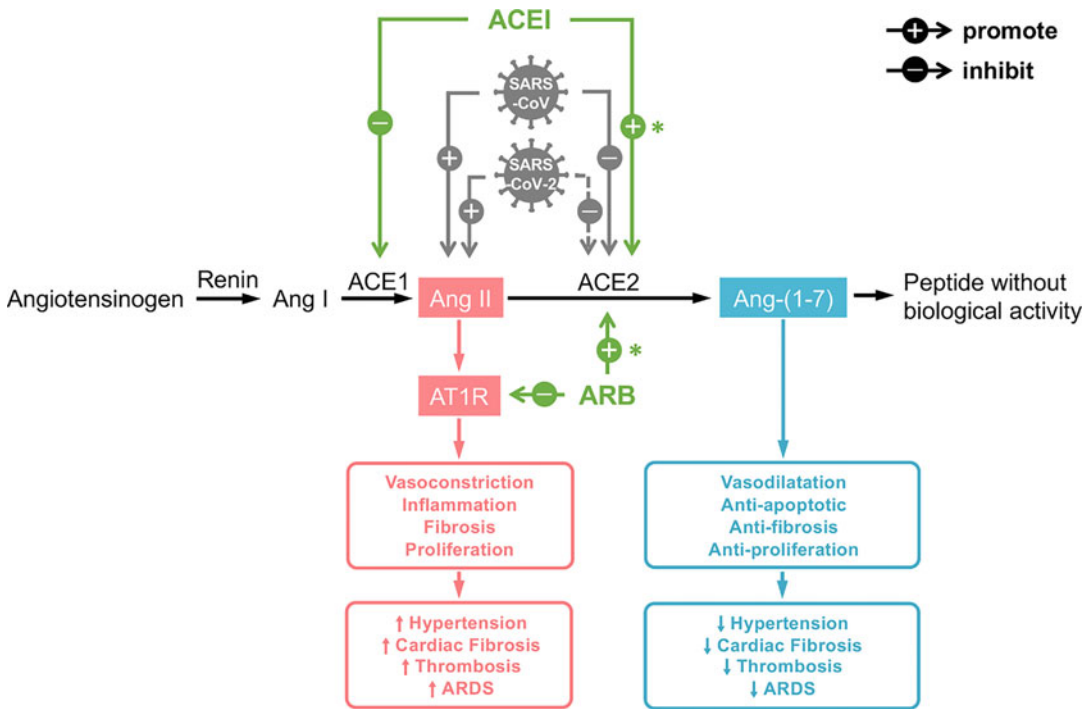
Fig. 3.3 The visualization of molecular action undergoing differentiation during COVID-19 Infection. HCoV-SARS binds to ACE2, which not only leads to its entry but also irregular balance between Ang molecules, resulting in the severity of the disease. ACE2 is also pharmacologically related to Angiotensin Receptor Blockers (ARBs), ARBs are inhibitors that dilate blood vessels to treat conditions such as hypertension. Permission to use figure sought from Guo et al. (2020a)

pro-inflammatory cytokines (Gheblawi et al. 2020; Guo et al. 2020a, b; Wang et al. 2020).

Additionally, sepsis may be a factor in COVID-19 patients, due to general physiology being impacted. Within damaged organs, endotoxin overload leads to septic shock, which induces AKI and renal damage (Henry and Lippi 2020). Works by Beyerstedt et al. (2021), Gheblawi et al. (2020), Guo et al. (2020a), Wang et al. (2020) go into more microscopic detail regarding ACE1/ACE2 gene polymorphism. The next section provides more depth surrounding immunobiology and the complement system. The next section will consider immunobiology and the complement system.

3.8 Immunobiology and The Complement System

Upon recognition of SARS-CoV-2, complement system becomes active and promotes pathogen response via lectins and the alternative pathway. The numerous anaphylatoxins, like C3a and C5a, bind to specific receptors, leading to stimulation of histamine, leukotrienes, and prostaglandins, which results in flushing, hypoxia, vasodilation, and hypotension (Murray et al. 2020). Additionally, an activated alternative pathway generates C5b-9 in tubules apical brush border as a response to the virus, leading to over-accumulation and tubulointerstitial damage (Henry and Lippi 2020).

The disruption of lymphocytes and role in the maintenance of immune hemostasis leads to lymphopenia, which has been observed in

patients with severe COVID-19 symptoms. As those cells contain ACE2 receptors, SARS-CoV-2 might target them, reducing the number of CD4+ and CD8+ T Cells. This results in unequal distribution of immune response, hyperactivation of the innate immune system and a long process of terminating the virus (Murray et al. 2020). Another factor of lymphopenia might be induced inflammatory responses, which prompts lymphocyte apoptosis, leading to lymphocyte ratio disproportion (Beyerstedt et al. 2021). Through analyses, patients with severe COVID-19 have expressed injury around the spleen and lymph nodes, which suggests that the virus can damage lymphatic organs reducing contribution to immune hemostasis (Mahase 2020).

There may be some overlap between immune responses, after the detection of a foreign pathogen, facilitating hypercoagulability. Initially, circulating pro-inflammatory chemicals activate blood monocytes (Chowell et al. 2015). Endothelial cells are activated by cytokines and virus particles, which create adhesion molecules and monocyte chemo-attractants, leading to the recruitment of activated monocytes to endothelial cells (Beyerstedt et al. 2021). Endothelial cells also use neutrophils, which conduct coagulation contact pathway, by realizing neutrophil extracellular traps, which activate platelets. Additionally, tissue factors might be exposed due to any endothelial damage. The blood viscosity increases as levels of oxygen decrease due to hypoxia induced by COVID-19 leading to the stimulation of thrombosis (Baral et al. 2020). Figure 3.4 provides an overview of the complement system's possible contribution to inflammatory response in severe COVID-19.

Thrombosis laboratory indexes like partial thromboplastin time, prothrombin time, and international normalized ratio are elevated, and D-dimer, which correlates with high mortality rate in COVID-19 patients (Yang et al. 2017). Additionally, peripheral blood smears express low fibrinogen levels and thrombocytopenia with schistocytes under morphology. Several factors may prompt microthrombi and microangiopathy, which elevate the risk of micro-infarctions across cardiovascular, respiratory, and renal physiological systems inducing irreversible damage where COVID-19 symptoms are present (Yang et al. 2017).

Understanding rhabdomyolysis is also important because it is caused by muscle breakdown arising from numerous factors, such as overexertion, trauma, toxic substances, or healthcare complications over time. Autopsy data of COVID-19 patients present acute proximal tubular damage and glomerular fibrin thrombi with ischaemic collapse (Henry and Lippi 2020). There are several theories suggesting viral-induced rhabdomyolysis. It might be induced by a cytokine storm damaging muscles, circulating toxins, muscle degeneration, or direct virus invasion. Due to the novelty of COVID-19, there is little transparency between a correlation surrounding rhabdomyolysis and AKI in symptomatic COVID-19 patients (Yang et al. 2017; Henry and Lippi 2020). The next section provides an overview of organ crosstalk and biomedical communication.

3.9 Organ Crosstalk and Biomedical Communication

Linked to COVID-19 is acute respiratory distress syndrome (ARDS). ARDS are life-threatening disorders wherein the lungs cannot take in oxygen for the body to maintain physiologically, leading to incapacities surrounding crosstalk between respiratory, cardiovascular, and renal systems (Povlsen et al. 2020; Park and Faubel 2021). As the COVID-19 pathology shares similar symptoms to ARDS, and within both groups of patients where AKI has been detected, it is postulated that AKI develops from organ crosstalk between the lung–kidney axis (Murray et al. 2020).

Several factors, including an inflammatory/immune response and the secretion of circulating compounds, can interact with kidney cells and cause harm to ARDS patients. The reduction of oxygen transport within organs also contributes to the development of AKI (Park and Faubel 2021). A study in 2019 showed, that 70% of patients
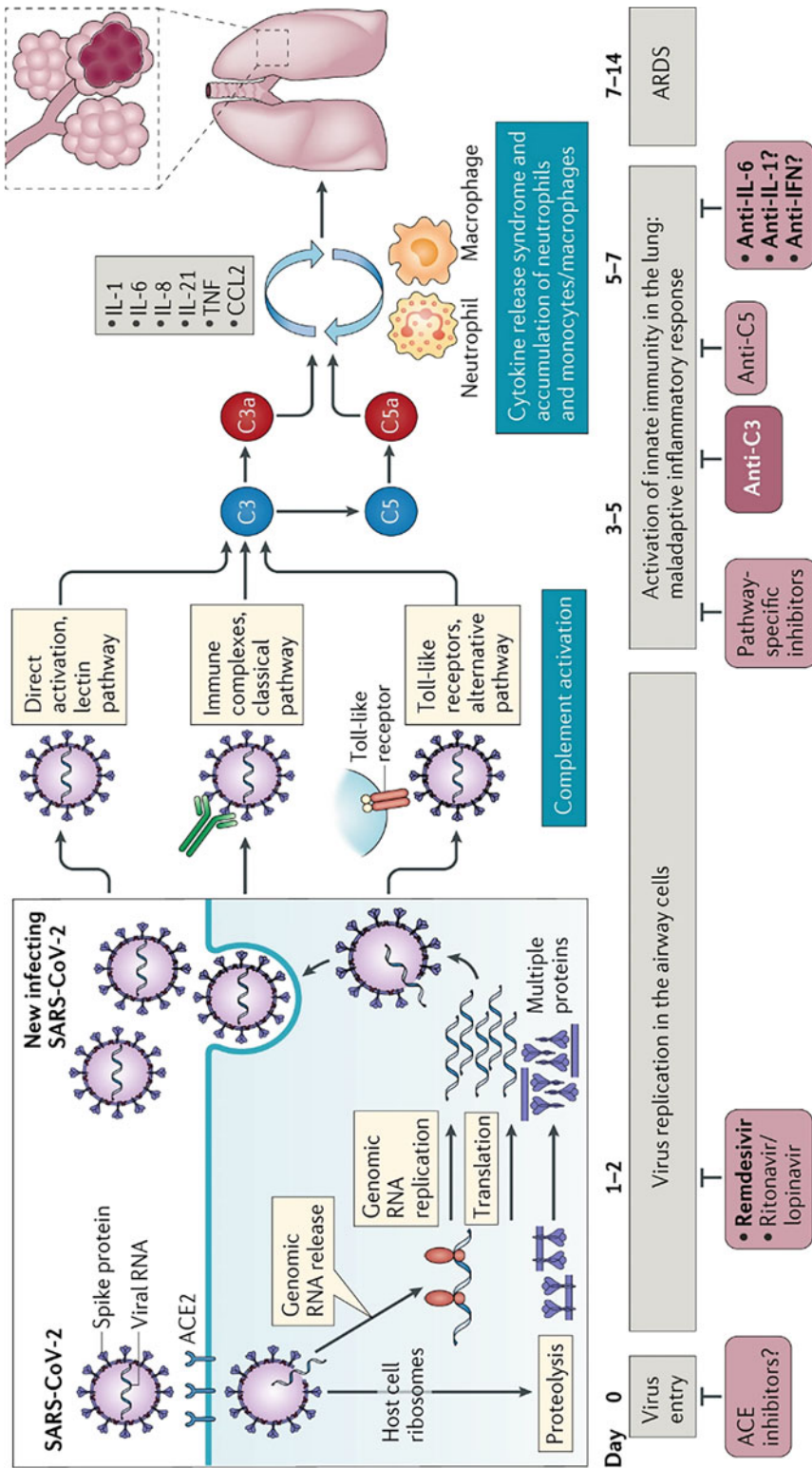
Fig. 3.4 The presentation of the complement system's possible contribution to inflammatory response in severe COVID-19 (Risitano et al. 2020)

with healthy kidneys and ARDS developed AKI, confirming lung involvement in the development of AKI, and suggesting comparable results for COVID-19 infection (Park and Faubel 2021).

3.10 Current Treatments and COVID-19

3.10.1 Reduction of Accessibility of SARS-CoV2 to ACE2 Receptors

The severity of COVID-19 has led to an increased focus on developing appropriate treatment against SARS-CoV-2 to decrease the impact of the pandemic and protect the most vulnerable patients (Florindo et al. 2020). The main aims of treatment focus on blocking the virus from attaching itself to the ACE2 receptor, which would stop the viral entry (Ni et al. 2020). Knowledge about receptors, action, and the reaction of each substance within the cells during SARS-COV-2 infection would contribute to the development of appropriate COVID-19 treatment (Ni et al. 2020).

One way to block the spread of SARS-COV-2 is to introduce genetically modified ACE2, called Human Recombinant Soluble (HRS) ACE2, which would reduce the number of viral attachments to the actual cells. The drug APN01 contains HRS ACE2 and is currently in Phase II trial testing for lung disease (Abd El-Aziz et al. 2020). Previously, Arbidol 20 has been used in treatment against influenza virus, which impairs viral entry (Li et al. 2021). It works as a virus-host cell fusion inhibitor and due to its broad-spectrum antiviral application is currently clinically tested against SARS-CoV-2 (Li et al. 2021).

A similar effect can be observed with the use of a soluble form of ACE2 (Krishnamurthy et al. 2021). Soluble ACE2 is naturally found within plasma (Yeung et al. 2021). Increasing its concentration in plasma would promote the attachment of SARS-CoV-2, reducing the number of pathogens entering the cells (Beyerstedt et al. 2021). This approach not only reduces severity of disease but also preserves tissue ACE2 (Yeung et al. 2021).

3.11 Anti-Virals on COVID-19

Antivirals, which are used for different viral infections, are currently being tested for SARS-Cov-19. As some of them have a broad range application, this also allows them to be investigated in suppressing the infection. Some Antivirals include:

3.11.1 Lopinavir

After the SARS-CoV epidemic, the drug Lopinavir was approved as an effective antiviral due to its ability to inhibit viral action in in-vitro environments (Tripathy et al. 2020). Lopinavir is a protease inhibitor, which blocks protease's action, preventing the virus from creating progeny within the cell. Originally, this treatment was dedicated to HIV patients but due to a positive decrease in mortality among patients with SARS-CoV, it has been suggested that it might have potential against SARS-CoV2 as well. Unfortunately, there is no significant decrease in the mortality of COVID-19 patients (Yeung et al. 2021).

3.11.2 Hydroxychloroquine

Hydroxychloroquine is treatment with a safe profile used for several ailments, mainly malaria and due to anti-inflammatory properties for rheumatic diseases (Ben-Zvi et al. 2011). This pharmacotherapy affects viral entry by changing the pH of the vesicle, resulting in inhibition of several enzymes, and finally disabling endocytosis, if it is pH-dependent (Sinha and Balayla 2022). Additionally, glycosyltransferases are inhibited as well, stopping post-translational modifications of several viruses (Tripathy et al. 2020). Lack of viral replication would lead to reduced immune response, which would reduce the activation of

cytokine storm, and side effects of its action (Ye et al. 2020).

Theoretically, Hydroxychloroquine should be an essential treatment for COVID-19 disease. However, the examination of COVID-19 patients treated with hydroxychloroquine leads to inconsistent data showing both a significant decrease in mortality among COVID-19 patients and little effect in reducing mortality (Geleris et al. 2020). Additionally, hydroxychloroquine is associated with QT prolongation, which might cause arrhythmia, so it is not an ideal treatment for a patient who is taking other treatments for chronic diseases, such as chronic kidney disease (CKD) (Hooks et al. 2020).

3.11.3   Favipiravir

In China, a drug called Favipiravir is currently used to treat severe influenza (Shiraki and Daikoku 2020). It inhibits the action of the RNA polymerase enzyme, which disables transcription of the viral genome. This results in the prevention of translating essential viral proteins (Hassanipour et al. 2021). Preliminary data obtained from the examination of Favipiravir among patients with COVID-19 provided a promising solution for the current pandemic (Hassanipour et al. 2021). However, a review of over 2700 studies concluded that there was no evidence of reduced mortality among patients with COVID-19 (Özlüşen et al. 2021).

3.11.4   Remdesivir

Remdesivir, developed by Gilead Sciences, was developed to treat RNA-based viruses, which are most likely to induce a global pandemic, such as the Ebola virus, MERS, and SARS (Eastman et al. 2020). The activity against SARS and MERS led to suggest Remdesivir as a potential candidate for COVID-19 due to the similarity between those viruses (Eastman et al. 2020). It is a mutagenic nucleoside, which terminates pre-mature viral RNA (Snell 2001).

Within the presence of Remdesivir, a poliovirus was constantly mutating to create a defence mechanism against it (Crotty et al. 2001). Continually, the virus exposure to a high concentration of Remdesivir can lead to a 9.7-fold increase in mutations, which results in a genetic error of the virus and its infectivity reduced by 99.3% (Crotty et al. 2001).

Additionally, Remdesivir affects the DNA synthesis process by reducing the reactive hydroxyl group at the end chain terminators (Mitsuya et al. 1990). Figure 3.5 provides an overview of current treatments and COVID-19, and Fig. 3.6 provides a specific overview surrounding the inhibition of viral genome replication by Remdesivir.

Preliminary data presented informs that patients treated with Remdesivir recover quicker than those treated with a placebo (Beigel et al. 2020). It was also observed that Remdesivir improved patients' well-being during the infection comparing them to a group treated with a placebo (Beigel et al. 2020). Thanks to those results, the Food and Drug Administration (FDA) permitted the use of Remdesivir against COVID-19. Despite positive outcomes of Remdesivir usage, the mortality among patients treated with it is still high, and the drug alone is
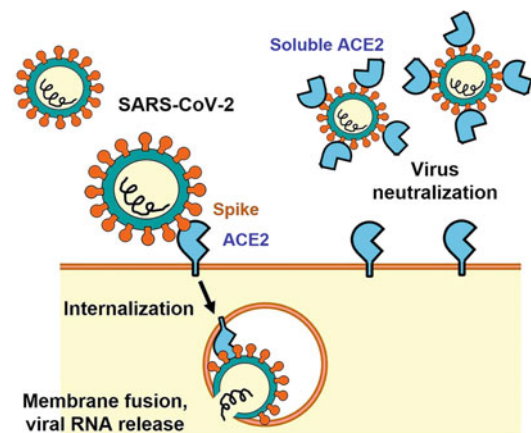
Fig. 3.5 An overview of Current Treatments and COVID-19. The standard mode of action, in which SARS-CoV-2 attaches to the membrane's ACE2 and enters the cell is presented on left. In the presence of soluble ACE2, SARS-CoV-2 attaches to those units, resulting in no membrane fusion (Kuba et al. 2021)
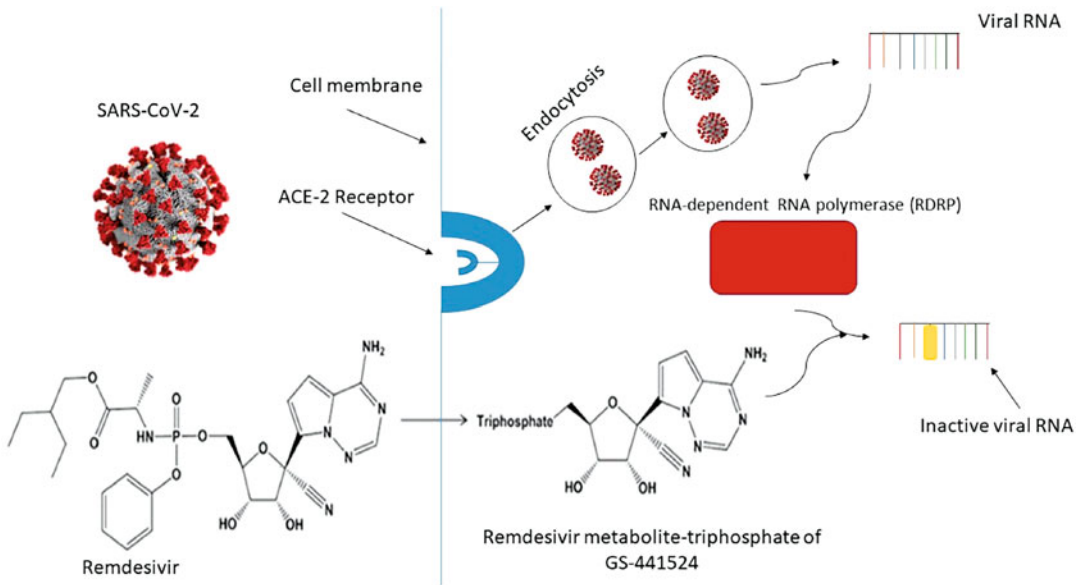
Fig. 3.6 Inhibition of viral genome replication by Remdesivir (Al-Tannak et al. 2020)

not sufficient in curing COVID-19 disease (Beigel et al. 2020).

3.12 Anti-Inflammatory Agents on COVID-19 Recipient

As mentioned before, many factors might induce organ dysfunction syndrome. Circulating cytokinesis storm, which might be induced by superimposed septic syndrome or directly by a virus, causes severe damage to the body (Beigel et al. 2020). To ease organ damage, the usage of anti-inflammatory drugs was suggested to ameliorate COVID-19 infections (Beigel et al. 2020).

3.12.1 Steroids

During the SARS-CoV outbreak in 2002–2003, the use of steroids was restricted due to the lack of beneficial results, and possibly harmful side effects like delayed viral clearance, avascular necrosis, diabetes, and psychosis (Russell et al. 2020). Corticosteroids were observed to increase mortality among SARS patients, which indicates

the danger of using steroids to ease COVID-19 symptoms (Russell et al. 2020).

3.12.2 JAK-STAT Inhibitors

The JAK/STAT signaling pathway is present within various cells and has been associated with various roles in immune responses like IL-2, IL-4, IL-6, IL-12 signaling, TH (T-Helper) 1, TH2, Treg cell and Th9, Th 17 cell differentiation, the proliferation of viral selective CD8+ T cells and B cell lymphoma (Satarker et al. 2020). The presence of cytokine storm is essential for dealing with a viral infection, however as mentioned before, cytokine overload might induce organ damage or severe conditions like ARDS (Luo et al. 2020). A solution has been suggested that JAK-STAT inhibitors might decrease the level of the pro-inflammatory cytokine, resulting in general improvement of health among COVID-19 patients (Luo et al. 2021). However, a lack of an appropriate titer of cytokines might lead to compromised immune responses and proliferation of SARS-CoV-2. Currently, studies of JAK-STAT inhibitor medication called Baricitinib, provide promising data, showing a

reduction in the number of deaths among COVID-19 patients (Mahase 2022).

While it is known that COVID-19 impacts renal function, leading to increased mortality, cytokine response of renal epithelium has not been studied in detail. One team reported on the genetic programs that activate human primary proximal tubule (HPPT) cells by interferons and suppression by Ruxolitinib, a Janus kinase (JAK) inhibitor used in COVID-19 treatment (Jankowski et al. 2021). Integration of future research linked to AKI and COVID-19, as well as other tissues, permit the avenue of kidney-specific interferon responses. Additionally, new drugs such as Ruxolitinib (dACE2) are being trialed; recently discovered isoform (dACE2) informs that initial data show promising results linked to HPPT cells of the kidneys aligned to ACE2, the SARS-CoV-2 receptor (Jankowski et al. 2021).

3.12.3 Mesenchymal Stem Cell Therapy

Cell-based therapy, particularly stem cell therapy, has emerged as a potential therapeutic, with many seeing prospects to heal incurable illnesses (Lopes-Pacheco et al. 2019). The research surrounding stem cells continues to generate intrigue due to the potential including a high proliferation rate, low invasive procedure, and are free of ethical issues (Turner et al. 2021). Among COVID-19 patients, stem cells focus on modifying immune cell function, immune responses and reducing inflammation-induced lung injury (Golchin et al. 2019). Those stem cells also produce growth factors, which promote cell proliferation and prevent apoptosis (Adas et al. 2021). Figure 3.7 provides an overview surrounding visualization and mode of action during mesenchymal stem cell therapy in COVID-19 patients.

The decrease in mortality has been observed in several studies, which focused on the usage of Mesenchymal Stromal (stem) Cell (MSC) therapy among COVID-19 patients (Metcalfe 2022). Additionally, mesenchymal stem cells

significantly shorten the time to clinical symptom improvement in COVID-19 patients (Lanzoni et al. 2021). Several clinical trials have shown that MSCs are effective and safe for the treatment of COVID-19 patients, particularly critically ill patients, reducing clinical symptoms, hospital stay, cytokine release, and mortality (Zumla et al. 2020).

3.13 Conclusion

There has been a surge in the literature surrounding mechanisms attributing to SARS-CoV and SARS-CoV-2 action on the immune response to a pathogen. SARS-CoV-2 patients present an increased level of blood coagulation factors and blood clotting complexities; the main mediators include thrombin, tissue factor, and fibrinogen (Beyerstedt et al. 2021). SARS-CoV-2 infection impairs the function of vascular endothelial function, resulting in increased production of thrombin and reduced fibrinolysin, which impacts clotting ability (Gheblawi et al. 2020). While it is known that COVID-19 impacts kidney function, leading to increased mortality, research surrounding interrogation of cytokine response on renal epithelium has not been substantiated.

3.14 Summary

There is an advantage to implementing ACE2 treatment to improve immune response against infection; ACE2 may also offer appropriate strategies for the management of symptoms that relate to SARS-CoV and SARS-CoV-2 in most immunocompromised or immunosuppressed patients (Murray et al. 2020). However, what is still not known is whether ACE2 should be assigned at a population level to totally prevent COVID-19 symptoms. That notwithstanding, advances in laboratory practice, allow the implementation of pathology assays and techniques including microscopy advances for visualization and analysis to understand host–pathogen communication to preclude kidney disease impact (Gheblawi et al. 2020; Beyerstedt et al. 2021).
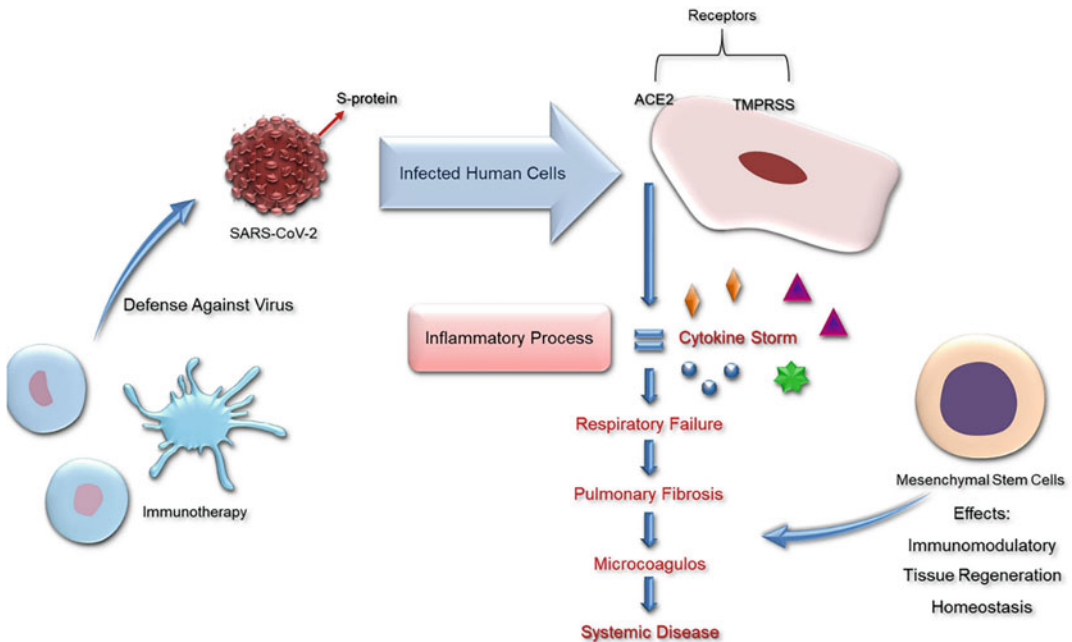
Fig. 3.7 Overview surrounding visualization and mode of action during mesenchymal stem cell therapy in COVID-19 patients (Câmara et al. 2021)

References

Abd El-Aziz T, Al-Sabi A, Stockand J (2020) Human recombinant soluble ACE2 (hrsACE2) shows promise for treating severe COVID19. Signal Transducti Target Ther. Available at https://www.nature.com/articles/s41392-020-00374-6.pdf. Accessed April 2022

Abdul-Fattah S, Pal A, Kaka N, Kakodkar P (2021) History and recent advances in coronavirus discovery. Methods Pharmacol Toxicol. doi: https://doi.org/10.1007/7653_2020_47. Accessed March 2022

Adas G, Cukurova Z, Yasar K, Yilmaz R, Isiksacan N, Kasapoglu P, Yesilbag Z, Koyuncu I, Karaoz E (2021) The systematic effect of mesenchymal stem cell therapy in critical COVID-19 patients: a prospective double controlled trial. Cell Transplant. https://doi.org/10.1177/09636897211024942. Accessed April 2022

Al-Tannak N, Novotny L, Alhunayan A (2020) Remdesivir—bringing hope for COVID-19 treatment. Sci Pharm 88(2):29. Accessed April 2022

Baral R, White M, Vassiliou VS (2020) Effect of renin-angiotensin-aldosterone system inhibitors in patients with COVID-19: a systematic review and meta-analysis of 28,872 patients. Curr Atheroscler Rep 22(10):61

Beigel J, Tomashek K, Dodd L, Mehta A, Zingman B, Kalil A, Hohmann E, Chu H, Luetkemeyer A, Kline S, Lopez de Castilla D, Finberg R, Dierberg K, Tapson V, Hsieh L, Patterson T, Paredes R, Sweeney D, Short W, Touloumi G, Lye D, Ohmagari N, Oh M, Ruiz-Palacios G, Benfield T, Fätkenheuer G, Kortepeter M, Atmar R, Creech C, Lundgren J, Babiker A, Pett S, Neaton J, Burgess T, Bonnett T, Green M, Makowski M, Osinusi A, Nayak S, Lane H (2020) Remdesivir for the treatment of Covid-19 – final report. N Engl J Med:1813–1826. Accessed April 2022

Ben-Zvi I, Kivity S, Langevitz P, Shoenfeld Y (2011) Hydroxychloroquine: from malaria to autoimmunity. Clin Rev Allergy Immunol 42(2):145–153. https://doi.org/10.1007/s12016-010-8243-x. Accessed April 2022

Beyerstedt S, Casaro EB, Rangel ÉB (2021) COVID-19: angiotensin-converting enzyme 2 (ACE2) expression and tissue susceptibility to SARS-CoV-2 infection. Eur J Clin Microbiol Infect Dis 40(5):905–919

Brake SJ, Barnsley K, Lu W, McAlinden KD, Eapen MS, Sohal SS (2020) Smoking upregulates angiotensin-converting enzyme-2 receptor: a potential adhesion site for novel coronavirus SARS-CoV-2 (COVID-19). J Clin Med 9:841

Câmara D, Porcacchia A, Lizier N, De-Sá-Júnior P (2021) A COVID-19 overview and potential applications of cell therapy. Biologics 1(2):177–188. Accessed May 2022

Chowell G, Abdirizak F, Lee S, Lee J, Jung E, Nishiura H et al (2015) Transmission characteristics of MERS and

SARS in the healthcare setting: a comparative study. BMC Med 13:210

Chu KH, Tsang WK, Tang CS, Lam MF, Lai FM, To KF, Fung KS, Tang HL, Yan WW, Chan HW, Lai TS, Tong KL, Lai KN (2005) Acute renal impairment in coronavirus-associated severe acute respiratory syndrome. Kidney Int 67(2):698–705

Crotty S, Cameron C, Andino R (2001) RNA virus error catastrophe: direct molecular test by using ribavirin. Proc Natl Acad Sci U S A 98(12):6895–6900. Accessed April 2022

Dhama K, Sharun K, Tiwari R, Dhawan M, Emran TB, Rabaan AA, Alhumaid S (2021) COVID-19 vaccine hesitancy - reasons and solutions to achieve a successful global vaccination campaign to tackle the ongoing pandemic. Hum Vaccin Immunother

Eastman R, Roth J, Brimacombe K, Simeonov A, Shen M, Patnaik S, Hall M (2020) Remdesivir: a review of its discovery and development leading to emergency use authorization for treatment of COVID-19. ACS Central Sci 6(5):672–683. Accessed April 2022

Florindo H, Kleiner R, Vaskovich-Koubi D, Acúrcio R, Carreira B, Yeini E, Tiram G, Liubomirski Y, Satchi-Fainaro R (2020) Immune-mediated approaches against COVID-19. Nat Nanotechnol 15(8):630–645

Geleris J, Sun Y, Platt J, Zucker J, Baldwin M, Hripcsak G, Labella A, Manson D, Kubin C, Barr R, Sobieszczyk M, Schluger N (2020) Observational study of hydroxychloroquine in hospitalized patients with Covid-19. N Engl J Med 382(25):2411–2418. https://doi.org/10.1056/nejmoa2012410. Accessed April 2022

Gheblawi M, Wang K, Viveiros A, Nguyen Q, Zhong JC, Turner AJ, Raizada MK, Grant MB, Oudit GY (2020) Angiotensin-converting enzyme 2: SARS-CoV-2 receptor and regulator of the renin-angiotensin system: celebrating the 20th anniversary of the discovery of ACE2. Circ Res 126(10):1456–1474

Golchin A, Farahany T, Khojasteh A, Soleimanifar F, Ardeshirylajimi A (2019) The clinical trials of mesenchymal stem cell therapy in skin diseases: an update and concise review. Curr Stem Cell Res Therapy 14(1): 22–33. Accessed April 2022

Guo J, Huang Z, Lin L, Lv J (2020a) Coronavirus disease 2019 (COVID-19) and cardiovascular disease: a viewpoint on the potential influence of angiotensin-converting enzyme inhibitors/angiotensin receptor blockers on onset and severity of severe acute respiratory syndrome coronavirus 2 infection. J Am Heart Assoc 9(7):e016219

Guo YR, Cao QD, Hong ZS, Tan YY, Chen SD, Jin HJ, Tan KS, Wang DY, Yan Y (2020b) The origin, transmission, and clinical therapies on coronavirus disease 2019 (COVID-19) outbreak - an update on the status. Mil Med Res 7(1):11

Guruprasad L (2021a) Human coronavirus spike protein-host receptor recognition. Prog Biophys Mol Biol 161: 39–53

Guruprasad L (2021b) Human SARS CoV-2 spike protein mutations. Proteins 89(5):569–576

Hassanipour S, Arab-Zozani M, Amani B, Heidarzad F, Fathalipour M, Martinez-de-Hoyo R (2021) The efficacy and safety of Favipiravir in treatment of COVID-19: a systematic review and meta-analysis of clinical trials. Sci Rep 11(1):11022. Accessed April 2022

Henry BM, Lippi G (2020) Chronic kidney disease is associated with severe coronavirus disease 2019 (COVID-19) infection. Int Urol Nephrol 52:1193–1194

Hooks M, Bart B, Vardeny O, Westanmo A, Adabag S (2020) Effects of hydroxychloroquine treatment on QT interval. Heart Rhythm 17(11):1930–1935. Accessed April 2022

Huang C, Wang Y, Li X, Ren L, Zhao J, Hu Y et al (2020) Clinical features of patients infected with 2019 novel coronavirus in Wuhan, China. Lancet 395(10223): 497–506

Jankowski J, Lee HK, Wilflingseder J, Hennighausen L (2021) JAK inhibitors dampen activation of interferon-activated transcriptomes and the SARS-CoV-2 receptor ACE2 in human renal proximal tubules. iScience 24(8):102928

Krishnamurthy S, Lockey R, Kolliputi N (2021) Soluble ACE2 as a potential therapy for COVID-19. Am J Phys Cell Phys 320(3):C279–C281

Kuba K, Yamaguchi T, Penninger J (2021) Angiotensin-converting enzyme 2 (ACE2) in the pathogenesis of ARDS in COVID-19. Front Immunol 12:732690. Accessed April 2022

Lanzoni G, Linetsky E, Correa D, Messinger Cayetano S, Alvarez R, Kouroupis D, Alvarez Gil A, Poggioli R, Ruiz P, Marttos A, Hirani K, Bell C, Kusack H, Rafkin L, Baidal D, Pastewski A, Gawri K, Leñero C, Mantero A, Metalonis S, Wang X, Roque L, Masters B, Kenyon N, Ginzburg E, Xu X, Tan J, Caplan A, Glassberg M, Alejandro R, Ricordi C (2021) Umbilical cord mesenchymal stem cells for COVID-19 acute respiratory distress syndrome: A double-blind, phase 1/2a, randomized controlled trial. Stem Cells Transl Med 10(5):660–673. Accessed April 2022

Li M, Yu T, Zhu J, Wang Y, Yang Y, Zhao K, Yi Y, He J, Li C, He J (2021) Comparison of the antiviral effect of arbidol and chloroquine in treating COVID-19. Ann Palliat Med 10(3):3307–3312

Lopes-Pacheco M, Robba C, Rocco P, Pelosi P (2019) Current understanding of the therapeutic benefits of mesenchymal stem cells in acute respiratory distress syndrome. Cell Biol Toxicol 36(1):83–102. Accessed April 2022

Luo W, Li Y, Jiang L, Chen Q, Wang T, Ye D (2020) Targeting JAK-STAT signaling to control cytokine release syndrome in COVID-19. Trends Pharmacol Sci 41(8):531–543. Accessed April 2022

Luo J, Lu S, Yu M, Zhu L, Zhu C, Li C, Fang J, Zhu X, Wang X (2021) The potential involvement of JAK-STAT signalling pathway in the COVID-19

infection assisted by ACE2. Gene 768:145325. Accessed April 2022

Lupala CS, Ye Y, Chen H, Su XD, Liu H (2022) Mutations on RBD of SARS-CoV-2 Omicron variant result in stronger binding to human ACE2 receptor. Biochem Biophys Res Commun 29(590):34–41

Mahase E (2020) Covid-19: Coronavirus was first described in The BMJ in 1965. BMJ 369:m1547

Mahase E (2022) Covid-19: anti-inflammatory treatment baricitinib reduces deaths in patients admitted to hospital, finds trial. BMJ 376:o573. Accessed April 2022

Mehrbod P, Eybpoosh S, Farahmand B, Fotouhi F, Khanzadeh Alishahi M (2021) Association of the host genetic factors, hypercholesterolemia, and diabetes with mild influenza in an Iranian population. Virol J 18(1):64

Metcalfe S (2022) Mesenchymal stem cells and management of COVID-19 pneumonia. Medicine in Drug Discovery, [online] 5, p. 100019. Available at https://pubmed.ncbi.nlm.nih.gov/32296777/. Accessed April 2022

Mitsuya H, Yarchoan R, Broder S (1990) Molecular targets for AIDS therapy. Science 249(4976): 1533–1544. Accessed April 2022

Murray E, Tomaszewski M, Guzik TJ (2020) Binding of SARS-CoV-2 and angiotensin-converting enzyme 2: clinical implications. Cardiovasc Res 116:e87–e89

Ni W, Yang X, Yang D, Bao J, Li R, Xiao Y, Hou C, Wang H, Liu J, Yang D, Xu Y, Cao Z, Gao Z (2020) Role of angiotensin-converting enzyme 2 (ACE2) in COVID-19. Crit Care 24(1):422

Özlüşen B, Kozan Ş, Akcan R, Kalender M, Yaprak D, Peltek İ, Keske Ş, Gönen M, Ergönül Ö (2021) Effectiveness of favipiravir in COVID-19: a live systematic review. Eur J Clin Microbiol Infect Dis 40(12): 2575–2583. Accessed April 2022

Park BD, Faubel S (2021) Acute kidney injury and acute respiratory distress syndrome. Crit Care Clin 37(4): 835–849

Povlsen AL, Grimm D, Wehland M, Infanger M, Krüger M (2020) The vasoactive mas receptor in essential hypertension. J Clin Med 9(1):267

Risitano A, Mastellos D, Huber-Lang M, Yancopoulou D, Garlanda C, Ciceri F, Lambris J (2020) Complement as a target in COVID-19? Nat Rev Immunol 20(6): 343–344

Russell C, Millar J, Baillie J (2020) Clinical evidence does not support corticosteroid treatment for 2019-nCoV lung injury. The Lancet 395(10223):473–475. Accessed April 2022

Sama IE, Ravera A, Santema BT, van Goor H, ter Maaten JM, Cleland JGF, Rienstra M, Friedrich AW, Samani NJ, Ng LL, Dickstein K, Lang CC, Filippatos G, Anker SD, Ponikowski P, Metra M, van Veldhuisen DJ, Voors AA (2020) Circulating plasma concentrations of angiotensin-converting enzyme 2 in men and women with heart failure and effects of renin–angiotensin–aldosterone inhibitors. Eur Heart J 41: 1810–1817

Satarker S, Tom A, Shaji R, Alosious A, Luvis M, Nampoothiri M (2020) JAK-STAT pathway inhibition and their implications in COVID-19 therapy. Postgrad Med 133(5):489–507. Accessed April 2022

Shiraki K, Daikoku T (2020) Favipiravir, an anti-influenza drug against life-threatening RNA virus infections. Pharmacol Ther 209:107512. Accessed April 2022

Sinha N, Balayla G (2022) Hydroxychloroquine and COVID-19. [online]. Available at https://pmj.bmj.com/content/postgradmedj/96/1139/550.full.pdf. Accessed April 2022

Snell N (2001) Ribavirin - current status of a broad spectrum antiviral agent. Expert Opin Pharmacother 2(8): 1317–1324. Accessed April 2022

Song Z, Xu Y, Bao L, Zhang L, Yu P, Qu Y et al (2019) From SARS to MERS, thrusting coronaviruses into the spotlight. Viruses 11(1):E59. https://doi.org/10.3390/v11010059. Accessed March 2022

Tripathy S, Dassarma B, Roy S, Chabalala H, Matsabisa M (2020) A review on possible modes of action of chloroquine/hydroxychloroquine: repurposing against SAR-CoV-2 (COVID-19) pandemic. Int J Antimicrob Agents 56(2):106028. Accessed April 2022

Turner L, Munsie M, Levine A, Ikonomou L (2021) Ethical issues and public communication in the development of cell-based treatments for COVID-19: lessons from the pandemic. Stem Cell Rep 16(11):2567–2576. Accessed April 2022

UK Health Security Agency (UKHSA) (2022.) Data series on deaths in people with Covid-19 – Technical summary - UK Heath Security Agency data series on deaths in people with COVID-19 (available at UK Heath Security Agency data series on deaths in people with COVID-19 publishing.service.gov.uk). Accessed March 2022

V'kovski P, Gultom M, Kelly JN, Steiner S, Russeil J, Mangeat B, Cora E, Pezoldt J, Holwerda M, Kratzel A, Laloli L, Wider M, Portmann J, Tran T, Ebert N, Stalder H, Hartmann R, Gardeux V, Alpern D, Deplancke B, Thiel V, Dijkman R (2021) Disparate temperature-dependent virus-host dynamics for SARS-CoV-2 and SARS-CoV in the human respiratory epithelium. PLoS Biol 19(3):e3001158

Wang K, Gheblawi M, Oudit GY (2020) Angiotensin converting enzyme 2: a double-edged sword. Circulation 142(5):426–428

Xu H, Zhong L, Deng J, Peng J, Dan H, Zeng X, Li T, Chen Q (2020) High expression of ACE2 receptor of 2019-nCoV on the epithelial cells of oral mucosa. Int J Oral Sci 12(1):8

Yang CW, Lu LC, Chang CC, Cho CC, Hsieh WY, Tsai CH, Lin YC, Lin CS (2017) Imbalanced plasma ACE and ACE2 level in the uremic patients with cardiovascular diseases and its change during a single hemodialysis session. Ren Fail 39(1):719–728

Ye Q, Wang B, Mao J (2020) The pathogenesis and treatment of the 'Cytokine Storm' in COVID-19. J Infect 80(6):607–613. Accessed April 2022

Yeung M, Teng J, Jia L, Zhang C, Huang C, Cai J, Zhou R, Chan K, Zhao H, Zhu L, Siu K, Fung S, Yung S, Chan T, To, K, Chan J, Cai Z, Lau S, Chen Z, Jin D, Woo P, Yuen K (2021) Soluble ACE2-mediated cell entry of SARS-CoV-2 via interaction with proteins related to the renin-angiotensin system. Cell 184(8): 2212–2228.e12

Zumla A, Wang F, Ippolito G, Petrosillo N, Agrati C, Azhar E, Chang C, El-Kafrawy S, Osman M, Zitvogel L, Galle P, Locatelli F, Gorman E, Cordon-Cardo C, O'Kane C, McAuley D, Maeurer M (2020) Reducing mortality and morbidity in patients with severe COVID-19 disease by advancing ongoing trials of Mesenchymal Stromal (stem) Cell (MSC) therapy – achieving global consensus and visibility for cellular host-directed therapies. Int J Infect Dis 96:431–439. Accessed April 2022

Part II

Radiology and Patient Care

The Evolution of Equipment and Technology for Visualising the Larynx and Airway

4

Duncan King and Alison Blair

Abstract

Laryngoscopy and endotracheal intubation are the core skills of an anaesthetist. The tools and equipment used today are unrecognisable from the methods used in the first recorded attempts at laryngoscopy over 200 years ago. The evolution of the modern-day laryngoscopes has mirrored advancements in technology within general society, and particularly with regard to computer and fibreoptic technology over the last 30 years. The development of these modern visualisation devices would not have been possible without those that went before it, as each new device has been influenced by the previous. Video laryngoscopes have quickly gained popularity as the primary intubating device in many scenarios, driven by ease of use as well as positive patient outcomes. While it is still debated whether videolaryngoscopes can replace direct laryngoscopy for routine intubations, their effectiveness in difficult airways is unquestioned. This chapter will cover the anatomy of the airway and the development of technology from the rudimentary creations in the early 1700s to the modern larynsgocopes created in the twenty-second century which allow the user to view the airway in more detail in order to secure endotracheal intubation even in an airway where intubation would be difficult.

4.1 Airway

The larynx is located in the anterior aspect of the neck at the level of the third to sixth cervical vertebral bodies and lies at the junction between the oesophagus and trachea. It is bordered by the hyoid bone superiorly and the cricoid cartilage inferiorly (Strandring et al. 2015). The primary function of the larynx is to protect the trachea from the aspiration of substances, by closing, in a sphincter valve-like mechanism, upon mechanical stimulation, typically during swallowing of food or liquid. The larynx also plays a crucial role in phonation and the regulation of breathing (Pohunek 2004; Isaacs and Sykes 2002).

The anatomy of the larynx can be described by its external anatomy and its internal anatomy.

It is composed of a rigid cartilaginous skeleton, and an inner lining of muscles. The skeleton consists of three large unpaired cartilages (epiglottis, thyroid, and cricoid) and three smaller

D. King
Northern Irish Medical and Dental Agency, Belfast, Northern Ireland

A. Blair (✉)
Craigavon Hospital, Southern Health and Social Care Trust, Craigavon, UK
e-mail: alison.blair@southerntrust.hscni.net

paired sets of cartilages (arytenoids, corniculate, cuneiform) (Strandring et al. 2015).

Epiglottis It is a leaf-shaped cartilage that flattens and moves down to cover the superior opening of the larynx, preventing aspiration during swallowing. It is attached by a "stalk" to the anterior aspect of the thyroid cartilage. A clinically important pair of pouch-like areas situated between the epiglottis and the base of the tongue are known as the valleculae. A Macintosh-style laryngoscope is placed into this space to allow a good view of the laryngeal inlet while intubating.

Thyroid Cartilage It is the biggest of the cartilages of the larynx. It is composed of two lamina and the anterior conjoint region between the two is known as the laryngeal prominence (colloquially known as the Adams apple) (Strandring et al. 2015). Superiorly, the lamina project to form superior horns, which attach to the hyoid bone via the thyrohyoid membrane. Inferiorly the lamina forms inferior horns which attach to the cricoid cartilage via the cricothyroid membrane (Isaacs and Sykes 2002).

Cricoid Cartilage It is a signet ring-shaped cartilage that encircles the airway. The cricoid ring consists of a tall posterior sheet or lamina and a much narrower anterior arch. The cricoid cartilage itself signifies the inferior border of the larynx and is found at the level of sixth cervical vertebra. It articulates with the thyroid cartilage as well as the arytenoids (Pohunek 2004). The cricoid is the only laryngeal cartilage that is a complete ring, a fact that is utilised clinically during emergency intubation or non-fasted patients. External pressure anteriorly over the cricoid cartilage causes compression of the oesophagus and theoretically reduces the risk of regurgitation and aspiration of stomach contents (Roberts et al. 1994).

The paired **arytenoids** cartilages are three-sided pyramidal shaped and they articulate with the border of the lamina of the cricoid. The apex of the arytenoids is where the corniculate cartilages articulate. The lateral extension of the arytenoids is known as the muscular process and serves as an attachment point for the cricoarytenoid muscles. The medial aspect of the base is known as the vocal process. The vocal ligament (part of the vocal cord) attaches at the vocal process and extends across to the thyroid cartilage (Strandring et al. 2015).

The epiglottis is attached to the arytenoids by the aryepiglottic ligament.

The **cuniform and corniculate** cartilages are embedded within these vocal folds. The corniculate cartilages attach to the apex of the arytenoids. They serve to reinforce and support the aryepiglottic folds.

There are several membranes and ligaments of the larynx that serve as support for the cartilaginous skeleton. These can be described as extrinsic if they attach the larynx to surrounding structures, or intrinsic, when they connect the various laryngeal cartilages together and hold it as one single functioning unit (Strandring et al. 2015).

4.1.1 Extrinsic

- Thyrohyoid membrane—connects the thyroid cartilage to the hyoid bone (which is not technically part of the larynx)
- Hyoepiglottic ligament—attaches the hyoid bone to the epiglottis
- Cricotracheal ligament—attaches the cricoid cartilage to the first tracheal ring.

4.1.2 Intrinsic

- Cricothyroid membrane—connects the cricoid and thyroid cartilages. It is composed of two parts; a single thickened median cricothyroid ligament and two lateral cricothyroid ligaments (also known as conus elasticus). The cricothyroid membrane is clinically important as the site of insertion of an emergency airway in a "Can't Intubate Can't Ventilate" scenario (Roberts et al. 1994).
- Quadrangular membrane—a relatively large membrane that stretches between the lateral aspect of the epiglottis and the arytenoid

cartilages. The lower margin is thickened to form the vestibular ligament, while the upper margin forms the aryepiglottic folds (Strandring et al. 2015).

The laryngeal cavity is the internal space between the laryngeal cartilages and extends from just below the epiglottis to the base of the cricoid cartilage. When viewed during laryngoscopy from above, there are two paired protrusions of soft tissue into the laryngeal cavity. The superior vestibular folds (or false vocal cords), and inferior to that the white vocal folds (or true vocal cords). The two-dimensional space in between the true vocal cords is known as the rima glottidis.

4.1.3   Laryngeal Muscles

The complex range of functions performed by the larynx is made possible by numerous sets of muscles. These again can be classified into intrinsic (which are involved in phonation) and extrinsic muscles (which move the whole larynx superiorly and inferiorly) (Roberts et al. 1994).

Extrinsic Muscles are compromised of the suprahyoid groups (which generally elevate the larynx) and the infrahyoid groups (which generally lower the larynx).

The **Intrinsic Muscles** together have three distinct functions

- To close the vocal cords and inlet during swallowing
- To open and relax the vocal cords during inspiration
- To tense the vocal cords during phonation

The cricothyroid muscle acts to tense and stretch the vocal cords and helps to create forceful speech. The thyroarytenoid muscle relaxes the vocal cords. The posterior cricoarytenoids abduct the vocal cords, while the lateral cricoarytenoids and the transverse arytenoid muscles adduct the arytenoids, closing the glottis. The oblique arytenoids and the aryepiglottic muscles adduct the arytenoids, closing the glottis (Pohunek 2004; Roberts et al. 1994).

4.1.4   Innervation of the Larynx

Laryngeal innervation is provided by two nerves, the recurrent laryngeal nerve and branches of the superior laryngeal nerve. Both are themselves branches of the vagus nerve. The superior laryngeal nerve has two important branches—the internal and the external branches. The *internal* receives sensory information from the glottis, the supraglottis and the inferior aspect of the epiglottis. The *external* branch provides motor innervation to the cricothyroid muscle only. The recurrent laryngeal nerve has sensory and motor function. It receives sensory information from the subglottis and provides motor innervation to all of the other intrinsic muscles of the larynx. Of important clinical note, the glossopharyngeal nerve provides sensory innervation to the tongue base and the vallecula. It is this that is stimulated during the process of laryngoscopy and endotracheal intubation (Strandring et al. 2015).

4.2   Endotracheal Intubation

Endotracheal intubation is the process of inserting a tube through the vocal cords and into the trachea. It is a common, and essential skill in anaesthesia and done to protect and control the patient's airway (Collins 2014). There are in effect an immeasurable number of indications for endotracheal intubation. These indications can be categorised into:

1. Protection of regurgitation of stomach contents—e.g. in patients with low conscious level.
2. Allow for mechanical ventilation during surgery where spontaneous ventilation is not possible or adequate such as when muscle relaxation is required.
3. Respiratory failure—due to any cause, such as low conscious level, severe infection or muscle weakness.
4. Partial or complete airway obstruction—which again can be due to any cause (low conscious level, infections, tumours).

5. To aid safe diagnostic procedures or management—e.g. in patients who are intoxicated or poorly co-operative, putting themselves or others at risk.
6. Shock syndrome of any cause—to allow tight control of gas exchange in ICU (Hagberg 2018).

Controlling a patient's airway is required in the case of airway obstruction, often because the patient has a low conscious level (through induction of anaesthesia, or other causes), resulting in tissues around the upper airway losing their tone and obstructing. Endotracheal tubes, when placed within the trachea, result in a sealed circuit once connected to a ventilator. This is achieved using a balloon "cuff" in the distal aspect of the tube. Inflating this cuff with air when placed in the trachea creates this seal, therefore protecting the airway from aspiration and allowing for positive pressure ventilation (Hagberg 2018).

4.2.1 Laryngoscopy

Laryngoscopy is the broad term used for visualisation of the larynx. It is a key practical skill involved in anaesthetics, as it allows for insertion of endotracheal tubes and is one of the earliest key skills developed in anaesthetic training.

Historically, humans have been obsessed with developing means to visualise the internal body structures, and the larynx is no different. Physicians interest in visualising the larynx can be traced to as early as mid-1700s (Burke 2004). However, the historical credit for whom created the laryngoscope as we know it is debated and serves its roots in some related inventions from the 1800s.

4.2.2 Early Devices

Despite the laryngoscope being the key tool of the modern-day anaesthetist, early devices were in fact created and used by surgeons. These early creations were fairly rudimentary, and alterations and adaptions have been made over the years by successive scientists and resulting in the laryngoscope we know today (Burke 2004). In 1743 a French surgeon named Leveret documented using a highly polished metal spatula to visualise the nasopharynx. He combined this with a snare-like device to remove nasal polyps.

In 1807 German Physician Philipp von Bozzini published a report on his device he called his "light conductor" or "Lichtleiter" (Roth 2008). He described his device as "a simple apparatus for the illumination of the internal cavities and spaces in the living animal body" (Roth 2008). Von Bozzini's device comprised a speculum with a set of parallel tubes inside it. He utilised light from a candle which is placed in one of the tubes. This light is reflected down the tube into the viewed body cavity, and the second metal tube is used for viewing. This use of an external light source differentiated his device from earlier reflective devices. While von Bozzini described using his device to visualise the nasopharynx and hypopharynx (among other cavities), he never described visualisation of the larynx (Bailey 1996; Pieters et al. 2015).

Benjamin Guy Babington in 1829 published a report to the Hunterian society on his invention the "glottoscope" which he used to view the larynx (Roth 2008). The "glottoscope" used sunlight for illumination and consisted of a system of mirrors as well as a separate tongue depressor which he successfully used to visualise the larynx (Pieters et al. 2015). The patient would be sitting with their back to the sun and the user would then hold a hand mirror, reflecting the sun's light to the back of the patient's throat. A small mirror, which was attached to a spatula, was then used to visualise the larynx. Although there was documentation of Babington being able to view the larynx, there was no reference made to the vocal cords and their function (Burke 2004).

Despite all these earlier examples and inventions, it is Manuel García who is generally credited with the rather dubious title of "father of Laryngology". It is he who is considered to have viewed the functioning glottis and vocal cords in their entirety. García was a singer by trade, and in a quest to improve his singing and teaching, he

wanted to learn how the vocal cords functioned. Again, using the sun as an external light source, García's device used two mirrors, and was able to observe his own functioning vocal cords and the upper segments of his trachea (Burke 2004). In his paper in 1855, García described the action of the vocal cords during inspiration and vocalisation and production of sound in the larynx (Bailey 1996).

Laryngoscopy in this period was greatly hindered by the requirement of an external light source. This was restricted to using the sun, or a candle, both of which were extremely impractical. It was not until Thomas Edison invented the lightbulb in 1878 that significant advances could be made.

4.2.3 From Indirect to Direct

All devices and methods used for visualising the larynx and vocal cords had been under indirect vision, i.e. through reflection using mirrors, that is until Alfred Kristein first described his device the "Autoscope" in 1895 (Hirsch et al. 1986). His device consisted of an electrical light source termed the "electroscope", which formed the handle of the Autoscope. The light rays were focused by a lens, and then reflected through 90 degrees by a prism. A thick, rounded blade was attached to the bottom of the handle, through which the light was transmitted. The blade was used to displace the tongue and epiglottis anteriorly, therefore allowing direct visualisation of the laryngeal inlet. Further developments by Kristein produced two distinct blades for his Autoscope. One which was placed into the vallecula, with anterior pressure elevating the epiglottis allowing visualisation of the larynx. The other, known as the "intralaryngeal blade", was placed beneath the laryngeal surface of the epiglottis (Fig. 4.1). Forward and upward pressure lifted the epiglottis, revealing the larynx below (Hirsch et al. 1986). These two blades are clear predecessors to the Macintosh and Miller blades. Kristein not only pioneered the predecessor to the modern-day direct laryngoscope, but he also understood the importance of patient positioning for successful
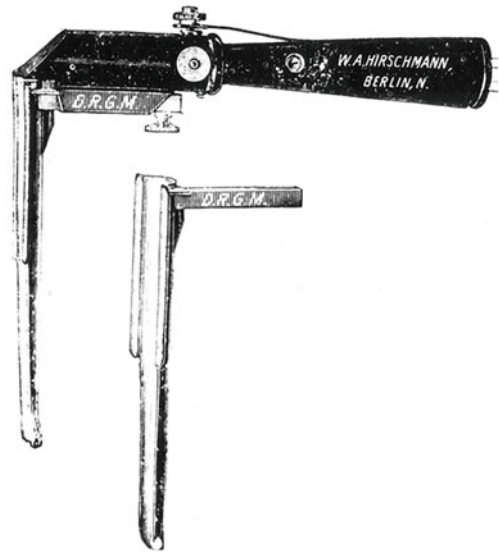
Fig. 4.1 Kirstein's modified autoscope. The standard blade is shown attached to the handle, with the intralaryngeal blade shown below. Medical Historical Library, Harvey Cushing/John Hay Whitney Medical Library. Reprinted with permission

laryngoscopy. He described "the body must be placed in such a position that an imaginary continuation of the laryngotracheal tube would fall within the opening of the mouth" (Hirsch et al. 1986). He understood that extension of the atlanto-occipital joint is required, in what is now colloquially termed the "sniffing the morning air" position (Pieters et al. 2015).

Chevalier Jackson was the first to combine direct laryngoscopy with endotracheal intubation. He invented a U-shaped laryngoscope with a handle and a blade with an incorporated distal light (Fig. 4.2). This differentiated his device from Kristein's earlier one, which used a proximal light source. Jackson's laryngoscope also incorporated a sliding base on the blade to allow easy passage of an endotracheal tube (Moon et al. 2021). He was also the first to introduce laryngoscopy in the supine position, rather than the sitting position that all previous methods had utilised. Jackson also further emphasised the importance of c-spine flexion with head extension for laryngoscopy (Pieters et al. 2015).

Up until this time, the laryngoscope (or earlier devices), were tools used by surgeons, primarily

Fig. 4.2 Jackson's laryngoscope. Wood library-Museum of Anesthesiology Reprinted with permission

for diagnostic purposes. It was clear that direct laryngoscopy showed potential benefits for anaesthesia, and it was an American anaesthetist, Henry Janeway, who was influential in popularising the use of direct laryngoscopy in anaesthetics. Surgery at the time was primarily performed using inhalation anaesthesia, by placing a cone over the patient's mouth and nose. There was no protection against collapse of the patient's upper airway and obstruction by the tongue, and there was also a high risk of aspiration of blood, mucus, or vomit during surgery. Janeway recognised these risks, and the potential for tracheal intubation to alleviate these and showed improved success of these surgeries by achieving this (Burke 2004). He noted the difficulty in achieving reliable and safe tracheal intubation, and so developed a laryngoscope with the sole purpose of aiding this (Pieters et al. 2015). His device, known as the "speculum", incorporated a battery-powered distal light source situated within the handle itself allowing more manoeuvrability of the device. He also added a central notch to the blade to guide the tube during placement, as well as a slight curvature to the distal tip to help direct the tip through the vocal cords (Burke 2004).

The horrifically disfiguring injuries sustained in World War 1, resulted in further advancements within the field of airway management in anaesthetics. Two British Anaesthetists, Sir Ivan W. Macgill and Edward S. Rowbotham,

described anaesthesia for reconstructive facial surgery for British soldiers. They realised that surgery for these soldiers was easier with the airway secured with an endotracheal tube. From the early 1920s, they described several alterations and advancements to laryngoscopy, each of which aimed at providing safe means to secure the patients airway for facial surgery (Magill 1930; Rowbotham and Magill 1921).

Rowbotham and Magill (1921) described using a laryngoscope developed similar to Janeway's earlier device, whilst incorporating a "guiding rod". This was a metal rod used to grasp the end of the endotracheal tube and direct it into the trachea under direct vision (Rowbotham 1920). Magill designed a U-shaped laryngoscope in 1926, which itself was a modification of the earlier Jackson laryngoscope (Magill 1926). Magill also altered his laryngoscope to be "folding"—similar to a modern direct laryngoscope device. He suggested an intubation technique of inserting the blade in a "paraglossal approach", i.e. inserting the blade at the side of the mouth rather than the midline, which helped improve the view. He also put batteries into the handle, continuing from Janeway's earlier advancement. Magill also introduced his now ubiquitous "Magill forceps", heavily based on Rowbotham's "guiding rod", which help to direct the tube into the trachea during endotracheal intubation (Magill 1930).

A wide range of ultimately very similar laryngoscopy blades were being described at this time. Robert Miller described his "straight" laryngoscopy blade, (the so-called "Miller Blade") in 1941 (Pieters et al. 2015; Miller 1941). While so-called "straight", there was still a slight curve to the blade two inches from the tip. The blade was designed to be placed under the epiglottis and directly lift it onto the anterior wall of the larynx, allowing a view of the vocal cords. In 1946 Miller produced an infant version, which proved extremely successful, and is still used today. Infant anatomy is still considered by many to be more suited to the use of a straight blade when performing laryngoscopy.

Probably the most significant and enduring advancement in the field of direct laryngoscopy

was made by Robert Macintosh. He described the endotracheal intubation prior to the advent of muscle relaxants as a "tour de force", and believed that the hallmark of a successful anaesthetist was "the ability to pass an endotracheal tube under direct vision" (Scott 2009; Macintosh 1943). The majority of anaesthetists at the time would often struggle to expose the vocal cords of their unparalysed patients. The ground-breaking 1942 paper on the first use of muscle relaxation (Griffith and Johnson 1942) was yet to be published, and it was necessary to deepen the patient with large doses of general anaesthesia before attempting intubation (Scott 2009). The invention of muscle relaxation allowed much easier exposure of the vocal cords, as well as easier passing of endotracheal tubes through relaxed cords. It also significantly reduced the rate of laryngospasm, the potentially life-threatening condition where the vocal cords spasm and clamp shut, preventing any air getting into the lungs (Hagberg 2018).

Macintosh felt that many anaesthetists were struggling to consistently intubate patients due to issues with poor technique. During direct laryngoscopy, the standard practice at the time involved passing a straight blade in the midline and lifting the epiglottis, even though Magill had clearly described the technique of paraglossal straight-blade laryngoscopy (Scott 2009). Macintosh disagreed with the midline approach. In his 1943 textbook, he wrote that using a straight blade in the midline could "make the tongue bulge over the blade and obscure the view" (Macintosh 1943). Poor straight-blade technique hindered laryngoscopy and set the stage for Macintosh to develop his famous laryngoscope (Scott 2009).

Macintosh experimented with different devices and found one day during tonsillectomy surgery, "Opening the mouth with the Boyle-Davis gag, I found the cords perfectly displayed . . . before the morning had finished" (Scott 2009), The "Boyle-Davis gag" was a curved metal device placed in the mouth and used to visualise the oropharynx and stabilise the tonsils for surgery. He got his assistant to solder this "Boyle-Davis gag" onto a laryngoscope blade, and thus the Macintosh blade was born.

Macintosh discovered that the key to achieving this "perfect display" of the laryngeal inlet was his new method of indirectly elevating the epiglottis: "the important point being that (with a blade shorter than other laryngoscopes) the tip finishes up proximal to the epiglottis" (Jephcott 1984). Macintosh was not the first to observe that the blade did not need to go beyond the epiglottis, he was however the first to suggest the standard of placing the blade tip within the vallecula (Scott 2009). He illustrated the fact that when the laryngoscope tip is placed in the vallecula and is "lifted . . . the epiglottis, because of its attachment to the base of the tongue, is drawn upwards and the (entire) larynx comes into view"(Macintosh and Bannister 1943) This new technique of indirectly elevating the epiglottis still remains the preferred method of direct laryngoscopy worldwide (Scott 2009).

Despite acknowledging the obvious curve of his own laryngoscope, Macintosh believed that people focused too much on the curve of the blade. He stated that "The precise shape or curve of the blade does not seem to matter much provided the tip does not go beyond the epiglottis" and providing the technique of the user was adequate (Macintosh 1944). Macintosh eventually settled on a curve that mimicked that of the, then-popular, Magill's endotracheal tube. In fact, in the early days Macintosh laryngoscopes could be bought with various curves, or even straight, illustrating that the point was not the curve, but rather the method of indirectly lifting the epiglottis with a shorter blade (Scott 2009).

The Macintosh and the Miller laryngoscope formed the cornerstone of anaesthetic airway management until modern times, and indeed are still the predominant laryngoscopes used in much of the world today (Fig. 4.3). There are a small, but significant number of people whom obtaining an adequate view of the glottis is either extremely difficult or impossible with the Macintosh and Miller laryngoscopes. As a result, there have been several attempts to modify these in order to overcome these situations (Hagberg 2018).
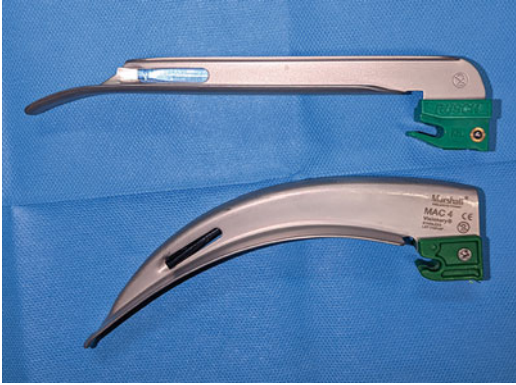
Fig. 4.3 Modern Miller (top) and Macintosh (bottom) laryngoscope blades

Before considering the modifications, it is useful to understand the components of the modern laryngoscope.

4.2.4 Modern Laryngoscope

The basic structure of a laryngoscope consists of a blade, a handle and a light source (Hagberg 2018). The main shaft of the blade is known as the spatula. Its function is to displace and compress the tongue and soft tissues. This allows the oral and pharyngeal axis to be aligned, providing a direct line of site between the laryngeal inlet and the operators eye (Figs. 4.4, 4.5, and 4.6). The blade can be straight or curved as previously discussed. The blade also comes in different sizes, from size 0 (used in neonates) to size 4 (used in large adults) (Fig. 4.7).

The upward projection on the top of the blade is known as the flange (Figs. 4.4, 4.5, and 4.6). On the Macintosh laryngoscope the flange is a reverse-Z shape, and functions to help displace and hold the tongue out of the field of vision. The tip of the laryngoscope (sometimes called the beak) is blunt and thickened in order to prevent any trauma to the soft tissues. The light source is located in close proximity to the tip, and is provided either directly by a lightbulb, or indirectly via fibreoptics from a light source at a distance. The handle of the laryngoscope contains the batteries for the light source and comes in
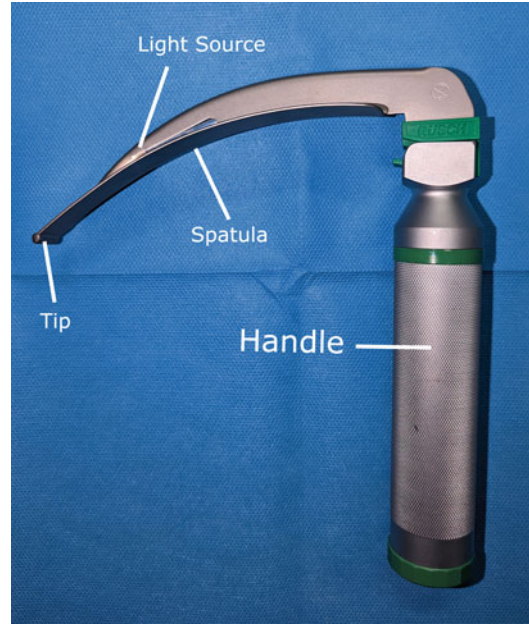
Fig. 4.4 Modern Macintosh blade and handle lateral view

various sizes. These are standard, paediatric (which is thinner to improve the balance with small paediatric blade) and a short handle (to improve ease of intubating obese patients or those with large breasts). The blade attaches onto the handle via a hook at the base of the blade. This base also contains an electrical contact that provides power from the battery to the light (Figs. 4.4, 4.5, and 4.6).

Despite the enduring popularity and success, even until present day, of the Macintosh and Miller largyngoscopes, there was a small but significant proportion of the population upon whom
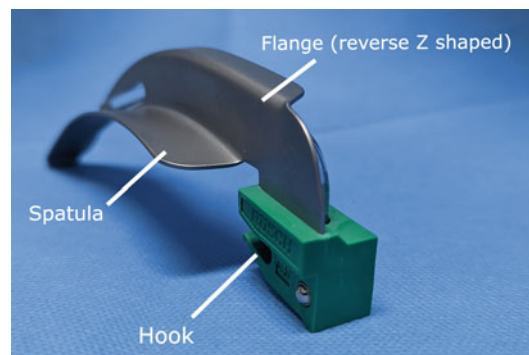
Fig. 4.5 Modern Macintosh blade and handle
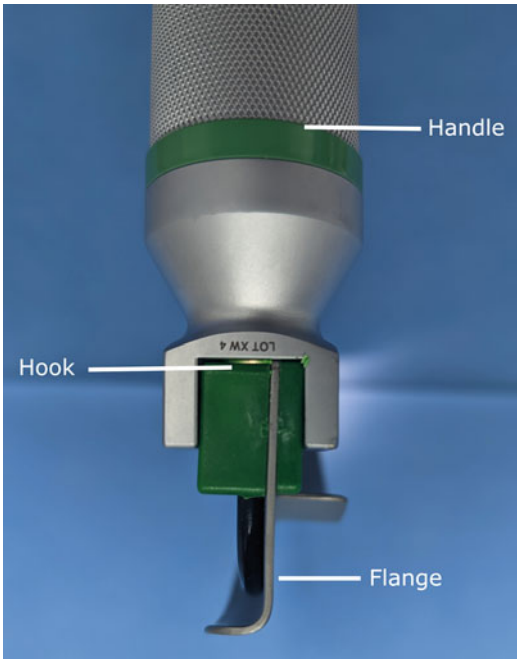
Fig. 4.6 Modern Macintosh blade (posterior view). Note reverse z-shaped flange

obtaining an adequate view of the vocal cords was either extremely difficult or impossible using these devices. There has over the years

Fig. 4.7 Modern Macintosh blade size (from top to bottom) 4, 3, 1, and 0

been numerous attempts, through functional adaptions to the "basic" Macintosh or Miller laryngoscope to try and rectify this.

4.2.5   Macintosh Related Curved Blades

One of the first adaptions to Macintosh's blade was by Dr. Parrott in 1951. He lengthened the blade by around 2.5 cm and created a more gradual curve. This was in an attempt to facilitate intubating patients with prominent teeth or a receding jaw, while the additional length was useful in larger patients (Parrott 1951). The Parrott laryngoscope was otherwise identical to the Macintosh.

While it was recognised that the straight and curved blades each had their own specific advantages, Drs. Bowen and Jackson created a laryngoscopy blade in 1958 that they hoped could be successful in all difficult scenarios. The blade was almost straight with a significant curve to the distal aspect, and the tip was split. This split allowed it to be placed deep into the vallecula, and in theory more effectively lift the epiglottis (Bowen and Jackson 1952).

A mirror-imaged version of the Macintosh laryngoscope exists, fairly oddly named the "left-handed laryngoscope", as it is conversely held in the user's right hand. It is identical in blade shape as the regular Macintosh laryngoscope, however the flange is orientated in the opposite direction. This could be used in patients with oropharyngeal abnormalities necessitating placement of the endotracheal tube in the left side of the patients' mouth (Pope 1960).

The distal spatula of a few blades has been reported as having a sharper curve than the Macintosh. Most noteworthy was one produced by Gubuya-Orkin, which was first described in 1959. This was distinctive for having an S-shaped blade and a 3 cm bendable distal portion which they described bending it through a range of 15–45°. The ideal intubating angle, according to the authors, is 35° from horizontal, which enables the instrument to lift the epiglottis indirectly (Gabuya and Orkin 1959). The blade,

which was discovered to be particularly successful in some cases when laryngoscopy using the Macintosh blade had failed, may have been the prototype for other blades having a distinct set or adjustable distal curvature (Hagberg 2018).

A significant improvement was made to the original Macintosh laryngoscope by Raez (1984). He altered the mid-blade by flattening the curve slightly and made slightly concave. These combined alterations should lessen the "crest-of-hill" effect, in which the convexity at the midblade can obstruct the direct line of vision between the user and the laryngeal inlet. This blade is known as the *Improved view Macintosh* (Raez 1984).

4.2.6   Miller Related Straight Blades

There have been numerous attempts at alterations to the classic Miller straight blade. Most notably are the Soper, the Wisconsin and the Phillips blades. The Soper was introduced in 1947, which was largely straight. It was produced in response to difficulty in lifting a long "flabby" epiglottis by the Macintosh blade (Soper 1947). It had a small transverse slot cut into the distal blade in order to prevent the epiglottis from slipping off the blade. The Wisconsin is entirely straight with a C-shaped flange that gradually increases in size from proximal to distal (Hagberg 2018). The Phillips blade was released in 1973 and is a combination of the slightly curved tip of the Miller and the shaft of the Jackson blade (Phillips and Duerksen 1973). The Soper, the Winsonsin and Phillips blades are all still in commercial use today.

4.2.7   Levering Tip Laryngoscope

The levered tip laryngoscope (Corazzelli-London-McCoy or CLM blade) was initially produced as an adaption to the Macintosh curved blade in 1993, although it is now readily available in both curved and straight blade configurations. These blades have a distal hinging tip that can be activated by a spring-loaded lever attached to the laryngoscopes handle. Pressing the lever elevates the tip, which is the final 2.5 cm of the blade, by around 70° (Figs. 4.8 and 4.9). This tip can act in the vallecula, providing good contact with the hyoepiglottic ligament, allowing lifting of the epiglottis. This can be particularly useful in situations of limited neck movement, where force through the blade could be detrimental, or situations of limited mouth opening (McCoy and Mirakhur 1993). In theory less force is required when using a CLM blade, and therefore less sympathetic stimulation is seen (increasing heart rate or mean arterial pressure) (McCoy and Mirakhur 1995). Some recent studies have shown using the CLM blade and engaging the tip may in fact worsen an otherwise easy view (Tuckey et al. 1996). This is thought to be due to the fact that in these "easy views" the tip would easily and fully engage the vallecula and lift the hyoepiglottic ligament. Further activation of the handle and tip in fact causes posterior displacement of the blade, as there is no further anterior displacement of the hyoepiglottic ligament possible, which causes worsening of the view (Levitan and Ochroch 1999). The CLM blade has been the most recent significant adaption to the classical indirect laryngoscopes.

Fig. 4.8 CLM laryngoscope

Fig. 4.9 CLM laryngoscope with hinging tip activated

4.2.8 Return to Indirect Laryngoscopy

While the Macintosh and Miller blades ensured that direct laryngoscopy was by far and away the most common method of endotracheal intubation, there have been numerous rigid indirect laryngoscopes introduced over the last 60 years. These rigid indirect laryngoscopes allow a view of the laryngeal inlet and vocal cords indirectly through the use of mirrors, fibreoptic cables, or video cameras (Hagberg 2018). They provide an advantage as they can "look round the corner", therefore potentially improving an otherwise difficult intubation. The structure of these indirect laryngoscopes can vary from a slightly adapted Macintosh blade to an entirely distinctive design altogether.

While the impression of these indirect laryngoscopes is that they are modern inventions, in fact the first widely available device was produced by Siker in 1959. He produced a blade with an incorporated mirror, which can be used to identify the epiglottis and laryngeal inlet if they cannot be directly visualised. Copper wiring attaches the mirror to the blade, allowing heat conduction in an attempt to prevent the mirror from steaming up. The mirror inverts the image, meaning that the process of tracheal intubation

takes a large amount of specific practice with the Siker device (Siker 1956).

McMorrow and Mirakhur developed a similar mirrored device. It was an adaption of the regular CLM laryngoscope but was unique in that activating the lever not only elevated the tip, but deployed a mirror posteriorly and inferiorly to the blade (McMorrow and Mirakhur 2003).

4.2.9 Prisms in Laryngoscopes

The use of prisms in laryngoscopes was not a new concept, as Kristen had done in the late nineteenth century, however Huffman (1968) re-introduced the concept. He attached a triangular prism to a Macintosh blade, allowing refraction of the light through 30 degrees, and allowing the user to "see round the corner" (Huffman 1968). This allowed improvement in obtainable view in particularly challenging intubations, and also allowed less force to be used when trying to obtain a view. He subsequently attached a second prism more proximally, creating a second device that allowed refraction of light through 80°.

The Airtraq device was the most commercially and clinically available Prism-assisted device. The blade of the Airtraq is designed to be "anatomically shaped", and thus at a more acute angle than the Macintosh blade. The concept was aimed at creating a device that would provide a view of the laryngeal inlet while not requiring alignment of the oral, pharyngeal, and tracheal axes (Hagberg 2018). This allows easy visualisation of the glottis while intubating. As the Airtraq is able to "look around the corner" of the tongue to obtain a laryngeal view while using minimal "lifting force", it is suggested it provides a clinical advantage in certain scenarios. These include patients with an anterior larynx (a term used within to describe the phenomenon of the laryngeal inlet appearing more anterior to the line of sight during laryngoscopy) or restricted neck movements from any cause (fractures and immobilisation collars, radiotherapy, burns etc.). The Airtraq consists of two adjacent channels. The "viewing channel" consists of various lenses and prisms and terminates at the proximal eye

piece on the laryngoscope handle. The adjacent channel acts as a "housing channel" for the endotracheal tube and allows easy advancement of the tube down the channel and through the vocal cords, under vision via the eyepiece. With the tube in position, it can be separated from the Airtraq device by "peeling". The battery-powered light source is found at the tip of the blade, as is a small heater, which heats and prevents fogging of the distal lens (Hagberg 2018).

4.2.10   Fibreoptics

The largest and most significant development with regard to laryngoscopy and intubation over the last 70 years has without doubt been the introduction of fibreoptics. Fibreoptic scopes were initially developed in the 1950s for use as endoscopes. Over time, bronchoscopes became more readily used, but it was not until the 1980s when fibre-optics were utilised in anaesthetic practice as part of rigid indirect laryngoscopes (Hagberg 2018).

Fibre-optic cables transmit their light by means of total internal reflection. This is the process by which light in a medium is completely reflected back into the medium by its surroundings. All light is refracted (or "bent") to a degree when it passes between two differing substances. This is because the substances have a different refractive index. A commonly seen example of this is viewing an object that is half submerged in water. Water and air have different refractive indices so the object will appear bent at the point it enters the water. Total internal reflection occurs when refraction is so great that the whole beam is bent (or reflected) back into the original material. This occurs when the angle between the light source and the boundary is greater than the critical angle.

A fibre-optic cable transmits information as light (photons) via incredibly thin (around 20 µm in diameter) strands of glass or plastic known as optical fibres. There are around 15,000 of these glass fibres in a fibre-optic scope. Fibreoptic devices have bundles of around 15,000 glass fibres, each about 20 µm in diameter.

These strands make up the core of the fibre-optic cable. The core is surrounded and encased by a layer of a different type of glass known as the cladding. It is the boundary between the core and the cladding that allows for total internal reflection. The cladding is surrounded by a protective coating, as well as strengthening and supportive Kevlar fibres in modern devices.

These fibre-optic scopes allow rapid and clear transmission of pictures, which has revolutionised medical practice, from endoscopes to view the gastrointestinal tract to bronchoscopes which allow fibre-optic intubations.

Rigid indirect fibre-optic laryngoscopes were the biggest evolutionary change in anaesthetics since Mactinosh's creation. While the popularity of the laryngoscopes individually was never great, they signalled a significant advancement in the technology in anaesthetic practice. They were introduced in the late 1980s in the form of the Bullard Laryngoscope. It features a rigid L-shaped blade and incorporates fibre-optic bundles that transmit the image to the proximal eye piece (Kastnelson and Straker 1996). The blade of the Bullard laryngoscope is anatomically shaped, allowing for indirect visualisation of the laryngeal inlet, without alignment of the oral, pharyngeal, and laryngeal orifices. It was conceived as a laryngoscope that is useful in patients who are difficult to intubate, particularly with minimal neck movement. It can also be used for awake intubation in patients as minimal "lifting force" is required for intubation. The Bullard laryngoscope features a "work channel" which lies posterior to the blade and can be used for suction as well as local anaesthetic or oxygen administration during laryngoscopy. The Bullard laryngoscope also features an attachable metal stylet, which can be used with a pre-loaded endotracheal tube to facilitate intubation. The eyepiece can either be used directly by the user or can be attached to a video camera for display on a large screen (Borland and Casselbrant 1990).

The UpsherScope is similar in design to the Bullard Laryngoscope, however, consists of a J-shaped rather than L-shaped blade (the blade has less of an acute angle to it), which is also thinner and flatter. Instead of an attached stylet,

the UpsherScope has a C-shaped channel posterior to the blade which is designed to help guide the endotracheal tube through the cords when intubating. It is simpler in design when compared to the Bullard laryngoscope, as it has no accessory channel for suctioning or administration of drugs. It is otherwise similar to a handle and fibre-optic viewing fibres that connect to an eye piece (Pearce and Shaw 1996).

The WuScope is the third of the common rigid fibreoptic scopes that were seen in clinical practice. It is similar in concept to the UpsherScope and the Bullard Laryngoscope, however differs in its design. It consists of two components: a removable flexible fibreoptic scope and a rigid blade laryngoscope structure. The blade itself consists of a handle, and a hollow tubular blade that contains two internal channels. One of these channels is the guiding passage for the endotracheal tube, while the other houses the fibreoptic endoscope. The tubular structure was designed in order to protect the endoscopic fibres from secretions or blood, as well as hold soft tissue structures of the airway out of the way. The WuScope also incorporates an oxygen channel next to the endoscopic fibres. The blade attaches to the handle of the device at 110° which was to allow for easy entry into the oropharynx (Wu and Chou 1994).

4.2.11   Flexible Fibre-Optic Scope Intubation

While rigid fibre-optic laryngoscopes are still a relatively recent invention, fibre-optic intubating bronchoscopes have been around since 1967 when Dr. Peter Murphy first demonstrated the procedure using a surgical choledochoscope. Quickly the practice of fibreoptic intubating bronchoscopes became more widespread, initially for normal intubations, but soon for difficult airways. Due to its obvious advantages compared to rigid devices, the flexible intubating bronchoscope became the gold standard throughout anaesthetic practice for intubating patients with difficult airways and cervical spine high-risk patients. It also became an extremely useful

diagnostic tool for assessing potentially difficult airways, confirming endotracheal tube placement (in particular double lumen tubes), as well as therapeutic management of foreign bodies/ secretions (Hagberg 2018).

The obvious main advantage of the flexible intubating bronchoscope is the minimally invasive nature, so the intubation can therefore be done awake with no muscle relaxants.

All flexible fibre-optic bronchoscopes have the same basic components: the *body*, the *insertion cord* and the *flexible tip.*

The body consists of the handle of the device on which is attached several key features. It contains an eyepiece and lens, or on more modern devices, a video output adapter or actual video screen. The handle also contains a light source which is either battery operated for portability or a connection cable for an external light source. The handle also contains a single plane control lever for controlling the direction of the tip (either up or down), as well as an attachment point for a suction channel (Hagberg 2018).

The body handle is attached to the insertion cord which is the part that enters into the patient. It is a thin flexible cord that passes into the patients' airway and be inserted orally or nasally. It contains several components that allow visualisation of the structures of the airway. The *fibreoptic light bundle* transmits light down to the tip from the light source, while the *fibreoptic image bundle* transmits the image in the form of light from the tip to the eye piece. The light bundles are made up of anywhere between 10,000 and 50,000 glass fibres, each 8 or 9 μm in diameter. Each of these strands is surrounded by a layer of cladding, as discussed earlier. Also contained withing the insertion tube are angulation wires. These run the length of the insertion tube and connect the control lever to the tip of the fibreoptic device. On flexing the control lever, these move the tip through a vertical plane allowing the user to direct the fibre scope. The final component of the insertion tube is a suction channel that runs from the tip to the suction port on the handle. This channel can alternatively be used to administer medications (such as local anaesthetics) or used as a biopsy port.

The final aspect of a fibre-optic scope is the flexible tip which contains a lens for focusing the light entering the scope.

Fibre-optic intubations can either be done orally or nasally. Oral fibreoptic intubation is generally seen to be a more challenging procedure as the tongue tends to collapse to the back of the oropharynx, even in an awake patient, making navigation with the fibreoptic scope more difficult. Several airway accessory devices have been introduced to assist with oral fibreoptic intubations. These devices, which include the Berman Intubating Airway (Figs. 4.10 and 4.11) and the Williams Airway Intubator, sit in the oropharynx and help guide the fibreoptic scope down towards the larynx and vocal cords. They also function to hold the tongue and soft tissues out the way to allow passage of the scope and have a "breakaway slit" to allow them to be peeled off the scope once it has passed through the vocal cords. Once this accessory device has been removed, the endotracheal tube, which had
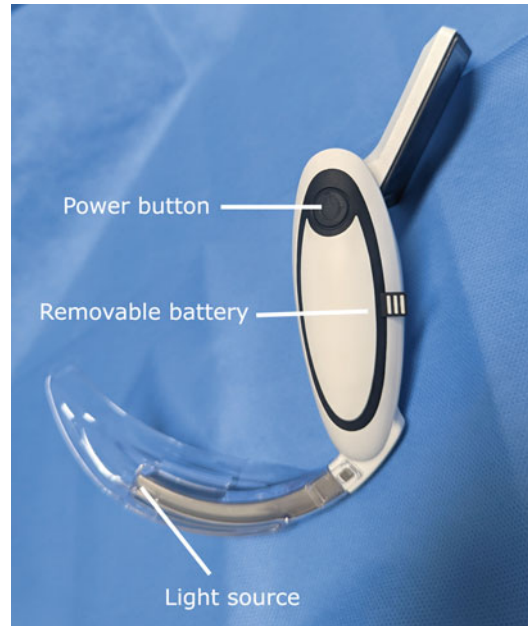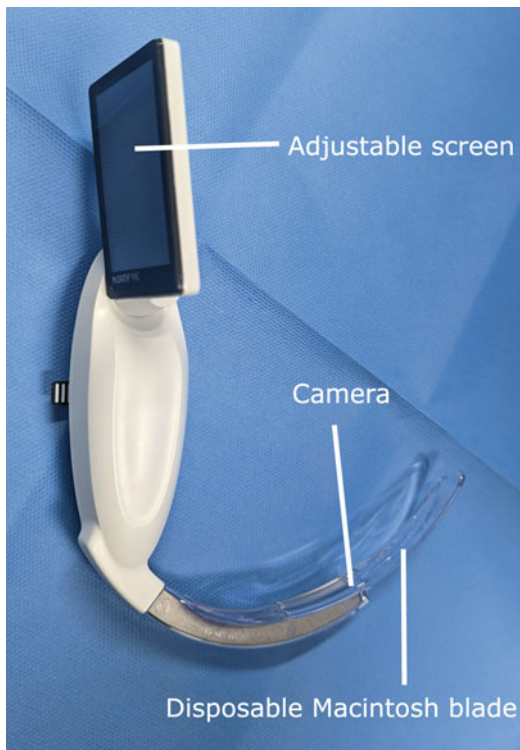

Fig. 4.11 McGrath videolaryngoscope, left lateral view

been pre-loaded onto the fibreoptic scope before starting, is then railroaded down the scope and through the cords.

Nasal fibreoptic intubation is often seen as simpler as the nasal passage helps guide the scope towards the vocal cords. The size of endotracheal tube that is used is restricted, however, generally to a size 6, due to the relatively small size of the nostrils. This has implications for ventilation, and particularly with ongoing management in intensive care afterwards, if applicable. For this reason, the user may often the elect to afterwards do an airway exchange for an oral endotracheal tube once nasal fibreoptic intubation has been achieved.

Fibreoptic intubations can be done either awake or unconscious. They major use benefit of fibreoptic intubations is in those patients with known or suspected difficult airways, most practitioners will elect to use awake fibreoptic intubations to keep the patient spontaneously breathing throughout should any difficulties arise.

Due to this ability to "bail out" from the intubation, awake fibreoptic intubation (AFOI) is the most risk-free method of intubation, so there does not in fact need to be a specific indication to use

Fig. 4.10 McGrath videolaryngoscope right lateral view

it. There are specific situations where AFOI is specifically indicated.

- It remains the gold standard for any patient with a known or expected difficult airway as mentioned, specifically for patients with oropharyngeal malignancies. It is not particularly effective for patients with tumours or strictures of the glottic or subglottic regions, however.
- Any patients with cervical spine instability.
- Those at risk of intubation trauma, e.g. loose teeth.
- Avoidance of aspiration in very high-risk patients.
- Allergy to muscle relaxant.
- Placement of double lumen tubes and tracheostomies.
- For cardiovascular stability—as induction once endotracheal tube is in situ is generally inhalational.

One of the biggest restrictions to the use of fibreoptic scopes is cost. Re-usable fibreoptic scopes produced by Olympus with accompanying screen and equipment costs upwards of £20,000 which is prohibitively expensive for many departments (Hagberg 2018). A cheaper alternative is the Ambu aScope, which is a disposable flexible scope utilising a camera and LED light source. The images are electronically transmitted to a screen rather than through the use of fibreoptics. However, it is a single use device, so waste is increased and the image quality is inferior to a fibreoptic scope.

There are few absolute contraindications to AFOI, however a uncooperative patient will make attempts at that method pointless. As it is a more specialised method of intubating, untrained staff also precludes AFOI. Near total airway obstruction (unless used for diagnostic purposes) is also a contra-indication, as would an allergy to local anaesthetics (Hagberg 2018).

4.2.12 Videolaryngoscopes

While rigid fibreoptic laryngoscopes were initially considered a niche development, they introduced the world of anaesthetics to the concept of videolaryngoscopes. These devices, however, remained fairly peripheral following their invention, as flexible fibreoptic bronchoscopes were by far the most popular devices for difficult airways. The trusted Macintosh laryngoscope was used for patients with "regular" airways.

The popularity and availability of the videolaryngoscope increased significantly from the early 2000s due to yet more technological advancements. The significant draw backs of the rigid indirect fibreoptic laryngoscopes discussed were the significant cost of the fibre-optics, as well as their bulky size. A Macintosh laryngoscope was easily transportable in the users' pocket, whereas the fibreoptic scopes were less portable, especially if being used with a screen (Chemsian et al. 2014).

The invention and availability of LCD (liquid-crystal display) screens, LED (light-emitting diode) lights, and CMOS (complementary metal-oxide semiconductor) video chip technology which are utilised in modern videolaryngoscopes has made these devices much cheaper, portable, and easier to use (Hagberg 2018).

Videolaryngoscopes tend to be categorised according to the shape of their blade. These categories are "Macintosh style blades", and "acute angulated blades". There often is a third category of videolaryngoscopes added which is "channelled devices" (Chemsian et al. 2014).

4.2.13 Macintosh Style Blades

These devices integrate video technology onto a modern Macintosh-styled laryngoscope. They have the added advantages of familiarity of blade shape, as well as being able to use the device for direct laryngoscopy if there was a failure with the video technology.

The **Mcgrath** laryngoscope is a portable videolaryngoscope, which is battery powered and has a small adjustable screen attached to the handle. It comes with the standard Macintosh sizes of disposable blades from 0 (baby) to size 4 (large adult). It also comes with an X-blade,

which is an acute angulation blade for difficult airways, making the Mcgrath an all-round videolaryngoscope (Shippey et al. 2008).

Due to its significant advantages of relatively low cost and portability, it has become the most widely utilised videolaryngoscope (Niforopoulou et al. 2010).

The **C-MAC,** which was produced by Storz medical, was the first videolaryngoscope to be widely commercially available. It also consists of a Macintosh laryngoscope with an incorporated video technology. It differs from the Mcgrath laryngoscope, in that the handle of the laryngoscope is attached to a distant larger screen via a cable. This provides the advantage of everyone in the room being able to see the view which helps in situations of teaching as well as patients with a difficult airway. The blade of the C-MAC is interchangeable from an infant to adult size 4 (Chemsian et al. 2014).

The **GlideScope direct** was the original GlideScope design with a metal, non-interchangeable size 3.5 Macintosh blade. The handle of the laryngoscope is attached to a distant monitor, similar to the C-MAC, and the device can be used for direct laryngoscopy, or indirect using the video function.

4.2.14 Acute Angulated Blades

Devices that incorporate a more acute angulation to their blades compared to the standard Macintosh blade. This acute angulation has been seen in several studies to improve glottic visualisation with minimal patient c-spine flexion. This has been seen to be useful in patients with known difficult airways, and those with an anterior positioned larynx. The drawback with these acute angled blades is that while the view is often improved, passing the endotracheal tube through the cords is more challenging due to the acute angulation, and an intubating stylet is usually required. Another major drawback is they cannot be used for direct laryngoscopy should the video equipment fail.

The **GlideScope** with the acute hyperangulation blade of 60°, and otherwise has

similar equipment to the non-angulated GlideScope. It comes with a specifically designed rigid stylet (GlideRite stylet) for use during intubating due to the acute angulation of the blade.

Mcgrath Series 5 is a portable laryngoscope with the small screen attached to the handle similar to the standard Mcgrath, however with an acute angled blade. The blade portion is fully detachable and its connection position on the handle can be altered. This clever feature allows for the blade to be first inserted into the patients' mouth, then connected to the handle, which is potentially useful in those obese patients or those with large breasts (Niforopoulou et al. 2010).

C-MAC D-Blade is an acutely curved version of the original, produced by Storz medical in 2010. The blade is curved, and functions, in a similar fashion to the GlideScope, and requires the use of an intubating stylet (Cavus et al. 2011).

King Vision laryngoscope was only released in 2017, so is one of the newest devices available. It has a similar design style to the Mcgrath in that it has a small screen attached at the top of the handle and is fully portable. It has two types of disposable blades, the standard aBlade which is an acute angle blade, or the channelled blade (Kriege 2017).

4.2.15 Channelled Devices

These devices use a side channel to direct the pre-loaded endotracheal tube through the vocal cords. With the endotracheal tube pre-loaded, there is no requirement for stylets or gum elastic bougies to assist with intubation.

The **King Vision** device as mentioned has an option of a channelled blade, and so can be categorised as a channelled device.

The **Airtraq** device, as discussed earlier in the chapter, while not strictly a video-laryngoscope, is often incorrectly categorised as a channelled videolaryngoscope. While not containing any video technology, the camera can be attached to the eyepiece of the device for display on a screen.

The **Pentax AWS** is a true videolaryngoscope with a side channel for guiding of the endotracheal tube. It is portable, with the screen attached to the handle. The screen displays a target mark which is aligned with the laryngeal structures, and the endotracheal tube is then advanced through the cords. As with all the channelled devices, when the endotracheal tube is through the vocal cords, it needs to be "peeled" off the laryngoscope in a lateral motion to allow removal of the device.

4.3 Conclusion

There have been clear and marked improvements in the available technology used for tracheal intubations, particularly over the last 40 years. These improvements are reflected in significant improvement in adverse outcomes and generally in patient safety with regard to intubations (Li and Warner 2009). Awake fibre-optic intubation quickly became the gold standard for patients with known or expected difficult airways. There were pitfalls however, mainly with regard to cost and requirement of an experienced team in AFOI. The advent of videolaryngoscopy over the last 20 years has changed the landscape dramatically. It is now well established that videolaryngoscopy improves the achievable laryngeal view when compared to direct laryngoscopy. Numerous recent studies have shown extremely high rates of success using Mcgrath (95% success rate) (Noppens and Möbus 2010), Pentax (95% success rate) (Asai et al. 2010), and GlideScope (96% success rate) (Aziz et al. 2011) in either confirmed or suspected difficult airways. The GlideScope even showed a 94% success rate as a rescue device following a failed attempt at direct laryngoscopy. This has been incorporated into studies, which suggest videolaryngoscopes showed no benefit when compared to direct laryngoscopy on patients with regular "easy" airways.

So, with videolaryngoscopy being as effective in "routine" airways, and clearly superior in difficult airways the expectation may be that videolaryngoscopy continues to proliferate in popularity and will in time fully displace direct laryngoscopy as the primary method of endotracheal intubation. Given that videolaryngoscopy has a clear benefit over direct laryngoscopy in teaching, due to the potential for a shared view between teacher and trainer, as well as its use in awake patients (using local anaesthetics and acute angulation blades), then that time may be not too far in the future.

References

Asai T, Liu E et al (2010) Use of the Pentax-AWS in 293 patients with difficult airways. Anesthesiology 110:898–904

Aziz MF, Healy D et al (2011) Routine clinical practice effectiveness of the GlideScope in difficult airway management: an analysis of 2,004 GlideScope intubations, complications, and failures from two institutions. Anesthesiology 28:34–41

Bailey B (1996) Laryngoscopy and laryngoscopes—who's first?: the forefathers/four fathers of laryngology. Laryngoscope 106:939–943

Borland LM, Casselbrant M (1990) The Bullard laryngoscope — a new indirect oral laryngoscope. Anaesth Analg 70:105–108

Bowen RA, Jackson I (1952) A new laryngoscope. Anaesthesia 7:254–256

Burke CM (2004) A historical perspective on use of the laryngoscope as a tool in anesthesiology. Anaesthesiology 100:1003–1006

Cavus E, Neumann T et al (2011) First clinical evaluation of the C-MAC D-blade videolaryngoscope during routine and difficult intubation. Anaesth Analg 112:382–385

Chemsian RV, Bhananker S, Ramaiah R (2014) Videolaryngoscopy. Int J Crit Illn Inj Soc 4(1):35–41

Collins S (2014) Direct and Indirect laryngoscopy: equipment and techniques. Respir Care 59(6):850–864

Gabuya R, Orkin L (1959) Design and utility of a new curved laryngoscope blade. Anaesth Analg 38:364–369

Griffith HR, Johnson G (1942) The use of curare in general anaesthesia. Anesthesiology 3:418–420

Hagberg CA (2018) Hagberg and Benumof's airway management, 4th edn. Elsevier, Philadelphia

Hirsch NP, Smith GB, Hirsch PO (1986) Alfred Kristein - pioneer of direct laryngoscopy. Anaesthesia 41:42–45

Huffman JP (1968) The application of prisms to curved laryngoscopes: a preliminary study. Anaesthesia 36:138–139

Isaacs RS, Sykes J (2002) Anatomy and physiology of the upper airway. Anesthesiol Clin North Am 20:733–745

Jephcott A (1984) The Macintosh laryngoscope. Anaesthesia 39:474–479

Kastnelson T, Straker T (1996) The Bullard laryngoscope and a "directional tip" RAE tube. J Clin Anesth 8:80–81

Kriege M (2017) Using King Vision video laryngoscope with a channeled blade prolongs time for tracheal intubation in different training levels, compared to non-channeled blade. PLoS One 12(8):e0183382

Levitan RM, Ochroch E (1999) Explaining the variable effect on laryngeal view obtained with the McCoy laryngoscope. Anaesthesia 54:599–601

Li G, Warner M (2009) Epidemiology of anesthesia related mortality in the United States, 1999–2005. Anesthesiology 110:759–765

Macintosh RR (1943) A new laryngoscope. Lancet 1:205

Macintosh RR (1944) Laryngoscope blades. Lancet 1:485

Macintosh RR, Bannister F (1943) Essentials of general anaesthesia, 3rd edn. Blackwell Scientific Publications, Oxford

Magill I (1926) An improved laryngoscope for anaesthetists. Lancet 207:500

Magill I (1930) Technique in endotracheal anaesthesia. Br Med J 2:817–819

McCoy EP, Mirakhur R (1993) The levering tip laryngoscope. Anaesthesia 48:516–519

McCoy EP, Mirakhur R (1995) A comparison of the stress response to laryngoscopy. Anaesthesia 50:943–946

McMorrow RC, Mirakhur R (2003) A new mirrored laryngoscope. Anaesthesia 58:998–1002

Miller RA (1941) A new laryngoscope. Anaesthesiology 2:317–320

Moon JS et al (2021) Epidemiology of anesthesia related mortality in the United States, 1999–2005. Anesthesiology 134:936

Niforopoulou P et al (2010) Video-laryngoscopes in the adult airway management: a topical review of the literature. Acta Anaesthesiol Scand 54:1050–1061

Noppens RR, Möbus S (2010) Evaluation of the McGrath Series 5 Videolaryngoscope after failed direct laryngoscopy. Anaesthesia 65:716–720

Parrott CM (1951) Modification of Macintosh's curved laryngoscope. Br J Med 2(4738):1031

Pearce AC, Shaw S (1996) Evaluation of the upsherscope. Anaesthesia 51:561–564

Phillips OC, Duerksen R (1973) Endotracheal intubation: a new blade for direct laryngoscopy. Anaesth Analg 52:691–697

Pieters B et al (2015) Pioneers of laryngoscopy: indirect, direct and video laryngoscopy. Anaesth Intensive Care 43(Suppl):4–11

Pohunek P (2004) Development, structure and function of the upper airways. Paediatr Respir Rev 5:2–8

Pope ES (1960) Left handed laryngoscope. Anaesthesia 15:326–328

Raez GB (1984) Improved vision modification of the Macintosh laryngoscope. Anaesthesia 39:1249–1250

Roberts JT et al (1994) Clinical management of the airway. WB Saunders, Philidelphia

Roth YK (2008) A brief history of tracheostomy and tracheal intubation, from the Bronze age to the space age. Intensive Care Med 34:222–228

Rowbotham S (1920) Intratracheal anaesthesia by the nasal route for operations on the mouth and lips. Br Med J 2:590–591

Rowbotham S, Magill I (1921) Anaesthetics in the plastic surgery of the face and jaws. Proc R Soc Med 14:17–27

Scott J (2009) How did the Macintosh laryngoscope become so popular? Paediatr Anesth 19(Suppl 1): 24–29

Shippey B, Ray D, McKeown D (2008) Use of the McGrath videolaryngoscope in the management of difficult and failed tracheal intubation. Br J Anaesth 100:116–119

Siker ES (1956) A mirrir laryngoscope. *Anaesthesiology* 17:38–42

Soper RL (1947) A new laryngoscope for anaesthetists. Br J Med 1:265

Strandring S et al (2015) Gray's anatomy: the anatomical basis of clinical practice. Elsevier, London

Tuckey JP, Cook TM, Rander CA (1996) An evaluation of the levering laryngoscope. Anaesthesia 51:71–73

Wu T, Chou H (1994) A new laryngoscope: the combination intubating device. Anaesthesiology 81:1085–1087

The Impact of Technological Innovation on Dentistry

5

Richard Zimmermann and Stefanie Seitz

Abstract

Technology has revolutionized the way dentists are able to treat their patients. These technological advances have paved the way for the creation of virtual patient models utilizing these 3-dimensional intra-oral patient models, cone bean computer tomography (CBCT) radiograph scans, extraoral 3-dimensional scans, and jaw motion tracings to create a patient-specific model. These models are advantageous in planning surgical treatments by providing 3-dimensional views of vital anatomical structures to accurately identify the location, size, and shape of a structure or defect in order to plan accordingly. Virtual augmentation of either hard tissue (bone) and/or soft tissue (i.e., gingiva) can also be accomplished.

Technology has allowed the capture of the dynamic motions of the jaw and combined them with the virtual patient to develop permanent restorations in harmony with the patient's orofacial complex. With the introduction of new technology in the realm of digital dentistry, patient care is being brought to a new and higher level. This creates a level of more optimal care that a dentist can deliver to patients.

5.1 Introduction

Advances in the area of digital dentistry have propelled the profession of dentistry into a completely new era. Historically, impressions of patients' teeth were taken using an alginate material and poured in dental stone to create models. These models were then utilized, along with 2-dimensional radiographic images, to evaluate bony structures. However, dentists now use wands that intraorally scan the patient and are able to create 3-dimensional virtual models of the patient's teeth. These 3D models from the scan allow for the beginning of the creation of virtual patients—both general models for educational use and patient-specific models (Joda et al. 2019). The creation of these comprehensive patient models can be accomplished with the combination of any number of components, including 3-dimensional intra-oral patient models or surface scans, cone bean computer tomography (CBCT) radiograph scans, 3-dimensional extraoral scans, and jaw motion tracings.

Definitive advantages are associated with these patient-specific models when planning various surgical treatments because they are able to

R. Zimmermann · S. Seitz (✉)

Department of Comprehensive Dentistry, UT Health San Antonio, San Antonio, TX, USA

e-mail: zimmermann@uthscsa.edu; seitz@uthscsa.edu

provide the dentist with 3-dimensional views of vital anatomical structures that may have not been able to be visualized on a traditional 2-dimensional radiograph. An enormous benefit associated with these new 3-dimensional views is that the models are to scale, allowing the surgeon to plan treatment effectively by providing enhanced accuracy in identifying the location, size, and shape of a structure or defect. Whether planning surgery on the maxilla (upper jaw) or mandible (lower jaw), the surgeon must be cognizant of the vital structures, such as blood vessels and nerves, that are located in these areas. If these structures are injured, it could result in extreme and/or prolonged harm to the patient. The knowledge of the location of these defects enables the surgeon to alter the plan to be able to lessen the effects the defect can have on the surgery. For example, one can virtually examine the complex anatomy of a sinus, location of various septa, and various neurovascular bundles of a patient prior to performing the actual surgical procedure. This translates into decreased surgical time as the surgeon is more familiar with the patient's anatomy prior to beginning the procedure. The need for virtual augmentation of either hard and/or soft tissue during a surgery can also be determined based on these virtual models, along with the ability of the surgeon to attain an accurate measurement of the amount of grafting material that will be utilized for the surgery.

In the area of restorative dentistry, the ability to conduct a 3-dimensional oral reconstruction of the patient's dentition is incredibly useful. This is accomplished by combination of intra-oral scans, facial photographs, and 3D radiographic images to create a "virtual model" of a patient. These virtual models allow the development of permanent restorations that are in harmony with the patient's orofacial complex—both esthetically and functionally. Specifically in esthetic dentistry, the virtual patient enables the dentist to evaluate the shape and position of the patient's teeth relative to their facial structure and create a virtual simulation of proposed restorations (Garcia et al. 2018). This virtual mock-up is incredibly useful for communication between the patient, dentist, and laboratory technician.

Historically, the fabrication of dental restorations was created on an analog articulator—a mechanical device on which the dentist would mount upper and lower jaw models to simulate the patient's functional jaw movement. However, this device is limited by linear movements, so it does not completely model the patient's function because jaw movement occurs in multiple planes. Nowadays, technology has allowed us to capture the dynamic motion of the jaw and combine it with the virtual patient to design patient-specific restorations that are in synergy with the patient's actual jaw movements (Lepidi et al. 2020).

A promising area emerging in digital dentistry is the utilization of diagnostic imaging of a patient's airway to aid in the diagnosis and treatment of sleep apnea which affects approximately 1 billion people worldwide. Therefore, development of these new technologies, both hardware and software, in the realm of digital dentistry, is bringing patient care to a new and higher level. This tremendously facilitates the role of the dentist in providing more optimal care that a dentist can deliver to their patients.

5.2 Creating the Virtual Patient

The creation of a virtual patient begins with a scan of the patient's teeth using the digital impression system. The scan renders a 3-dimensional virtual model of the teeth that can be created in two different ways. The first way involves scanning the traditionally made stone models with either a laboratory scanner or intra-oral scanner (IOS), while the second way involves directly scanning the patient's oral cavity with the utilization of an intra-oral scanner (Fig. 5.1).

Intra-oral scanning (IOS) has several distinct advantages over the conventional impression materials and techniques (Marques et al. 2021; Rutkūnas et al. 2017). For patients, IOS provides less discomfort by eliminating the need for impression trays loaded with a considerable amount of impression material that tends to elicit the gag reflex which is overall unpleasant. The second advantage which patients enjoy is the decreased amount of time needed for the
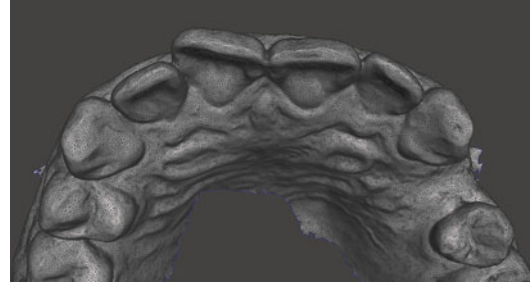
Fig. 5.1 Intra-oral scan of patient capturing both hard (teeth) and soft (gingiva) tissues. Color is picked up by the scanner

Fig. 5.2 Intra-oral scan of patient illustrating the point cloud that actually makes up virtual models

3-dimensional model. An experienced clinician is able to complete a scan in just a few minutes. For the clinician, digital impressions allow for a cleaner, faster, and more accurate representation of the patient's oral cavity. Utilizing the traditional method requires mixing and pouring dental stone into the impression, along with a period of time in which the dental stone must be set. After which, trimming and cleaning the models are needed. Also, legally, dentists are required to keep patient models for a specific number of years depending on where their practice is located because they are considered a part of the patient record. Virtual models facilitate this requirement by allowing the models to be stored virtually and not requiring an actual physical space. This is a considerable benefit to those clinicians with thousands of patients in their practices.

Intra-oral scanners are handheld devices that typically consist of a wand with a camera in the tip. The wands are moved to capture all angles of the patient's teeth, taking hundreds of pictures as it progresses. The ability to scan is easily accomplished and dentists find that there is a short learning curve associated with it. While the technology used in these scanners varies, the result of the pictures is a 3D mesh created from a point cloud using a mathematical algorithm. This 3D mesh is the virtual model of the patient's dental arch, capable of capturing both hard and soft tissue (Fig. 5.2).

Intra-oral scanners are most often used to scan a patient's oral cavity while the individual is

sitting in the dental chair, which is the reason they are often referred to as chairside scanners. There are numerous scanners on the marker with features that target different types of users. Some of these scanners employ the technology that also allows the capture of various shades and colors of the anatomical structures and embeds that information in the 3D mesh, creating life-like recreations of the patient's intra-oral cavity (Haddadi et al. 2019). This colored mesh is an advantage over the monochromatic lab scanners because it allows for the visualization of a more realistic virtual model of the patient, which can aid in some diagnostic procedures.

Chairside scanners embed 3-dimensional positioning coordinates into the digital scans during the scanning process (Fig. 5.3). These coordinates provide the relationship of the maxilla, to that of the mandible, whenever the scans are viewed in the software. However, this captured relationship between the dental arches is static and only represents when the two jaws are biting together fully. While this is useful and might be all that is necessary for some applications (for example— smile analysis), other applications require the dynamic movement of the mandibular arch with respect to the maxillary arch (ex—fabrication of nightguard for teeth grinding or a crown). Some intra-oral scanners claim to capture this dynamic movement; however, these scanners are only capturing the beginning and end, which results in a straight line of movement. This is not a true representation of the human body and the movement of the temporo-mandibular joint, which is
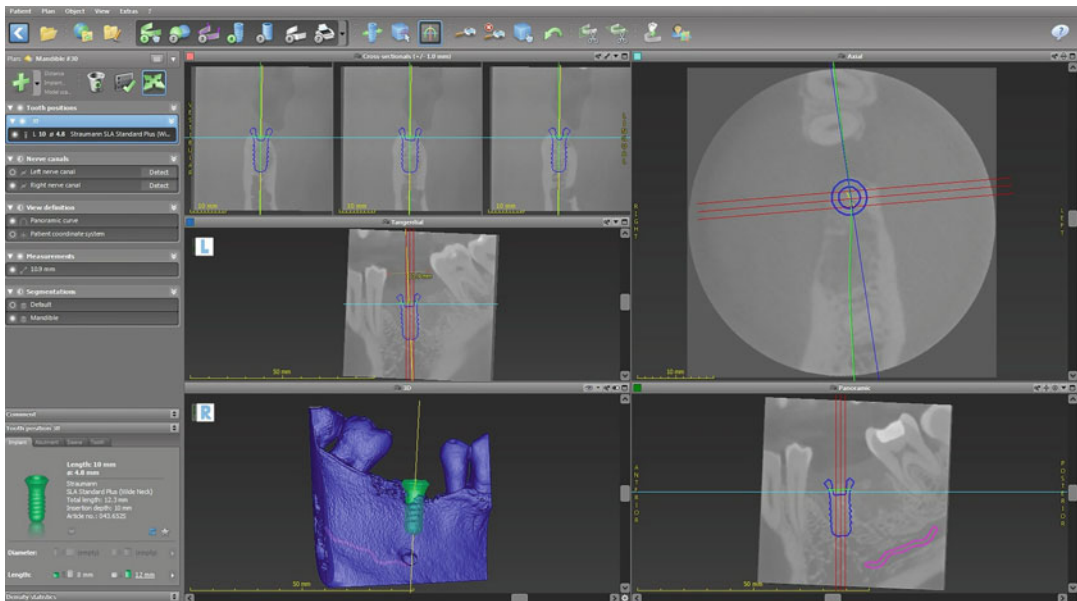
Fig. 5.3 Implant planning software demonstrating the integration of virtual models (blue) to the CBCT to facilitate planning

more fluid and more curvilinear in nature (Clayton et al. 1971).

5.3 Utilization of the 3-Dimensional Model

Cone-beam computed tomography (CBCT) is a radiographic imaging technique that utilizes round or cone-shaped x-rays to capture numerous images as the scanner rotates around the patient. This type of image creates certain advantages over traditional 2D radiographs, including the elimination of image magnification, overlapping of anatomical structures, and image distortion. These images are saved as Digital Imaging and Communications in Medicine (DICOMs) files, which consist of a collection of voxels—the unit of graphic information that defines a point in three dimensions. This radiographic imaging method provides an accurate, 3-dimensional model of hard tissue structures that is accomplished

through either "surface" or "volume" rendering. Surface rendering utilizes gray scales of the CBCT to create the model. The model can be used for digitalization of 3D landmarks; it also can be aligned with other 3D meshes, and even enables the user to plan virtual osteotomies or bone removal surgery. Volume rendering creates the model by using the volume of voxels, to which parameters are set based on the shading algorithms. The disadvantage of this method is the inherent inability to perform virtual surgeries or the lack of the ability to align the model with other 3D meshes. The utilization of CBCT scans has become quite widespread and essential in dentistry in all disciplines. Not only are they used for diagnosis and treatment planning, but also for the creation of detailed patient-specific models and surgical guides (Baan et al. 2021).

For oral and maxillofacial surgery, the use of a CBCT allows for the determination of the precise location of anatomical features, such as neurovascular bundles and tumors, as well as

impacted and supernumerary teeth. For Endodontics, a specialty that focuses on teeth requiring root canals and their associated pathologies, CBCTs allow for the differentiation of apical pathologies, visualization of fractured teeth, and visualization of complex root morphology. For periodontics, CBCTs can aid in the diagnosis of furcation involvement due to bone loss, bone defects around teeth, pathologies, and periodontal cysts. The primary use of CBCTs in orthodontics is to aid in assessing age, adolescent facial growth, and disruptions in tooth eruptions. CBCTs have created one of the largest impacts in implant dentistry. The technology allows for the measurement of the patient's bone height and width. It also enables localization of important anatomical structures in the area of the planned implant placement, as well as provides the capability to assess the need for additional surgical procedures such as bone grafting.

As in all radiographs, any metal present in the oral cavity like amalgams (silver fillings), crowns, or existing implants can create radio-opacities. These radio-opacities result in the decreased quality of the CBCT due to masking and distorting of the anatomical structures and tooth morphology being evaluated for diagnosis on the X-ray. Several methods exist to decrease the amount of scatter and improve the CBCT scan, however, these do not help restore accurate morphology if it has been distorted. To overcome discrepancies within the oral cavity related to scatter, certain software allows the merging, or fusion, of a patient's CBCT DICOMs with their 3-dimensional digital model created by the intra-oral scan (Fig. 5.4).

This fusion creates an accurate 3-dimensional model of the patient's oral cavity, replicating both hard and soft tissue in both radiographic and dental model forms. In addition to the creation of this fused virtual model of the oral cavity, certain specialty areas of dentistry also require the ability to relate the oral cavity with external landmarks and features of the patient's face. This is of key importance when performing esthetic reconstructions either through oral and

Fig. 5.4 Patient stone models being mounted onto articulator

maxillofacial surgery or with dental restorations. The simplest and most common approach at this time is to align the intra-oral digital models to a 2-dimensional photograph of the patient. While this accomplishes the goal of enabling the use of facial features in treatment planning and restoration design, there are inherent limitations.

The first limitation, and the one with the largest impact, relates to the alignment of a 3-dimensional dental model to a 2-dimensional object, the patient photograph. Malalignment of the patient models can result in a tilt of the occlusal plane, the plane of the chewing surfaces of the teeth, compared to the patient's true occlusal plane. This will have a negative influence on the esthetic reconstruction which may not be possible to recognize until treatment is rendered. For this reason, this method is primarily used in esthetics involving dental restorations; the proposed design can be fabricated in temporary restorations,

allowing the dentist to identify the issue and correct it before proceeding to the fabrication of the final restorations. A second limitation is the ability to only view this type of virtual reconstruction from the anterior, or front. One cannot rotate the model to view from different angles due to the constraints inherent with a 2-dimensional photograph. The ability to rotate the images through various viewpoints could be an advantage as it would help evaluate the reconstructions in a more realistic 3-dimensional environment.

In order to overcome these limitations associated with 2-dimensional photographs, 3-dimensional scans of a patient's head can be obtained utilizing specialized equipment and can be accomplished by two methods. The first method involves the integration of a facial scanner within a CBCT machine. This method accurately relates the 3-dimensional head scan to the patient's DICOMs, which can then be aligned to intra-oral digital models. There is a limitation associated with this method. It requires the patient to obtain a full CBCT of the maxillofacial region, which may be unnecessary if the patient is not going to have any surgical procedures and results in more radiation exposure than needed for the patient. The second method involves the use of a "handheld" scanner that captures a photorealistic 3-dimensional image of the patient's head. For alignment, additional scans are needed which incorporate specialized markers that allow for the accurate alignment to the 3-dimensional facial scan. This method involves several more steps in order to achieve optimum alignment but does not expose the patient to unnecessary radiation. While each of these methods has advantages and disadvantages, both result in a 3-dimensional model of the patient that can be viewed from any angle, both with and without facial features. This provides the dental provider an accurate and more complete virtual patient model that allows for comprehensive diagnosis and treatment planning, something that had not previously existed. It also leads to enhanced interdisciplinary communication among various providers.

These virtual models discussed above are generally excellent tools for certain diagnosis and treatment planning, interdisciplinary communication, and help keep a record of the patient as they are presented in the dental chair. However, the majority of dental treatment takes place in the stomatognathic system, a functional environment that is composed of skeletal structures, muscles of mastication, the temporomandibular joint, and the dental arches (maxillae/mandible). This system is an incredibly dynamic environment, meaning it is in motion for most of its various functions—speaking, chewing, parafunctional habits, etc. (Peck 2016).

From the simplest restorations to complex full-mouth rehabilitations, this dynamic jaw movement must be taken into consideration, otherwise it could lead to the failure of the restoration(s). While simple dental restorations (i.e.—fillings) are easily done directly in the mouth and, therefore, adjusted to this dynamic movement intraorally, more complex restorations (i.e.—crowns) are created indirectly on the patient's dental models. Traditional methods consisted of these restorations being fabricated on stone dental models of the patient's upper and lower arches which were mounted on a dental articulator through the utilization of a facebow record.

A facebow (Fig. 5.5) is an intra-oral dental device that records the position of the patient's arches and then translates that position to the articulator. Articulators can range from simple to fully adjustable models, but all share the same limitation—they are mechanical devices, which are limited in the range of motion they can mimic because of the dynamic and non-linear movement of the lower arch.

In today's world, digital workflows for the fabrication of dental prostheses can also generate basic mandibular movement. This is accomplished by the movement of the surface scan, or 3-dimensional model, of the mandible in a direction (right, left, forward) along a flat plane that exists between the maxilla and mandible. When the mandibular scan collides with the maxillary
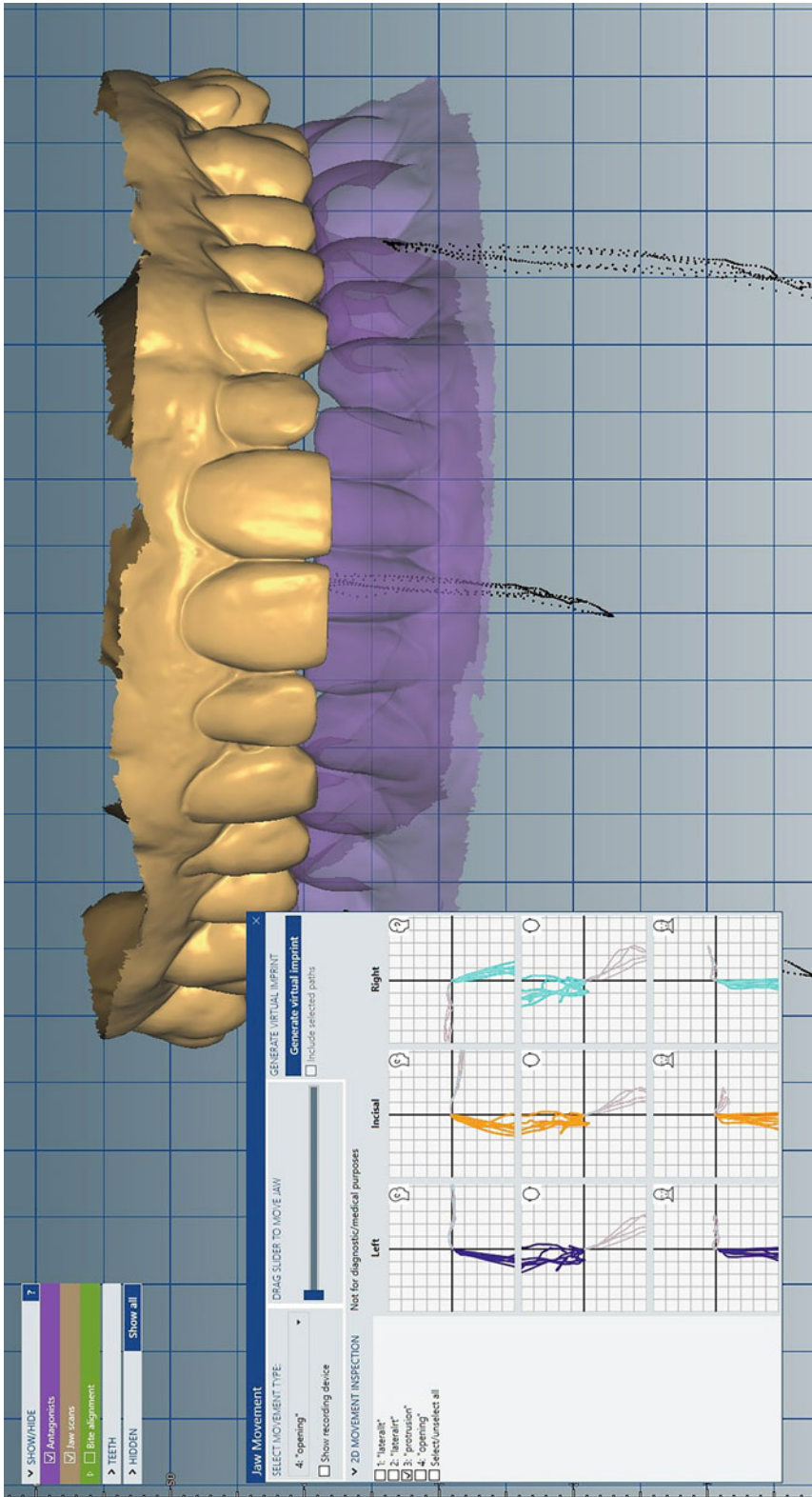
Fig. 5.5 Digital pathways of mandible being illustrated with virtual models in design software illustrated by the black dots

scan, the software will continue to move the scan but make adjustments that eliminate the intersection of the scans. This movement mimics intraoral mandibular movement in that it replicates tooth-guided movement. However, the generation of this movement fails to consider the influence of the neuro-musculature system. To counteract this issue, specialized extraoral systems have been developed that capture the dynamic motion of the mandible (Kwon et al. 2019). These systems vary in the way data is captured but are consistent in that the dynamic motion is transferred into the design software. This allows the software to mimic the actual movement of the patient's mandible, with all factors included. Deviations, non-linear pathways, and other 3-dimensional movements can be recreated within the software, eliminating the solely mechanical movements associated with mechanical articulators (Fig. 5.6).

This digital workflow is comprised of digital versions of the facebow and articulator. In order to capture the movement of the jaw, sensors are attached to the patient's head that act as a digital facebow. The first step is registering the maxilla

Fig. 5.6 Sensors embedded in the cranial apparatus are used to track sensors located in the mandibular apparatus, which is attached to the patient's teeth

to the sensors, and then registering it to the mandible.

After this is completed, the patient is instructed to move their mandible through specific positions, during which the sensors record the 3D movement pathway of the mandible. This data is imported into specific software that allows the user (either clinician or dental technician) to accurately replicate the patient's actual curvilinear jaw motion with the patient's mandibular virtual model. This allows the user to evaluate the mandibular path of movement as it relates to maxillary arch and recognize "interferences" or occurrences where the movement is limited, between the teeth of the opposing dental arches. This technology can be used in combination with CBCT to diagnose temporomandibular joint disorder, or TMD (Liao 2021). Evaluation of the jaw movements, along with the analysis of both the shape and wear in the condyle and fossa of the joint, can aid the dentist in diagnosing the causes specific for each patient to determine the most effective treatment for that individual. The ability to record and analyze a patient's actual mandibular movement is important in the evaluation of temporomandibular jaw disorders and the ability to track them over time. More research is currently needed in this area, but it indicates huge potential for this field of dentistry.

The digital applications described above are being routinely done today for the creation of dental restorations. Clinicians are also using these 3-dimensional virtual models to better evaluate and discuss treatment options, with their patients and other oral health care providers. The intra-oral scan is the simplest and most basic 3D model of a patient, and it is also the foundation upon which other technologies can be utilized.

A limitation that currently exists with digital dental technology is the inability to create a patient model that combines all of the various digital scans into one virtual model that is able to mimic the dynamic movement of the patient's extraoral soft tissue during mandibular movement that is smile, or any other facial animation. This type of virtual model would prove incredibly beneficial and would have the greatest impact in

the area of *esthetic* dentistry and smile design. These two areas require the analysis of a patient's animated lip line to be able to achieve the optimal *esthetic* outcomes for the patient.

So far in this chapter, it has been explained how a patient-specific model for dentistry is created, including the advantages and disadvantages of the pathways and the limitations of these virtual models. The use of virtual models is easily appreciated in reference to the fabrication of various dental prostheses due to the fact that they are a replacement for traditional stone models. However, there are numerous other ways in which these virtual models are being used in general dentistry and the various dental specialties that warrant discussion in further detail.

5.4   Virtual Model Utilization in Oral Maxillofacial Surgery

One of the areas that benefits the most from these virtual models is oral maxillofacial surgery, which was first discussed at the beginning of the chapter. From orthognathic jaw surgery to implant surgery, virtual models have become mainstream in the diagnosis and treatment planning for these surgeons (Otranto de Britto Teixeira et al. 2020). Orthognathic surgery is used to correct deformities in the upper or lower jaw and the associated incorrect positioning of the teeth. To do this effectively, the surgeon utilizes a specialized software that allows the user to simulate various osteotomies (ex-sagittal split or vertical ramus osteotomy) on the virtual model while taking into consideration the patient's specific anatomical structures. For example, when planning mandibular osteotomies with a virtual model, the user is able to virtually track the inferior alveolar canal (IAC), a canal that houses an important neurovascular bundle, and creates a mesh of the pathway as it goes through the length of the lower jaw. This mesh provides the user a 3-dimensional view of the IAC pathway, allowing for more precise planning to avoid the vital

structures within. This is incredibly important because any damage to the inferior alveolar nerve can cause symptoms including: numbness, pain, burning or tingling in the lips, chin, and gums; drooling; or impaired speech. In addition, once the virtual osteotomies are performed, the sections can be repositioned and allows for a virtual generation of the model that depicts the proposed surgical outcome.

In addition to creating a virtual rendering of the final surgical results of osteotomies, surgeons are able to use certain specialized software to predict the soft tissue and hard tissue outcomes of orthognathic surgery. The software utilizes databases of documented cases to predict the soft tissue outcome based on the hard tissue changes. It has been shown that the predicted outcome for hard tissue changes is reasonably accurate, within 1 mm of the actual surgical outcomes. However, the predictions for soft tissue outcomes are more varied with the greatest area needing improvement being the region around the lower lip.

5.5   Virtual Model Utilization in Orthodontics

In the area of orthodontics, the use of lateral cephalometric analysis via a 2D image more widely used over CBCT due to the reduced amount of radiation exposure to the patient. However, there are certain cases when the CBCT and 3D visualization are superior for diagnosis and treatment planning. The primary advantage in 3D visualization is due to the inherent issue with 2D radiographic images; the fact that impacted teeth are superimposed over the other anatomical structures, and it is difficult to ascertain the exact position or impact on the tooth or anatomical structure. The 3D models allow complete visualization of these areas (Baan et al. 2020).

One of these cases involved the impaction of maxillary canines, which are the second most

commonly impacted tooth, after third molars (wisdom teeth). Impacted teeth are teeth in which tissue, bone, or another tooth has prevented it from reaching its normal position in the mouth. The surgical exposure of these teeth is one of the most common indications for CBCT imaging in orthodontics. In this type of case, the virtual model improves the treatment planning by allowing visualization of the precise location in the arch, including the proximity to adjacent teeth and other vital structures. In addition, it allows for a more accurate evaluation of the tooth follicle and enables the assessment and extent of any existing adjacent tooth resorption. This visualization enables the orthodontist to better plan the surgical access, orthodontic bracket placement, and extrusion path for the impacted tooth, which results in a better outcome for the patient.

Supernumerary teeth are extraneous teeth that can develop anywhere in a person's mouth. The most common area for these teeth to be found is in the anterior maxillae and they can be difficult to differentiate from normal dentition. These teeth are usually impacted or unerupted. Virtual models allow the orthodontist to precisely locate the teeth and determine their true morphology. This is important as it will aid in treatment planning and help determine whether the teeth are retrievable and able to be retained or if they need to be extracted.

5.6 Virtual Model Utilization in Endodontics

In dentistry, endodontics is the area that focuses on the dental pulp, the roots of teeth, and the tissue surrounding the roots. The majority of endodontics revolves around the treatment of the root canals of teeth. Root canal morphology is a complex three-dimensional structure that varies between teeth and is even found to be distinct within certain populations. Maxillary molars present with numerous variations that challenge even the most experienced endodontist. Traditional 2-dimensional radiographs are the most widely used method to diagnose and treatment plan endodontic therapy, however, these images provide limited information and are influenced by X-ray angulation, the overlapping of anatomical structures, and contrast. For these reasons, the use of CBCT has been shown to be incredibly useful for complex cases.

The ability of a clinician to navigate through a 3D image of a tooth allows for better visualization and, therefore, a better understanding of the root canal morphology (Shah and Chong 2018). Curves, accessory canals, and even fractures of the root can be seen from different angles, allowing the clinician to better diagnose, plan, and provide treatment for the patient. It has also been used to help differentiate between endodontic and non-endodontic pathologies. Emerging dental software allows the user to virtually plan endodontic treatment by identifying anatomical abnormalities, calculating exact measurements, and choosing which instruments should be used prior to the actual treatment. Currently, the main drawback in using CBCT and virtual modeling for endodontics lies with the amount of radiation exposure, which is higher than the conventional 2D radiographs. For this reason, the use of CBCT in endodontics is only recommended for complex cases at this time.

5.7 Virtual Model Utilization in Implant Dentistry

Dental implantology involves the combination two different areas of dentistry—surgery and prosthetics—to provide treatment for a patient. This treatment can range from a simple, single-tooth replacement to full arch reconstruction supported by numerous dental implants. For any case, accurate placement is essential to achieve optimal esthetic and functional prosthetic outcomes. However, patient anatomy may limit the proposed location of the implant, requiring additional planning or even a completely different approach (Kernen et al. 2020).

The first step in digital treatment planning of a dental implant is the acquisition of surface scans of the patient. For dentate patients, this is accomplished with the use of an intra-oral scanner, as discussed previously. Edentulous patients,

however, are more complex as soft tissue can be more challenging to capture and does not exhibit a definitive shape like hard tissue due to its mobility. For this reason, there are distinctive and different pathways to create virtual models for dentulous and edentulous patients.

For edentulous patients, a well-fitting removable prosthesis (denture) is required—one that is well adapted to the patient's soft tissue. At the CBCT scanning appointment, fiduncles (specialized small metal spheres for use in CBCT). are attached to the patient's current prosthesis. The patient is then scanned with the modified prosthesis in place. Subsequently, the prosthesis itself is scanned separately while sitting on a CBCT table. Afterwards, the CBCT scan of the patient wearing the prosthesis and the prosthesis alone are imported into a specific dental implant planning software that utilizes artificial intelligence to align the patient CBCT to the prosthesis CBCT using the fiduncles. The software will take the prosthesis CBCT scan data and create a virtual replica (mesh) of the prosthesis. The position of the prosthesis to the patient's hard tissue is accomplished by the alignment of the fiduncles. The next step in the software is to create a virtual mesh of the soft tissue by reverse engineering the tissue side of the prosthesis. Once completed, a virtual model of the patient's bone with overlying tissue mesh is formed (Fig. 5.7).

For both edentulous and dentate patients, the next step after merging of the surface scans to the CBCT file comes the actual planning of the implant case.

Dental implants come in a wide range of lengths, diameters, and shapes. Historically, 2-dimensional radiographs (panographs), along with acetate overlays depicting different implant sizes, were used to plan for surgical placement. Surgical guides were then fabricated on stone models that had a diagnostic wax-up of the proposed final restorations. The main limiting factor with this method was the inability to take the patient-specific anatomy into consideration when planning. While some anatomical structures are visible on 2D radiographic film (ex-inferior alveolar nerve), others are hidden due to overlapping of other anatomical structures (ex-palatal foramen).

For dentate patients, a proposed design of the prosthesis replacing the missing teeth must be created. By doing this, the restorative doctor is conveying to the surgeon the ideal position of the implant based on the patient's existing dentition. This proposal takes into account a number of factors including the placement of the final restoration with respect to adjacent teeth and opposing dentition. The goal is to place dental implants in positions that will support final restorations that are in harmony with the patients existing dentition and maxillomandibular relationships. Failure to do this results in a significantly higher probability of a broken prosthesis and/or failed implant. Current dental technology supports the virtual design of the patient's final prosthesis by allowing the restoring dentist to create a virtual prosthesis that takes all of these important factors into consideration and ensures the final prosthesis is in harmony with the patient's dentition. Once completed, the design is integrated into the surface scan and aligned with the patient's CBCT. Afterwards, the surgeon can plan and place the implant in the optimal location using the proposed prosthesis as a reference.

Once the planning for both the prosthesis and the implant is complete, either in dentate or edentulous patients, a surgical guide can be created based on the virtual implant plan. Surgical guides are aids that help the surgeon orient the implant during the implant surgery to achieve the proposed correct location, depth, and angulation needed for the prosthesis. Surgical guides can be utilized in simple, straightforward cases requiring the replacement of some teeth with implants, or in more complex cases. Complex cases require more advanced guides, usually multiple guides for a single case, which require advanced virtual modeling techniques to create.

In certain implant rehabilitation cases, an alveoloplasty (bone reduction) is needed to create restorative space for the final prosthesis. The workflow is similar to the ones already stated, however, during the implant planning phase, the amount of bone needing to be removed can be determined based on the restorative components.
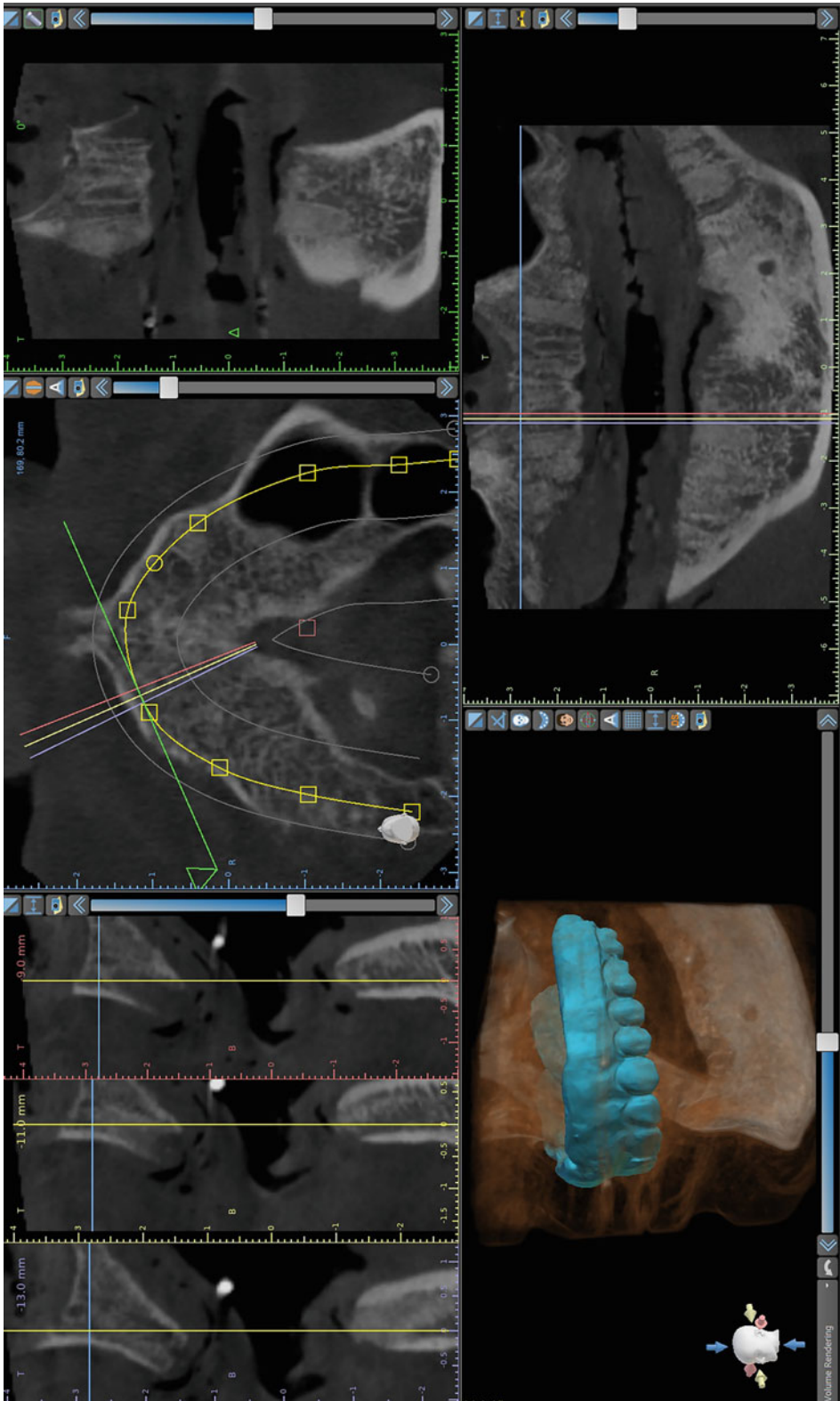
Fig. 5.7 Patient intra-oral scan aligned to patient CBCT for implant planning

Once the surgeon virtually arranges the implant along with the restorative components in place, the amount of bone needed to be removed can be measured on the virtual model. Once that amount is determined, the software will allow the user to remove and recontour the bone, creating a virtual bone reduction that gives the surgeon a guide for what has to be done to accomplish the alveoloplasty. This workflow is best undertaken by experienced clinicians who have a thorough understanding of bone physiology and remodeling and who can predict the outcome of the bone reduction surgery. Once this workflow is completed, the complex surgical guide can be designed. The original, unaltered virtual model is used to create the first part of the guide, while the modified model that has undergone the virtual alveoloplasty, is utilized to create the bone reduction and implant placement. While there are limitations to these complex surgical guides, it has been shown that the use of these guides decreases surgical time and improves prosthetic outcomes, which warrants the time spent creating them.

It is not uncommon for some type of bone grafting procedure to be necessary in conjunction with implant placement. While it is difficult to determine the real-world outcome of virtual grafting due to various factors, such as patient health and behavior, virtual modeling allows the surgeon to predict if grafting is going to be needed and the amount of graft material that should be used. It is well established that at least 1.5 mm of bone is needed to surround a dental implant for successful integration. If it is determined that the proposed implant location lacks the 1.5 mm of bone in an area while virtually planning the implant, the surgeon can plan for the placement of a bone graft. There are various types of bone that can be utilized for a bone graft and the amount of bone grafting needed aids the surgeon in determining which of these materials will be the best fit for the specific situation.

An additional area that commonly requires bone grafting is the maxillary sinus region. Often, the sinus is located too low for the desired implant to be completely encased in bone, so additional bone is placed in the bottom of the sinus to ensure the implant is fully in bone and does not protrude into the sinus. It is not uncommon for a sinus lift to be performed at the same time of the implant placement. This procedure can also benefit from virtual planning for numerous reasons.

The most common approach for a sinus lift is to access the sinus through a lateral window that is surgically cut into the lateral wall of the sinus and the sinus membrane is carefully elevated from the floor of the sinus. Once the access is made, grafting material is then placed below the sinus membrane and the bone window is replaced. During the planning phase, a virtual model can illustrate the position of any septa or deviation in the internal area of the sinus that could complicate the surgical approach. More importantly, the model allows for the visual tracking of the posterior superior alveolar artery and nerve to determine the best approach to avoid injury. Some implant planning software will even allow the user to determine a specialized model of the sinus and calculate the amount of bone grafting material needed to accomplish the sinus lift (Fig. 5.8).

This aids in eliminating the unnecessary waste of bone grafting material by providing the amount needed. An alternative approach to accessing the sinus is through the residual crestal ridge of the jaw. However, for this approach to be successful, certain anatomical features must be present. For example, the area must be free of any septa and have a certain amount of bone thickness remaining. If not, then the lateral window approach is recommended. While there has been many of these surgeries accomplished before patient-specific modeling, this technology has helped to better prepare the surgeon and decrease the surgical time.

Examples of some cases are provided below:

5.7.1   Case Example #1

A patient presented with a removable appliance ("flipper") replacing her four anterior teeth. The patient was happy with the existing esthetics of the appliance, including the tooth shape and
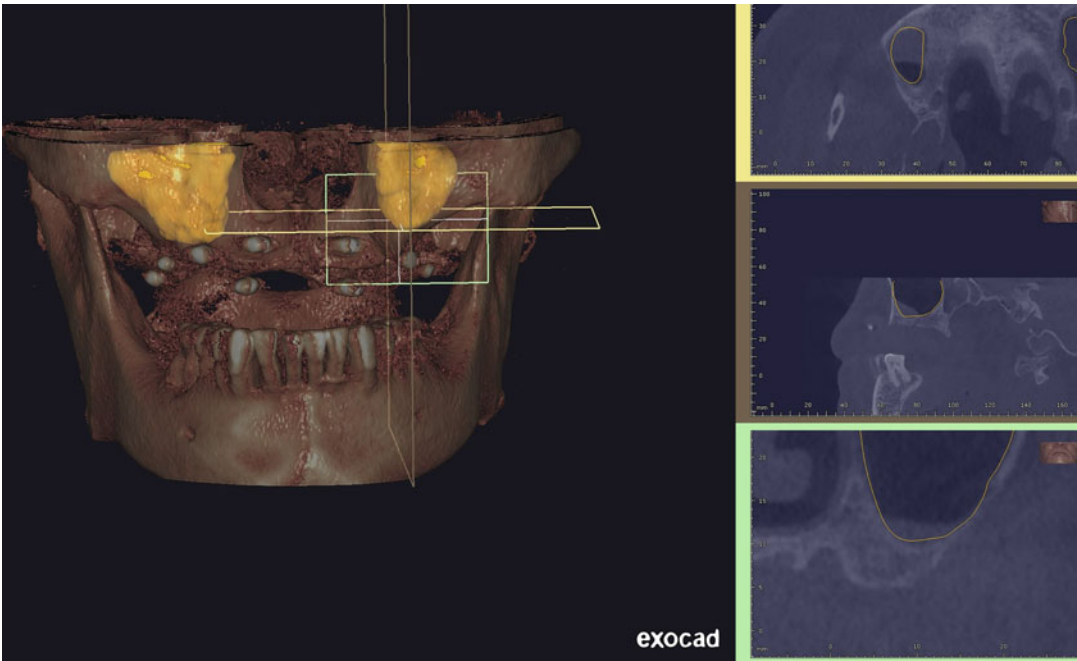
Fig. 5.8 The yellow areas outline the patient sinus in this implant planning software which aid in planning of implants in this region

position of the teeth, but did not like the poor fit and the fact that it was removable and not a fixed prosthesis (Fig. 5.9).

The patient was interested in obtaining a more permanent fixed restoration that could mimic her natural teeth, so she was referred for implant therapy.

Initially, a traditional panogragh was taken and a clinical examination of the patient's maxillary alveolar ridge was performed. Both the panogragh and the clinical examination revealed that the patient had an adequate alveolar height and the necessary ridge width for the placement of implants (Fig. 5.10).

The standard of care at this clinic required the dentist to obtain a CBCT for all patients receiving dental implant therapy, so the patient was referred

Fig. 5.9 Intra-oral picture of patient wearing their removable appliance
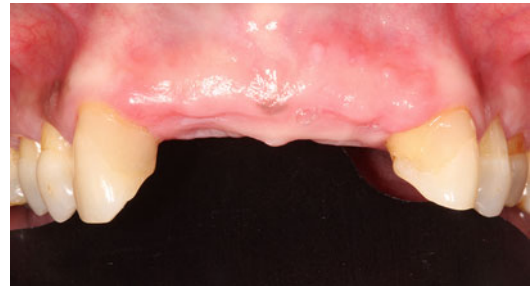
Fig. 5.10 Intra-oral picture of patient without the removable appliance

Fig. 5.11 Virtual model of patient rendered from CBCT

to the Radiology clinic for the CBCT and subsequent radiology interpretation. Intra-oral scans were also taken of the patient's maxillary and mandibular arches, along with her existing removable partial appliance to be used as a diagnostic wax-up for the final prosthesis.

Upon interpretation of the CBCT, it was determined that the alveolar ridge had more buccal-lingual resorption than what was initially observed, with alveolar defects due to previous extractions. It also revealed thin and immature bone, as opposed to the more solid buccal cortical plate (Fig. 5.11).

When placing implants, the density and volume of existing bone are critical for successful osseointegration. If the existing bone is not ideal, bone grafting or more advanced surgical procedures are required. In this particular case, a virtual model of the patient was created to better visualize the situation that revealed the true extent of the bone loss in the anterior region. While virtual models from CBCT's are not 100% accurate, they can provide the clinician with a clearer picture of the clinical situation. Given the anterior location of the planned dental implants, the patient's concern for the most esthetic outcome, and the amount of bone loss observed, it was decided to virtually plan the implant case.

The first step was the creation of the virtual model from the patient's CBCT. For this case, the teeth were segmented in the maxillary bone to better visualize the trajectory of the roots of the canines (Fig. 5.12).

When segmenting different areas of the model, it has been found that the ability to assign a different color to each area and adjust the transparency of each segment are useful tools for the dentist. These tools allow for better visualization of the different areas, including bone, roots of the teeth, etc. It is particularly useful when overlaying various surface scans that contain multiple segmentations.

After the CBCT model was completed, the surface scans (maxillary and mandibular) were then aligned to it, followed by the scan of the interim appliance (Fig. 5.13).

For this case, a virtual scan of the face would have been useful given the importance placed on esthetics. However, due to the fact that the patient was happy with the esthetics of the current removable appliance, it was decided to import a scan of it to aid in planning. At this point, a complete virtual model of the patient had been created within the dental implant planning software.

The replacement of anterior teeth with dental implants can be esthetically challenging, especially with multiple missing teeth complicated by bone loss. In this case, it had to be determined whether two implants and a bridge or four implants with separate crowns would be used to replace the missing teeth. There are advantages and disadvantages associated with both, however, the existing bone architecture and the possibility of necessary additional procedures must be considered to achieve the desired outcome.
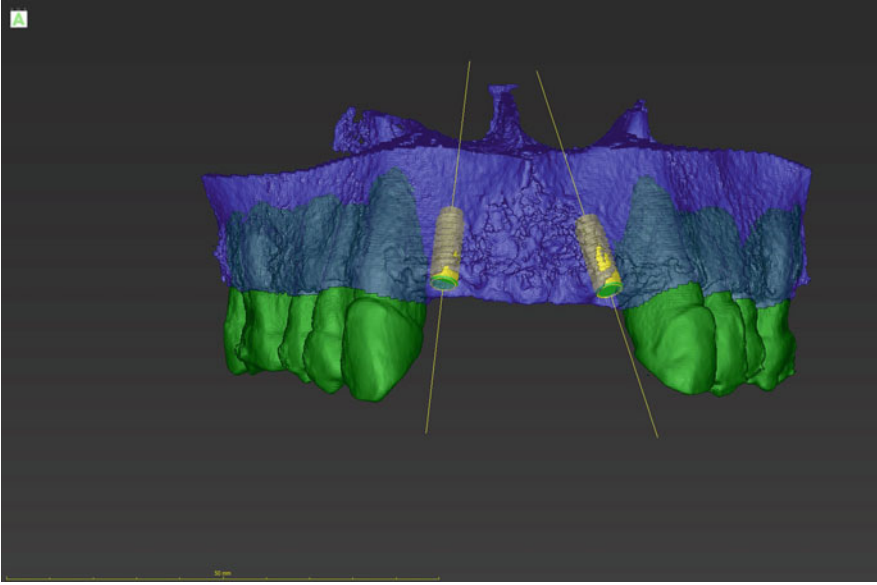
Fig. 5.12 Virtual model of patient showing segmentation of teeth/roots and proposed implant locations
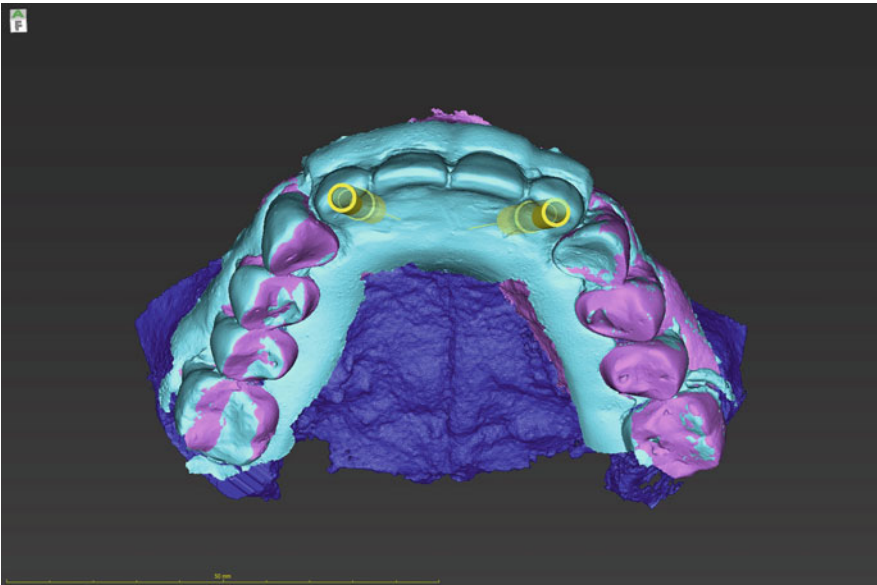
Fig. 5.13 Virtual model of implant planning showing proposed position of implants (yellow) to the patient's removable appliance (light blue)

Once the full virtual model was completed and the virtual planning of the case had begun, it was realized that the width of the remaining ridge was insufficient for the placement of four dental implants without requiring a large bone graft. It was also determined that the placement of just

two dental implants at certain positions would only require a minimal grafting procedure.

The ability to place implants in the virtual model also provides visualization of the necessary implant trajectory. This is important in the restorative phase of implant therapy as it will dictate the type of restoration that can be placed. Therefore, when planning an implant, the desired restorative plan must be balanced with the available bone to achieve optimal outcomes. This is where the scan of the patient's existing prosthesis becomes important. By overlaying her appliance in the virtual model, the clinician can visualize the effect that the trajectory of the implant will have on the final prosthesis. In this particular case, it was determined that the preferred method of restoration would not be feasible since the trajectory emerged from the incisal, or bottom edge of the teeth. The decision had to be made either to change the restorative design or perform larger and more complex grafting techniques. After consulting with the patient and informing her of the possibilities, she elected not to undergo additional large surgical procedures and the restorative plan was changed to accommodate the necessary implant trajectory. Once the implant size and position were finalized, a surgical guide was fabricated to facilitate the planned placement of the implants into the proposed positions. As with all implant surgeries, the surgical guide was fabricated using additive technology (3D printing) and a specialized biocompatible sterilizable resin was utilized.

At the time of surgery, a full-thickness periosteal flap was created and reflected, which allowed complete visualization of the alveolar ridge. In the model, the center point of the ridge appeared rough and thin—this is usually indicative of thin, immature bone. While in the photograph the bone appears to be solid clinically, it was thin and porous (Fig. 5.14).

As predicted by the virtual model, a small grafting procedure was needed.
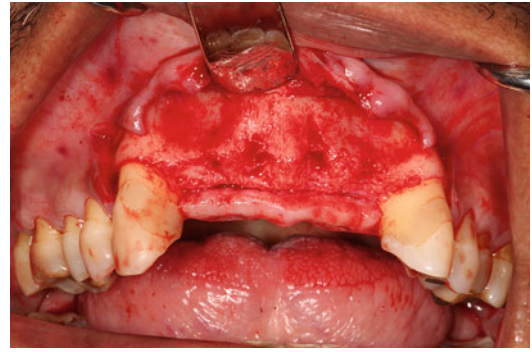
Fig. 5.14 Intra-oral picture showing osseous architecture after reflection of soft tissue

5.7.2 Case Example #2

When performing prosthetic reconstructions of patients' dentitions, one must take the mandibular movement into account, otherwise the restorations will fail, or the patient will generate temporomandibular symptoms. In traditional analog workflows, the first step is to obtain a maxillomandibular relationship utilizing a facebow. Facebow complexity ranges from simple to fully adjustable, with the fully adjustable being the most complex and requiring hours for an experienced clinician to use. The facebow is then used to transfer the position of the maxillary arch to an articulator to represent the patient's temporomandibular joint and both upper and lower arches. The movement allowed by the articulator depends on the model used—a simple articulator only allows for an open/close movement, while the fully adjustable models allow for more complex movements which more accurately mimic the patient's jaw movement. However, it is still a mechanical device that is limited by the features and build—namely the moving parts are restricted to flat rails. Therefore, the natural movement of the mandible is not accurately reflected. For example, when a patient open and closes, the mandible may not move in a straight vertical line but has a deviation to either side

during the movement. This deviation could be the result of the person's natural joint, previous trauma to the joint, or a result of temporomandibular disorder. Due to the lack of movement accuracy, the provider will need to perform chairside adjustments in order to get the prosthesis in harmony with the patient's oral complex. The amount of time required for these adjustments is related to the extent/size of the restoration being done. A single tooth may be five to ten minutes, while a full-mouth rehabilitation can take several hours. Additionally, the more accurately the articulator mimics the natural movement of the patient, the less time is spent in adjustments at the time of delivery.

As mentioned earlier, digital technology that allows for the capture of a patient's mandibular movement can be used with surface scans to create an accurate virtual model of a patient's orthognathic system. This model can be used for numerous diagnostic and therapeutic treatments, but its biggest advantage lies with the development of patient-specific restorations. To create this type of virtual model, intra-oral scans of the maxillary and mandibular arches are taken. The next step is to capture the mandibular movement. To do this, specialized headgear containing infrared cameras is placed on the patient. A sensor is then used with specialized bite plates to register the position of the maxillae and then the mandible. At this point, the same information from the traditional facebow has been obtained.

The next step in this digital process involves the attachment of the sensor to the mandibular biteplate and having the patient perform jaw movements in a specific order. As the patient goes through the motions, the infrared cameras in the headset capture the 3-dimensional movement of the sensor on the biteplate. The software then creates a demonstration of all mandibular movements performed by the patient. At the same time, the software creates tracings of the patient's condyles that can be used for diagnosis (Fig. 5.15). These tracing can be used in identification of pathologies or unusual jaw movement, as discussed previously.

Once the movements are tracked, the intra-oral scans are imported into dental-specific Computer-aided design (CAD) software along with the algorithm from the digital facebow. The algorithm orients the surface scans onto a virtual articulator, creating a virtual setup resembling the traditional analog articulator.

The CAD software can replicate the patient's mandibular movement without any limitations. The user is able to see any deviations from normal and the software creates visual aids by displaying a series of dotted pathways the mandible goes through during functional movements. Specific movements (example—left lateral movement), may be individually selected and visualized. Since these movements are in the virtual world, they will reflect any deviation that the patient may have in reality.

The software is also capable of generating meshes of individual movement pathways, which prove incredibly useful for the development of prostheses by eliminating various interferences that would have been present if only a static relationship was used.

Interferences arise when tooth cusp tips hit opposing teeth prematurely or out of harmony with the other parts of the orthognathic system. These interferences were referenced earlier and are the cause of necessary chairside adjustments that extend the time the patient must be in the chair. When activated, the CAD software will utilize the dynamic jaw movements to create a restoration that will function most effectively for the patient (Fig. 5.16).

These pictures illustrate such a case. This patient needed two full coverage posterior restorations. For various reasons, the most posterior tooth in an arch is a little more challenging to develop a proper occlusion when restoring. For these restorations, the digital facebow was taken, along with intra-oral scans of the patient. The virtual patient was created as described above. During the design process, the user was able to visualize and toggle among the various occlusal contacts on both the existing dentition and the proposed prostheses to determine the best occlusion for the final restorations. In addition, the user was also able to move the virtual mandible through various motions to help better visualize
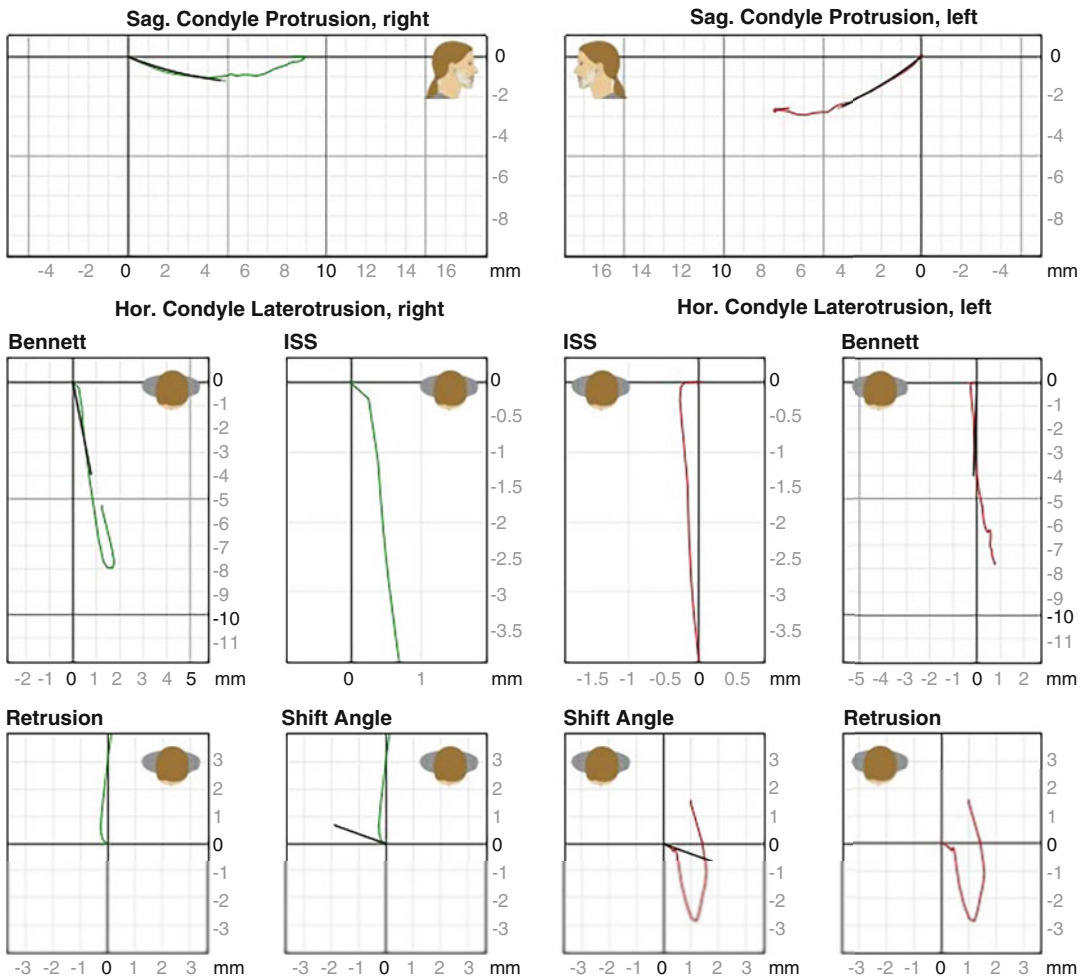
Fig. 5.15   Condylar pathway tracings obtained from mandibular tracking

the mandibular pathway and possible interferences.

The software is able to illustrate the patient's occlusion utilizing a heatmap to demonstrate the degree of contact. Red and yellow colors indicate intersection of surfaces, while the blues indicate areas of contact—light blue indicates a heavy contact while dark blue indicates light contact between teeth. When the restorations are first generated by the software, they have red and yellow spots indicating they are actually intersecting with the opposing surface scan (Fig. 5.17).

Using the adapt function, the software adjusted the proposed design of the restoration to be in harmony with the rest of the patient's dentition (Fig. 5.18).

During the try-in of the two restorations, the patient was instructed to go through all the various mandibular movements while marking paper was placed between the restorations and opposing dentition. One can see how close the markings on the final restorations align with those indicated in the design software (Fig. 5.19).

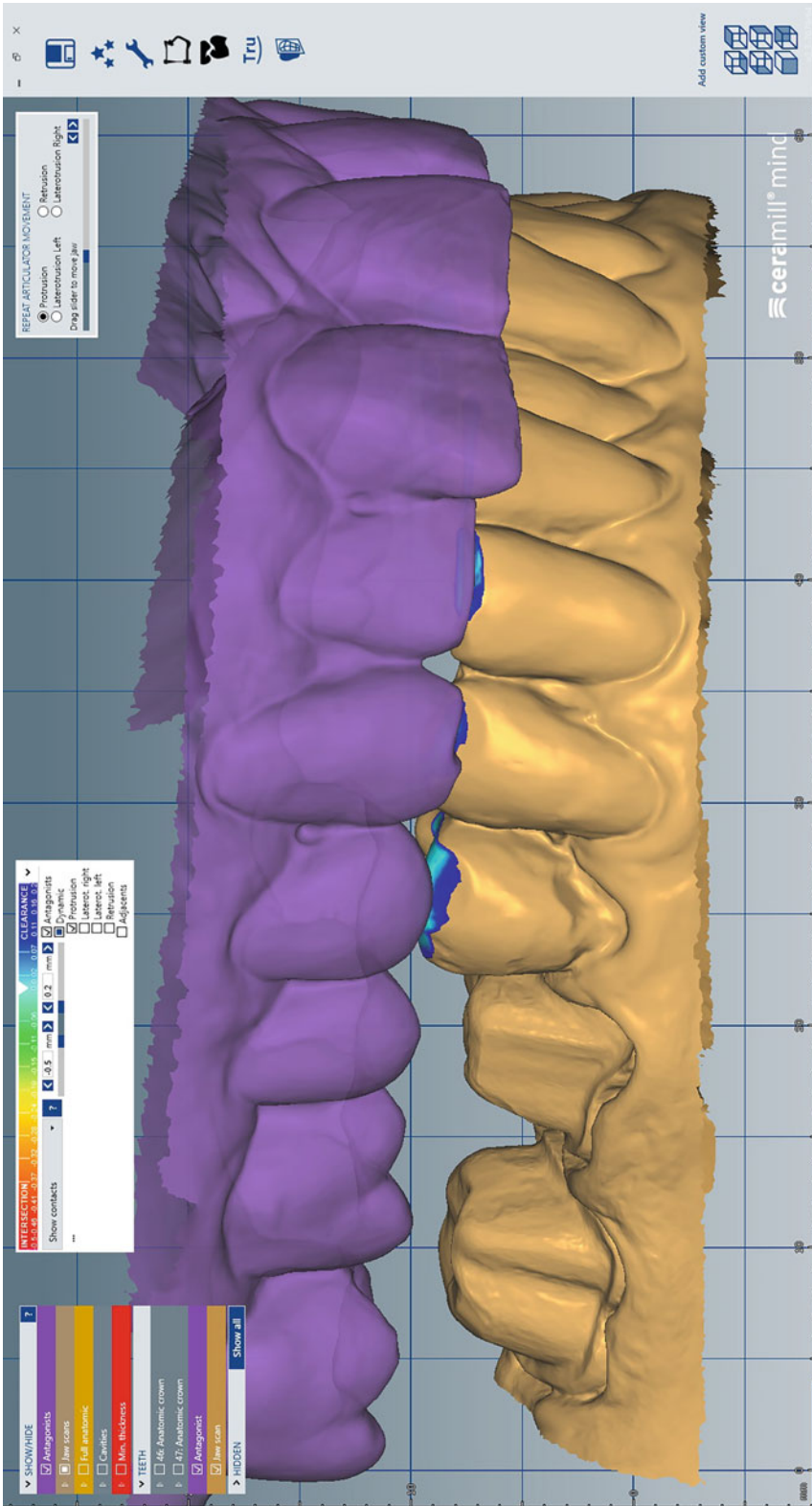This demonstrates the accuracy involved in how the digital facebow translates both

Fig. 5.16 Virtual models in lateral excursion with heat map visible (blue/light blue on teeth) illustrating interfering points
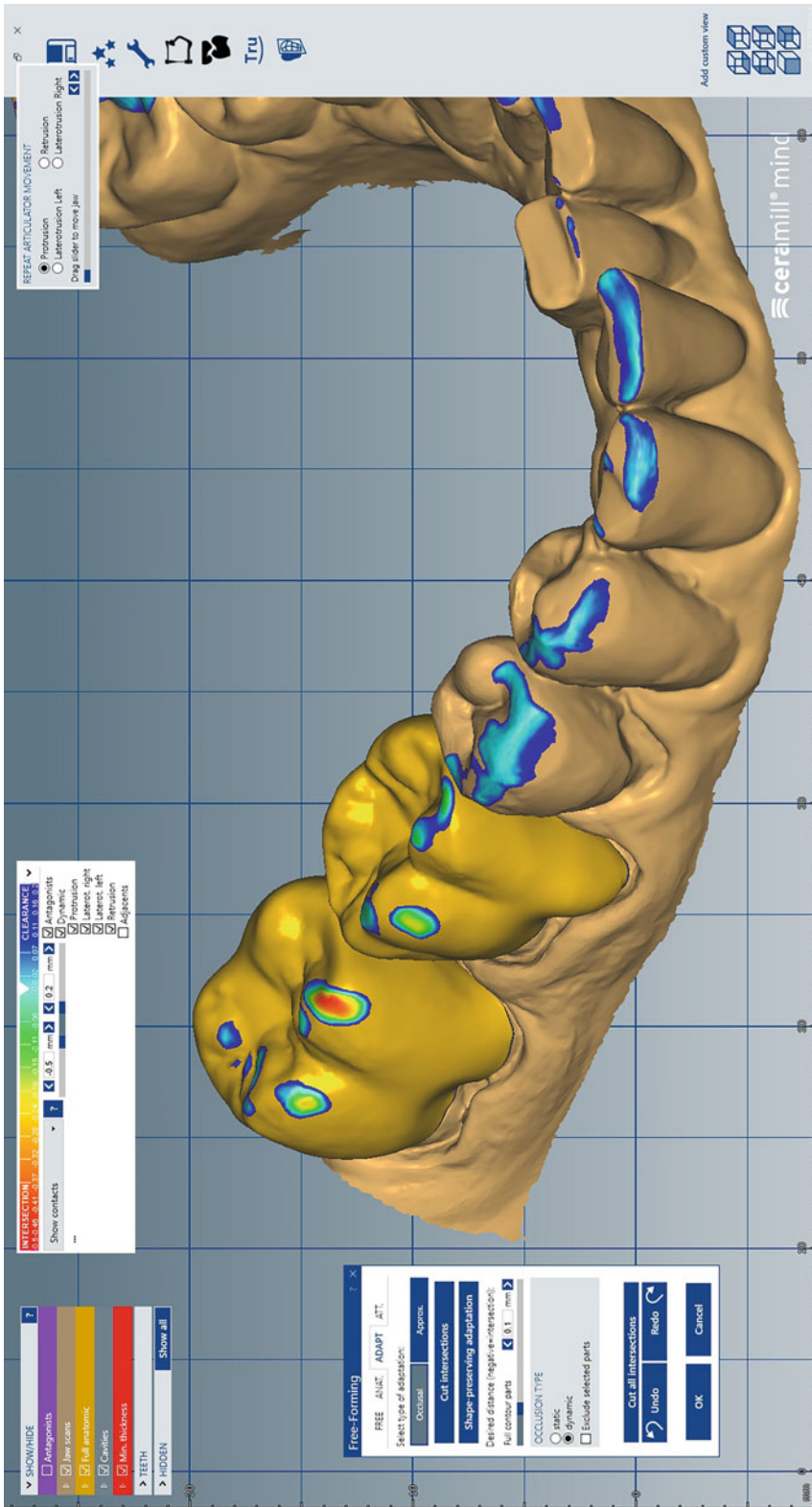
Fig. 5.17 Virtual model of patient with proposed crowns (yellow) design showing interferences via heat map
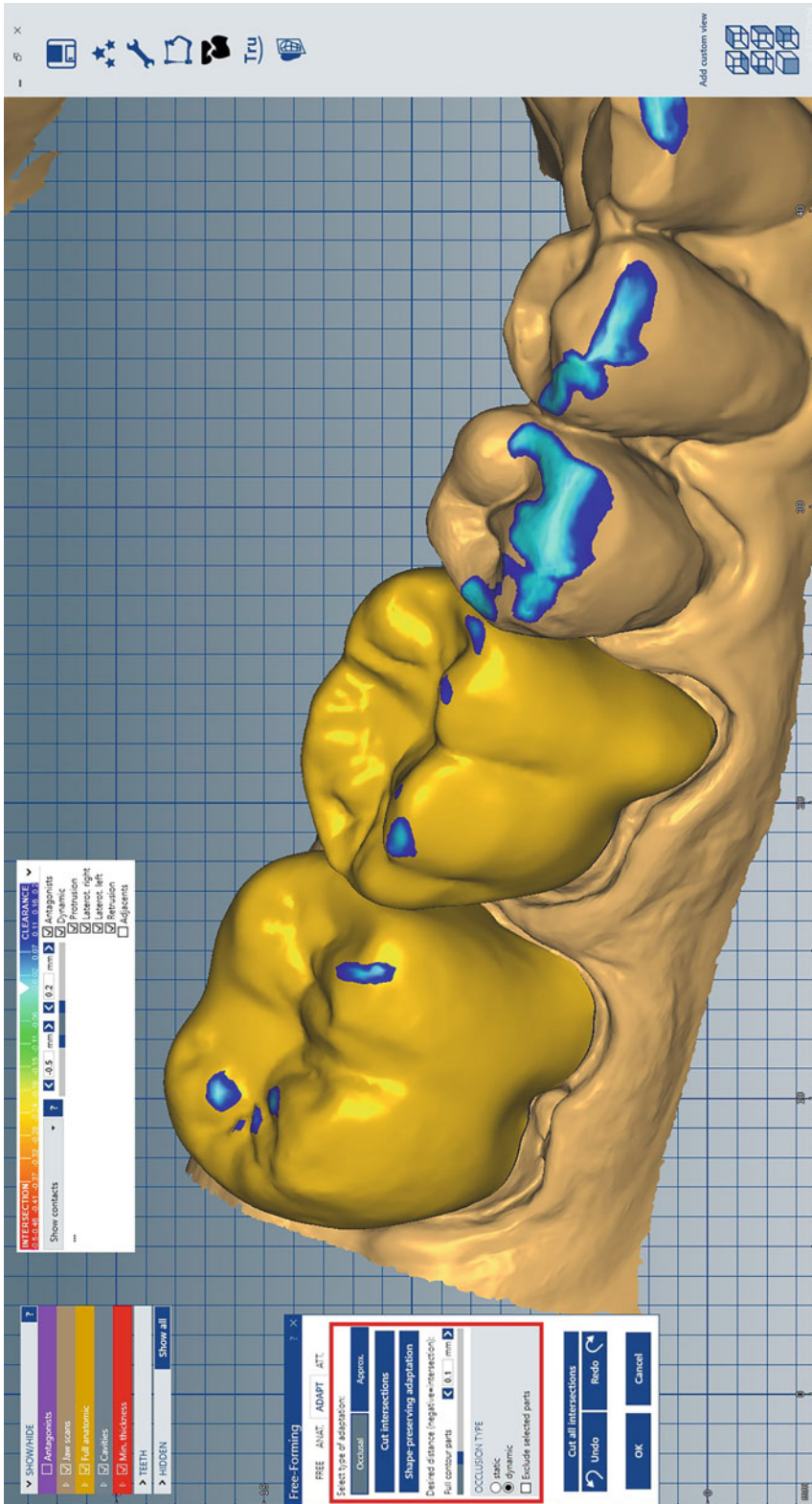
Fig. 5.18 Proposed crown design after adjustment for interferences

Fig. 5.19 intra-oral picture of crowns at initial try-in

maxillomandibular relationships and mandibular movement. While this case illustrates the use of virtual models and workflows to increase the accuracy of restorations, one can easily appreciate the benefit of using this technology on larger cases as well.

5.8 Conclusion

The exponential rate at which digital technology is advancing in dentistry is apparent in the discussion in this chapter. Consequently, the outcomes for both dentists and patients are constantly improving. New developments in both hardware and software are allowing for better diagnosing, planning, and treatment with the creation and utilization of virtual models and virtual patients. Dental procedures will be associated with less treatment timeframe and fewer complications for the patients, along with many other advantages, due to these advances. However, based on recent technological developments, it seems the best is yet to come.

References

Baan F, de Waard O, Bruggink R, Xi T, Ongkosuwito EM, Maal TJJ (2020) Virtual setup in orthodontics: planning and evaluation. Clin Oral Investig 24(7):2385–2393. https://doi.org/10.1007/s00784-019-03097-3

Baan F, Bruggink R, Nijsink J, Maal TJ, Ongkosuwito EM (2021) Fusion of intra-oral scans in cone-beam computed tomography scans. Clin Oral Investig 25(1):77–85. https://doi.org/10.1007/s00784-020-03336-y

Clayton JA, Kotowicz WE, Zahler JM (1971) Pantographic tracings of mandibular movements and occlusion. J Prosthet Dent 25(4):389–396. https://doi.org/10.1016/0022-3913(71)90229-0

Garcia PP, da Costa RG, C. M., Ritter, A. V., Correr, G. M., da Cunha, L. F., & Gonzaga, C. C. (2018) Digital smile design and mock-up technique for esthetic treatment planning with porcelain laminate veneers. J Conserv Dent 21(4):455–458. https://doi.org/10.4103/JCD.JCD_172_18

Haddadi Y, Bahrami G, Isidor F (2019) Accuracy of intra-oral scans compared to conventional impression in vitro. Prim Dent J 8(3):34–39. https://doi.org/10.1308/205016819827601491

Joda T, Gallucci G, Wismeijer D, Zitzmann N (2019) Augmented and virtual reality in dental medicine: a systematic review. Comput Biol Med 108:93–100. https://doi.org/10.1016/j.compbiomed.2019.03.012

Kernen F, Kramer J, Wanner L, Wismeijer D, Nelson K, Flügge T (2020) A review of virtual planning software for guided implant surgery - data import and visualization, drill guide design and manufacturing. BMC Oral Health 20(1):251. https://doi.org/10.1186/s12903-020-01208-1

Kwon JH, Im S, Chang M, Kim JE, Shim JS (2019) A digital approach to dynamic jaw tracking using a target tracking system and a structured-light three-dimensional scanner. J Prosthodont Res 63(1):115–119. https://doi.org/10.1016/j.jpor.2018.05.001

Lepidi L, Galli M, Mastrangelo F, Venezia P, Joda T, Wang HL, Li J (2020) Virtual articulators and virtual mounting procedures: where do we stand? J Prosthodont 30(1):24–35. https://doi.org/10.1111/jopr.13240

Liao PL (2021) Evaluation of temporomandibular joint dysfunction by a mandibular tracing system: a case report. J Curr Res Dent 1(1):8–12. https://doi.org/10.54646/bijcrid.002

Marques S, Ribeiro P, Falcão C, Ferreira Lemos B, Ríos-Carrasco B, Ríos-Santos J, Herrero-Climent M (2021) Digital impressions in implant dentistry: a literature review. Int J Environ Res Public Health 18(3):1020. https://doi.org/10.3390/ijerph18031020

Otranto de Britto Teixeira A, Almeida MAO, Almeida RCDC, Maués CP, Pimentel T, Ribeiro DPB, Medeiros PJ, Quintão CCA, Carvalho FAR (2020) Three-dimensional accuracy of virtual planning in

orthognathic surgery. Am J Orthod Dentofacial Orthop 158(5):674–683. https://doi.org/10.1016/j.ajodo.2019.09.023

Peck CC (2016) Biomechanics of occlusion-implications for oral rehabilitation. Oral Rehabil 43(3):205–214. https://doi.org/10.1111/joor.12345

Rutkūnas V, Gečiauskaitė A, Jegelevičius D, Vaitiekūnas M (2017) Accuracy of digital implant impressions with intraoral scanners. A systematic review. Eur J Oral Implantol 10(Suppl 1):101–120

Shah P, Chong BS (2018, Mar) 3D imaging, 3D printing and 3D virtual planning in endodontics. Clin Oral Investig 22(2):641–654. https://doi.org/10.1007/s00784-018-2338-9

Advanced 3D Visualization and 3D Printing in Radiology

6

Shabnam Fidvi, Justin Holder, Hong Li, Gregory J. Parnes, Stephanie B. Shamir, and Nicole Wake

Abstract

Since the discovery of X-rays in 1895, medical imaging systems have played a crucial role in medicine by permitting the visualization of internal structures and understanding the function of organ systems. Traditional imaging modalities including Computed Tomography (CT), Magnetic Resonance Imaging (MRI) and Ultrasound (US) present fixed two-dimensional (2D) images which are difficult to conceptualize complex anatomy. Advanced volumetric medical imaging allows for three-dimensional (3D) image post-processing and image segmentation to be performed, enabling the creation of 3D volume renderings and enhanced visualization of pertinent anatomic structures in 3D. Furthermore, 3D imaging is used to generate 3D printed models and extended reality (augmented reality and virtual reality) models. A 3D image translates medical imaging information into a visual story rendering complex data and abstract ideas into an easily understood and tangible concept. Clinicians use 3D models to comprehend complex anatomical structures and to plan and guide surgical interventions more precisely. This chapter will review the volumetric radiological techniques that are commonly utilized for advanced 3D visualization. It will also provide examples of 3D printing and extended reality technology applications in radiology and describe the positive impact of advanced radiological image visualization on patient care.

6.1 Introduction

Medical imaging is of vital importance in depicting the internal visualization of organ systems and their function. Computed Tomography (CT), Magnetic Resonance Imaging (MRI) and Ultrasound (US) are the core modalities used in biomedical imaging that display

S. Fidvi (✉) · J. Holder · S. B. Shamir
Department of Radiology, Montefiore Medical Center, Bronx, NY, USA
e-mail: sfidvi@montefiore.org; juholder@montefiore.org; sshamir@montefiore.org

H. Li · G. J. Parnes
Department of Radiology, Jacobi Medical Center, Bronx, NY, USA
e-mail: lih18@nychhc.org; parnesg1@nychhc.org

N. Wake
GE Healthcare, Aurora, OH, USA

Center for Advanced Imaging Innovation and Research, NYU Langone Health, New York, NY, USA
e-mail: Nicole.Wake@ge.com

two-dimensional (2D) images in fixed orientations. Advanced volumetric medical imaging expands upon this 2D imaging by creating three-dimensional (3D) images to be displayed on the conventional 2D imaging screens which are viewed by physicians, patients, and their families alike. 3D processing techniques facilitate diagnosis and enable quantitative analysis of the acquired images.

3D printing, augmented reality (AR), and virtual reality (VR) are 3D imaging methods used to create anatomic models. Creating 3D models from radiological imaging data is a complex process that involves manipulating the original 2D images into a volume that represents patient-specific anatomy. 3D anatomic model creation includes image acquisition, image segmentation, and computer-aided design (CAD) modeling. The manipulated data is then optimized for the advanced visualization method of choice—3D printing, AR, or VR. All forms of 3D modeling transform biomedical information into a visual display that renders abstract and complex diseases readily comprehensible. 3D modeling from medical imaging data elucidates complex anatomic structures and highlights pathology which enables clinicians to plan surgical procedures more effectively and enhance patient outcomes. For example, 3D models are used to plan tumor resections within the abdomen, pelvis, breast, and musculoskeletal systems, as well as to facilitate many cardiac and neurointerventional procedures. In addition to clinical applications, 3D models have been used to improve trainee and patient education.

3D modeling has been used in medical education for generations to demonstrate both normal anatomy and complex pathologies, and many medical student and radiology residency training programs implement 3D printing and extended reality technologies (Burns et al. 2022). Institutions also use these models to assist patients and their families in understanding medical conditions, surgical goals and surgical approaches. Patient specific, anatomically accurate 3D models enhance patient education and the consent process by helping the patient and their family to better understand their pathology as

well as the surgery that will be performed and the inherent risks the procedure entails (Eisenmenger et al. 2017; Tzavellas et al. 2020). This leads to more effective communication, elevated patient satisfaction, and confidence in selecting a treatment plan (Mitsouras et al. 2015).

This chapter provides an overview of the benefits and limitations of the traditional imaging modalities of CT, MRI, and Ultrasound. Furthermore, the chapter highlights the volumetric radiological techniques that are commonly utilized for advanced 3D visualization and provides examples of 3D printing and extended reality technology applications in radiology. The chapter discusses examples that demonstrate how advanced medical imaging techniques facilitate myriad cardiovascular and neurointerventional procedures. Additionally, the chapter focuses on how the use of 3D imaging can be used to plan tumor resections in the abdomen, pelvis, breast, and musculoskeletal system. In summary, the chapter highlights the tremendous positive impact of advanced radiological image visualization techniques like 3D printing in revolutionizing patient care.

6.2   Medical Imaging Technologies

Imaging modalities including CT, MRI, and ultrasound are often used for advanced 3D image visualization or to create 3D printed and extended reality models (Wake et al. 2022). There are many texts that describe these imaging modalities in detail (Seutens 2009; Kalendar 2011; Brown et al. 2014; Zagzebski 1996). Herein, the basics are described in order to provide a background for the 3D imaging and visualization methods commonly used in radiology and medicine.

Computerized Tomography is used most often for advanced 3D image visualization and modeling due to the ease of post-processing CT data. A CT scan involves a series of X-rays delivered through a patient that is subsequently detected by the scanner detector after passing through the body. The quantity of X-rays absorbed by the body determines the number of X-rays that reach the CT detector, which in turn

utilizes software to assign grayscale levels defined as Hounsfield Units (HU) to various tissues. Tissues that do not absorb many X-rays appear black, such as fat and air, while those that absorb these rays appear white, such as bone and intravenous contrast. Most organs and vascular structures fall somewhere in between, as varying degrees of gray. CT is thus able to distinguish and isolate pathological processes from the background tissue based on the differing levels of white, gray, and black. The radiologist defines and separates objects on the acquired images to generate 3D models, and the pathology must be demarcated from the background tissue through the post-processing step. This modeling process thus works most effectively if the organ can be easily separated from its environment, and if the pathology can be accurately separated from the organ. CT is conducive to this as there is a solitary color scale to evaluate and the images are often acquired in a standard, axial plane (Mitsouras et al. 2015).

Magnetic Resonance Imaging is a more complex imaging modality that provides good tissue contrast without ionizing radiation. MRI uses varying electromagnetic fields applied to a patient in multiple configurations and directions to generate images in unlimited planes. There are consequently many sequences available (e.g., T1, T2, proton density, diffusion, dynamic contrast enhanced) that highlight different tissues in various ways and in different orientations. The signal of tissue can have multiple different colors, or intensities, depending on the pathology and sequence used for display. MRI is more difficult to use than CT for 3D image visualization and 3D printing. MRI has some limitations in distinguishing pathology from background tissue because it has thicker slabs than CT which results in more structural overlap and impairs the radiologist's ability to diagnose with precision. Finally, MRI is particularly susceptible to artifacts that can distort images, which renders contouring and isolating structures challenging (Graves and Mitchell 2013; Morelli et al. 2011; Bernstein et al. 2006). Setting these challenges aside, what makes MRI so effective in radiology is its excellent soft tissue contrast and the wealth of information content in MR images.

Ultrasound is commonly used for advanced 3D imaging visualization. This imaging modality employs high-frequency sound waves that spread through the body, bounce off deep tissues, and return to the machine to be processed (Prince and Links 2006). The generated image is determined by the different speeds and directions of soundwaves emitted from the various tissues and structures detected by the machine. Although ultrasound is excellent for 3D image visualization, it poses a challenge for 3D modeling as ultrasound images are not obtained in the standard transverse, coronal, and sagittal orientations. However, the use of specialized probes and image processing software enhance the ability to perform a 3D ultrasound (Sepulveda et al. 2012). This has allowed the progressive incorporation of 3D-US into the routine fetal anatomical survey to allow evaluation of select fetal anatomical landmarks and serve as a complement to evaluate detected fetal anomalies (Sepulveda et al. 2012). The other limitation of ultrasound is that the image appearance is entirely dependent on manual transducer positioning and there is high variability in organ and pathology orientations and appearances (Wake et al. 2022).

6.3 3D Image Visualization

Volumetric medical images can be visualized on a 2D screen or a 3D display which effectively represents the spatial relationships between adjacent structures. In order to properly visualize anatomic structures in 3D or to create accurate anatomic 3D models from medical imaging data, the slice thickness must be sufficiently narrow (e.g., 1 mm or less). If the slice thickness is too large, then the 3D anatomical region of interest will be distorted. For CT and MRI, 3D acquisitions with isotropic resolution (e.g., $1 \times 1 \times 1$ mm) permit visualization of the anatomy from any orientation, enabling proper depiction of any pertinent anatomic structure.

Volume rendering is an important data visualization technique used to create a 3D

representation of volumetric medical imaging data, typically CT. Direct volume rendering methods generate 3D representations of the volume data directly (Levoy 1988). An optical model is applied to map data values to optical properties such as color and opacity (Max 1995).

Fundamental CT algorithms include Maximum Intensity Projection (MIP), Minimum Intensity Projection (MinIP), and Shaded Surface Volume Renderings (SS-VRT). MIP images are obtained by projecting the voxel with the highest attenuation value on every view throughout the image volume, whereas MinIP images display only the lowest attenuation value encountered in a specific volume. MIP images are useful for the detection of small lung nodules and MinIP images are particularly useful for analyzing the biliary tree and pancreatic duct. SS-VRT allows for 3D visualization from volumetric data by representing object surfaces (Udupa et al. 1991; Hong and Freeny 1999; Fishman et al. 2006). SS-VRT, which is particularly useful for visualizing bone or vasculature, provides a 3D perspective of that specific tissue. An important variation of SS-VRT is virtual endoscopy wherein the surface of the gastrointestinal tract lumen, such as the colon, is displayed so that lesions and polyps are readily detected. There are thus multiple post-processing algorithms that can be applied to 2D images to generate clinically useful 3D images.

6.4 Image Segmentation

Image segmentation, the process of subdividing an image into its constituent regions or objects, is a highly relevant task in medical image analysis and is important for many clinical applications. Segmentation algorithms for grayscale images are typically based on one of two basic categories, both of which deal with properties of intensity values: (1) discontinuity (partitioning an image based on abrupt changes in gray level) and (2) similarity (partitioning an image into regions that are similar). Common segmentation techniques available in most medical image

post-processing platforms include thresholding, edge detection, and region growing.

Thresholding is the simplest method of image segmentation and can be used to generate binary images from a volumetric grayscale image dataset. To differentiate pixels of interest, a comparison of each pixel intensity value with respect to a threshold is performed. If the pixel's intensity is higher than the threshold, the pixel is set to one value, i.e., white, and if it is lower than the threshold, it is set a second value, i.e., black (Fig. 6.1).

Edge detection is a technique that finds the boundaries of objects (edges) within images. Edge detection works by detecting discontinuities in brightness between adjacent structures and is used most frequently for segmenting images based on sudden local changes in intensity.

Region growing is a simple region-based image segmentation method. It is classified as a pixel-based image segmentation method since it involves the selection of initial seed points. Once a seed point or set of points has been identified, a region is grown by appending to each set of neighboring pixels that have predefined properties similar to the seed.

In the USA, when medical image post-processing software is marketed for patient care (i.e., Clinical Care or Diagnostic Use), the software needs to have Food and Drug Administration (FDA) clearance. FDA-cleared software is not required for research in the US. Outside the USA, regulations vary. Table 6.1 highlights some of the software products available for medical image post-processing.

6.5 3D Printing

3D printing and extended reality technologies are increasingly being used in medicine for a wide range of applications including pre-surgical planning, simulations, intraoperative guidance, trainee education, and patient education. 3D printing technologies can also be used to create patient-specific surgical guides, implants, and prosthetics.

Also known as additive manufacturing or rapid prototyping, 3D printing uses an additive
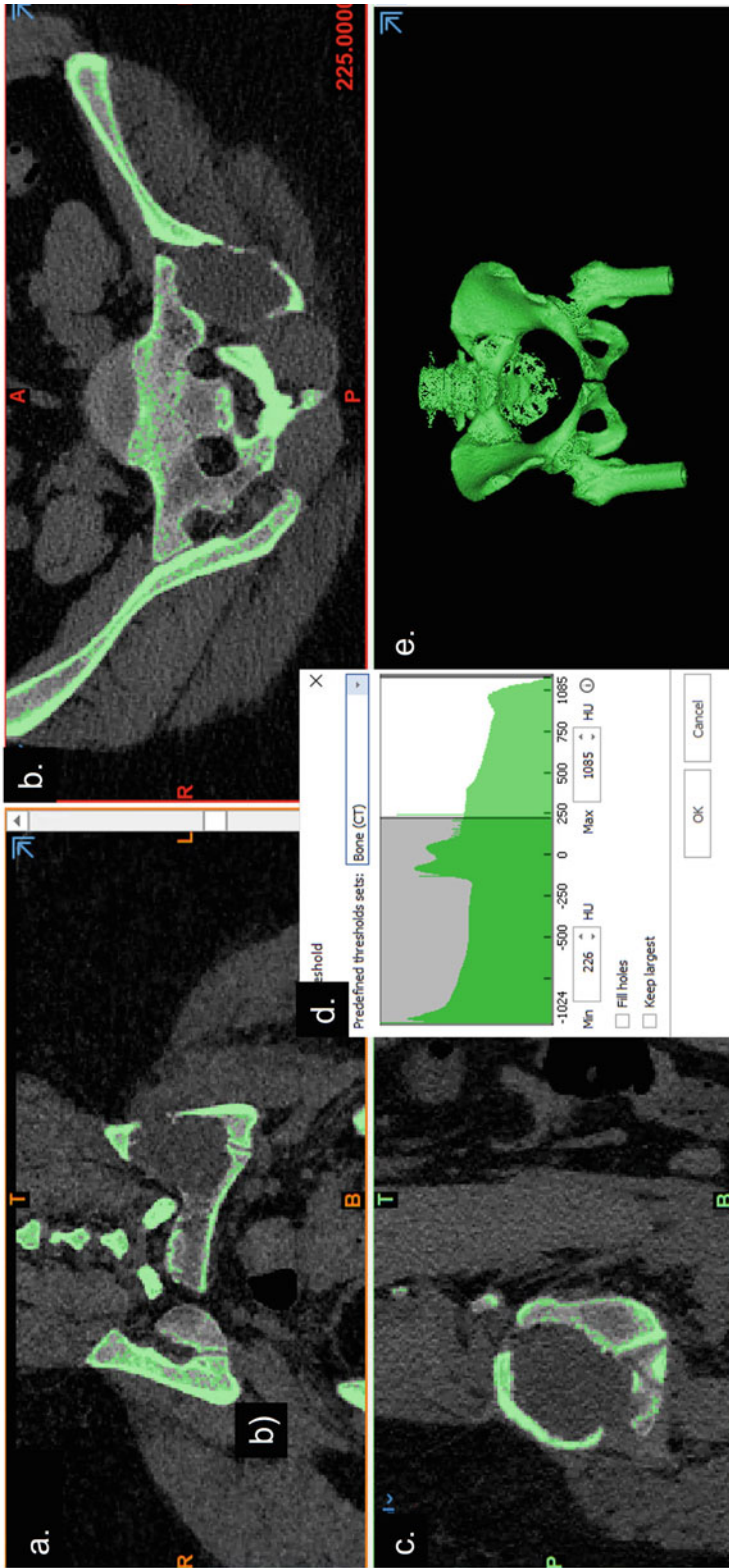
Fig. 6.1 Example of bone thresholding from CT data using HU 226–1085. (**a**) Coronal view, (**b**) axial view, (**c**) sagittal view, (**d**) threshold settings, (**e**) 3D visualization of segmented bone. Images courtesy of Nicole Wake, PhD, GE Healthcare

Table 6.1 3D visualization and segmentation programs utilized in radiology

Product	Company	Website	FDA Clearance
3D Slicer	Brigham and Women's Hospital	www.slicer.org	None
Amira	Thermo Fisher Scientific	https://www.thermofisher.com/us/en/home/electron-microscopy/products/software-em-3d-vis/amira-software.html	3D Visualization
Analyze/ Analyze Pro	Analyze Direct	www.analyzedirect.com	None
AnatomicsRx	Anatomics	www.anatomicsrx.com	None
AW Server	GE	www.gehealthcare.com	3D Visualization
D2P	3D Systems	www.3Dsystems.com	3D Printing
Dolphin 3D Surgery	Dolphin/Patterson Dental	www.dolphinimaging.com	3D Visualization
F.A.S.T	Fovia	www.fovia.com	3D Visualization
IBM iConnect	IBM	https://www.ibm.com/products/iconnect-access	3D Visualization
iNtuition	TeraRecon	www.terarecon.com	3D Visualization
Itk-SNAP	University of Utah & UPENN	www.itksnap.org	None
MeVisLab	Mevis	www.mevislab.de	None
Mimics	Materialise	www.materialise.com	3D Printing
Mirrakoi	Rhino3D Medical	https://mirrakoi.com/rhino3dmedical_for_engineers/	None
NemoFAB	Nemotec	www.nemotec.com	None
OsiriX Lite	Pixmeo	www.osirix-viewer.com	None
OsiriX MD	Pixmeo	www.osirix-viewer.com	3D Visualization
Ossa 3D	Conceptualiz	http://www.conceptualiz.org/products_ossa.html	None
Ricoh 3D for Healthcare	Ricoh, USA, Inc	https://www.ricoh-usa.com/en/industries/healthcare/3d-printing-for-healthcare	3D Printing
Seg3D/ Biomesh3D	University of Utah	https://www.sci.utah.edu/cibc-software/seg3d.html	None
Simpleware	Synopsis	www.synopsis.com	3D Printing
Vitrea	Vital Images/ Canon	www.vitalimages.com	3D Visualization

method to create a 3D physical object layer by layer. First patented in 1986 by Chuck Hull, 3D printing technologies have quickly developed over the years (Hull 1986). Although all 3D printers use the basic additive fabrication method that involves building the part one layer at a time, they differ on the material types and techniques used. Today, according to the American Society for Testing Materials, there are seven major 3D printing technologies (ISO 2021). These technologies include binder jetting, direct energy deposition, material extrusion, material jetting, powder bed fusion, sheet lamination and vat photopolymerization (Table 6.2).

3D printed models play a crucial role in transforming surgical interventions by facilitating pre-surgical planning and simulation, intraoperative navigation, and physician training. 3D models are valued by many surgeons as they provide spatial comprehension, tactile feedback, and a better understanding of patient-specific anatomical characteristics and variations (Tzavellas et al. 2020). In conjunction with computer-aided surgery simulation, 3D models

Table 6.2 Description of 3D printing technologies

Printing technology type	Description of method
Binder Jetting	Process in which a liquid bonding agent is selectively deposited to join powder materials.
Direct Energy Deposition	Process in which focused thermal energy is used to fuse materials by melting as they are being deposited.
Material Extrusion	Process in which material is selectively deposited through a nozzle.
Material Jetting	Process in which droplets of photosensitive build material are selectively deposited and solidified with ultraviolet light.
Powder Bed Fusion	Process in which thermal energy selectively fuses regions of a powder bed.
Sheet Lamination	Process in which sheets of material are bonded to form a part.
Vat Photopolymerization	Process in which liquid photopolymer in a vat is selectively cured by light-activated polymerization.

are an invaluable tool in the preparation for a safer and more cost-effective surgical pelvic reconstruction minimizing operative time and maximizing precision outcomes (Hung et al. 2019). Models manufactured with materials fulfilling biocompatibility standards can be sterilized using predefined protocols and brought to the surgical field (Fang et al. 2019). Using 3D models can allow for a reduction in overall operative and fluoroscopic times, a decrease in intraoperative blood loss, increased accuracy of reduction and fixation and a decrease in complications such as iatrogenic nerve injuries (Tzavellas et al. 2020). Current 3D printing technologies can be limited regarding material type and color capabilities, although technologies are continuously improving, and it is expected that new material types and color options will be more easily accessible and affordable in the future.

6.6 3D Visualization and Modeling for Cardiovascular Applications

Planning cardiovascular surgery is a collaborative effort that integrates imaging expertise of radiologists and clinical expertise of cardiologists and cardiac surgeons to determine the best therapeutic options while optimizing operative time. Over the last 10 years, 3D image visualization has been used extensively for the planning of cardiovascular procedures such as transcatheter aortic valve replacement (TAVR), widely established as the most common FDA-approved treatment for patients with severe symptomatic aortic stenosis who are at moderate (or greater) risk for surgical valve replacement (Hosny et al. 2019). This endovascular procedure employs a catheter-based delivery system using femoral arterial access to implant a balloon-expandable bioprosthetic valve within a diseased aortic valve. Although in widespread use, the complex 3D anatomy of the aortic root makes it difficult to predict how the prosthetic aortic valve will adapt in the patient and achieving a personalized prosthetic valve fit for every patient remains a surgical challenge. Oversizing the prosthetic valve can lead to annular rupture, and under-sizing can result in an ineffective seal/paravalvular leak or prosthetic valve embolization. Characterization of aortic root anatomy and aortic annular measurements are an important starting point for determining appropriate valve size, but additional patient-specific factors such as the degree of annular eccentricity and the relative distribution of calcified deposits on valve leaflets and in the LVOT all influence valve anchoring and seal efficacy (Hosny et al. 2019). Figure 6.2 shows aortic images from a patient with significant plaque on the annulus.

3D printed heart and aortic models are used preoperatively and intraoperatively in the management of complex congenital heart disease (CHD), acquired cardiovascular anomalies, cardiac tumors and in percutaneous cardiology procedures such as TAVR (Levin et al. 2020; Yoo et al. 2015, 2017; Marro et al. 2016). Anatomic models facilitate improved spatial acuity to
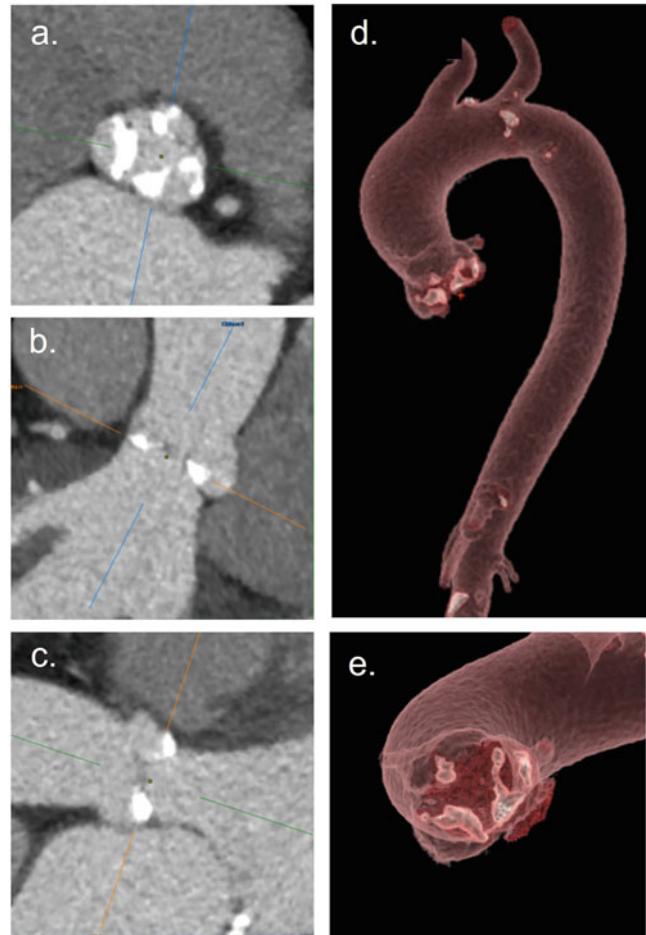
critical structures with reduction in operative time including cardiopulmonary bypass times. Operative rehearsals with patient-specific 3D printed models reveal potential pitfalls to the surgeon, the preferred approach and optimal instrumentation, while providing a preview of anatomic nuances and opportunity to improve technique (Yoo et al. 2017; Hussein et al. 2020; Hermsen et al. 2017). 3D printed models assist in educating surgical trainees by simulating specific anatomy and allowing various surgical approaches to be practiced in a stress-reduced environment without harming the patient. Soft tissues can be mapped and reconstructed, effectively moving important decisions from the time-constrained operating room to the preoperative setting (Costello et al. 2015; Ballard et al. 2018). Cardiothoracic surgeons find the models suitable for practicing

closure of septal defects, application of baffles (surgically-created tunnels used to redirect blood flow) within the ventricles, reconstructing the aortic arch, and the arterial switch procedure (Yoo et al. 2015). In addition, patient-specific 3D models are valuable for enhancing engagement with parents and improving communication between cardiologists and parents resulting is a positive impact in parents' and patients' psychological adjustment to living with congenital heart disease (CHD) (Biglino et al. 2015).

CHD such as Ventricular Septal Defects (VSD), Tetralogy of Fallot, and Double Outlet Right Ventricle (DORV) cause significant hemodynamic and functional consequences necessitating surgical repair. 3D-printed replicas of the patient's heart permit precise understanding

of complex cardiac anatomy and hands-on simulation of surgical and interventional procedures.

As an example, DORV (Fig. 6.3) is a cardiac anomaly in which both the aorta and the pulmonary artery originate predominantly or entirely from the right ventricle. In this situation, the left ventricle (LV) has no direct outlet to either great vessel and must eject blood into the right ventricle (RV) through a VSD. Rarely, in the absence of a VSD, the LV is very hypoplastic. The physiological picture and the type of surgical correction depend on the arrangement of the great vessels and the anatomy of the VSD, both of which are well depicted by imaging. The most common variant, the Fallot type, has a normal arrangement of the great vessels, a subaortic VSD and is often associated with pulmonic stenosis. DORV may also be associated with an anterior aorta and a subpulmonic VSD, called the Taussig-Bing anomaly. Surgical correction for the Fallot type variant consists of VSD patch closure which
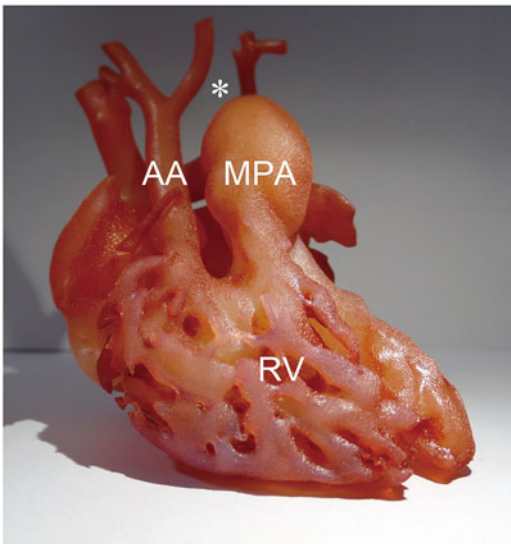
Fig. 6.3 Patient-specific 3D printed hollow cardiac model printed with a flexible material (TangoPlus, Stratasys) and created from 3D cardiothoracic CT data obtained preoperatively in an infant with DORV and interrupted aortic arch type B. Both the smaller AA and dilated MPA arise from DORV. The aortic arch is interrupted (asterisk) between the left common carotid artery and the left subclavian artery, indicating type B of interrupted aortic arch. *MPA* main pulmonary artery. Reproduced with open-access permission from Goo et al. (2020)

directs blood to the aorta and correction of pulmonic stenosis. For the Taussig-Bing variant without pulmonary obstruction, surgical correction consists of patch closure of the VSD and arterial switch. In the presence of pulmonary obstruction, LV flow is tunneled through the VSD to the aorta and an RV-PA pathway is created- the so-called Rastelli procedure (Quail and Taylor 2020).

3D-printed heart models are of value in training for and performing corrective surgery for Hypertrophic Cardiomyopathy (HCM). HCM is a genetic myocardial disease characterized by marked hypertrophy of the LV and occasionally the RV, possible obstruction of the LV outflow tract (LVOT), life-threatening arrhythmias and sudden cardiac death. Septal reduction therapies, including surgical myectomy and percutaneous transluminal septal myocardial ablation are established treatments for drug refractory symptomatic HCM. Poor visualization of the left ventricular cavity in the operative field and heterogeneous LVOT anatomy can make this surgical procedure challenging (Hamatani et al. 2017). The preferred method of treatment, surgical septal myectomy (SM), has potential complications of iatrogenic ventricular septal defect, residual left ventricular outflow tract (LVOT) obstruction and mitral regurgitation (MR) (Andrushchuk et al. 2018). Anatomic models help avoid these complications by optimizing visualization of complex intracardiac morphology and the mitral apparatus and permitting superior intraventricular septum resection volume and shape (Ali et al. 2020). 3D-printed HCM heart models also allow for patient-specific preoperative simulation of a low-volume, low-visibility, high-risk surgical procedure that is traditionally difficult to teach (Hermsen et al. 2017).

3D modeling is also commonly used in cardiology for left atrial appendage (LAA) occlusion (Goitein et al. 2017; Liu et al. 2016; Hong et al. 2022; Kim et al. 2022; Hachulla et al. 2019; Morcos et al. 2018). The LAA is a common site for thrombus formation in patients with atrial fibrillation (AF), the most common cardiac arrhythmia. Its incidence increases with age to

>8% in those >80 years of age, and embolic strokes originating in the LAA are associated with a higher morbidity and mortality, emphasizing the need for effective stroke prevention in AF. While the mainstay of treatment is pharmacological therapy with anticoagulants, LAA occlusion/exclusion devices such as the Watchman device (Boston Scientific, Marlborough, MA) are a viable alternative in patients in whom contraindications to anticoagulant therapy exist or who are at high risk of bleeding. Occlusion is defined as placement of a device into the LAA percutaneously, while exclusion refers to the application of an external ligature to isolate the LAA from the circulation (Athanassopoulos 2016).

The correct sizing and the optimal implantation position of the closure device pose a challenge due to complex and variable LAA shapes. The risks of under- or oversizing are LAA perforation, pericardial effusion, interference with the mitral valve or the ostium of the pulmonary veins, compression of the left circumflex artery and device embolization (Hachulla et al. 2019). Precise understanding and measurements of the dimensions of the LAA ostium, landing zone and maximum length of the main anchoring lobe are essential elements in occlusion procedures and especially important in patients with variant anatomy (Fig. 6.4).

Obtaining accurate LAA dimensions is also crucial to minimize intraprocedural improvisations and device changes, recapture maneuvers, and prolonged procedure times (Morcos et al. 2018). Periprocedural noninvasive imaging modalities utilized to evaluate the LAA include fluoroscopy, 2D or 3D transesophageal echocardiography (TEE), intracardiac echocardiography (ICE) and cardiac CT. 3D printed LAA models are valuable tools in the identification of the optimal device size and position eliminating incomplete sealing and peri-device leaks. Added benefits include technique optimization with simulation of the LAA closure procedure and a reduction in the device implantation learning curve (Hachulla et al. 2019).

Advanced 3D image visualization and printing have also been used for patients with mitral annular calcification (MAC), a degenerative process involving the mitral annulus which progresses to involve the leaflets and subvalvular apparatus causing valvular obstruction or regurgitation. In patients with severe MAC who are not surgical candidates, transcatheter mitral valve replacement (TMVR) is a feasible therapeutic option but remains surgically challenging due to the complexity of the mitral valve apparatus and its geometric relationship with the left ventricular anatomy. The calcified mitral annulus can vary in rigidity, size, and shape, all of which can affect anchoring of the deployed transcatheter valves and predispose to paravalvular leaks (PVL). The proximity of the mitral apparatus to the left ventricle can lead to LVOT obstruction during TMVR, either by direct prosthetic valve protrusion or by displacing the anterior mitral valve leaflet into the LVOT. Furthermore, the bulky calcified annulus can lead to underexpansion and dislodgement of the balloon-expandable valves. Given the anatomical challenges, meticulous pre-procedural 3D planning is warranted (Wang et al. 2016, 2018). 3D printed cardiac models are valuable adjuncts to assess prosthesis sizing, anchoring, expansion, paravalvular gaps, LVOT obstruction and extra-annular calcium extension (El Sabbagh et al. 2018) (Fig. 6.5). Simulation with 3D models helps trial the complex navigational maneuvers needed to advance catheters from the aorta to the left ventricle, preprocedurally select the size of the deflectable guiding catheter and to optimize catheter tip positioning between the two papillary muscles and close to the mitral annulus (Valverde 2017).

Another major use of advanced 3D image visualization in cardiac applications is for cardiac tumors. To safely resect or debulk a cardiac tumor, it is imperative to understand its intricate interplay with critical local cardiac structures to help devise a safe surgical strategy while protecting the coronary circulation. 3D printed cardiac tumor models such as that shown in Fig. 6.6 provide vital structural insight into tumor size and location and are used to identify the spatial relationship between the tumors and the coronary arteries in addition to gauging their depth and infiltration (Riggs et al. 2018).

Fig. 6.4 Example of a cauliflower-shaped LAA. (**a**) Cardiac CT and (**b**) TEE which both predicted a 25-mm Amulet device. Two different Amulet sizes were tested on the 2D printed model: (**c**) a 25 mm sized device and (**d**) a 22 mm sized device (Reproduced with open-access permission from Hachulla et al. (2019)
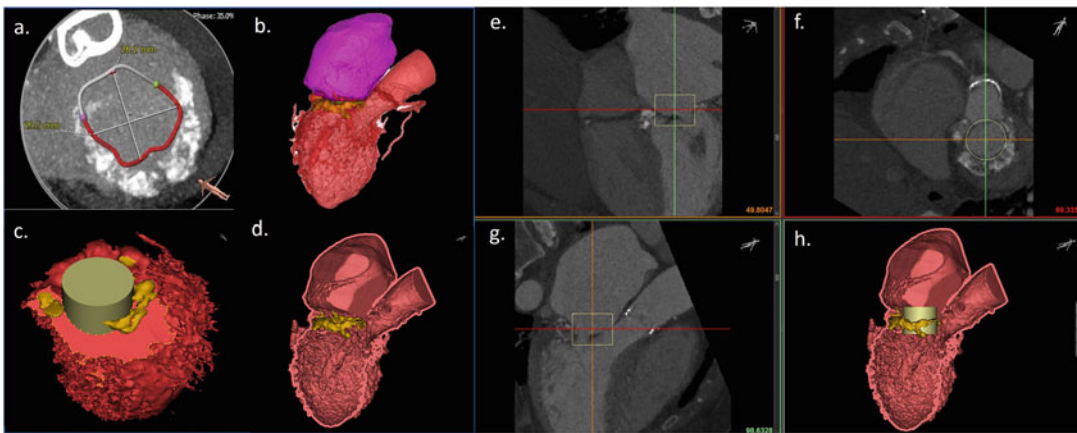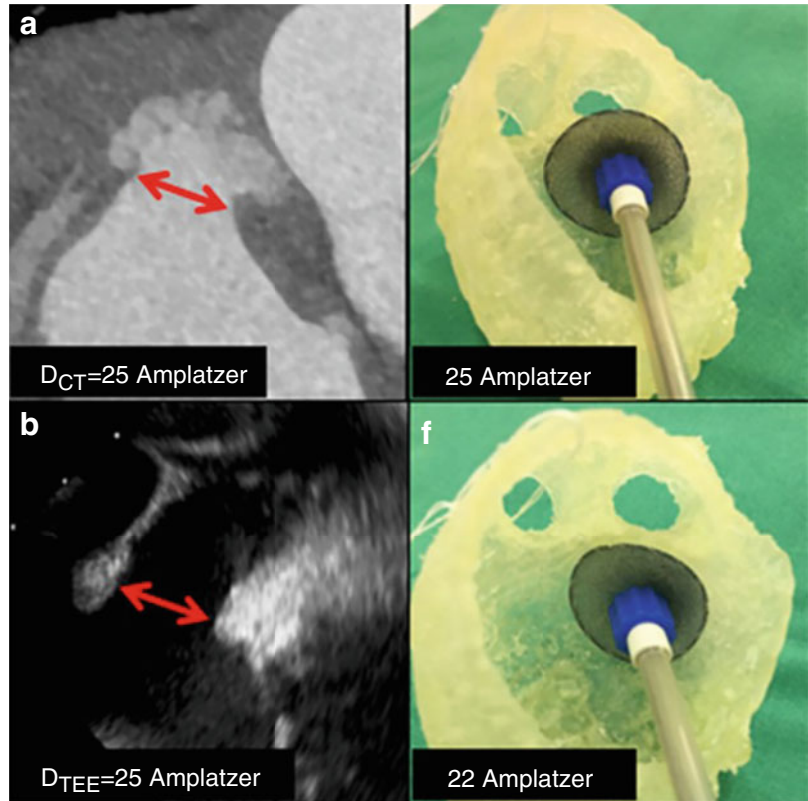
Fig. 6.5 3D modeling and surgical planning for TMVR in a patient with severe MAC. (**a**) cross-section of the mitral annulus with estimated area measurement shown. (**b**) 3D model of the hollowed left ventricle and atrium with aortic outflow (red), left atrium (purple), and calcified plaque (yellow). (**c**) en-face projection of mitral valve plane with simulated valve dark yellow. (**d**) hollowed left-sided heart view showing mitral calcification. (**e**) CT showing 4 chamber view with simulated valve (yellow box), (**f**) CT showing en-face mitral annulus view with simulated valve (yellow circle). (**g**) CT showing 2-chamber view with aortic outflow tract and simulated valve (yellow box). (**h**) 3D model of the hollowed left ventricle and atrium with the simulated valve placed (light yellow). Images courtesy of Nicole Wake, PhD, GE Healthcare

Fig. 6.6 Photographs of a physical 3D printed heart model (white) with a tumor (transparent) showing the left circumflex artery coursing through the tumor [Reproduced with open-access permission from Riggs et al. (2018)]


Finally, open surgical repair of abdominal aortic aneurysms (AAA) has given way to catheter-based endovascular aneurysm repair (EVAR) which requires specialized skills and training (Bastawrous et al. 2018). Endovascular repair of complex aortic aneurysms involving the origin of aortic branches, extreme angulations, complex aneurysm neck anatomy, and short landing zones can be technically challenging. Pertinent information sought from preoperative CT angiograms includes assessment of access (common femoral artery) for its diameter (large enough to accommodate delivery system), presence of plaques or calcifications which can hinder access, iliac artery diameters at landing zones and iliac vessel tortuosity (Chepelev et al. 2015). Simulation on 3D printed aortic phantoms is beneficial in the preoperative planning and teaching of aneurysm repairs by identifying the best projections for angiography, the best catheter and wire combinations to navigate the anatomy and in determining appropriate stent size, design, and position (Sommer et al. 2018, 2021; Meess et al. 2017) (Fig. 6.7). Haptic feedback elicited from manipulation of guidewires and catheters also aids complex endovascular interventions, increasing operator confidence (Chepelev et al. 2018).

6.7 3D Visualization and Modeling for Musculoskeletal Applications

3D image post-processing is routinely performed to better visualize musculoskeletal pathologies such as complex shoulder fractures (Fig. 6.8). 3D printed-assisted operations for comminuted and intraarticular proximal humeral fractures shortened surgery duration and time to fracture union, improved healing in an anatomical position and shoulder function, reduced blood loss volume, the number of fluoroscopies during surgery and minimized postoperative complications (Li et al. 2022).

In the setting of pelvic trauma, 3D visualization of the fractured hemi-pelvis provides surgeons an accurate understanding of fracture configuration, allowing the manipulation of bone fragments in a virtual simulation and creation of personalized treatment plans utilizing the best surgical approach and reduction technique as well as optimal interfragmentary screw trajectories (Hurson et al. 2007). Surgery around the bony pelvis poses unique challenges due to complex anatomy, deep exposures and narrow safe corridors required to avoid critical neurovascular and visceral structures (Fang et al. 2019); and 3D visualization is a much more powerful tool as compared to traditional radiological assessment of pelvic fractures involving plain X-rays and CT (Hurson et al. 2007).
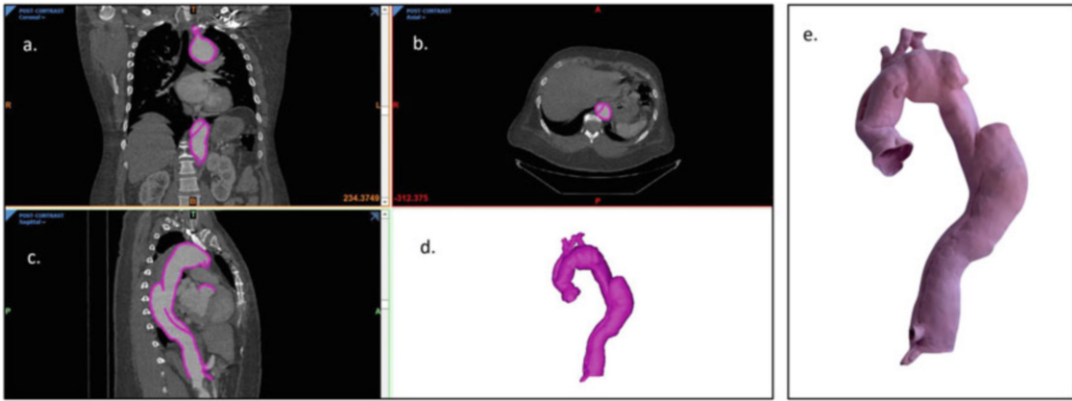
Fig. 6.7 Case with an abdominal aortic aneurysm with a dissection showing image contours generated from image segmentation and subsequent hollowing of the blood pool on the (**a**) coronal, (**b**) axial, and (**c**) sagittal CT images. (**d**) Virtual 3D model of the anatomic region of interest. (**e**) 3D printed model of the printed aortic aneurysm model printed with jet fusion technology. Images courtesy of Nicole Wake, PhD, GE Healthcare
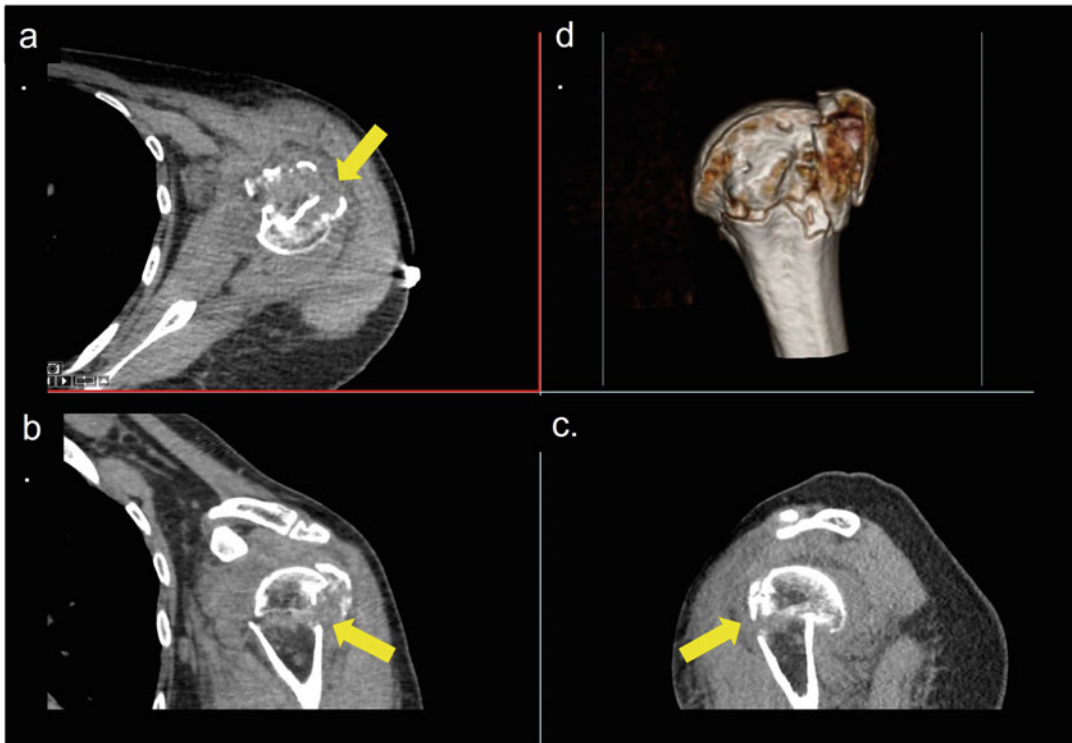
Fig. 6.8 Humeral head fracture (yellow arrow) shown on (**a**) axial, (**b**) coronal, and (**c**) sagittal CT images with (**d**) corresponding 3D model of the fracture. Images courtesy of Nicole Wake, PhD, GE Healthcare

3D printing the mirror image of the opposite intact anatomy can also play an invaluable role in the accurate pre-contouring of fixation plates, ensuring optimal implant positioning, minimizing dissection of adjacent soft tissues, reducing surgeon fatigue, and minimizing the need for implant repositioning (Fang et al. 2019; Hung et al. 2019). An example of mirroring is shown in Fig. 6.9.

3D visualization is also commonly used to reconstruct the bony anatomy for joint replacement and repair, such as the knee and shoulder. Using CT data, these 3D reconstructions allow improved comprehension of conditions such as osteoarthritis and allow for precise surgical planning using custom devices that match the patient's specific anatomy (Berhouet et al. 2017; Koch et al. 2021; Kwon et al. 2005; Lei et al. 2020). In patients with shoulder osteoarthritis, disproportionate posterior load bearing deforms the glenoid leading to bony thinning, retroversion, and biconcavity of its articular surface. Surgical techniques for shoulder replacement surgery total shoulder arthroplasty (TSA), shoulder hemiarthroplasty (SHA), and reverse shoulder arthroplasty (RSA) with adjunctive measures such as bone grafting and glenoid reaming. Surgical objectives include restoration of normal glenoid version and osteophyte removal to rebalance the humeral head, restore normal biomechanics, achieve durable hardware fixation, and provide lasting symptomatic relief and functional ability. The small volume of glenoid bone stock in conjunction with complex biomechanical forces and its relative avascularity and low strength (Wang et al. 2019) leads to loosening of the glenoid component, which is widely recognized as the primary limitation in the mid- and long-term durability of TSA (Al Najjar et al. 2018). The bony morphology of the glenoid is therefore a critical factor in the selection of appropriate surgical technique and preoperative planning for implant placement to ensure arthroplasty durability. As shown in Fig. 6.10, 3D printed models create realistic anatomic-scale representations of glenoid morphology including osteophytes, bony thinning, retroversion, and biconcavity.

3D visualization and modeling are also used in patients with spinal deformities such as idiopathic scoliosis, kyphosis, and meningomyeloceles to facilitate the study of joint inclination, false articulations and pedicle size (Fig. 6.11). In the preoperative setting, these models serve as a guide to curve correction and pedicle screw placement, resulting in a safer and more optimized surgical outcome.

Patient-specific 3D printed models can be highly valuable in cases of orthopedic oncology (Fig. 6.12). In addition, in these cases, surgical guides can also be created directly from volumetric images to guide corrective bone resections or complex tumor resections. In addition, as reconstructive and restorative surgeries have advanced in scope and complexity in the field of Orthopedics, 3D printing technology holds the potential for bringing personalized medicine and patient-centered healthcare closer to reality by enabling the fabrication of patient-specific implants. Despite the availability of multiple standardized commercial implants, a subset of patients fall outside the window of available devices and benefit from the design and production of individually tailored prostheses and orthotics (Mitsouras et al. 2015). Consequences of an improperly fitted implant include patient embarrassment and discomfort, decreased patient compliance and even depression (Ballard et al. 2018).

At this time, most implants created using additive technologies are created by original equipment manufacturers with 510 K FDA clearance to manufacture and sell the intended part. Typically, the design of a patient-specific implant utilizes the concept of "Mirroring" to create a template of patient anatomy in the setting of severe pathologic unilateral deformities. As humans exhibit plane symmetry though the midline sagittal plane, the non-pathologic side can be mirrored and computationally overlapped with the diseased side allowing rapid and accurate patient-specific reconstruction. This technique enables the creation of patient-specific surgical guides which allow the precise excision of bone and soft tissue tumors, optimization of the resection volume, conservation of healthy tissue and subsequent placement of the custom implant
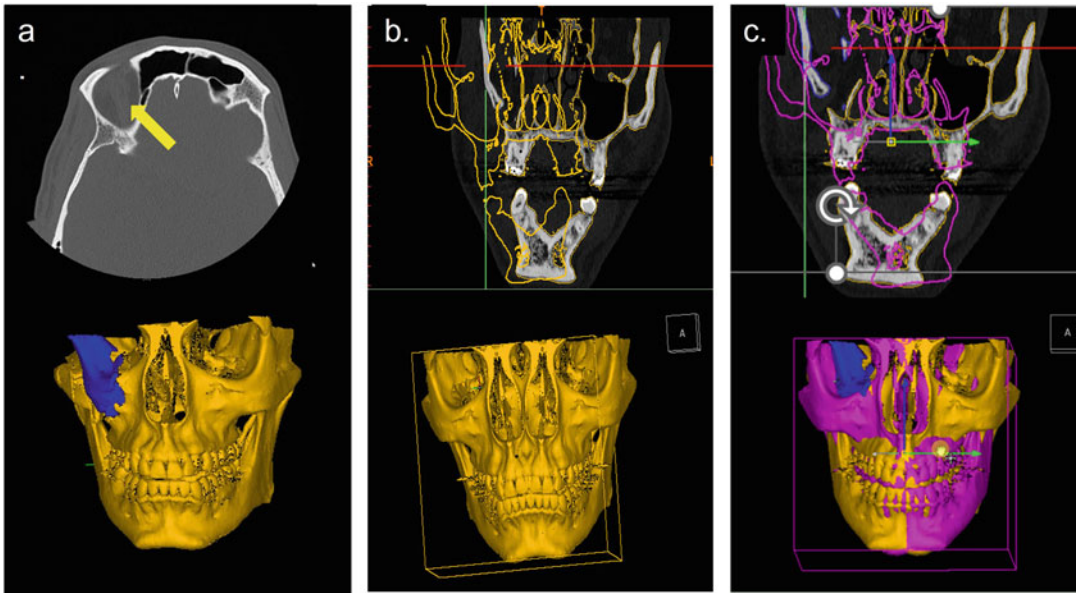
Fig. 6.9 (**a**) Axial CT image demonstrating tumor (yellow arrow) with corresponding 3D model with bone (yellow) and tumor (blue). (**b**) Image of the left side, mirrored to the right, with the plane vertically at the center of the nose. (**c**) Mirror image depicted in purple with the original bone (yellow) and tumor (blue). Note that rotation would be performed next to ensure proper alignment. Images courtesy of Nicole Wake, PhD, GE Healthcare

flush with the excision site (Chepelev et al. 2015). 3D-printed implants are used for tumor endoprosthetic reconstruction in cases of osteosarcomas, pelvic chondrosarcomas and tumors of the spine, clavicle, scapula and calcaneus. Custom-made implants are accompanied with a set of individualized tools for replicating the planned bone cuts, custom-made trial implants and drill guides to facilitate accurate placement of the prosthesis. Full-scale models for preoperative planning and intraoperative reference and guidance are also provided. Accurate intraoperative placement can, however, be challenging due to absence of intraoperative flexibility and the design and manufacture of these models are time-intensive and costly (Fang et al. 2019).

Finally, 3D printing of personalized orthotics (externally worn medical devices used to modify the structural and functional characteristics of the neuromuscular and skeletal system) using medical imaging data can allow for personalized solutions that can be advantageous as compared to standard devices. Orthotics are typically used in the setting of cerebral palsy, stroke, traumatic brain injuries, multiple sclerosis, and clubfoot to support the lower leg and correct imbalance. 3D printing technology offers design freedom and manufacture of patient-specific orthotics with theoretically optimized biomechanics, improved functionality, better fit, and aesthetics. Their relatively low cost is an important factor for children requiring multiple replacements as they grow (Matsumoto et al. 2015).

6.8 3D Visualization and Modeling for Abdominal Applications

The use of 3D printing in abdominal interventions and clinical scenarios is becoming increasingly common, with applications for surgical planning at the forefront. Image segmentation is challenging in abdominal structures as they demonstrate similar grayscale shades, which renders differentiation between them and their surrounding
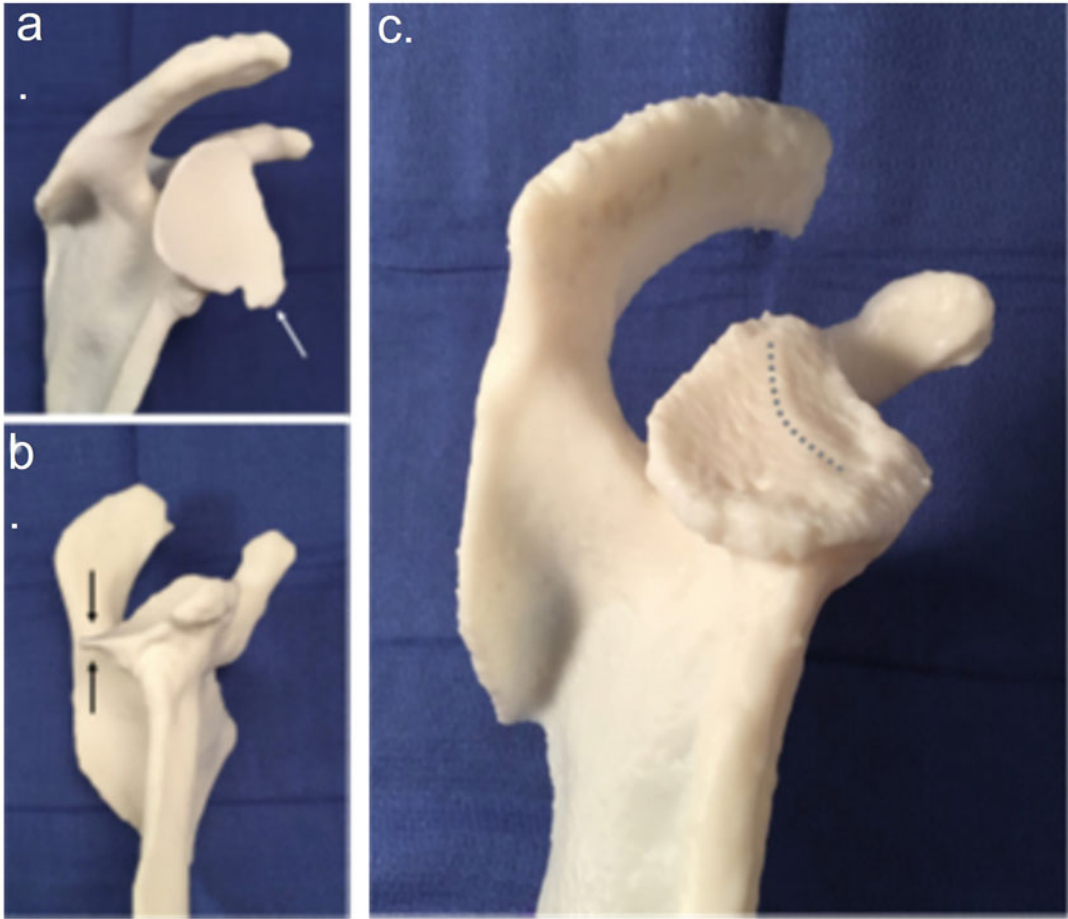
Fig. 6.10 3D model printed of the scapula created with selective laser sintering printing technology. (**a**) View from lateral demonstrates a large anteroinferior glenoid osteophyte (arrow). (**b**) View from inferior shows glenoid retroversion and posterior bony thinning (arrows). (**c**) 3D model printed using a stereolithography printer. View from inferolateral demonstrates glenoid biconcavity with a ridge between the two depressions in the glenoid surface (dotted line). Reproduced with permission from Wang et al. (2019)

vessels and fat difficult to process. Many solid organ tumors have similar grayscale appearances compared to the surrounding organ parenchyma, which makes delineation difficult. In addition, hepatic parenchyma, vascular, and biliary structures are closely opposed to each other and can often overlap or are difficult to distinguish on conventional 2D images. Furthermore, the vascular and biliary structures often take oblique, non-linear courses which are similarly challenging to comprehend on 2D images (Mitsouras et al. 2015). However, medical teams find 3D

modeling beneficial as abdominal anatomy can be relatively complex.

For abdominal applications, the two organ systems for which 3D modeling is most widely performed are hepatobiliary and renal structures (Mitsouras et al. 2015). These organs are clearly visible in medical images (CT and MRI) with smooth, regular borders that make them amenable to segmentation and reconstruction (Pietrabissa et al. 2020).

Liver transplant surgeries have been a frequent subject of 3D modeling (Mitsouras et al. 2015). There is a relative paucity of cadaveric donors for
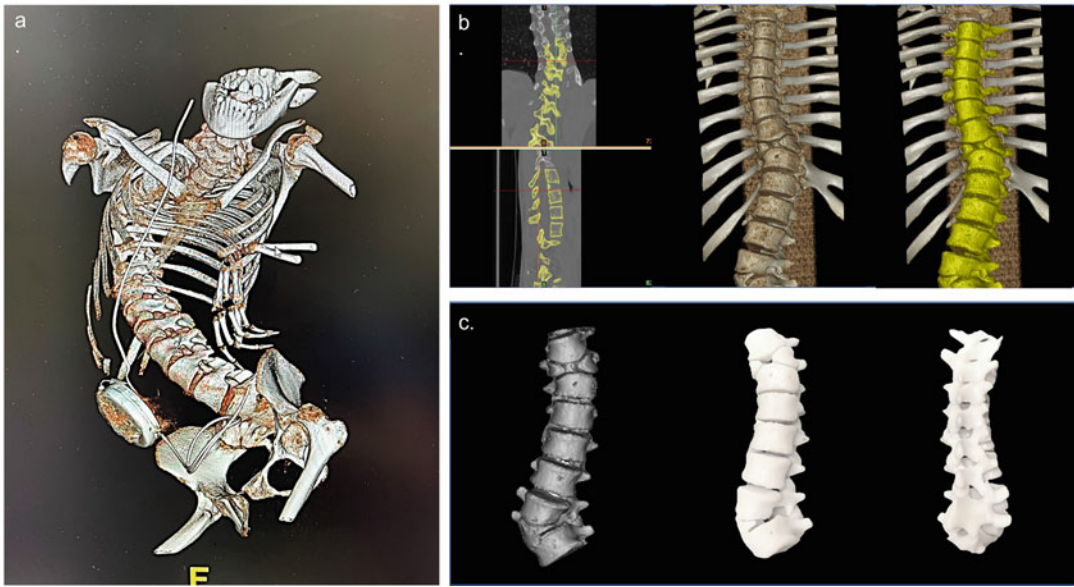
Fig. 6.11 (**a**) Shaded surface volume rendering of a patient with severe scoliosis. (**b**) Segmentation and visualization of a patient with scoliosis and a butterfly vertebra. (**c**) Virtual 3D model and 3D printed spine models (bottom right). Images courtesy ofNicole Wake, PhD, GE Healthcare

the transplant procedures, and many transplant procurement operations rely on living, healthy individuals undergoing lobectomies, which can have high morbidity. Much of this morbidity is due to inaccurate preoperative characterization of biliary and vascular structures and suboptimal estimates of liver volume (Zein et al. 2013).

Determining the volume of the donor's liver and individual lobes is an important component of operative planning as it ensures adequate postoperative reserve. Traditionally, these volumes are generated using modeling software on computer workstations (Fig. 6.13), although several studies have shown that 3D printed models have been more accurate in assessing liver volumes when compared to ex-situ surgical specimens (Zein et al. 2013). The same volumetric calculation and anatomic delineation can help when large portions of liver must be resected for other reasons than transplantations, such as solitary tumor resections. The tumor's relationship to adjacent vascular and biliary structures, as well as location within a segment, can be clarified with these printed models (Fang et al. 2015).

3D modeling also aids in the planning of partial nephrectomies for renal tumor resections (Silberstein et al. 2014). The kidney normally has an oblique position within the upper abdomen, which can be difficult to visualize on 2D imaging, and has multiple vascular and excretory structures that must be carefully considered in surgical planning, similar to the liver. 3D printing clarifies the relations between tumors and these structures for preoperative planning (Fig. 6.14) (Mitsouras et al. 2015; Wake et al. 2017, 2018, 2019). 3D printed models have also been used to plan the removal of kidneys from living donors in renal transplantation planning, as well as the removal of renal stones percutaneously (Pietrabissa et al. 2020).

The same goals of elucidating tumor location and relationship to adjacent structures have been described in the resection of pancreas, spleen, and bowel tumors and in treating anorectal fistulae (Marconi et al. 2017; Hamabe and Ito 2017). The technology has also been implemented in preoperative planning of abdominal wall hernias
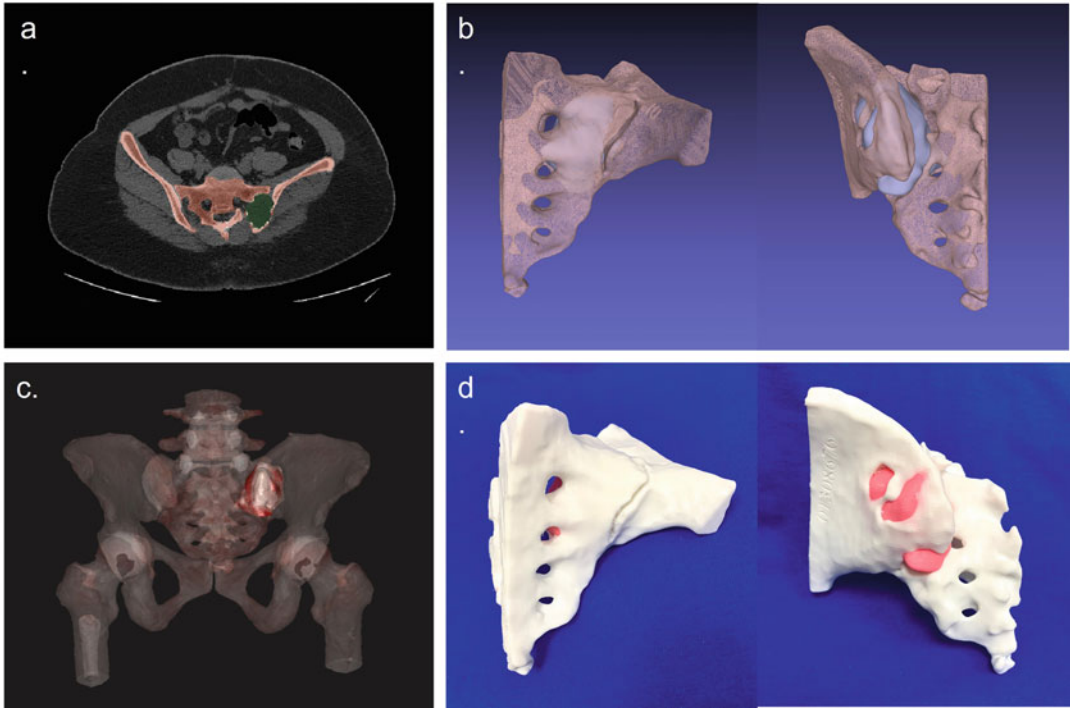
Fig. 6.12 Patient with a complex pelvic tumor showing (**a**) axial view with bone segmentation (red) and tumor segmentation (green), (**b**) 3D visualization of the left hemi-pelvis with tumor in the posterior and anterior views, (**c**) 3D visualization of the whole pelvis with tumor, and (**d**) Posterior and anterior photographs of the 3D printed left hemi-pelvis model printed with material extrusion technology with the bone (white) and tumor (pink). Images courtesy of Nicole Wake, PhD, GE Healthcare

and surgical mesh development (Ballard et al. 2018).

3D imaging is also commonly used during virtual colonoscopy studies for colon cancer screening. During these exams, carbon dioxide gas or room air is insufflated directly into the colon and a CT scan is performed in the axial plane. These conventional 2D axial images are then often processed to generate 3D views to enhance polyp detection (Geenen et al. 2004). These views include endoluminal displays, which mimic the viewpoint of conventional endoscopic colonoscopy, or virtual dissection views which display the entire lumen surface as a flattened image (Silva et al. 2006) (Fig. 6.15).

For prostate cancer, MRI is often used to localize lesions for biopsy, and many clinicians attempt to determine whether the cells detected in the resected specimen after prostatectomy match the findings predicted on the preoperative MRI. The difficulty in comparing the resected gland to the MRI is that the prostate is very soft and often deforms when removed, rendering its shape and morphology different than that on imaging. To ameliorate this pitfall, institutions have developed MRI-based patient-specific 3D models to serve as a mount for the removed gland (Makinen and Makinen 1971; Newman 1971; Wu et al. 2019). The model holds the prostate in place as it is sliced to match the location and orientation of the MRI lesions. One study found that using these patient-specific mounts was more accurate in correlating histology and MRI imaging than using standard slicing techniques (Costa et al. 2017). Some urologists also use 3D models for preoperative planning of prostatectomies and partial gland treatment, particularly in assessing the location of
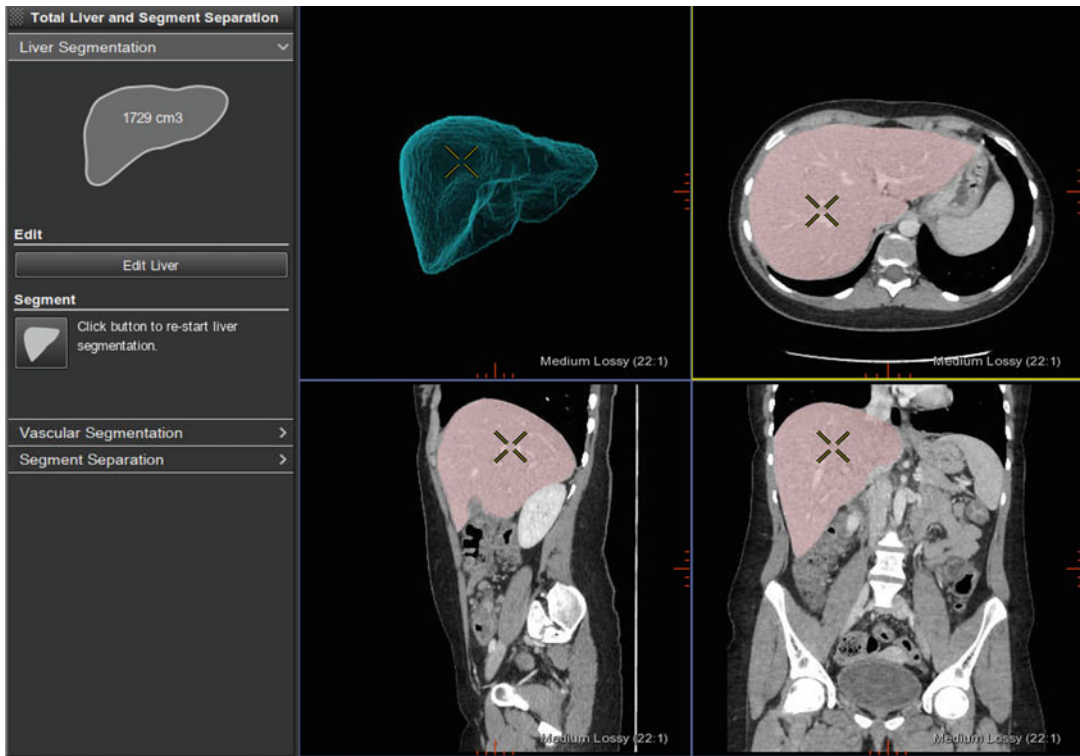
Fig. 6.13 Automated liver volume analysis performed on the GE AW workstation showing liver segmentation, 3D visualization, and total volume calculation. Images courtesy of Nicole Wake, PhD, GE Healthcare
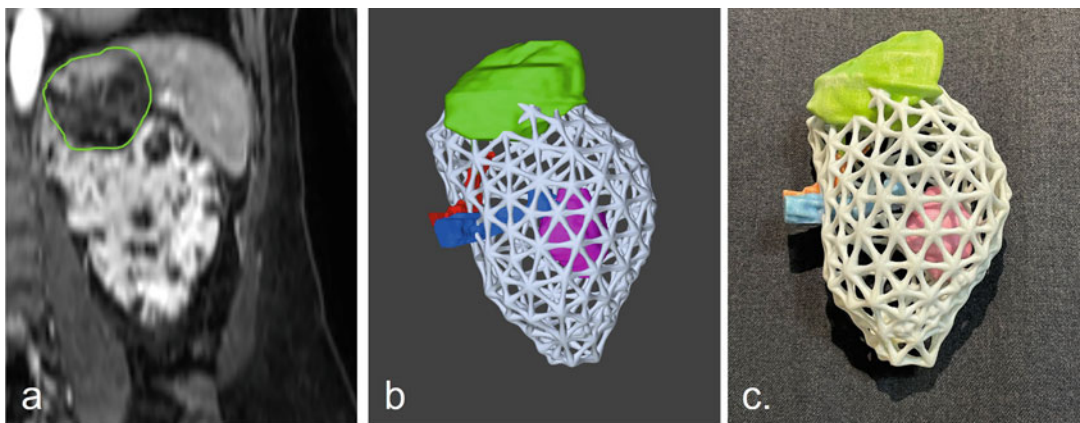
Fig. 6.14 Patient with Tuberous Sclerosis and multiple angiomyolipomas showing (**a**) coronal MR image with a left upper pole mass (Tuberous Sclerosis complex associated renal cell carcinoma) highlighted in green, (**b**) 3D model shown on computer screen with a lattice design for the kidney parenchyma, and (**c**) photograph of the 3D printed model. The kidney parenchyma was designed as a lattice structure so the internal anatomy could be properly visualized in the 3D printed model which was printed with binder jetting technology (CJP 660, 3D Systems). Images courtesy of Nicole Wake, PhD, GE Healthcare
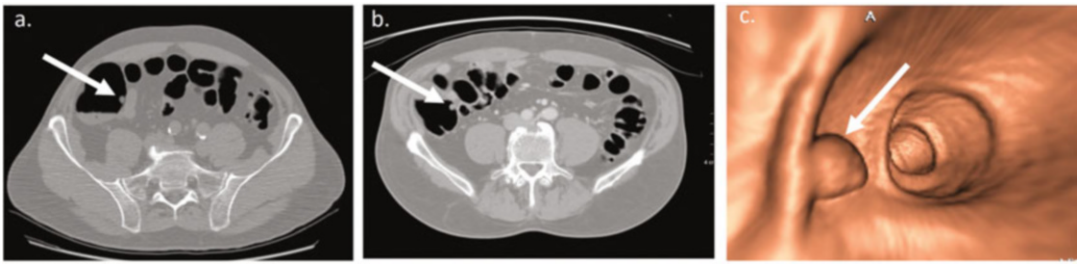
Fig. 6.15 CT Colonography with 3D processing. (**a**) supine and (**b**) prone axial CT images demonstrating a polyp in the ascending colon (arrow). (**c**) 3D reconstruction highlights the polyp (arrow). Images courtesy of Dr. Judy Yee, Montefiore Medical Center

neurovascular bundles and of the bladder neck to ensure that these are avoided (Jomoto et al. 2018; Wake et al. 2016, 2020, 2021).

6.9 3D Visualization for Neurological Applications

Neurological disorders such as brain tumors, strokes, and hemorrhage represent a major global health burden. In neuroradiology, 3D reformats of CT head and neck images are commonly used clinically for improved visualization of complex facial fractures and vertebral body injuries, where these reconstructions have been shown to improve the delineation of fracture line extent and displacement (Kaur and Chopra 2010). 3D reconstructed fracture maps of thoracic and lumbar vertebral bodies also improve understanding of fracture patterns to improve clinical decision-making (Su et al. 2019).

Similar to conventional CT, CT angiography (CTA) examinations are crucial for the evaluation of cerebrovascular pathology. In cases of multiple intracranial aneurysms, CTA source images can be used to determine the pattern and location of hemorrhage, as well as to determine the acuity of hemorrhage and the presence of active bleeding (Sanelli et al. 2005).

MRI is another valuable data source for high-resolution visualization of neuroanatomy. Techniques imaging the cerebral vasculature such as MR angiography (MRA) or contrast-enhanced MRA are now increasingly utilized in their 3D form to help provide a more comprehensive analysis prior to surgical and/or endovascular interventions. For the surgical management of meningiomas and intracranial arteriovenous malformations, high temporal and spatial resolution 3D MRA studies have been shown to reduce the number of invasive diagnostic angiograms by identifying and classifying fistulas, and by illustrating major feeding arteries in the evaluation of the meningiomas (Reinacher et al. 2007). In addition, MR techniques such as diffusion spectrum imaging can also be used to characterize the 3D diffusional displacement of water molecules, allowing for enhanced comprehension of the connectivity pathways in the brain (Wedeen et al. 2005; Callaghan 1993). Advanced image visualization and analysis can also help to quantify brain structures (e.g., tumor size and shape) and highlight their subtle changes over time.

6.10 3D Printing in Neurosurgery

Studies reporting on 3D printing in neurosurgery have primarily been focused on the creation of patient-specific models for surgical planning (Fig. 6.16). Surgical planning for brain tumor resection typically involves using MRI to separate tumor and surrounding normal tissue. Despite this technology, anatomic relationships demonstrated on 2D MRI images may still be difficult to appreciate before and during the procedure. 3D printing technology permits MRI data
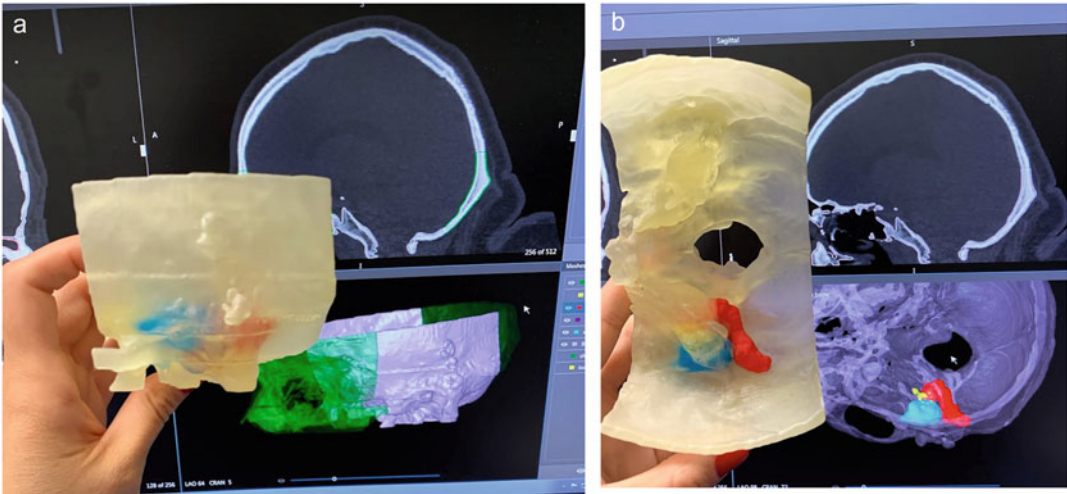
Fig. 6.16 Multi-colored 3D printed model of a skull base tumor (blue) shown alongside associated vasculature (red) and bone (clear). The model was printed using material jetting and is shown with corresponding images from the (**a**) side view and (**b**) top-down view. The model helped to guide the surgical approach for tumor resection. Images courtesy of Nicole Wake, PhD, GE Healthcare

to be converted to patient-specific models, improving comprehension of complex anatomic relationships between tumor, blood vessels, bone, and adjacent normal tissue, and facilitating surgeons' conceptualization of the location and extent of neoplastic tissue (Oishi et al. 2013; Spottiswoode et al. 2013) (Fig. 6.17).

Printed neurological models illustrating the associations of tumor to its surrounding anatomical structures have also allowed surgeons to simulate surgical approaches (Oishi et al. 2013). For ventriculostomy procedures, 3D-printed simulators are a cost-effective alternative to virtual haptic simulators while providing a realistic training experience (Bova et al. 2013; Ryan et al. 2015; Waran et al. 2014c, 2015). These simulators involve a reusable base segment and a disposable segment for practicing the technique. Some of these devices involve using a fluid-filled ventricular system providing variable pressure to simulate pathology (Ryan et al. 2015; Waran et al. 2015). Another simulator makes use of an electromagnetic tracking system registered to a virtual image of positioning once the skin, skull and dura are traversed (Bova et al. 2013).

An additional role of 3D printing in simulation development is in the field of transsphenoidal endoscopic pituitary removal. Multiple studies have made use of skull replicas to practice this surgical approach (Inoue et al. 2013; Waran et al. 2012). The printed skulls are registered to surgical navigation software to better depict the surgical procedure and to allow the model to be paired in real-time with the neuroimages (Waran et al. 2012, 2014c).

With the shift towards endovascular treatment of aneurysms, simulation plays a key role for trainees due to the lack of realistic cadaveric tissue. 3D printed replicas of hollow elastic aneurysms improve trainees' procedural expertise by offering the opportunity to visualize aneurysm shape and to practice aneurysm clipping (Mashiko et al. 2015). A more realistic simulation of the different tissue types is provided by using materials with varying densities and consistencies. Li et al. found in a large-scale study that medical students using 3D printed models had a significantly improved understanding of fracture anatomy when compared with students using conventional CT images, but no difference in the use of 3D models vs. virtual

Fig. 6.17 3D printed cervical spine tumor (C2 chordoma) model showing (**a**) axial MR image with tumor segmentation (green), (**b**) axial CT image showing bone and vertebral artery segmentation (yellow and red respectively), (**c**) Virtual 3D model showing the bone (white), vertebral arteries (red) and tumor (green), and (**d**) 3D printed model printed in multiple colors with binder jetting technology (CJP 660, 3D Systems, Rock Hill, SC). Images courtesy of Nicole Wake, PhD, GE Healthcare
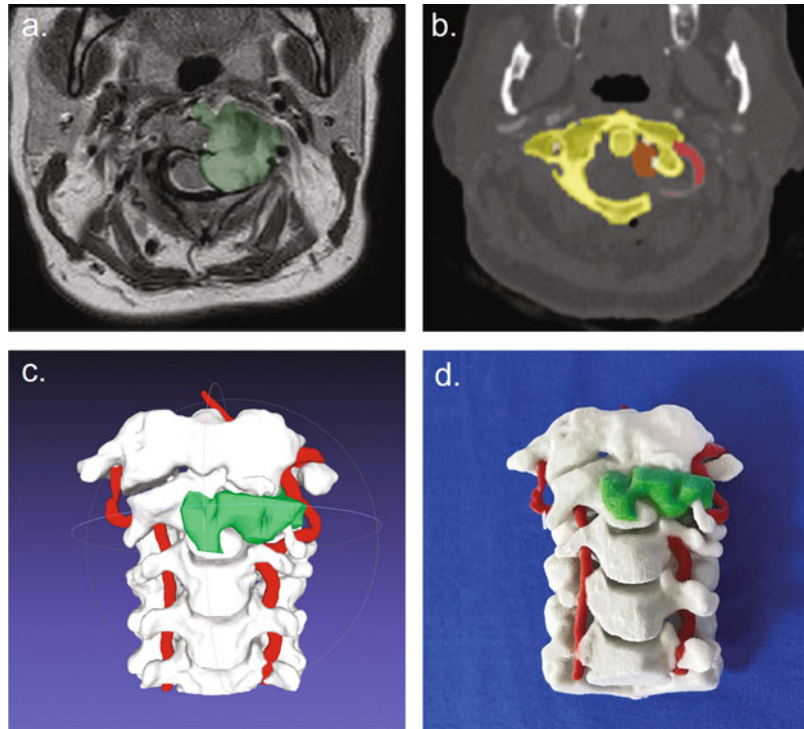
renderings (Mashiko et al. 2015). Finally, 3D printed neurosurgical models have also been useful for training for brain biopsies, with studies demonstrating that with the use of 3D printed simulators, less experienced trainees required shorter duration and fewer attempts to complete the task (Waran et al. 2014a, b).

6.11 Digital Technologies in Craniomaxillofacial Surgery

Virtual oral and maxillofacial surgeries using templating with 3D technologies originated in the mid-1990s (Xia et al. 2000). Digital osteotomies are simulated in computer-aided-design software during these procedures and transferred directly to the patient with a patient-specific surgical guide designed from the medical images. Providing personalized, tailored solutions in the operating room can improve surgical accuracy and minimize surgical time, thereby improving patient outcomes (Ballard et al. 2020, Arce et al. 2020, Alexander and

Wake 2022). Common surgical procedures that utilize these technologies include orthognathic surgery (also known as corrective jaw surgery), distraction osteogenesis (a treatment to lengthen the craniofacial skeleton), and free flap reconstruction (Christensen 2018).

In orthognathic surgery, 3D printing has been used to create anatomic models, occlusal splints, osteotomy guides, repositioning guides, fixation plates/implants, and spacers (Lin et al. 2018). For distraction osteogenesis procedures, 3D-printed surgical guides decrease operative and ventilation times, as well as reduce hospital stays compared to traditional treatments (Mao et al. 2019). In mandibular free flap procedures, the jaw is rebuilt using either autologous or donor bone. The most common autologous bone used for this purpose is the fibula, the smaller of the two bones in the lower leg. Creating patient-specific cutting guides from CT data precisely delineates the length and angles at which both the mandible and fibula are cut and optimizes autologous bone fitting to the resected area (Alexander and Wake 2022).

6.12   Intraoperative Navigation

Intraoperative navigation is a valuable tool for complex neurosurgical procedures such as craniofacial surgeries, orthognathic procedures and endoscopic sinus surgeries to ensure proper tumor resection, bone segment repositioning, and timely bone graft reconstruction (Andrews et al. 2015; Zavattero et al. 2015; Bolzoni Villaret et al. 2014).

CT or MRI-guided stereotactic neurosurgery enhances safe and accurate targeting of deep brain structures. Neurosurgeons can insert a probe into many lesions or anatomic locations in the brain through this imaging guidance to perform location-specific procedures such as lesion biopsy, abscess drainage, pharmaceutical agent instillation, or electrode implantation (Lunsford 2012). In otolaryngology, 3D stereotactic guided sinus surgery is routinely used in the field of endoscopic sinus surgery. Due to the fatality of the complications which can arise from endoscopic sinus surgery, even the most experienced surgeons value as much information as possible intraoperatively. Clinically, studies have found that the various CT/MRI-guided navigation systems have an accuracy of approximately 1 mm and have the benefit of increased margin of intraoperative safety (Caversaccio and Freysinger 2003).

6.13   3D Visualization and Modeling for Breast Applications

Breast cancer is impacted by a multitude of factors, including cancer stage, prognostic factors and patient-specific factors (Santiago et al. 2019). Early-stage breast cancer is typically treated with breast conservation surgery (BCS) using a combination of radiation and/or chemotherapy in place of a mastectomy. Treatment is guided by the need to balance achievement of tumor-free margins with satisfactory cosmesis (Santiago et al. 2019). The utilization of 3D imaging for breast cancer management, including CT, MRI, and 3D mammography, allows for optimized

patient autonomy, improved tumor-free margins for BCS, and advances in treatment. Furthermore, the ability for a patient to hold a tangible depiction of their breast lesion can help patients understand the potential treatment options for their cancer and allow them to take an active role in decision-making (Fig. 6.18).

3D imaging and printing provides the surgeon with a more complete conceptualization of a breast lesion, reduces operating times, and limits the number of repeat operations (Schulz-Wendtland et al. 2017) Utilizing MRI information, a study created personalized 3D printed models and bra-like plastic locators, allowing surgeons to mark the edges of a tumor on the breast surface and to inject blue dye into the breast 1 cm from the tumor edges (Barth Jr. et al. 2017). This technique allowed for accurate localization of 18 of 19 cancers with all 68 blue dye injections sufficiently beyond the tumor edges (Barth Jr. et al. 2017). An additional study demonstrated that the utilization of 3D printed molds as a guide for BCS resulted in preserving normal breast tissue while achieving negative margins (Rao et al. 2018). Further, a study has shown potential for semi-automated delineation of a breast lesion using MRI information to create subsequent 3D printing (Schulz-Wendtland et al. 2017), which has potential to expedite prototyping.

The literature provides a case of breast cancer that was favored to be treated with mastectomy, as BCS was thought to necessitate significant breast size alteration due to the extent of disease (Santiago et al. 2019). Upon review of a 3D printed model of this particular patient's tumor, the patient and surgeon agreed on BCS, and not only was adequate cosmesis achieved, but postoperative imaging demonstrated no recurrent disease at 6 months (Santiago et al. 2019). This example illustrates the utility of 3D printing for complex breast cancer patients, and explains why institutions, such as MD Anderson routinely create models, as seen in the provided examples (Figs. 6.19, 6.20, and 6.21).

Accurate surgical resection relies on palpation, which can make for imprecise breast lesion localization (Schulz-Wendtland et al. 2017). Though

Fig. 6.18 Patient with a large breast mass showing (**a**) 3D visualization of the skin (pink) shown with the segmented tumor (purple), and arterial supply (red). (**b**) 3D printed model of the tumor and vasculature. (**c**) 3D printed model of the tumor (red) shown with the breast from the chest wall perspective. Images courtesy of Nicole Wake, PhD, GE Healthcare
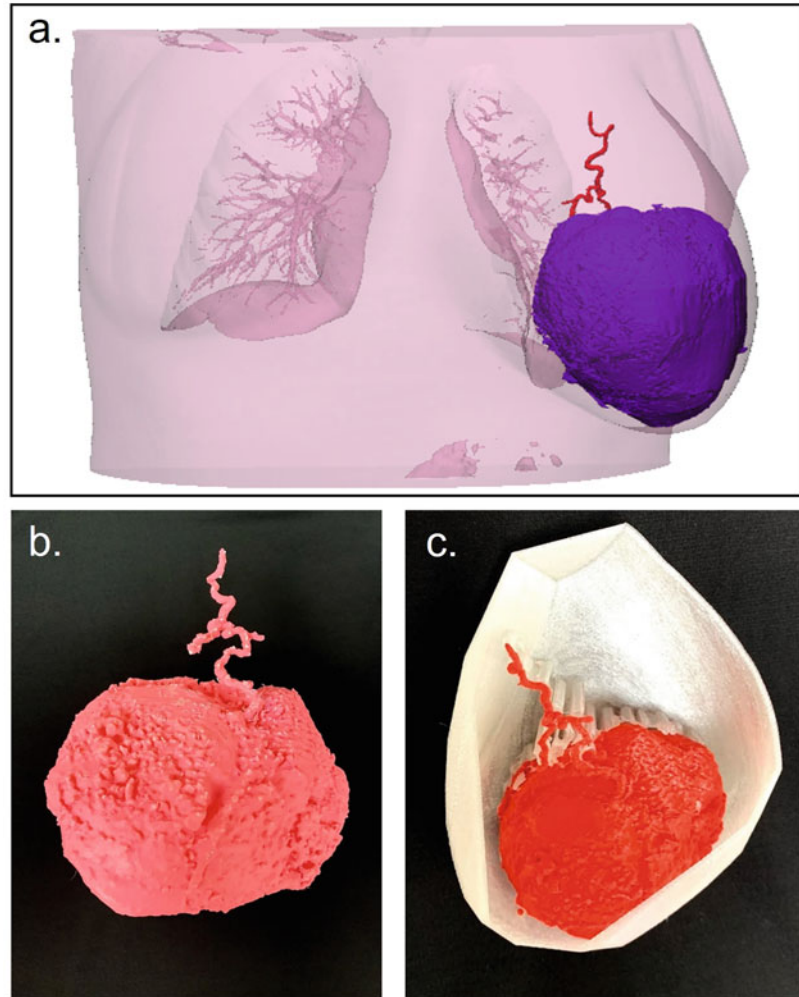
preoperative lesion size assessments are accurate for most women, numerous factors including tumor size and breast density may influence preoperative assessment of a breast lesion (Schulz-Wendtland et al. 2017). Often a woman will have a wire localization procedure prior to excision of nonpalpable breast cancer, wherein a radiologist localizes the cancer's location using a wire with imaging guidance. Alternatively, localization can be performed with alternate markers, such as radioactive seeds and radiofrequency identification tags. Despite the utilization of wire localization, the technique still requires the surgeon to estimate the 3D position of a cancer from 2D mammographic images (Barth Jr. et al. 2017). Furthermore, wires may enter the breast at a substantial distance from the site of the cancer. It follows that this imprecision results in positive margins requiring re-excisions in 22 to 34% of cases (Barth Jr. et al. 2017; Lovrics et al. 2011; Schnabel et al. 2014; Chagpar et al. 2015; Rao et al. 2018), and in some subgroups, the repeat excision rate can be as high as 40% (Schulz-Wendtland et al. 2017).

3D imaging also has potential treatment advances for breast cancer. High dose rate (HDR) breast brachytherapy, radiation utilized for breast cancer treatment, can potentially be optimized utilizing 3D technology. For instance, a study found that using a combination of a catheter optimization procedure and a computer-controlled robotic 3D ultrasound system allowed
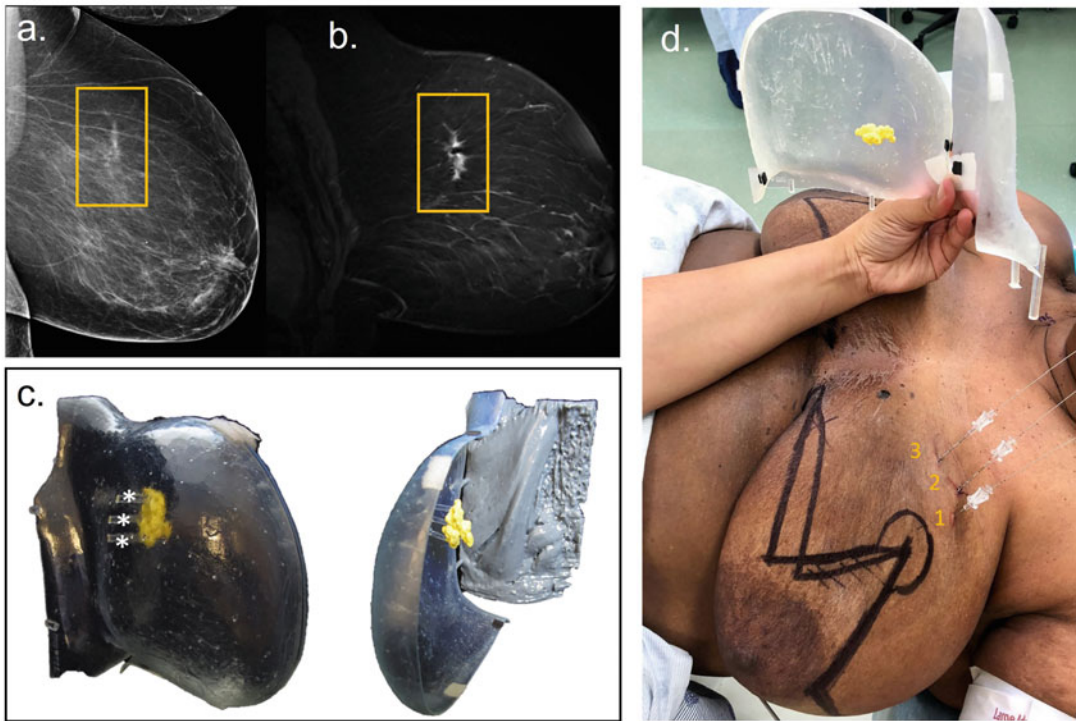
Fig. 6.19 68-year-old woman with left breast invasive ductal carcinoma with micropapillary and mucinous features and DCIS cribriform with micropapillary growth patterns and comedonecrosis. (**a**) Lateromedial mammogram demonstrates a focal asymmetry (rectangle). (**b**) Sagittal dynamic contrast-enhanced MRI demonstrates non-mass clumped enhancement (rectangle) in the upper inner quadrant with a post-biopsy clip corresponding to the focal asymmetry noted by mammography. (**c**) Lateral views of the 3D printed model with (left) overlying skin obscuring the tumor detail and without (right) the overlying skin, both printed at 65% scale with the skin (clear), tumor (yellow), and pectoris muscle (gray). Support structures for the tumor arise from the medial skin (asterisk). (**d**) Photograph of the patient with the models demonstrating significant lateral gland displacement when the patient is in the supine position. Disease localized wires (numbered) corresponding to the area of disease (yellow) in the 3D printed model. Images courtesy of Dr. Lumarie Santiago, MD Anderson Cancer Center

for real-time, rapid guidance and planning for treatments down to 14 and 12 catheters (Poulin et al. 2015). Additionally, utilization of a 3D template has been shown to be a safe and reproducible method to assess the lesion volume for HDR multicathether brachytherapy (Aristei et al. 2019). Finally, 3D printing has potential to reduce heart and lung radiation doses during post-mastectomy radiotherapy, via creating customized virtual boluses of electron beam therapy (Yang et al. 2019). These results are important as the rate of ischemic heart disease has been shown to be proportional to the mean cardiac dose of radiotherapy for breast cancer (Darby et al. 2013), thus dose optimization can have a potentially profound impact on long-term longevity of breast cancer survivors.

6.14 3D Visualization and Modeling for Fetal Medicine

While 2D Ultrasound is of paramount importance in the examination of fetal anatomy and antenatal detection of congenital anomalies, 3D ultrasound and MRI are important complementary imaging modalities which can enhance pregnancy management in select congenital fetal malformations.

The two main barriers to high-quality obstetrical 3D ultrasound are bone shadowing and fetal
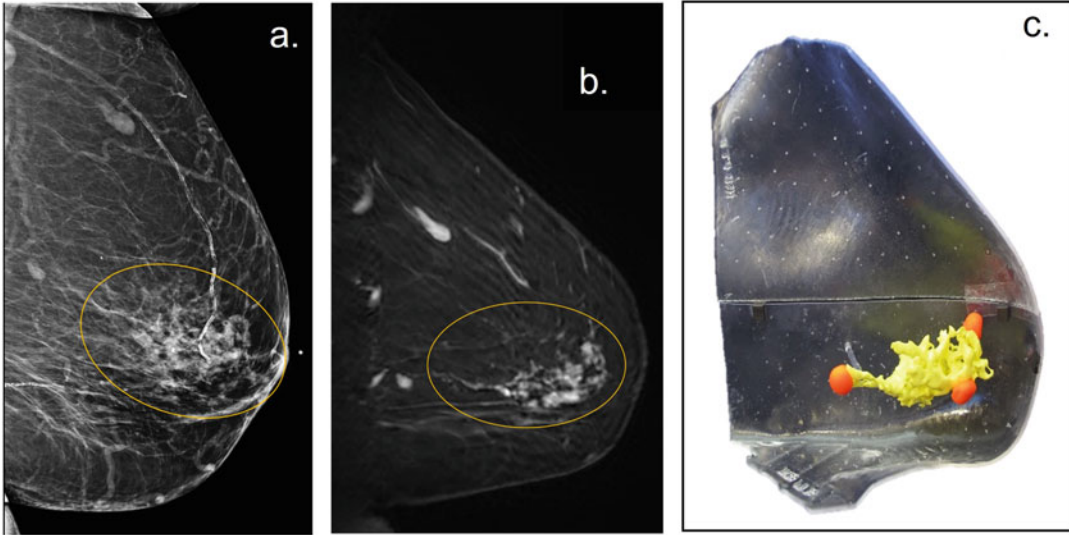
Fig. 6.20 72-year-old woman with the left breast DCIS solid type with focal cribriform differentiation with focal central necrosis and involvement by calcifications preoperative imaging including mammogram and breast MRI. (**a**) Lateromedial mammogram demonstrates a focal asymmetry associated with calcifications in the left breast (oval). (**b**) Dynamic contrast-enhanced sagittal breast MRI image of the left breast demonstrates non-mass, clumped enhancement in the upper outer quadrant (oval) corresponding to the focal asymmetry and calcifications noted by mammography. (**c**) lateral view of the 3D printed model depicting I-125 seed placement in red corresponding to their location in the post-procedure mammogram circles. Images courtesy of Dr. Lumarie Santiago, MD Anderson Cancer Center
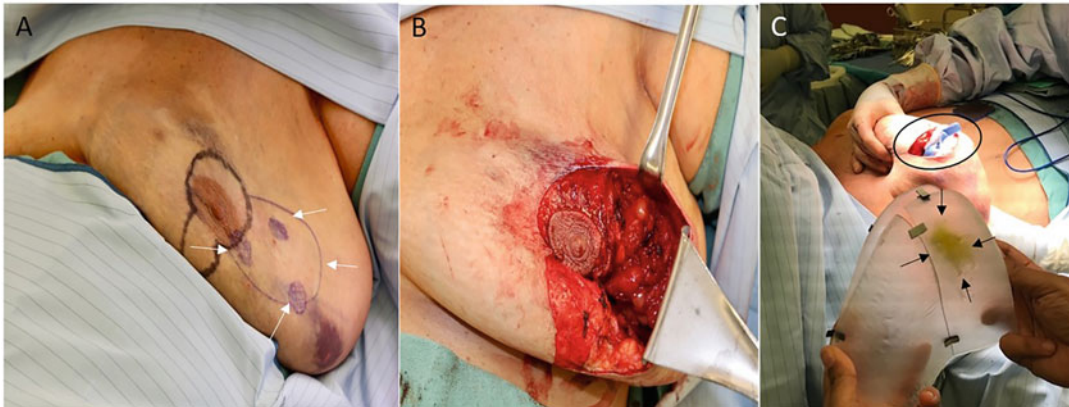
Fig. 6.21 Photographs of the patient from this figure showing (**a**) Significant lateral displacement of the breast with I-125 seed activity marked on the skin arrows. (**b**) Circumvertical incision provided excellent exposure for excision of the bracketed area of disease. (**c**) Smaller scale 3D printed model obtained from imaging and prone position versus expected ptosis from macromastia in supine position. Images courtesy of Dr. Lumarie Santiago, MD Anderson Cancer Center

movement, both of which require a high degree of operator skill. The lack of uniformity in industry standards regarding the storage format for volume datasets generated by 3D ultrasound also limits widespread use (Gonçalves 2016).

3D ultrasound allows superior depiction of fetal surface anomalies and contributes to the improved first-trimester prenatal diagnosis of neurological defects (anencephaly, acrania, encephalocele, and holoprosencephaly), craniofacial anomalies (orofacial clefts and cyclopia), abdominal wall defects (omphalocele and gastroschisis) and musculoskeletal dysplasias. The more severe malformations are an important cause of childhood mortality and morbidity, with the latter having long-term financial and psychosocial implications for the affected child and their family. The use of 3D ultrasound, particularly the surface rendering mode, allows parents to better conceptualize the malformation, thereby enhancing their ability to participate in prenatal counseling and make informed decisions (Araujo Júnior et al. 2015).

Figure 6.22 illustrates this concept with an example of anencephaly, a lethal open neural tube defect characterized by absence of the cranial vault with variable amounts of angiomatous stroma at the base of the skull (Callen 2009; Nyberg et al. 2003; Akinmoladun et al. 2020).

Holoprosencephaly is a rare congenital brain malformation characterized by partial or total failure of separation of the brain tissue in early development. In its most severe form, alobar holoprosencephaly, cleavage fails with a resultant single midline forebrain with a primitive monoventricle, often associated with a large dorsal cyst (Winter et al. 2015). Associated craniofacial anomalies include proboscis (a snout-like protrusion from the face/forehead) and cyclopia (a single palpebral fissure and a single midline orbit) as depicted in Fig. 6.23 (Sepulveda et al. 2012).

Visualization of the fetal face is an important component of obstetrical 2D ultrasound which can diagnose and classify orofacial clefts (Callen 2009, Nyberg et al. 2003) by depicting the fetal profile, upper lip and alveolar ridge in the sagittal, coronal, and axial views, respectively. The advent of 3D ultrasound with its surface rendering mode (Fig. 6.24) can generate detailed views of the fetal face at different stages of development, allowing the diagnosis of cleft lip and palate as early as the first trimester when a flat palate and absence of shadowing from adjacent non-ossified bones permits better visualization (Sepulveda et al. 2012; Werner et al. 2010).

The excellent soft tissue contrast capabilities of MRI have led to it surpassing ultrasound in the diagnosis and prognostication of congenital fetal anomalies of the brain and heart. The principal disadvantages of MRI are image data disruption due to fetal motion and maternal breathing. To minimize these, fetal MRI acquisition protocols are restricted to two-dimensional sequences with high-resolution reconstruction of 3D motion-corrected data (Davidson et al. 2021).

While 2D and 3D ultrasound can easily detect fetal neck masses and associated polyhydramnios due to impaired swallowing; an important limitation of these techniques is the inability to directly visualize the airway, thus limiting assessment of the degree of airway obstruction. MRI plays a crucial role in identifying fetuses at a risk of perinatal asphyxia by assessing the size, location, and internal characteristics of the mass as well as the degree of tracheal deviation, compression of the upper airway and oropharyngeal extension as shown in Fig. 6.25. The advent of ex-utero intrapartum life-saving treatment measures in specialist centers has proved life-saving in fetuses with a critical airway and is reliant on the complex anatomical detail provided by MRI (Sepulveda et al. 2012).

MRI volumetry allows precise estimates of total lung volume, assisting neonatal and pediatric surgical specialists in planning the prenatal and postnatal care of babies with congenital diaphragmatic hernia, congenital pulmonary airway malformations and anterior abdominal wall defects (Davidson et al. 2021).

Medical imaging, including ultrasound, CT, and MRI, plays a valuable role in the evaluation of shared anatomy in all types of conjoined twins (e.g., ventral, dorsal, or lateral union) and is instrumental in decision-making in terms of prenatal planning and managing parental
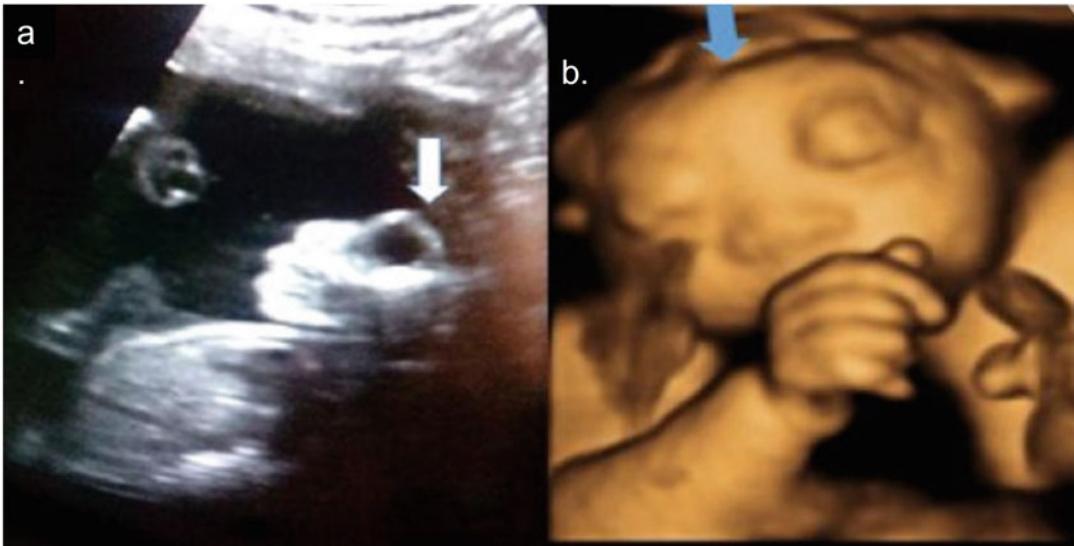
Fig. 6.22 (**a**) 2D ultrasound image of a fetus showing absence of the cranium (anencephaly) giving a frog eye appearance (white arrow). (**b**) 3D image of the fetus confirming the absent cranium (blue arrow). Reproduced with open-access permission from Akinmoladun et al. (2020)

Fig. 6.23 Facial features in a fetus with holoprosencephaly. (**a**) 2D ultrasound shows proboscis and severe midfacial hypoplasia. (**b**) 3D ultrasound surface rendered image shows proboscis, cyclopia, and arrhinia. (**c**) a photograph of the neonate with severe facial malformations. Reproduced with permission from Sepulveda et al. (2012)

expectations. Prenatal counseling in these cases focuses on the expected survivability without and with separation as well as the identification of additional anomalies affecting one of the conjoined twins. 3D printed models allow the surgical team to discuss planes of separation and devise an approach to the multi-stage separation procedure.

One example of conjoined twins, craniopagus, is a form of dorsal conjoined twinning with fusion at the skull (Fig. 6.26). CT is crucial to evaluate the degree of calvarial bony fusion and MRI is vital for assessment of the brain and spinal cord anatomy (Mehollin-Ray 2018). Furthermore, 3D visualization and printing technologies can allow for the separation of these twins at a young age,
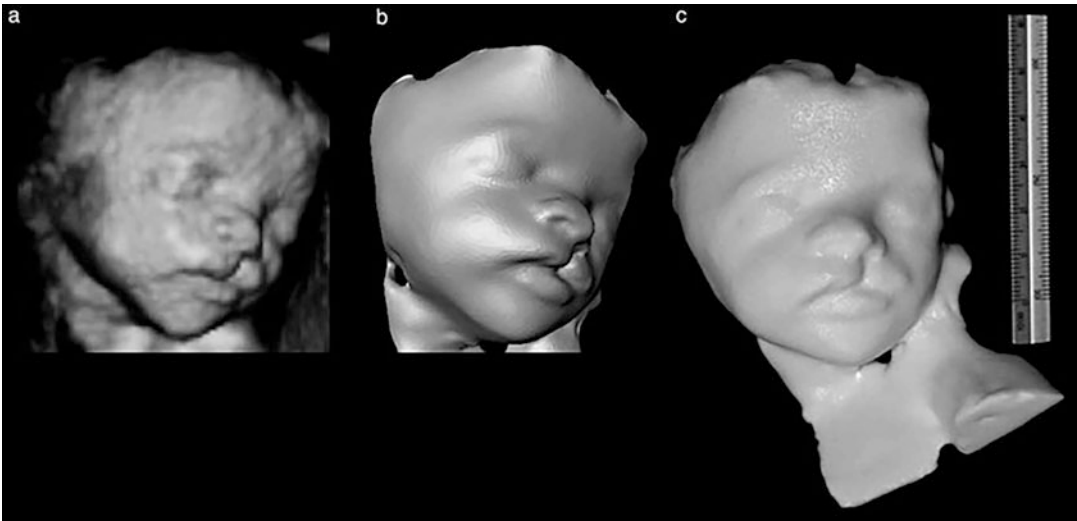
Fig. 6.24 Fetus with a cleft lip at 28 weeks' gestation. (**a**) 3D ultrasound image, (**b**) 3D virtual model and (**c**) physical 3D printed model built using a powder-based system. Reproduced with permission from Werner et al. (2010)
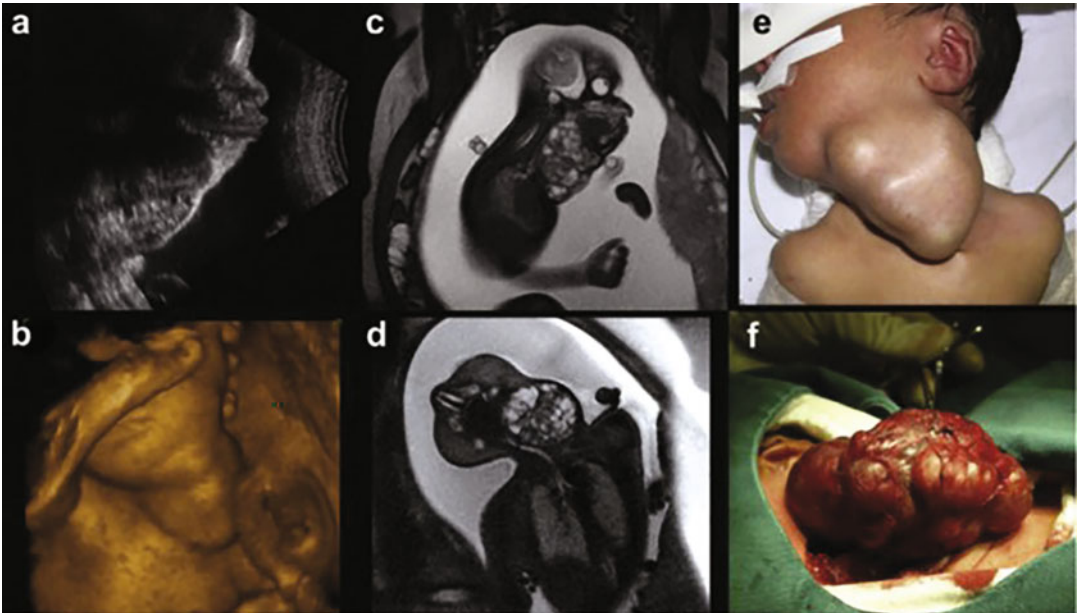
Fig. 6.25 Fetal cervical teratoma case. A fetal neck mass is clearly depicted with (**a**) 2D ultrasound and (**b**) 3D-ultrasound. Fetal MRI shows the internal characteristics of the mass, polyhydramnios, and partial compression of the upper airway (**c**, **d**). (**e**) Photograph of the mass at birth and (**f**) at the time of surgery (Reproduced with permission Sepulveda et al. 2012)
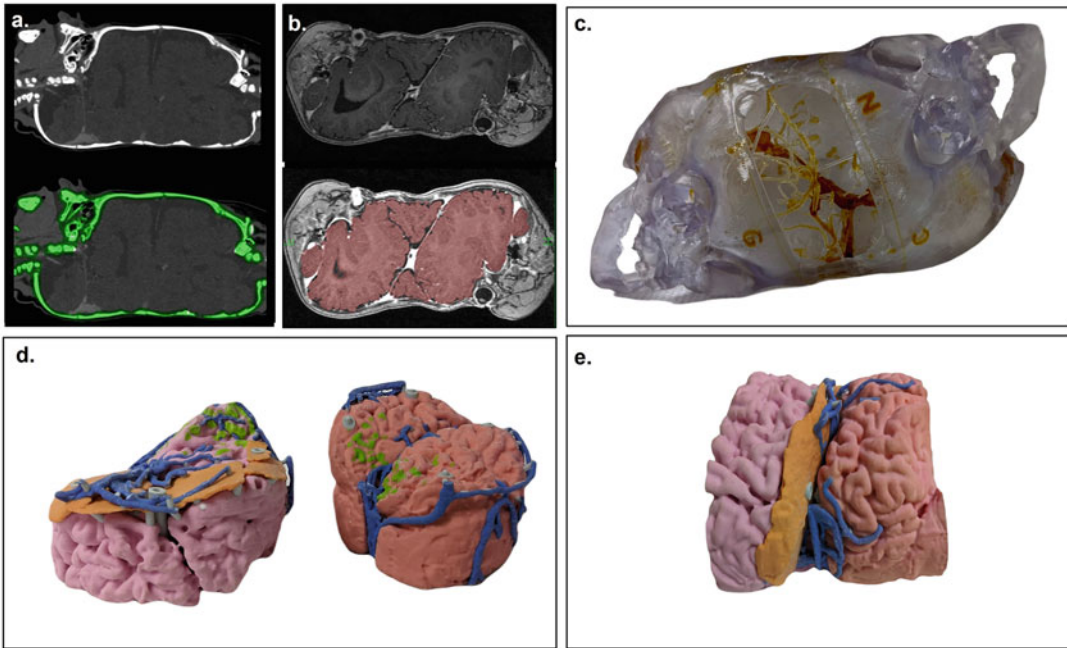
Fig. 6.26 Craniopagus twins showing (**a**) CT cross-section with bone segmentation, (**b**) MRI cross-section with brain tissue segmentation. (**c**) 3D printed skull models printed with stereolithography (3D Systems, Rock Hill, SC) showing internal vasculature with letters indicating proper placement for guides. (**d**) 3D printed brain models printed with binder jetting technology (CJP 660, 3D Systems, Rock Hill, SC) as two parts to demonstrate the intended separation plan with the venous sinus. (**e**) 3D-printed brain models shown placed together. Images courtesy of Nicole Wake, PhD, GE Healthcare

therefore harnessing the regenerative capacity of the brains (Heuer et al. 2019).

6.15 Extended Reality Technologies and Potential Future Applications

Advanced 3D medical imaging is used to support a wide range of surgical operations and for monitoring disease progression. Combining 3D imaging methods with the use of new technologies such as 3D printing can help improve patient outcomes by reducing operating times, enhancing precision, and decreasing risk. In addition to 3D printing, other advanced technologies such as extended reality can be used to better visualize medical imaging data. Extended reality is a term used to describe all real and virtual combined environments with human-machine interactions that are generated by computer technologies. Regarding these technologies, the most popular are Virtual Reality (VR) and Augmented Reality (AR). VR is the use of computer technology to create a completely immersive simulation of a 3D environment that can be interacted with in a realistic, physical method by a person using hand controllers (Heilig 1960). In contrast, AR uses computer technology to place virtual 3D objects within the real environment in the form of an overlay (Sutherland 1968).

Improved image visualization has been made possible with advancements of computer power; however, advanced image post-processing typically is a laborious time-consuming process. Automated workflows that utilize machine learning technologies are expected to reduce the time required to create this 3D content and to improve the accuracy, thereby allowing 3D

modeling to be performed and implemented more routinely.

In the realm of 3D printing, there is ongoing research into the clinical applications of 3D printing of biomaterials. For example, animal studies involving 3D-printed biocompatible scaffolds demonstrate encouraging results for tracheal reconstruction (Park et al. 2015; Chang et al. 2014; Goldstein et al. 2015). Studies including customized tympanic membrane printing with improved resistance compared to the temporalis fascia and customized septal buttons for septal perforations with superior compliance and effectiveness have been published (Kozin et al. 2016; Onerci Altunay et al. 2016). For the treatment of intervertebral disc degeneration, pre-clinical studies are currently ongoing to 3D print an elastic scaffold and deposit substrate/cells to form a regenerated intervertebral disc as an alternative to spinal fusion or artificial disc replacement surgery (Whatley et al. 2011). Combining advanced radiological imaging methods with bioprinting has huge potential for advancing personalized medicine and positively impacting patient care.

References

Akinmoladun JA, Oboro VO, Adelakun TI (2020) Initial experience with 3d-ultrasound as an adjunct to 2dultrasound in fetal anomaly diagnosis in a Nigerian diagnostic facility. Ann Ib Postgrad Med 18:170–177

Al Najjar M, Mehta SS, Monga P (2018) Three dimensional scapular prints for evaluating glenoid morphology: an exploratory study. J Clin Orthop Trauma 9:230–235

Alexander AE, Wake N (2022) 3D printed anatomic models and guides. Medical imaging technologies and imaging considerations for 3D printed anatomic models. 3D printing for the radiologist. Elsevier

Ali A, Ballard DH, Althobaity W, Christensen A, Geritano M, Ho M, Liacouras P, Matsumoto J, Morris J, Ryan J, Shorti R, Wake N, Rybicki FJ, Sheikh A (2020) Clinical situations for which 3D printing is considered an appropriate representation or extension of data contained in a medical imaging examination: adult cardiac conditions. 3D Print Med 6:24

Andrews BT, Thurston TE, Tanna N, Broer PN, Levine JP, Kumar A, Bradley JP (2015) A multicenter experience with image-guided surgical navigation: broadening clinical indications in complex craniomaxillofacial surgery. J Craniofac Surg 26:1136–1139

Andrushchuk U, Adzintsou V, Nevyglas A, Model H (2018) Virtual and real septal myectomy using 3-dimensional printed models. Interact Cardiovasc Thorac Surg 26:881–882

Araujo Júnior E, Rolo LC, Tonni G, Haeri S, Ruano R (2015) Assessment of fetal malformations in the first trimester of pregnancy by three-dimensional ultrasonography in the rendering mode. Pictorial essay. Med Ultrason 17:109–114

Arce K, Morris JM, Alexander AE, Ettinger KS (2020) Developing a point-of-care manufacturing program for craniomaxillofacial surgery. Atlas Oral Maxillofac Surg Clin North Am 28:165–179

Aristei C, Lancellotta V, Piergentini M, Costantini G, Saldi S, Chierchini S, Cavalli A, Di Renzo L, Fiorucci O, Guasticchi M, Bini V, Ricci A (2019) Individualized 3D-printed templates for high-dose-rate interstitial multicatheter brachytherapy in patients with breast cancer. Brachytherapy 18:57–62

Athanassopoulos GD (2016) 3D Printing for left atrial appendage (LAA) modeling based on transesophageal echocardiography: a step forward in closure with LAA devices. Cardiology 135:249–254

Ballard DH, Trace AP, Ali S, Hodgdon T, Zygmont ME, Debenedectis CM, Smith SE, Richardson ML, Patel MJ, Decker SJ, Lenchik L (2018) Clinical applications of 3D printing: primer for radiologists. Acad Radiol 25:52–65

Ballard DH, Mills P, Duszak R Jr, Weisman JA, Rybicki FJ, Woodard PK (2020) Medical 3D printing cost-savings in orthopedic and maxillofacial surgery: cost analysis of operating room time saved with 3D printed anatomic models and surgical guides. Acad Radiol 27:1103–1113

Barth RJ Jr, Krishnaswamy V, Paulsen KD, Rooney TB, Wells WA, Rizzo E, Angeles CV, Marotti JD, Zuurbier RA, Black CC (2017) A patient-specific 3D-printed form accurately transfers supine MRI-derived tumor localization information to guide breast-conserving surgery. Ann Surg Oncol 24:2950–2956

Bastawrous S, Wake N, Levin D, Ripley B (2018) Principles of three-dimensional printing and clinical applications within the abdomen and pelvis. Abdom Radiol (NY) 43:2809–2822

Berhouet J, Gulotta LV, Dines DM, Craig E, Warren RF, Choi D, Chen X, Kontaxis A (2017) Preoperative planning for accurate glenoid component positioning in reverse shoulder arthroplasty. Orthop Traumatol Surg Res 103:407–413

Bernstein MA, Huston J III, Ward HA (2006) Imaging artifacts at 3.0T. J Magn Reson Imaging 24:735–746

Biglino G, Capelli C, Wray J, Schievano S, Leaver LK, Khambadkone S, Giardini A, Derrick G, Jones A, Taylor AM (2015) 3D-manufactured patient-specific models of congenital heart defects for communication in clinical practice: feasibility and acceptability. BMJ Open 5:e007165

Bolzoni Villaret A, Battaglia P, Tschabitscher M, Mattavelli D, Turri-Zanoni M, Castelnuovo P, Nicolai

P (2014) A 3-dimensional transnasal endoscopic journey through the paranasal sinuses and adjacent skull base: a practical and surgery-oriented perspective. Neurosurgery 10(Suppl 1):116–120. discussion 120

Bova FJ, Rajon DA, Friedman WA, Murad GJ, Hoh DJ, Jacob RP, Lampotang S, Lizdas DE, Lombard G, Lister JR (2013) Mixed-reality simulation for neurosurgical procedures. Neurosurgery 73(Suppl 1): 138–145

Brown RN, Yu-Chung N, Haacke EM, Thompson MR, Venkatesan R (2014) Magnetic resonance imaging: physical principles and sequence design, p Wiley-Blackwell

Burns J, Mansouri M, Wake N (2022) 3D Printing in radiology education. Medical imaging technologies and imaging considerations for 3D printed anatomic models. 3D printing for the radiologist. Elsevier

Callaghan P (1993) Principles of nuclear magnetic resonance microscopy. Oxford University Press

Callen PW (2009) Ultrasonography in obstetrics and gynecology, vol 251, 5th edn. Radiology, pp 650–651

Caversaccio M, Freysinger W (2003) Computer assistance for intraoperative navigation in ENT surgery. Minim Invasive Ther Allied Technol 12:36–51

Chagpar AB, Killelea BK, Tsangaris TN, Butler M, Stavris K, Li F, Yao X, Bossuyt V, Harigopal M, Lannin DR, Pusztai L, Horowitz NR (2015) A randomized, controlled trial of cavity shave margins in breast cancer. N Engl J Med 373:503–510

Chang JW, Park SA, Park JK, Choi JW, Kim YS, Shin YS, Kim CH (2014) Tissue-engineered tracheal reconstruction using three-dimensionally printed artificial tracheal graft: preliminary report. Artif Organs 38:E95–e105

Chepelev L, Hodgdon T, Gupta A, Wang A, Torres C, Krishna S, Akyuz E, Mitsouras D, Sheikh A (2015) Medical 3D printing for vascular interventions and surgical oncology: a primer for the 2016 radiological society of North America (RSNA) hands-on course in 3D printing. 3D Print Med 2:5

Chepelev L, Wake N, Ryan J, Althobaity W, Gupta A, Arribas E, Santiago L, Ballard DH, Wang KC, Weadock W, Ionita CN, Mitsouras D, Morris J, Matsumoto J, Christensen A, Liacouras P, Rybicki FJ, Sheikh A (2018) Radiological Society of North America (RSNA) 3D printing Special Interest Group (SIG): guidelines for medical 3D printing and appropriateness for clinical scenarios. 3D Print Med 4:11

Christensen AM (2018) The digital thread for personalized craniomaxillofacial surgery. Digital technologies in craniomaxillofacial surgery. Springer

Costa DN, Chatzinoff Y, Passoni NM, Kapur P, Roehrborn CG, Xi Y, Rofsky NM, Torrealba J, Francis F, Futch C, Hagens P, Notgrass H, Otero-Muinelo S, Pedrosa I, Chopra R (2017) Improved magnetic resonance imaging-pathology correlation with imaging-derived, 3d-printed, patient-specific whole-mount molds of the prostate. Investig Radiol 52:507–513

Costello JP, Olivieri LJ, Su L, Krieger A, Alfares F, Thabit O, Marshall MB, Yoo SJ, Kim PC, Jonas RA, Nath DS (2015) Incorporating three-dimensional printing into a simulation-based congenital heart disease and critical care training curriculum for resident physicians. Congenit Heart Dis 10:185–190

Darby SC, Ewertz M, Mcgale P, Bennet AM, Blom-Goldman U, Brønnum D, Correa C, Cutter D, Gagliardi G, Gigante B, Jensen MB, Nisbet A, Peto R, Rahimi K, Taylor C, Hall P (2013) Risk of ischemic heart disease in women after radiotherapy for breast cancer. N Engl J Med 368:987–998

Davidson JR, Uus A, Matthew J, Egloff AM, Deprez M, Yardley I, De Coppi P, David A, Carmichael J, Rutherford MA (2021) Fetal body MRI and its application to fetal and neonatal treatment: an illustrative review. Lancet Child Adolesc Health 5:447–458

Eisenmenger LB, Wiggins RH, Fults DW, Huo EJ (2017) Application of 3-dimensional printing in a case of osteogenesis imperfecta for patient education, anatomic understanding, preoperative planning, and intraoperative evaluation. World Neurosurg 107: 1049.e1–1049.e7

El Sabbagh A, Eleid MF, Matsumoto JM, Anavekar NS, Al-Hijji MA, Said SM, Nkomo VT, Holmes DR, Rihal CS, Foley TA (2018) Three-dimensional prototyping for procedural simulation of transcatheter mitral valve replacement in patients with mitral annular calcification. Catheter Cardiovasc Interv 92:E537–e549

Fang C, Fang Z, Fan Y, Li J, Xiang F, Tao H (2015) Application of 3D visualization, 3D printing and 3D laparoscopy in the diagnosis and surgical treatment of hepatic tumors. Nan Fang Yi Ke Da Xue Xue Bao 35: 639–645

Fang C, Cai H, Kuong E, Chui E, Siu YC, Ji T, Drstvenšek I (2019) Surgical applications of three-dimensional printing in the pelvis and acetabulum: from models and tools to implants. Unfallchirurg 122:278–285

Fishman EK, Ney DR, Heath DG, Corl FM, Horton KM, Johnson PT (2006) Volume rendering versus maximum intensity projection in CT angiography: what works best, when, and why. Radiographics 26:905–922

Geenen RW, Hussain SM, Cademartiri F, Poley JW, Siersema PD, Krestin GP (2004) CT and MR colonography: scanning techniques, postprocessing, and emphasis on polyp detection. Radiographics 24: e18

Goitein O, Fink N, Guetta V, Beinart R, Brodov Y, Konen E, Goitein D, Di Segni E, Grupper A, Glikson M (2017) Printed MDCT 3D models for prediction of left atrial appendage (LAA) occluder device size: a feasibility study. EuroIntervention 13:e1076–e1079

Goldstein TA, Smith BD, Zeltsman D, Grande D, Smith LP (2015) Introducing a 3-dimensionally printed, tissue-engineered graft for airway reconstruction: a

pilot study. Otolaryngol Head Neck Surg 153:1001–1006

Gonçalves LF (2016) Three-dimensional ultrasound of the fetus: how does it help? Pediatr Radiol 46:177–189

Goo HW, Park SJ, Yoo SJ (2020) Advanced medical use of three-dimensional imaging in congenital heart disease: augmented reality, mixed reality, virtual reality, and three-dimensional printing. Korean J Radiol 21:133–145

Graves MJ, Mitchell DG (2013) Body MRI artifacts in clinical practice: a physicist's and radiologist's perspective. J Magn Reson Imaging 38:269–287

Hachulla AL, Noble S, Guglielmi G, Agulleiro D, Müller H, Vallée JP (2019) 3D-printed heart model to guide LAA closure: useful in clinical practice? Eur Radiol 29:251–258

Hamabe A, Ito M (2017) A three-dimensional pelvic model made with a three-dimensional printer: applications for laparoscopic surgery to treat rectal cancer. Tech Coloproctol 21:383–387

Hamatani Y, Amaki M, Kanzaki H, Yamashita K, Nakashima Y, Shibata A, Okada A, Takahama H, Hasegawa T, Shimahara Y, Sugano Y, Fujita T, Shiraishi I, Yasuda S, Kobayashi J, Anzai T (2017) Contrast-enhanced computed tomography with myocardial three-dimensional printing can guide treatment in symptomatic hypertrophic obstructive cardiomyopathy. ESC Heart Fail 4:665–669

Heilig M (1960) Stereoscopic-television apparatus for individual use. United States patent US 2955156A. https://patents.google.com/patent/US2955156A/en?oq=2955156

Hermsen JL, Burke TM, Seslar SP, Owens DS, Ripley BA, Mokadam NA, Verrier ED (2017) Scan, plan, print, practice, perform: development and use of a patient-specific 3-dimensional printed model in adult cardiac surgery. J Thorac Cardiovasc Surg 153:132–140

Heuer GG, Madsen PJ, Flanders TM, Kennedy BC, Storm PB, Taylor JA (2019) Separation of craniopagus twins by a multidisciplinary team. N Engl J Med 380:358–364

Hong KC, Freeny PC (1999) Pancreaticoduodenal arcades and dorsal pancreatic artery: comparison of Ct angiography with three-dimensional volume rendering, maximum intensity projection, and shaded-surface display. AJR Am J Roentgenol 172:925–931

Hong D, Moon S, Cho Y, Oh I-Y, Chun EJ, Kim N (2022) Rehearsal simulation to determine the size of device for left atrial appendage occlusion using patient-specific 3D-printed phantoms. Sci Rep 12:7746

Hosny A, Dilley JD, Kelil T, Mathur M, Dean MN, Weaver JC, Ripley B (2019) Pre-procedural fit-testing of TAVR valves using parametric modeling and 3D printing. J Cardiovasc Comput Tomogr 13:21–30

Hull CW (1986) Apparatus for production of three-dimensional objects by stereolithography. United States patent application

Hung CC, Li YT, Chou YC, Chen JE, Wu CC, Shen HC, Yeh TT (2019) Conventional plate fixation method versus pre-operative virtual simulation and three-dimensional printing-assisted contoured plate fixation method in the treatment of anterior pelvic ring fracture. Int Orthop 43:425–431

Hurson C, Tansey A, O'donnchadha B, Nicholson P, Rice J, McElwain J (2007) Rapid prototyping in the assessment, classification and preoperative planning of acetabular fractures. Injury 38:1158–1162

Hussein N, Honjo O, Haller C, Hickey E, Coles JG, Williams WG, Yoo SJ (2020) Hands-on surgical simulation in congenital heart surgery: literature review and future perspective. Semin Thorac Cardiovasc Surg 32:98–105

Inoue D, Yoshimoto K, Uemura M, Yoshida M, Ohuchida K, Kenmotsu H, Tomikawa M, Sasaki T, Hashizume M (2013) Three-dimensional high-definition neuroendoscopic surgery: a controlled comparative laboratory study with two-dimensional endoscopy and clinical application. J Neurol Surg A Cent Eur Neurosurg 74:357–365

ISO 2021 Additive manufacturing – General principles – Fundamentals and vocabulary

Jomoto W, Tanooka M, Doi H, Kikuchi K, Mitsuie C, Yamada Y, Suzuki T, Yamano T, Ishikura R, Kotoura N, Yamamoto S (2018) Development of a three-dimensional surgical navigation system with magnetic resonance angiography and a three-dimensional printer for robot-assisted radical prostatectomy. Cureus 10:e2018

Kalendar W (2011) Computed tomography: fundamentals, system technology, image quality, applications. Publicis

Kaur J, Chopra R (2010) Three dimensional CT reconstruction for the evaluation and surgical planning of mid face fractures: a 100 case study. J Maxillofac Oral Surg 9:323–328

Kim WD, Cho I, Kim YD, Cha MJ, Kim SW, Choi Y, Shin SY (2022) Improving left atrial appendage occlusion device size determination by three-dimensional printing-based preprocedural simulation. Front Cardiovasc Med 9:830062

Koch M, Frankewycz B, Voss A, Kaeaeb M, Herrmann S, Alt V, Greiner S (2021) 3D-analysis of the proximal humeral anatomy before and after stemless shoulder arthroplasty - a prospective case series study. J Clin Med 10:259

Kozin ED, Black NL, Cheng JT, Cotler MJ, Mckenna MJ, Lee DJ, Lewis JA, Rosowski JJ, Remenschneider AK (2016) Design, fabrication, and in vitro testing of novel three-dimensionally printed tympanic membrane grafts. Hear Res 340:191–203

Kwon YW, Powell KA, Yum JK, Brems JJ, Iannotti JP (2005) Use of three-dimensional computed tomography for the analysis of the glenoid anatomy. J Shoulder Elb Surg 14:85–90

Lei K, Liu LM, Xiang Y, Chen X, Fan HQ, Peng Y, Luo JM, Guo L (2020) Clinical value of CT-based patient-

specific 3D preoperative design combined with conventional instruments in primary total knee arthroplasty: a propensity score-matched analysis. J Orthop Surg Res 15:591

Levin D, Mackensen GB, Reisman M, McCabe JM, Dvir D, Ripley B (2020) 3D printing applications for transcatheter aortic valve replacement. Curr Cardiol Rep 22:23

Levoy M (1988) Display of surfaces from volume data. IEEE Comput Graph Appl 8:29–37

Li K, Liu Z, Li X, Wang J (2022) 3D printing-assisted surgery for proximal humerus fractures: a systematic review and meta-analysis. Eur J Trauma Emerg Surg 48(5):3493–3503

Lin HH, Lonic D, Lo LJ (2018) 3D printing in orthognathic surgery - a literature review. J Formos Med Assoc 117:547–558

Liu P, Liu R, Zhang Y, Liu Y, Tang X, Cheng Y (2016) The value of 3D printing models of left atrial appendage using real-time 3D transesophageal echocardiographic data in left atrial appendage occlusion: applications toward an era of truly personalized medicine. Cardiology 135:255–261

Lovrics PJ, Goldsmith CH, Hodgson N, McCready D, Gohla G, Boylan C, Cornacchi S, Reedijk M (2011) A multicentered, randomized, controlled trial comparing radioguided seed localization to standard wire localization for nonpalpable, invasive and in situ breast carcinomas. Ann Surg Oncol 18:3407–3414

Lunsford LD (2012) Modern stereotactic neurosurgery. Springer

Makinen PL, Makinen KK (1971) Azo dye binding proteins as interfering factors in enzyme assays based on azo coupling. Anal Biochem 39:208–217

Mao Z, Zhang N, Cui Y (2019) Three-dimensional printing of surgical guides for mandibular distraction osteogenesis in infancy. Medicine (Baltimore) 98:e14754

Marconi S, Pugliese L, Botti M, Peri A, Cavazzi E, Latteri S, Auricchio F, Pietrabissa A (2017) Value of 3D printing for the comprehension of surgical anatomy. Surg Endosc 31:4102–4110

Marro A, Bandukwala T, Mak W (2016) Three-dimensional printing and medical imaging: a review of the methods and applications. Curr Probl Diagn Radiol 45:2–9

Mashiko T, Konno T, Kaneko N, Watanabe E (2015) Training in brain retraction using a self-made three-dimensional model. World Neurosurg 84:585–590

Matsumoto JS, Morris JM, Foley TA, Williamson EE, Leng S, McGee KP, Kuhlmann JL, Nesberg LE, Vrtiska TJ (2015) Three-dimensional physical modeling: applications and experience at Mayo Clinic. Radiographics 35:1989–2006

Max NL (1995) Optical models for direct volume rendering. IEEE Trans Vis Comput Graph 1(2):97–108

Meess KM, Izzo RL, Dryjski ML, Curl RE, Harris LM, Springer M, Siddiqui AH, Rudin S, Ionita CN (2017) 3D printed abdominal aortic aneurysm phantom for image guided surgical planning with a patient specific fenestrated endovascular graft system. Proc SPIE Int Soc Opt Eng 10138:101380P

Mehollin-Ray AR (2018) Prenatal and postnatal radiologic evaluation of conjoined twins. Semin Perinatol 42:369–380

Mitsouras D, Liacouras P, Imanzadeh A, Giannopoulos AA, Cai T, Kumamaru KK, George E, Wake N, Caterson EJ, Pomahac B, Ho VB, Grant GT, Rybicki FJ (2015) Medical 3D printing for the radiologist. Radiographics 35:1965–1988

Morcos R, Al Taii H, Bansal P, Casale J, Manam R, Patel V, Cioci A, Kucharik M, Malhotra A, Maini B (2018) Accuracy of commonly-used imaging modalities in assessing left atrial appendage for interventional closure: review article. J Clin Med 7:441

Morelli JN, Runge VM, Ai F, Attenberger U, Vu L, Schmeets SH, Nitz WR, Kirsch JE (2011) An image-based approach to understanding the physics of MR artifacts. Radiographics 31:849–866

Newman E (1971) Vocational evaluation and work adjustment – a future thrust of the rehabilitation movement. Rehabil Rec 12:13–15

Nyberg DA, McGahan JP, Pretorius DH, Pilu G (2003) Diagnostic imaging of fetal anomalies. Lippincott Williams and Wilkins, Philadelphia

Oishi M, Fukuda M, Yajima N, Yoshida K, Takahashi M, Hiraishi T, Takao T, Saito A, Fujii Y (2013) Interactive presurgical simulation applying advanced 3D imaging and modeling techniques for skull base and deep tumors. J Neurosurg 119:94–105

Onerci Altunay Z, Bly JA, Edwards PK, Holmes DR, Hamilton GS, O'Brien EK, Carr AB, Camp JJ, Stokken JK, Pallanch JF (2016) Three-dimensional printing of large nasal septal perforations for optimal prosthetic closure. Am J Rhinol Allergy 30:287–293

Park JH, Park JY, Nam IC, Hwang SH, Kim CS, Jung JW, Jang J, Lee H, Choi Y, Park SH, Kim SW, Cho DW (2015) Human turbinate mesenchymal stromal cell sheets with bellows graft for rapid tracheal epithelial regeneration. Acta Biomater 25:56–64

Pietrabissa A, Marconi S, Negrello E, Mauri V, Peri A, Pugliese L, Marone EM, Auricchio F (2020) An overview on 3D printing for abdominal surgery. Surg Endosc 34:1–13

Poulin E, Gardi L, Fenster A, Pouliot J, Beaulieu L (2015) Towards real-time 3D ultrasound planning and personalized 3D printing for breast HDR brachytherapy treatment. Radiother Oncol 114:335–338

Prince JL, Links JM (2006) Medical imaging systems and signals. Pearson Education, Inc

Quail MA, Taylor AM (2020) Congenital heart disease: general principles and imaging. Grainger and Allsion's Diagnostic Radiology

Rao N, Chen K, Yang Q, Niu J (2018) Proof-of-concept study of 3-D-printed mold-guided breast-conserving surgery in breast cancer patients. Clin Breast Cancer 18:e769–e772

Reinacher PC, Stracke P, Reinges MH, Hans FJ, Krings T (2007) Contrast-enhanced time-resolved 3-D MRA:

applications in neurosurgery and interventional neuro-radiology. Neuroradiology 49(Suppl 1):S3–S13

Riggs KW, Dsouza G, Broderick JT, Moore RA, Morales DLS (2018) 3D-printed models optimize preoperative planning for pediatric cardiac tumor debulking. Transl Pediatr 7:196–202

Ryan JR, Chen T, Nakaji P, Frakes DH, Gonzalez LF (2015) Ventriculostomy simulation using patient-specific ventricular anatomy, 3D printing, and hydro-gel casting. World Neurosurg 84:1333–1339

Sanelli PC, Mifsud MJ, Zelenko N, Heier LA (2005) CT angiography in the evaluation of cerebrovascular diseases. AJR Am J Roentgenol 184:305–312

Santiago L, Adrada BE, Caudle AS, Clemens MW, Black DM, Arribas EM (2019) The role of three-dimensional printing in the surgical management of breast cancer. J Surg Oncol 120:897–902

Schnabel F, Boolbol SK, Gittleman M, Karni T, Tafra L, Feldman S, Police A, Friedman NB, Karlan S, Holmes D, Willey SC, Carmon M, Fernandez K, Akbari S, Harness J, Guerra L, Frazier T, Lane K, Simmons RM, Estabrook A, Allweis T (2014) A randomized prospective study of lumpectomy margin assessment with use of MarginProbe in patients with nonpalpable breast malignancies. Ann Surg Oncol 21:1589–1595

Schulz-Wendtland R, Harz M, Meier-Meitinger M, Brehm B, Wacker T, Hahn HK, Wagner F, Wittenberg T, Beckmann MW, Uder M, Fasching PA, Emons J (2017) Semi-automated delineation of breast cancer tumors and subsequent materialization using three-dimensional printing (rapid prototyping). J Surg Oncol 115:238–242

Sepulveda W, Ximenes R, Wong AE, Sepulveda F, Martinez-Ten P (2012) Fetal magnetic resonance imaging and three-dimensional ultrasound in clinical practice: applications in prenatal diagnosis. Best Pract Res Clin Obstet Gynaecol 26:593–624

Seutens P (2009) Fundamentals of medical imaging. Cambridge University Press

Silberstein JL, Maddox MM, Dorsey P, Feibus A, Thomas R, Lee BR (2014) Physical models of renal malignancies using standard cross-sectional imaging and 3-dimensional printers: a pilot study. Urology 84:268–272

Silva AC, Wellnitz CV, Hara AK (2006) Three-dimensional virtual dissection at CT colonography: unraveling the colon to search for lesions. Radiographics 26:1669–1686

Sommer KN, Shepard L, Karkhanis NV, Iyer V, Angel E, Wilson MF, Rybicki FJ, Mitsouras D, Rudin S, Ionita CN (2018) 3D Printed cardiovascular patient specific phantoms used for clinical validation of a CT-derived FFR diagnostic software. Proc SPIE Int Soc Opt Eng 10578:105780J

Sommer KN, Bhurwani MMS, Tutino V, Siddiqui A, Davies J, Snyder K, Levy E, Mokin M, Ionita CN (2021) Use of patient specific 3D printed neurovascular phantoms to simulate mechanical thrombectomy. 3D Print Med 7:32

Spottiswoode BS, Van Den Heever DJ, Chang Y, Engelhardt S, Du Plessis S, Nicolls F, Hartzenberg HB, Gretschel A (2013) Preoperative three-dimensional model creation of magnetic resonance brain images as a tool to assist neurosurgical planning. Stereotact Funct Neurosurg 91:162–169

Su Q, Zhang Y, Liao S, Yan M, Zhu K, Yan S, Li C, Tan J (2019) 3D computed tomography mapping of thoracolumbar vertebrae fractures. Med Sci Monit 25:2802–2810

Sutherland I (1968) A head-mounted three-dimensional display. Proc AFIPS 68:757–764

Tzavellas AN, Kenanidis E, Potoupnis M, Tsiridis E (2020) 3D printing in orthopedic surgery. 3D printing: applications in medicine and surgery. Elsevier

Udupa JK, Hung HM, Chuang KS (1991) Surface and volume rendering in three-dimensional imaging: a comparison. J Digit Imaging 4:159–168

Valverde I (2017) Three-dimensional printed cardiac models: applications in the field of medical education, cardiovascular surgery, and structural heart interventions. Rev Esp Cardiol (Engl Ed) 70:282–291

Wake N, Chandarana H, Huang WC, Taneja SS, Rosenkrantz AB (2016) Application of anatomically accurate, patient-specific 3D printed models from MRI data in urological oncology. Clin Radiol 71:610–614

Wake N, Rude T, Kang SK, Stifelman MD, Borin JF, Sodickson DK, Huang WC, Chandarana H (2017) 3D printed renal cancer models derived from MRI data: application in pre-surgical planning. Abdom Radiol (NY) 42:1501–1509

Wake N, Bjurlin MA, Rostami P, Chandarana H, Huang WC (2018) Three-dimensional printing and augmented reality: enhanced precision for robotic assisted partial nephrectomy. Urology 116:227–228

Wake N, Wysock JS, Bjurlin MA, Chandarana H, Huang WC (2019) "Pin the tumor on the kidney:" an evaluation of how surgeons translate CT and MRI data to 3D models. Urology 131:255–261

Wake N, Rosenkrantz AB, Sodickson DK, Chandarana H, Wysock JS (2020) MRI guided procedure planning and 3D simulation for partial gland cryoablation of the prostate: a pilot study. 3D Print Med 6:33

Wake N, Rosenkrantz AB, Huang WC, Wysock JS, Taneja SS, Sodickson DK, Chandarana H (2021) A workflow to generate patient-specific three-dimensional augmented reality models from medical imaging data and example applications in urologic oncology. 3D Print Med 7:34

Wake N, Vincent J, Robb F (2022) Medical imaging technologies and imaging considerations for 3D printed anatomic models. 3D printing for the radiologist. Elsevier

Wang DD, Eng M, Greenbaum A, Myers E, Forbes M, Pantelic M, Song T, Nelson C, Divine G, Taylor A, Wyman J, Guerrero M, Lederman RJ, Paone G,

O'neill, W. (2016) Predicting LVOT obstruction after TMVR. JACC Cardiovasc Imaging 9:1349–1352

Wang DD, Eng MH, Greenbaum AB, Myers E, Forbes M, Karabon P, Pantelic M, Song T, Nadig J, Guerrero M, O'neill, W. W. (2018) Validating a prediction modeling tool for left ventricular outflow tract (LVOT) obstruction after transcatheter mitral valve replacement (TMVR). Catheter Cardiovasc Interv 92: 379–387

Wang KC, Jones A, Kambhampati S, Gilotra MN, Liacouras PC, Stuelke S, Shiu B, Leong N, Hasan SA, Siegel EL (2019) CT-based 3D printing of the glenoid prior to shoulder arthroplasty: bony morphology and model evaluation. J Digit Imaging 32:816–826

Waran V, Menon R, Pancharatnam D, Rathinam AK, Balakrishnan YK, Tung TS, Raman R, Prepageran N, Chandran H, Rahman ZA (2012) The creation and verification of cranial models using three-dimensional rapid prototyping technology in field of transnasal sphenoid endoscopy. Am J Rhinol Allergy 26:e132–e136

Waran V, Narayanan V, Karuppiah R, Owen SL, Aziz T (2014a) Utility of multimaterial 3D printers in creating models with pathological entities to enhance the training experience of neurosurgeons. J Neurosurg 120: 489–492

Waran V, Narayanan V, Karuppiah R, Pancharatnam D, Chandran H, Raman R, Rahman ZAA, Owen SLF, Aziz TZ (2014b) Injecting realism in surgical training-initial simulation experience with custom 3D models. J Surg Educ 71:193–197

Waran V, Pancharatnam D, Thambinayagam HC, Raman R, Rathinam AK, Balakrishnan YK, Tung TS, Rahman ZA (2014c) The utilization of cranial models created using rapid prototyping techniques in the development of models for navigation training. J Neurol Surg A Cent Eur Neurosurg 75:12–15

Waran V, Narayanan V, Karuppiah R, Thambynayagam HC, Muthusamy KA, Rahman ZA, Kirollos RW (2015) Neurosurgical endoscopic training via a realistic 3-dimensional model with pathology. Simul Healthc 10:43–48

Wedeen VJ, Hagmann P, Tseng WY, Reese TG, Weisskoff RM (2005) Mapping complex tissue architecture with diffusion spectrum magnetic resonance imaging. Magn Reson Med 54:1377–1386

Werner H, Dos Santos JR, Fontes R, Daltro P, Gasparetto E, Marchiori E, Campbell S (2010) Additive manufacturing models of fetuses built from three-dimensional ultrasound, magnetic resonance imaging and computed tomography scan data. Ultrasound Obstet Gynecol 36:355–361

Whatley BR, Kuo J, Shuai C, Damon BJ, Wen X (2011) Fabrication of a biomimetic elastic intervertebral disk scaffold using additive manufacturing. Biofabrication 3:015004

Winter TC, Kennedy AM, Woodward PJ (2015) Holoprosencephaly: a survey of the entity, with embryology and fetal imaging. Radiographics 35:275–290

Wu HH, Priester A, Khoshnoodi P, Zhang Z, Shakeri S, Afshari Mirak S, Asvadi NH, Ahuja P, Sung K, Natarajan S, Sisk A, Reiter R, Raman S, Enzmann D (2019) A system using patient-specific 3D-printed molds to spatially align in vivo MRI with ex vivo MRI and whole-mount histopathology for prostate cancer research. J Magn Reson Imaging 49:270–279

Xia J, Samman N, Yeung RW, Shen SG, Wang D, Ip HH, Tideman H (2000) Three-dimensional virtual reality surgical planning and simulation workbench for orthognathic surgery. Int J Adult Orthodon Orthognath Surg 15:265–282

Yang K, Park W, Ju SG, Chung Y, Choi DH, Cha H, Park JY, Shin JS, Na CH (2019) Heart-sparing radiotherapy with three-dimensional printing technology after mastectomy for patients with left breast cancer. Breast J 25: 682–686

Yoo SJ, Thabit O, Kim EK, Ide H, Yim D, Dragulescu A, Seed M, Grosse-Wortmann L, Van Arsdell G (2015) 3D printing in medicine of congenital heart diseases. 3D Print Med 2:3

Yoo SJ, Spray T, Austin EH III, Yun TJ, Van Arsdell GS (2017) Hands-on surgical training of congenital heart surgery using 3-dimensional print models. J Thorac Cardiovasc Surg 153:1530–1540

Zagzebski J (1996) Essentials of ultrasound physics. Mosby

Zavattero E, Viterbo S, Gerbino G, Ramieri G (2015) Navigation-aided endoscopic sinus surgery. J Craniofac Surg 26:326–327

Zein NN, Hanouneh IA, Bishop PD, Samaan M, Eghtesad B, Quintini C, Miller C, Yerian L, Klatte R (2013) Three-dimensional print of a liver for preoperative planning in living donor liver transplantation. Liver Transpl 19:1304–1310

3D Visualisation of the Spine

7

Scarlett O'Brien and Nagy Darwish

Abstract

The 3D visualisation of the spine is thought of from multiple viewpoints. Firstly, radiological imaging is considered, with plain radiography, CT and MRI imaging discussed in detail with relevant applications to spinal surgery.

3D printing can be used in spinal surgery with multiple applications including education, pre-operative planning for complex cases and making patient-specific guides and implants. The rapidly growing field of intraoperative navigation and robotics have been discussed, in addition to their benefits and limitations within spinal surgery, as well as some technical tips.

An understanding of relevant anatomy and biomechanics is necessary for any surgeon, and so this chapter describes the key concepts to be familiar with, particularly the spinal motion segment and the different methods for classifying spinal injuries and how that relates to stability. The concepts discussed have been brought together by applying this knowledge to some interesting clinical cases. They highlight the importance of 3D visualisation of the spine, which must be considered throughout the decision-making process when managing patients. Spinal surgeons use multiple imaging modalities, knowledge of anatomy and biomechanics, as well as considering the need for navigation in more complex cases, all on a daily basis. With the advancement of technology available for 3D visualisation of the spine, we will be able to improve patient outcomes even further in the future.

7.1 Introduction

Significant developments in technology have enabled us to visualise the details of the human spine anatomy and abnormalities.

W.C. Rontgen, professor of physics in Wurzburg, Bavaria, reported the discovery of the X-ray in 1896 (Röntgen 1896), which is still essential today for the evaluation and management of the spine. Computed tomography (CT) was the first 3D radiological imaging, which provided more information than plain radiographs, allowing further classification of injury patterns and pathology of the spine. This was invented by Sir Godfrey Hounsfield (1980) at the EMI central research laboratories in 1967, and the first CT scan was performed in Wimbledon, England.

S. O'Brien · N. Darwish (✉)
Spinal Trauma Centre, Royal Victoria Hospital, Belfast, UK

Queen's University, Belfast, UK

Ten years later, moving away from radiation technology, Raymond Vahan Damadian, an American physician, was the first inventor of the MR (Magnetic Resonance) scanner (Young 2004). This revolutionary discovery enabled us to visualise not only bony skeletal structures but also to visualise in detail the soft tissues including, ligaments, neural and discal structures in all planes (axial, coronal and sagittal).

3D printing technology allows us to produce signature models for individual spines. Surgeons can now design a prosthetic that fits perfectly in the patient's body, Dr. Ralph Mobbs, a neurosurgeon in Sydney, Australia, was the first surgeon to implant a 3D-printed spinal implant to replace a tumour in the cervical spine and thus restore stability to the patient's spine.

Currently, navigation-assisted spine surgery technology allows the surgeon to access three-dimensional (3D) and virtual images of the spine in relation to the surgical instruments intraoperatively. The Human–Computer Interaction (HCI) concept improves the accuracy of dealing with the human spine. Robotic spine is the future; it has expanded the horizon of spine surgery. It is accurate, safe and minimally invasive.

This chapter will provide the current experiences of the authors as spinal orthopaedic surgeons, combined with a review of the literature. When discussing spinal patients, we mean any patient with pathology related to their spine at any level. This could be in the form of trauma, such as fractures, ligamentous injuries or spinal cord injuries, or atraumatic pathology such as degenerative disease, tumours and infections.

This chapter has been divided into five sections: Radiological Visualisation, 3D printing, Navigation and Robotics, Biomechanics, Clinical Cases.

7.1.1 Radiological Visualisation

Multiple imaging modalities are currently used to aid in the management of spinal patients. Radiological imaging has been available since the late nineteenth century. Imaging now encompasses both two-dimensional and three-dimensional scanning, with huge advances since the first X-rays were used. Commonly used imaging in spinal surgery includes plain film radiographs, computed tomography and magnetic resonance. Each modality may be used for different reasons in different situations, with each having a range of benefits, as well as risks and contraindications. In this section, each modality will be considered in detail, including the origins, modes of action and how we use each modality every day in spinal surgery.

7.2 Radiography

7.2.1 Background

Wilhelm Roentgen, a physics professor in Bavaria, first discovered the X-ray accidentally in 1895 (Rontgen 1896). At the time, he was testing cathode rays, trying to identify if they could pass through glass. A cathode ray is a beam of electrons in a vacuum tube travelling from the negatively charged electrode (cathode) at one end to the positively charged electrode (anode) at the other, across a voltage difference between the electrodes. During his experiment, he noticed that the rays were able to leak out through the cathode tube and emit a fluorescent glow on a nearby screen. He was unsure what this fluorescent ray was, and so termed it 'x-ray', with 'x' meaning unknown. The rays themselves are termed X-rays, whilst the images the rays produce when projected onto a screen are termed radiographs. The first radiograph taken was of Professor Roentgen's wife's hand (Fig. 7.1). Roentgen went on to win the Nobel Prize for Physics in 1901 for his discovery.

The medical community was quick to realise the potential for radiographs to be used in patients to identify fractures or locate bullets or shrapnel without having to open the body. Within a few years, the use of X-ray for making diagnoses was widespread in the United States and Europe. By 1900, radiographs were considered an essential element in patient care, particularly for their

Fig. 7.1 Professor Roentgen's first radiograph (Baumrind 2011)

ability to identify foreign bodies and fractures (Stimson 1899).

7.2.2 Mechanism of Action

A radiograph is produced when a negatively charged electrode is heated by electricity and electrons are released, therefore producing energy. That energy is directed towards a plate, or anode, at high speed. A radiograph is produced when the energy collides with the atoms in the metal plate. When X-rays meet the detector and create an image, there are five main densities that can be visualised; air, fat, soft tissue or fluid, calcium or bone, and metal. They are a direct result of how many X-rays have passed through the subject and arrived at the detector. For example, when passing through air, all the X-rays will continue on to the plate, and none will be absorbed by the air. This means that the area on the radiograph will be black as there is no density to it. Metal, on the other hand, is very dense, and so almost no X-rays will pass through it and onto the anode. This means that metal is white on a

radiograph. The densities in between air and metal vary in how they appear and will be various shades of grey. Whilst original radiographs were printed onto films and displayed on light boxes, electronic systems are now used to display the radiograph on computer screens which allows for higher-definition images that we can review in more detail (Fig. 7.2).

7.2.3 Use in Spinal Surgery

For several spinal conditions, plain radiographs are detailed enough to make a diagnosis, and no more advanced imaging is required. A good example is simple osteoporotic fractures of the vertebrae, where the fracture is low energy and unlikely to be unstable (Fig. 7.3). Repeated radiographs can be taken over time to assess for further compression or development of kyphosis. Commonly in practice, we will repeat the radiograph when the patient is weight-bearing to assess for further compression of the vertebrae.

Another example of simple radiography is identifying and monitoring scoliosis (Fig. 7.4). Over time, the patient's spinal curvature may worsen or change, and various measurements can be performed on a radiograph to quantify this. One such measurement is the Cobb angle, which is defined as the greatest angle at a particular region of the vertebral column, when measured from the superior endplate of a superior vertebra to the inferior endplate of an inferior vertebra, and refers to angles in the coronal plane (Coley 2013). An angle of >10 degrees is highly suggestive of scoliosis, with increasing angles making intervention or surgery more likely to be required.

7.2.4 Intraoperative X-Ray

C-Arm systems are used regularly in spinal surgery. C-Arms are fluoroscopy machines which use image intensifiers. This allows high-resolution X-ray images to be taken and displayed on a monitor in real time (Fig. 7.5). Modern C-arms can perform 12 distinct motions, allowing

Fig. 7.2 Normal Anterior-posterior (AP) and lateral radiograph of cervical spine
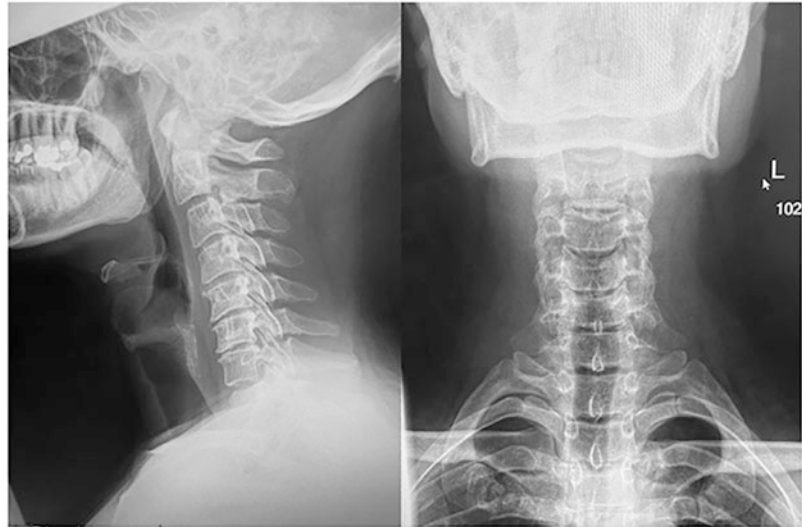
for the acquisition of almost any radiographic view (Pally and Kreder 2013). Their name is derived from their 'C' shape. This shape allows the machine to move around the body easily in order to achieve orthogonal views. They are used widely in orthopaedic surgery (Ojodu et al. 2018). The major advantages of intraoperative imaging are quick and easy identification of operative level, monitoring fracture reduction in multiple planes and confirming appropriate implant position, meaning any errors can be corrected whilst the patient is still in theatre. It does, however,

have the disadvantage of being quite operator dependent. It can be difficult to get true AP or lateral images due to the mobile nature of the C-Arm, meaning it can be difficult to interpret the images. There is also the radiation risk to both the patient and the surgical team, meaning lead must be worn to protect those near the C-Arm. There is also potential to de-sterilise the operative field with the C-arm (Biswas et al. 2008).

When performing spinal surgery, intraoperative X-ray is most commonly used to

Fig. 7.3 Vertebral fracture pre- and post-operatively
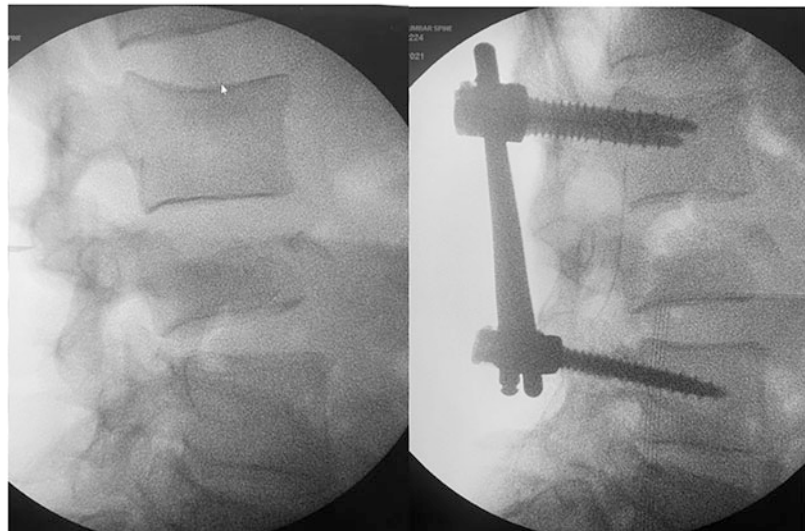
Fig. 7.4 Scoliosis case, pre- and post-operatively
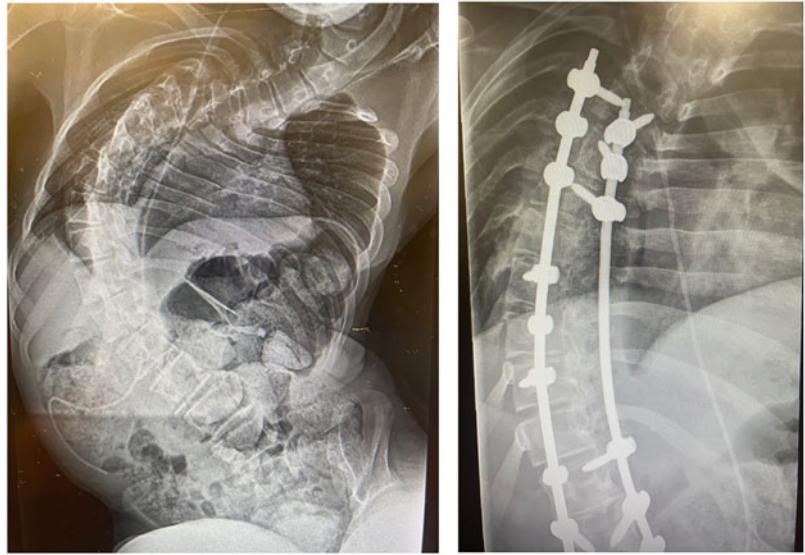
determine the correct vertebral level. For example, when performing an anterior cervical discectomy and fusion (ACDF), the C-Arm will be used prior to incision to ensure that the correct level is chosen to be operated on. The level from the intraoperative X-ray will be compared to the level identified on the MRI scan, which will also be displayed in theatre. Use of MRI scanning in spinal surgery will be covered in detail later. It will also be used during the procedure to confirm the correct level has been chosen, and this detail will always be recorded in the operation note. Images are also often taken when screws and plates are inserted, to confirm correct positioning within bone. For any procedure where an implant of any kind is inserted, a post-operative radiographic check will be taken to compare the intraoperative position to current position, again ensuring the implant is positioned correctly.

7.3   Computed Tomography (CT)

7.3.1   Background

CT uses multiple X-ray images stacked together to develop a three-dimensional image. CT was first developed by Sir Godfrey Hounsfield in

Fig. 7.5 Intraoperative C-Arm in use

1967, using theoretical calculations developed by Allan McLeod Cormack (Hounsfield 1980). Hounsfield was an engineer and inventor, whilst McLeod Cormack was a physicist. They aimed to develop X-ray technology, to create a three-dimensional image which would look inside an object without opening it. The first CT scan was performed in 1971 in London. The first scan was a CT brain performed in Atkinson Morley's Hospital in October 1971 (Fig. 7.6). They went on to win the Nobel prize in Medicine for their invention in 1979. The early CT scans took 30 minutes to perform, and several hours to process and reconstruct the image, often having to be done at another site. CT is now widely available in almost all hospitals in the UK. A CT cervical spine can be performed in around 5 minutes, and images are uploaded to the imaging system for review within a few minutes. CT is highly accurate in trauma. Ninetey-eight percent of cervical spinal injuries can be detected with CT, compared to radiography missing up to 57% of injuries (Jimenez et al. 2008). The major disadvantage of CT compared to radiography is radiation exposure. A CT of cervical spine has 90 times more radiation exposure than a series of radiographs (Jimenez et al. 2008).
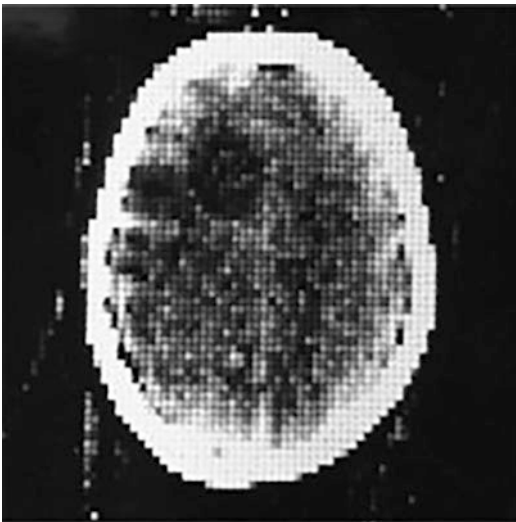
Fig. 7.6 The first CT Brain (Maier et al. 2018)

7.3.2 Mechanism of Action

CT uses multiple X-ray images to build up a cross-sectional image of an area of the body. Similarly, to plain X-ray, the X-ray beam is emitted from a source, passes through the area of the body, and then hits a detector. In CT, the source rotates around the patient, with the detector also rotating. When each beam is emitted, the detector will be opposite to the source, and so they move together. This allows images to be taken from multiple different angles thus gathering information regarding depth.

CT is performed based on different tissues having different densities. These densities can be measured from the calculation of the attenuation coefficient. The attenuation coefficient is a measure of how easily a material can be penetrated by an incident energy beam. Hounsfield developed a scale of densities of tissues with the human body. He used Hounsfield units (HU) to quantify the density based on four discreet tissues; air (-1000 HU), fat (-30 to -70 HU), water (0HU) and cortical bone ($+1000$ HU) (Kamalian et al. 2016). All tissues are therefore compared to these densities, and from this, all materials can be given a density in HU.

7.3.3 Use in Spinal Surgery

7.3.3.1 Trauma

CT is extremely useful in identifying bony injuries. CT imaging of the spine is carried out frequently in patients presenting with trauma to emergency departments. Spinal fractures can have many patterns and can be due to many different mechanisms. They can be easily missed if not investigated. CT is now the modality which should be used in the first instance in most cases to identify a cervical spine injury, with plain radiographs rarely used if there is a high level of suspicion of injury. The National Institute for Health Care Excellence (NICE) guideline for head injury recommends many patients with head injury also have their cervical spine imaged via CT ((NICE) 2014). The incidence of cervical

spine injury associated with head injury is between 4% and 8% (Holly et al. 2002), meaning it is vital that CT cervical spine is performed alongside CT brain to ensure cervical spine injury is not missed.

In addition to the initial identification of fracture, CT allows for fractures to be fully classified. This means the exact anatomical position of the fracture, number of elements or columns involved and inherently the stability of the injury can be identified. This allows surgeons to decide on the most appropriate management, either operative or non-operative. If operative management is indicated, CT imaging allows for operative planning. CT also identifies if any bony fragments are present within the spinal canal (Fig. 7.7) and will prompt clinicians to consider further imaging with Magnetic Resonance Imaging (MRI) if cord injury is suspected.

7.3.3.2   Tumour

Tumours of the spine can either be benign or malignant. Malignant tumours are either primary bone tumours or secondary metastatic disease. Common metastases arise from renal, lung, breast, thyroid and prostate primaries. The most common primary bone malignancy in spine is multiple myeloma (Kelley et al. 2007). CT can accurately identify the tumour and give important

Fig. 7.7 Axial CT of the lumbar spine demonstrating multifragmentary fracture with fragments in the canal

information such as size, elements of bone involved and if stability is compromised. CT is more sensitive than MRI in determining the extent of bony destruction, which is useful in pre-operative planning to determine if operative intervention is indicated and how it should be carried out.

7.3.3.3   CT Myelogram

Myelography is an imaging modality which utilises intrathecal injection of contrast to delineate spinal conditions. The pathologies myelography is used to diagnose or monitor include degenerative spondylosis, nerve root impingement from any cause and tumours. In neurosurgery, they are useful for identifying arachnoid lesions. Prior to the advent of MRI, it was widely used, both with fluoroscopy and later CT. The main indication presently is in patients who have contraindications to MRI, such as an incompatible pacemaker or spinal stimulator but require cross-sectional imaging of their spine and especially thecal sac and contents. Whilst it provides very useful diagnostic information, it has the disadvantage of morbidity associated with radiation and need to inject the subarachnoid space.

7.4   Magnetic Resonance Imaging (MRI)

7.4.1   Background

MRI is an imaging modality which creates images in multiple planes using non-ionising radiation. Both static and functional imaging can be produced. Nuclear magnetic resonance (NMR), later shortened to magnetic resonance, was discovered in 1945 by Felix Bloch and Edward Purcell, who were both physicists (Giunta and Mainz 2020). This principle formed the basis for MRI scanning. They won the Nobel prize in Physics in 1952 for this work. In 1969 Dr. Raymond Damadian theorised that cancerous cells could be detected using NMR, as cancerous cells hold more water, and would show up in MR due to increased numbers of hydrogen ions.

Raymond Damadian published the results of his experiments in 1971.

Also, in 1971 Paul Lauterbur theorised a method using NMR to obtain two-dimensional and three-dimensional images of living tissue. The following year, Lauterbur used his NMR technique to examine two test tubes containing water. He was able to generate an accurate cross-sectional image of the test tubes. His paper was accepted and published by Nature (Lauterbur 1973). Separately, Peter Mansfield published his research into using magnetic field gradients to create three-dimensional MR images in 1973 (Garroway et al. 1974). Damadian then created the first whole-body human scanner in 1977 (Fig. 7.8). Mansfield and Lauterbur were awarded the Nobel prize for Medicine in 2003 for their discoveries regarding magnetic resonance imaging.

MRI has the advantage of not requiring ionising radiation, therefore removing this risk for patients. This means that for patients where radiation is particularly damaging, such as young children or pregnant women, MRI is a safe alternative. However, given the magnetisation involved in MRI, it is not suitable for patients with any indwelling metalwork, such as certain medical implants. It is also quite a lengthy test, with a whole spine MRI taking around 45 minutes. This, combined with the noise and the small space, can make it difficult for some patients to tolerate.

7.4.2 Mechanism of Action

MRI produces cross-sectional images in any spatial direction; coronal, sagittal, axial, oblique. NMR relies on the interaction between atomic nuclei, strong magnetic fields and radiofrequency energy. NMR utilises the hydrogen protons within our bodies, within water, fat and carbohydrate molecules. These protons usually spin, creating a small magnetic charge. When a strong magnetic field is introduced, from the MRI scanner, the protons will align with this field. A radiofrequency pulse is then introduced, which will disrupt each proton, causing it to rotate

90 or 180 degrees. When the pulse is switched off, the protons will then return to their natural position, and this process releases electromagnetic energy. Differing tissues will release this energy at different rates, through varying relaxation processes. The receiving coil then measures the energy signal coming back from the protons. This signal then goes to the computer, which uses a formula to convert the signal to an image (Berger 2002).

When identifying spinal pathology, three sequences are commonly used in the MRI scan; T1 weighted, T2 weighted and Short tau inversion recovery (STIR). The timing of radiofrequency pulse sequences used to make T1 images results in images which highlight fat tissue within the body. The timing of radiofrequency pulse sequences used to make T2 images results in images which highlight fat and water. The timing of the pulse sequence used to make STIR sequences acts to suppress signal coming from fatty tissues, and so only water is highlighted (Patel et al. 2015) (Fig. 7.9).

7.4.3 Use in Spinal Surgery

7.4.3.1 Trauma

Vertebral fractures are increasingly common, with vertebral compression fractures being the second most common osteoporotic fracture (Svensson et al. 2016). It can be unclear if a fracture is acute or chronic, and patients may have multilevel fractures. As vertebral compression fractures are so common, patients presenting with back pain may have had previous imaging; either plain radiograph or CT. MRI can be useful in determining if the fracture is acute or chronic, as an acute fracture will be bright on the STIR sequence. It is also useful in determining the extent of fracture, for example, if it had been previously unclear if the posterior elements were involved or not. MRI is the only modality which will determine if any ligamentous instability has occurred, particularly of the anterior or posterior longitudinal ligaments. Ligamentous tear or rupture, combined with some fracture patterns, will make the spinal construct unstable (Fig. 7.10).

Fig. 7.8 Dr. Raymond Damadian's MRI Scanner 1977 (Winans 2018)
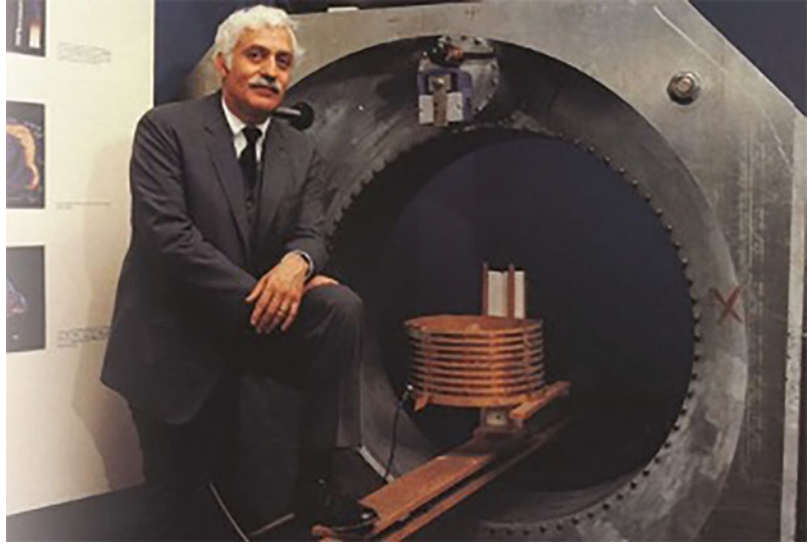
The concept of differing fracture patterns and their relative stability is discussed later in the biomechanics section. The major indication for MRI scanning in a spinal fracture is in patients with neurological deficits on examination. This usually indicates a spinal cord, cauda equina or spinal nerve root injury caused by the fracture. There are also many spinal cord injuries, which may not be associated with a fracture, such as central cord syndrome. These will also require an urgent MRI to make the diagnosis and guide management.

7.4.3.2   Degenerative Disease

One of the most common presentations to the spinal outpatient department is chronic neck or back pain, often associated with radiculopathy or another neurological deficit. If atraumatic, or if a fracture is excluded on plain imaging, degenerative disease is likely. This is often attributable to spondylosis (degenerative disc disease) (Fig. 7.11), spondylolisthesis (degenerative slip), facet joint hypertrophy or ligamentous hypertrophy. All these conditions have the potential to irritate nerve roots or the spinal cord and cause

Fig. 7.9 T1/T2/STIR Sagittal images of lumbar spine to show comparison
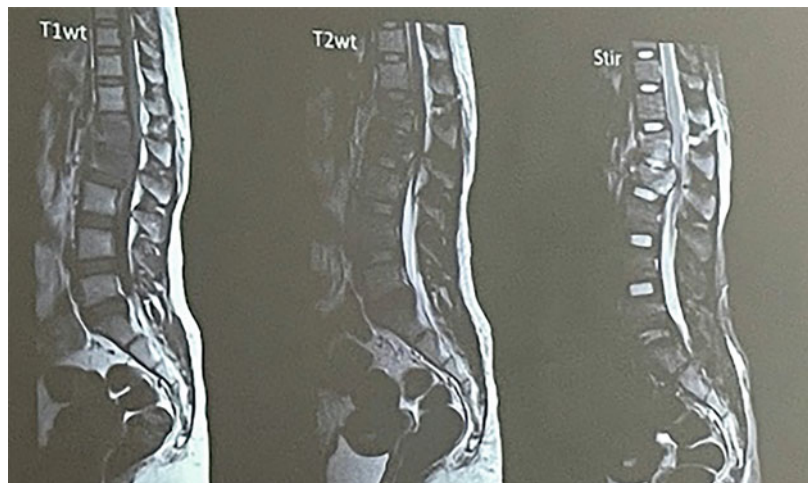
Fig. 7.10 Anterior longitudinal ligament injury with associated fracture

associated symptoms. The best way to image these conditions is with MRI.

7.4.3.3 Tumour

As previously mentioned in the section, discussing CT scans, malignant tumours in or around the spine are commonly seen in the tertiary centre. If the diagnosis is uncertain, for example, it may be difficult to differentiate between infection and tumour; therefore, MRI scanning can provide further information to aid the diagnosis. MRI is useful in classifying the tumour as extradural, intradural-extramedullary and intramedullary (Dasarju et al. 2020). This helps to determine management. When a known tumour is associated with neurological compromise, metastatic spinal cord compression (MSCC) should be considered. MSCC is a condition requiring urgent management, and so access to MRI for diagnosis should be available 24 hours a day (NICE 2008).

7.4.3.4 Cauda Equina Syndrome (CES)

CES is a relatively rare but disabling condition which can result in motor and sensory deficits, incontinence of urine and faeces, and loss of sexual function. Any patient with a possible diagnosis of threatened/partial/complete CES requires urgent investigation. MRI scanning must be undertaken in an emergency in the patient's local hospital and should take precedence over routine scans ((SBNS) 2018).

7.4.3.5 Recent Advances in MRI

A recent development in MRI is the use of zero echo time (ET) pulse sequences. A major difficulty with traditional MRI scanning is the loud noise generated from the rapidly switching currents in the magnetic field gradient coils.

Fig. 7.11 Multilevel degenerative disease of lumbar and cervical spine

Zero ET pulse sequences minimise gradient switching, and so, almost eliminate noise completely (Ljungberg et al. 2021). The sequences required are also shorter, and so scans can be more efficient. Whilst this technology is not yet readily available, it will be interesting to see what developments this advance in MRI will bring to spinal surgery.

7.5   Conclusion

Radiological imaging has advanced exponentially over the past century. Easy access to multiple imaging modalities is now available, which enhances the ability to visualise the human spine in three dimensions. Within spinal surgery, we use imaging to make a diagnosis, monitor a condition, make decisions about patient management and to guide our decision-making intraoperatively. As discussed later in the chapter, the future will involve using CT intraoperatively to navigate surgery, as a further advancement from intraoperative radiographs.

7.5.1   3D Printing

3D printing is also called additive manufacturing or rapid prototyping. It was first developed by Charles Hull in the 1980s (Hull 1986), when he patented the stereolithography device. The technique uses multiple 2D images, very similar to the axial cross-sectional images we would be familiar with from CT and MRI, and as the 2D images are laid down one on top of the other, a 3D image is then created.

There are now several different methods for creating 3D-printed items, but all follow this basic technique. The three methods currently in use are: fused deposition modelling (FDM), stereolithography (SLA) and selective laser sintering (SLS). FDM uses a heated polymer that is sequentially layered with a computer extrusion nozzle. It is widely used commercially, as it is relatively low cost and can be done quickly. However, the products tend not to be stable under significant heat, making them difficult to sterilise,

and therefore not used in surgery. SLA uses light-curable resin to sequentially add layers. The resin then undergoes photopolymerisation, where it is hardened by exposure to a light source. SLS uses a focused energy source such as an electron beam or laser to sinter fine powder, in other words, to convert powder particles into a solid construct sequentially. Both SLA and SLS can withstand heat, and thus can be sterilised, making them options for surgical implants.

7.5.1.1   Use in Spinal Surgery (Sheha et al. 2019)

Pre-operative planning	3D models can be printed from patients imaging. A 3D model of unusual anatomy or more complex pathology, allows surgeons to visualise their plan for surgery.
Intraoperative guides	Patient-specific drill guides and templates can be printed, allowing for more accurate screw placement.
Patient-specific implants	In cases where there is to be a large resection due to a large tumour, infection or significant trauma, an implant will need to be fitted to fill the gap where the resection has been taken. A specific implant allows a more anatomical fit to the patient and requires a less-extensive dissection, maintaining the structural integrity of their spine.
Education	At the most basic level, printed models can demonstrate anatomy and pathology in 3D, making it easier for students to visualise and understand. For surgical trainees, models can be printed to be used as surgical simulators. Trainees can learn techniques on the models, before transferring them to the operating theatre.

Many units have access to a 3D printer, which is connected to the CT imaging system. This means rapid access to live 3D printing, which can be used to plan for cases of severe deformity or complex fractures (Fig. 7.12). These models are used to visualise the pathology and determine the exact operative intervention required.

Fig. 7.12 3D printed deformity case in thoracolumbar spine and post-operative posterior stabilisation which have been printed in our unit

7.5.2 Navigation and Robotics

#### 7.5.2.1 Basics of Navigation and Robot-Assisted Surgery

Robotic surgery has become commonplace in many surgical specialties including spinal surgery, general surgery, gynaecology and urology. Robotic-assisted surgery has also become more widespread within orthopaedic surgery, particularly in knee arthroplasty. Robotic surgery systems can either be autonomous, where once set up, the robot performs most of the operation, or haptic, where the surgeon is required throughout the procedure to steer the robot to carry out the tasks.

7.5.2.2 Use within Spinal Surgery

Within spinal surgery, robotic surgery has been useful in the insertion of pedicle screws (Fig. 7.13), which are required for most spinal stabilisation and fusion procedures. The use of computer-aided navigation in spinal surgery was first reported by Nolte et al. (1995) where they used a combination of pre- and intraoperative information to insert pedicle screws more accurately in an open procedure. Improving the efficiency and accuracy of pedicle screw placement has many advantages for patients. Screw

malposition can lead to significant neurovascular complications, with so many important structures in and around the spinal column. Potential complications include dural tearing, neural damage and vascular or visceral complications. Many complications lead to serious morbidity and can necessitate return to theatre, with further anaesthetic complications and increased risk of systemic problems. A meta-analysis (Tang et al. 2014) suggests that complication rates and screw accuracy can be improved by intraoperative navigation techniques.

The ExcelsiusGPS system (Fig. 7.14) (Globus Medical; Audobon, PA, USA) is a robotic system
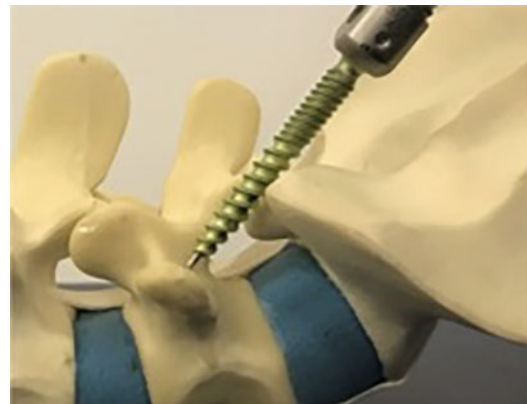
Fig. 7.13 Usual position for pedicle screw placement

Fig. 7.14 The ExcelsiusGPS system

in use in some UK centres. This system requires a pre-operative CT scan. Screw position will be planned from this imaging (Fig. 7.15). The patient is positioned and prepped as usual. The dynamic reference base arrays and surveillance markers are positioned in the bone.

An intraoperative CT using O-arm (Fig. 7.16) (Medtronic; Dublin, Ireland) is then performed, which is compared to their pre-operative scan. Planned screw position will now be confirmed and any adjustments made.

Small incisions are made, ensuring soft tissues were adequately dissected. The robotic end effector arm then moves into position to guide all movements along this planned trajectory. A pilot hole is made, then the hole is drilled and tapped, under navigation ensuring the correct trajectory is maintained. The screw is finally positioned, and placement is confirmed by the robot to match the planned position. The surgeon receives immediate feedback that the screw is positioned correctly.

Whilst additional equipment is required, with more moving components, there has not been an increase in surgical site infections associated with intraoperative navigation. A single-unit study found no significant difference in cases where no imaging, C-arm fluoroscopy or O-arm intraoperative CT were used (Kumagai et al. 2022). It was also initially felt that using navigation would increase surgical times. However, Khanna et al. (2016) found that whilst operative times were longer when navigation was first introduced to a unit, over time, operative time was actually decreased when the surgical team became more familiar with the equipment. As navigation becomes more commonplace, it should also become more efficient than current fluoroscopic or freehand screw placement.

Advantages and Disadvantages of Robotic Spinal Surgery (Alluri et al. 2021).
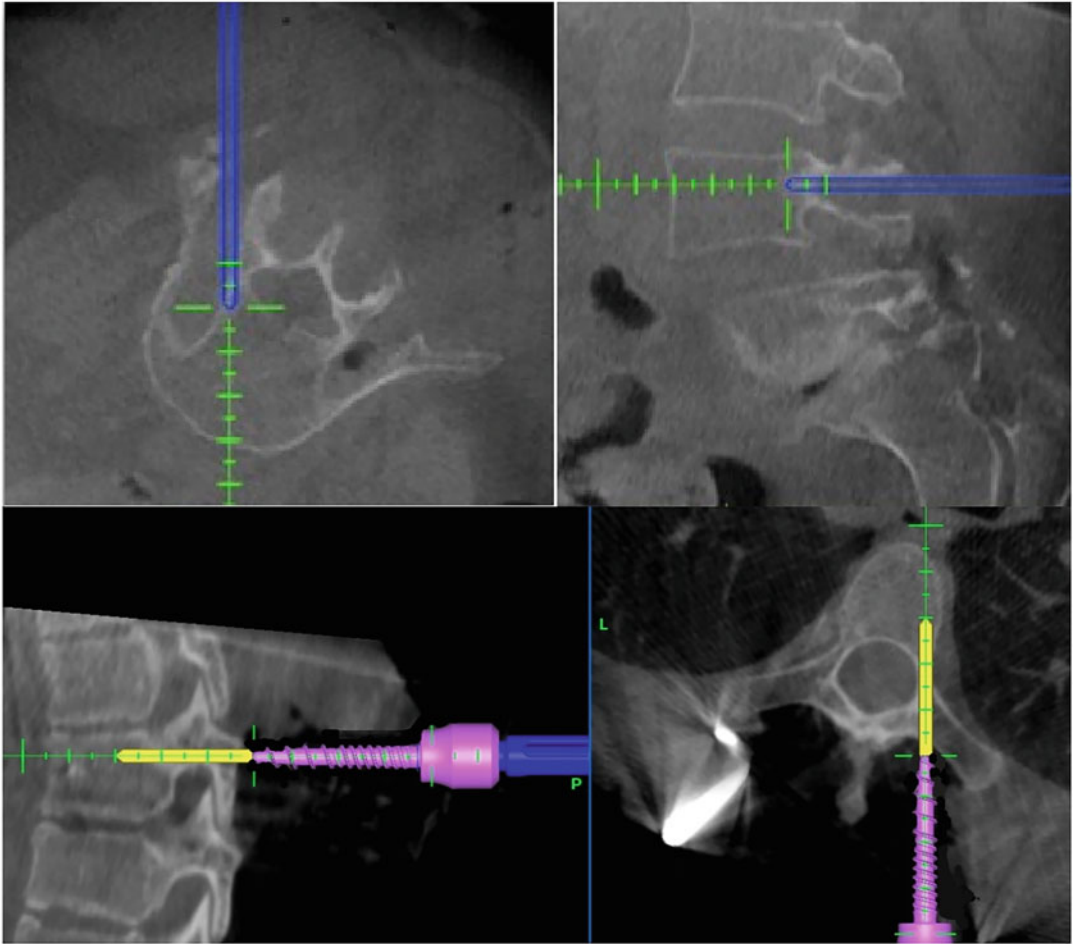
Fig. 7.15 Examples of CT navigation images in the thoracolumbar spine

Fig. 7.16 O-arm intraoperative CT

Advantages	Disadvantages
Improved clinical outcomes and reduced complications	Increased training required for the surgical team (Fig. 7.17)
Increased pedicle screw placement accuracy	Increased cost of equipment and software systems
Avoidance of breach of spinal canal, and so reduced risk of development of adjacent segment disease and spinal cord damage	Operative time not decreased until surgeons and team become familiar with system – Can take significant time to become proficient
Reduced radiation risk when compared to fluoroscopic guided instrumentation techniques	Technical issues can be associated with equipment or software
Reduced operative time and increased efficiency	

Fig. 7.17 Theatre team members using simulation to train in robotic-assisted navigation

Tips to Improve Spinal Navigation Surgery (Cawley et al. 2020)

1. The patient should be positioned prone on the Jackson table with arms abducted and elbows flexed. Ensure enough clearance below table for the navigation system.

2. It is important to dissect only what is required, as excessive dissection will alter spinal flexibility and therefore position, which will make navigation less accurate.

3. The reference frame must be placed solidly in position and protected throughout the case. Ensure the frame is not unnecessarily obscured by drapes.

4. Ensure the drill guide is held firmly, as any movements of this will alter the trajectory when drilling.

5. When drilling, power instruments should be used to increase accuracy and efficiency.

6. The starting point for each drill hole should first be made by a burr or serrated drill guide to help anchor the drill and prevent slippage, in turn protecting the trajectory. The navigation system allows a more lateral entry point for screw insertion, which allows a longer trajectory and so a broader construct triangulation. This in turn increases the pull-out strength of the screw.

7. The templating intraoperatively is carried out by the circulating surgical team. This increases the entire team's awareness of the need to accurately save the templated image and communicate the screw size clearly.

8. Using a wire and a cannulated screw technique is useful, particularly when achieving the correct entry point is more difficult.

9. When inserting the screw, it is vital to keep reviewing the images on screen to prevent over-tightening or perforation of the far cortex. This minimises the risk of nerve root irritation.

10. Navigation can also be used to deliver intrathecal analgesia, which is usually done freehand by the anaesthetist. The navigated method is more accurate, with lower complications.

7.5.3 Biomechanics

The spine has multiple functions. It supports the body by providing a structure that loads can be transmitted through, it allows the spinal cord and neural structures to be protected, and it allows motion of the body in multiple 3D planes.
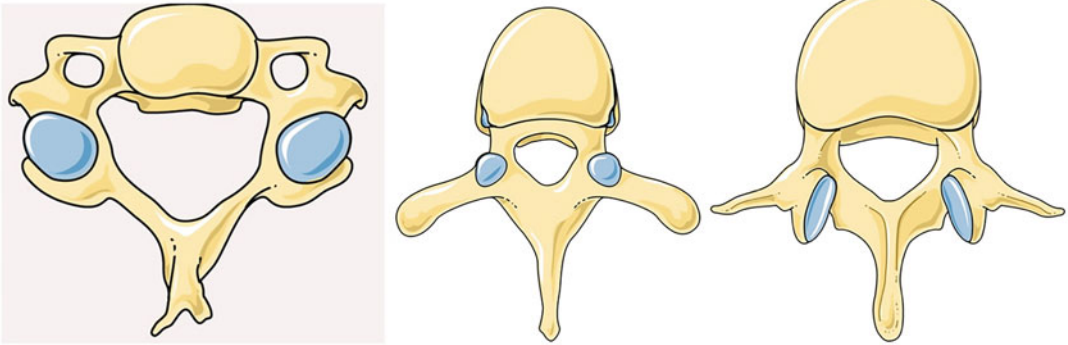
Fig. 7.18 Cervical, thoracic and lumbar vertebrae

7.5.3.1 Spinal Anatomy

The spinal column consists of 7 cervical, 12 thoracic, 5 lumbar, 5 fused sacral and 5 fused coccygeal vertebrae. In the sagittal plane, these are arranged with four curves; cervical lordosis, thoracic kyphosis, lumbar lordosis and sacrococcygeal kyphosis (sagittal balance). A typical vertebra contains common features; vertebral body, facet joints, spinous and transverse processes; however, the overall shape varies widely between different spinal segments (Fig. 7.18).

7.6 Vertebral Body

The vertebral body is the main load-bearing component of the spine. The main force requiring opposition is compression, which comes from the weight of the body above the vertebrae. The structure of the vertebral body allows axial compressive forces to be converted into transverse tensile forces. The central portion is cancellous bone, which is surrounded by cortical bone. The trabecular pattern of the cancellous bone allows the compressive forces to be distributed throughout the area evenly. The bone is arranged in vertical columns and horizontal beams. Their structure allows the vertebral body to be lightweight enough to be carried easily, whilst strong enough to withstand significant force. Increasing the number of columns and beams will proportionally increase the tensile strength of the unit. A

solid structure would be less able to withstand the load as the forces could not be distributed as easily.

7.7 Facet Joints

Facet joints make up part of the posterior elements of the spinal column and allow motion between vertebrae as well as increasing spinal stability. They consist of the superior and inferior articular processes of the superior and inferior laminae. Different segments of the spinal column move in slightly different planes as the inclination of the joint and shape of the joints change. The cervical spine has a lot of movement, especially rotation between C1 and C2, as well as flexion, extension and lateral flexion. The thoracic spine also has rotation and lateral flexion, but minimal flexion and extension. In the lumbar spine, the superior facets are concave and the inferior facets are convex, allowing significant flexion, extension and lateral flexion but almost no rotation. They also have a load-bearing function and can carry up to 30% of the load in combination with the intervertebral discs.

7.8 Intervertebral Discs

The intervertebral disc consists of a central, gelatinous nucleus pulposus and a peripheral annulus fibrosis. Annulus fibrosis consists of concentric

layers of collagen fibres. The fibres are arranged 30° to the vertical in alternating directions. The nucleus pulposus is mostly water and generates hydrostatic pressure. This hydrostatic pressure exerts tensile stresses in the annulus fibrosis. There are also the superior and inferior vertebral end plates which are made up of hyaline cartilage, and connect the disc to the vertebral body. The discs are avascular structures, and so rely on the end plate blood supply for their nutrients. As the disc is loaded, the hydrostatic pressure increases, exerting tension on the annulus fibrosis, increasing the disc stiffness. When the disc is loaded the fibres of the annulus fibrosis flatten, which produces circumferential hoop stresses.

7.9   Spinal Ligaments

From anterior to posterior, there are five main ligaments associated with the vertebral column: anterior longitudinal ligament anterior to the vertebral body, posterior longitudinal ligament posterior to the vertebral body, ligamentum flavum between laminae of adjacent vertebrae, interspinal ligament between the spinous processes and supraspinous ligament posterior to the spinous processes. The main function of these ligaments is to provide support to the spinal column by converting axial loads into tension. They allow protection of the spinal cord by restricting the movement of the spinal motion segment and by absorbing some of the forces. Conversely, they also permit motion and help maintain the correct orientation of the vertebral column.

7.10   Spinous and Transverse Processes

These bony protrusions provide areas for muscles and ligaments to attach. They do not offer much support in terms of load bearing or stability of the unit.

7.10.1   Spinal Motion Segments

The spine works in multiple functional units which allow motion between vertebral levels. Each motion segment consists of two vertebrae and the disc between them (Fig. 7.19). The intervertebral disc allows flexibility in the unit. Motion occurs at both the facet joints and the intervertebral joints. The planes of movement are flexion and extension in the sagittal plane, lateral flexion in the coronal plane and rotation in the axial plane.

7.10.2   Spinal Column Stability

The spinal column is considered stable if normal mechanical loading does not cause any significant displacement of the spinal motion segment and more importantly, causes no change in neurological status. This means in practice, that the spinal column is considered unstable if there is deformation when a patient axially loads, i.e. stands or sits upright. The question of stability is one of the most important things to consider when assessing a patient with spinal trauma.

Several classification systems are available which help to determine the stability of the thoracolumbar spine. In 1963, Holdsworth (1963) published his two-column classification system. In this, he defined the anterior column to begin at the anterior longitudinal ligament and finish at the posterior longitudinal. Elements posterior to the posterior longitudinal ligament are deemed the posterior column. He deemed that the posterior ligament complex was vital in determining stability. If both anterior and posterior columns were injured, the injury was unstable. If a single column was injured, the stability depended on the integrity of the posterior ligaments, and so the posterior column involvement. The only imaging modality available to Holdsworth was plain radiography.

This two-column classification system has now largely been superseded by the three-column classification developed by Denis (1983) in the 1980s. With the advent of CT, Denis had more

Fig. 7.19 Spinal motion segment, including two vertebrae and their intervertebral disc
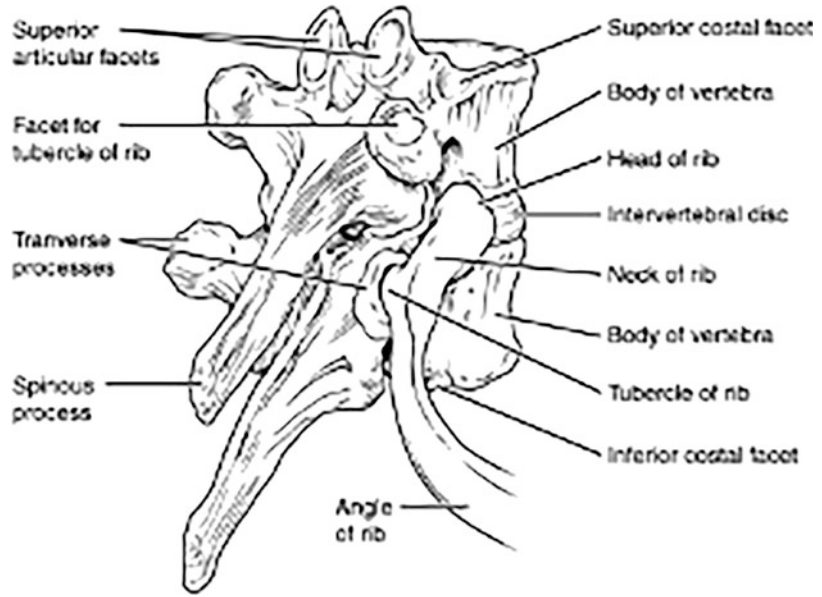
information available and expanded the columns. The anterior column now involved the anterior longitudinal ligament and the anterior half of vertebral body and intervertebral disc. The middle column included the posterior half of the vertebral body, disc and posterior longitudinal ligament. The posterior column was the same, including all posterior elements. Single-column injuries were all deemed stable. Three-column injuries were unstable. Two-column injuries involving the middle column are usually unstable.

More recently we are using the revised AO classification (Vu and Gendelberg 2020). This system includes three groups of fractures: compression (Type A), distraction (Type B) and torsional injuries (Type C) (Fig. 7.20). Type A injuries are simple compression injuries, Type B injuries are due to failure of the anterior or posterior tension band without gross translation, and Type C injuries are dislocation, rotational or displacement-type injuries. Within each type, there are subgroups which describe the severity and stability of the injury. A higher number indicates a more complex or unstable injury, for example, an A4 injury is a complete burst fracture involving both endplates and the posterior wall, but with the posterior ligaments intact. It is much more complex than an A1 injury, which includes

a simple end plate, with no involvement of the posterior elements. In clinical practice, all A type fractures and B1 fractures can be managed non-operatively. B2 can be managed either non-operatively or operatively, whilst B3 and C fractures are all unstable and require operative stabilisation.

Clinical clues to an unstable spine include increased pain on axial loading, neurological compromise and significant deformation.

7.10.3 Clinical Cases

7.10.3.1 Gunshot

A 35-year-old male presented with a gunshot wound to his back. He was a usually fit and well male, with a history of previous substance misuse. He sustained a single entry wound at the level of his lumbar spine. On initial examination, he had a right-sided neurological deficit. He had altered sensation at L3-S1, with reduced power 3/5 in this distribution. He also had absent knee and ankle reflexes. There was no associated bowel or bladder disturbance. Initial imaging was carried out with a CT trauma scan of head, cervical spine, chest, abdomen and pelvis (Fig. 7.21). This identified a comminuted fracture
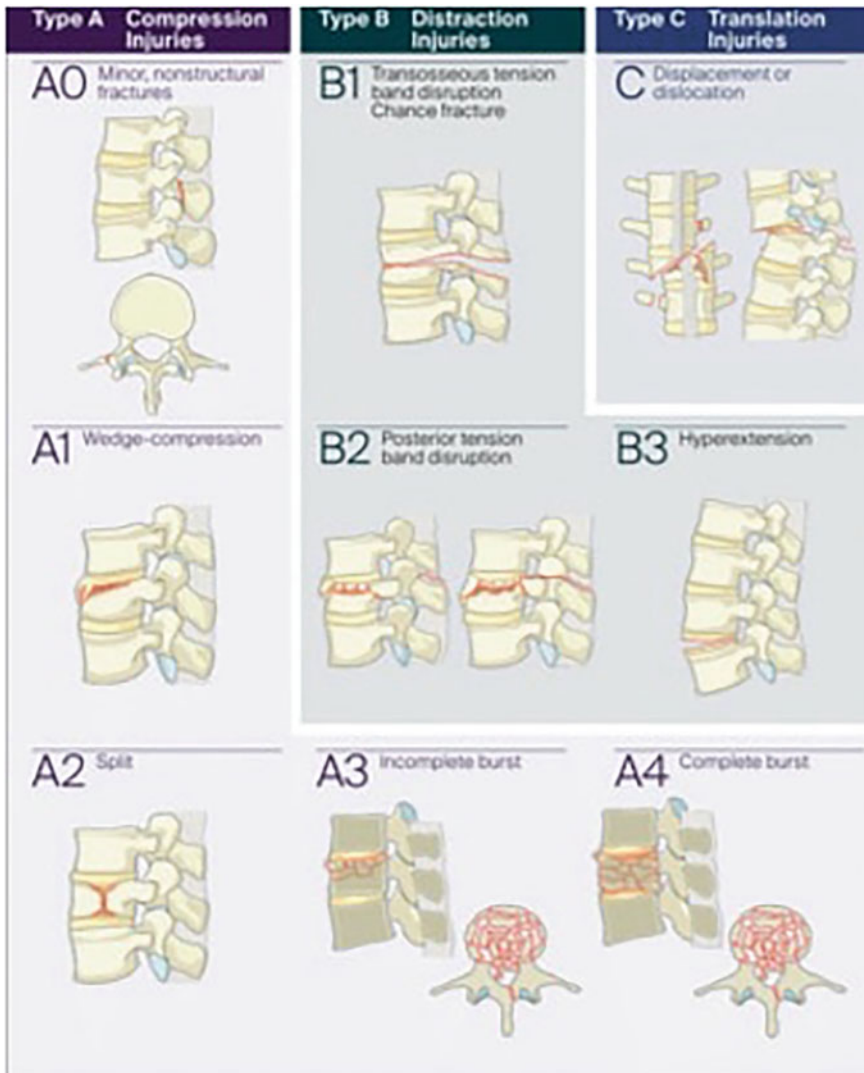
Fig. 7.20   Revised AO Classification of Spinal Fractures

of L3, with the bullet lodged in the right pedicle. The fracture extended through the posterior elements of L3 as well as involved the L2 spinous process. Bony fragments were identified within the spinal canal at the L2/3 level. Multiple gas locules were demonstrated tracking from the skin. Imaging also presented a left grade V renal injury with extensive perinephric haematoma.

This gentleman was initially managed with suitable resuscitation in the emergency department. He required blood products, intravenous fluids and significant analgesia. This was treated

as an open injury, which was likely to be contaminated. As such, he was managed as per the British Orthopaedic Association (BOA) and British Association of Plastic and Reconstructive Surgeons (BAPRAS) guidance on open fractures (1). He received intravenous antibiotics and a tetanus vaccine as well as tetanus immunoglobulin. A urinary catheter was inserted, with the urology team providing input for his renal injury.

He proceeded to the theatre the next morning for operative intervention for his spinal injury. At the time of surgery, the fracture was noted in the
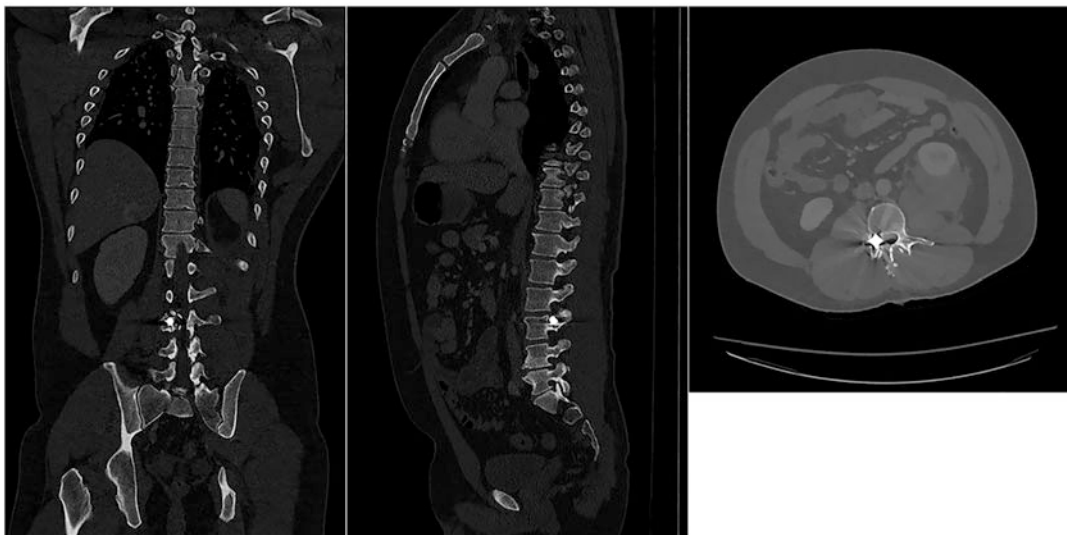
Fig. 7.21 Pre-operative coronal, sagittal and axial CT images

L3 pedicle. The bullet was successfully removed in one piece and sent to police as evidence. The spine was then stabilised with pedicle screws L2-L4 and pre-contoured rods. Intraoperative fluoroscopy (Fig. 7.22) confirmed all screws were appropriately sited. The gunshot tract was extensively washed and debrided.

Post-operatively the patient made good progress. His renal injury was managed non-operatively. A check radiograph was performed when stable (Fig. 7.23), which showed pedicle screws and rods to be appropriately positioned, and good overall lumbar alignment. At review, his sensation and power had improved, and he was managing to mobilise independently without any walking aid.

Diagnosis and operative planning would have been impossible in this case without 3D radiological imaging. His initial trauma scan was reconstructed into a 3D image which could be rotated, allowing the bullet to be easily visualised in relation to his bony anatomy. Intraoperative imaging was also vital to confirm the correct level and ensure all metalwork was positioned accurately.

7.10.3.2 Fracture on Background of Ankylosing Spondylitis

The next case is that of a 67-year-old male who was involved in a road traffic collision. He was a restrained driver, who was hit head-on by another motorist. He was able to self-extricate and initially to mobilise at the scene; however, he did have significant thoracic back pain. He has a history of both ankylosing spondylitis and rheumatoid arthritis and was on biological therapy. He had previous vertebroplasty surgery treating collapse fractures of the thoracic spine, as well as multiple non-operatively managed thoracic vertebral fractures. On examination, he had no focal neurological deficit. He was haemodynamically stable. His main complaint was of thoracic back pain. No other injury was identified outside his spine on primary or secondary survey.

Initial imaging was performed with a CT of the thoracic spine (Fig. 7.24). This identified a three-column, unstable T10 fracture on the background of significant ankyloses. He had subsequent imaging with a CT of the cervical and lumbar spine to complete the series of CT imaging.

Initially, a fracture through the C6/7 disc space was queried. At this stage, the patient was transferred to the tertiary spinal unit and had an MRI Whole Spine (Fig. 7.25). The injury at C6/7 was

Fig. 7.22 Intraoperative imaging
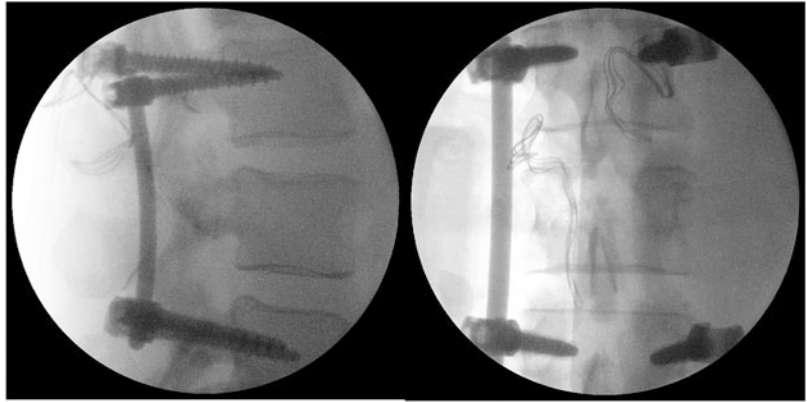
felt to be long-standing on this imaging and no cord injury was identified; however, a posterior epidural haematoma and anterior longitudinal ligament injury were detected. Combining this information, the patient was felt to have a highly

unstable T10 fracture and proceeded to theatre the same day as an emergency.

He had posterior stabilisation of T10 with pedicle screws and rods from T7-L2. Levels were checked pre-operatively, and screw position was

Fig. 7.23 Post-operative radiographs
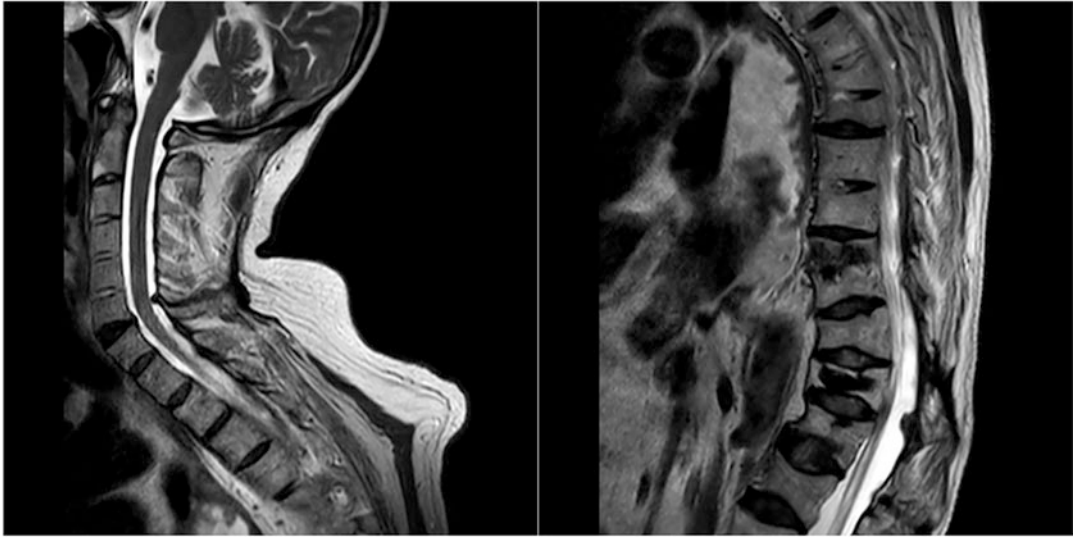
Fig. 7.24 Pre-operative sagittal MRI of cervical and thoracolumbar spine. Demonstrating the T10 fracture, as well as excluding a new cervical injury

checked intraoperatively using fluoroscopy (Fig. 7.26).

Post-operatively he recovered well. There was no neurological deficit and he has been able to mobilise independently. Post-operative radiographs (Fig. 7.27) obtained showed metalwork to be in the appropriate position.

This case highlights the importance of recognising the extensive instability of this fracture pattern in patients with ankylosing spondylitis, and to a lesser extent, diffuse idiopathic skeletal hyperostosis (DISH). Their spine is significantly stiffer than a spinal column with no underlying condition, and therefore they are likely to sustain more significant injuries with a higher risk of neurological compromise. It was vital to obtain completion imaging of the whole spine, as injuries at other sites are common, with the incidence being quoted as 13.1% (Lukasiewicz et al. 2016). With consideration of all these factors, these injuries should be treated as an emergency and should have posterior stabilisation on the same day.

7.10.3.3 Cauda Equina Syndrome

This case is of a 43-year-old male who had a long-standing history of lower back pain. For many years he also had radicular pain in his right leg. He presented to the emergency department with 1 week of increased lower back pain. His radiculopathy had progressed to bilateral pain over 3 days. He had 36 hours of difficulty with urination, having difficulty initiating a urinary stream. He was an otherwise fit and healthy gentleman. On examination, his power was intact throughout all myotomes and sensation intact throughout all lower limb dermatomes. He did have altered sensation in the S2–4 dermatomes in the perianal area; however, anal tone was intact. On presentation, he had difficulty initiating a urinary stream, and so was catheterised. He was found to have less than 200 ml residual volume in his bladder.

An MRI was arranged by the emergency department, which demonstrated a large L5/S1 disc protrusion which was causing cauda equina compression (Fig. 7.28). He proceeded to the theatre the following day for L5/S1 discectomy and decompression.

Fig. 7.25 Sagittal CT of thoracic spine and axial CT of T10. Arrow demonstrates the significant anterior opening
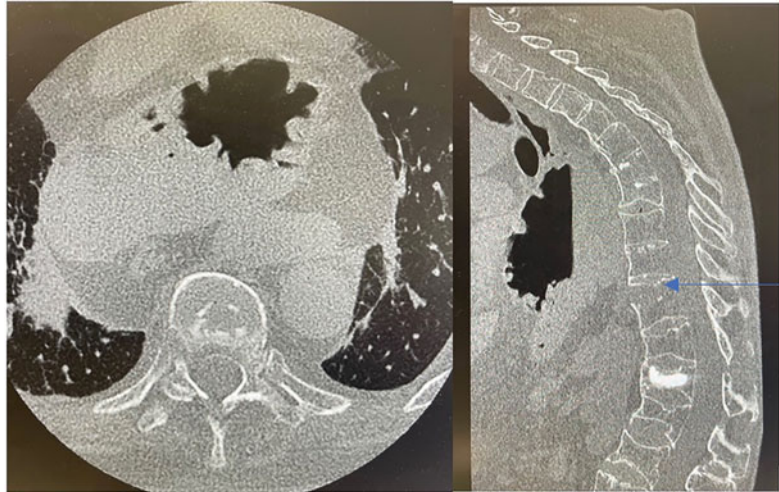
Post-operatively he recovered well. He had no ongoing neurological deficit and was discharged on day 3 post-operatively.

This gentleman presented with classical symptoms of cauda equina syndrome. He had back pain, bilateral leg pain, urinary disturbance and perianal sensory disturbance. Excellent emergency access to MRI scanning afforded this gentleman the ability to be managed in a timely fashion and thus avoided long-term neurological compromise.

Fig. 7.26 Intraoperative imaging

7.10.3.4 Acute Thoracic Disc with Neurological Compromise

The next case is that of a 46-year-old male who presented with thoracic back pain, leg weakness and loss of bladder control. He had no previous significant medical history. Initially, he was catheterised, with no significant residual volume and was able to feel the catheter. He had normal sensation in all lower limb dermatomes and normal power in all lower limb myotomes.

He proceeded to MRI (Fig. 7.29) which demonstrated a T10/11disc extrusion with cord compression.

At this stage, given there was no neurological deficit, the decision was made to manage this patient non-operatively. His bladder symptoms resolved over 48 hours and his catheter was successfully removed. Unfortunately, he subsequently went into urinary retention and had to be re-catheterised a few days later. Power and sensation remained intact in his lower limbs. Operative management was then felt to be in his best interest, and so he proceeded to theatre for posterior decompression of T10/11.

The operation was performed as a dual consultant case and a satisfactory decompression was achieved, meaning both operating consultants felt that the spinal cord was completely free with no pathological tissue indenting it. The level was confirmed on intraoperative imaging above. Unfortunately, the patient developed a complete

Fig. 7.27 Post-operative AP and lateral radiographs
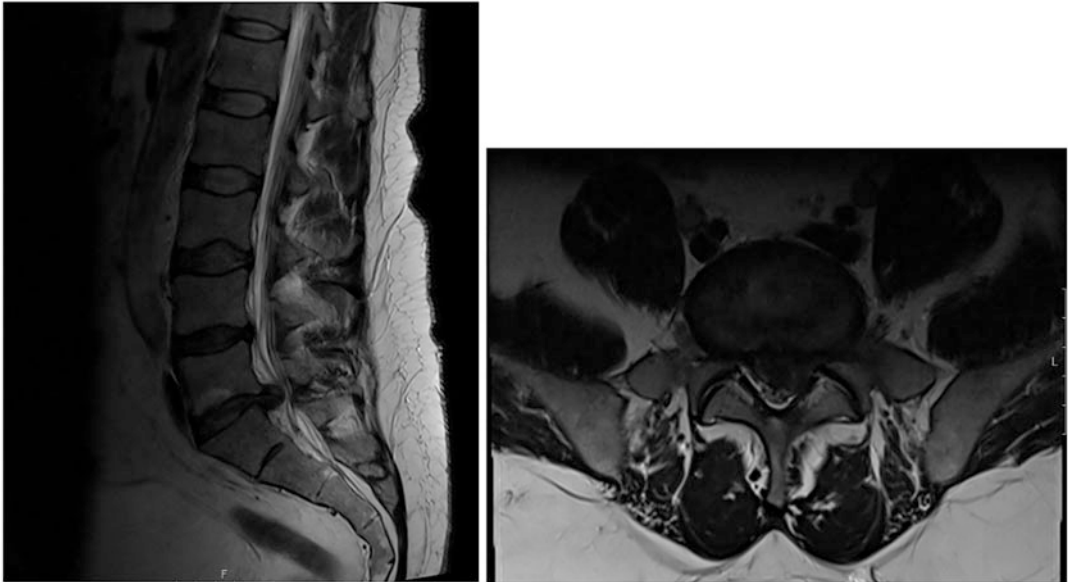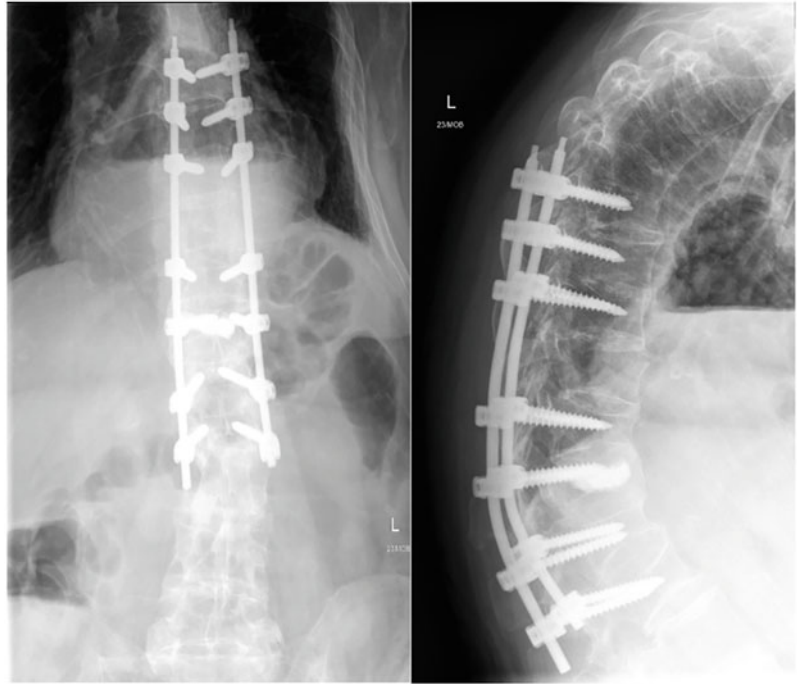
Fig. 7.28 Axial and sagittal MRI of lumbar spine, demonstrating large L5/S1 disc with cauda equina compression

loss of power in lower limbs bilaterally in recovery. He had a sensory level at L1 and was unable to feel the catheter. An emergency MRI was arranged (Fig. 7.30).

The MRI confirmed that a satisfactory posterior decompression had been performed at the correct level. There was no evidence of epidural haematoma, but cord signal change was evident.

Fig. 7.29 Axial and sagittal MRI images of thoracic disc

However, given the significant neurological deficit, the decision was made to proceed to anterior decompression. Thoracic surgeons gained access to the chest anteriorly and an anterior hemi corpectomy, discectomy and cage was performed (Fig. 7.31).

Post-operatively he was initially managed in the high-dependency unit; however, he was discharged to the ward within 48 hours.

His MRI was then repeated one week following the initial surgery (Fig. 7.32).

This demonstrated a reduction in cord oedema, but ongoing disc extrusion. The patient then proceeded to revision discectomy and posterior stabilisation T9-T12 (Fig. 7.33).

This patient made little neurological improvement despite intensive intervention. Following his admission, he had a period of rehabilitation in the spinal injuries unit where he made some improvements and was wheelchair independent with most activities of daily living on his discharge.

This case discusses thoracic disc disease with compression of the spinal cord. MRI imaging was vital for operative planning, and management was changed by MRI appearances. Our learning point from this case highlighted that navigation would be useful in a complex case like this, to minimise complications and prevent neurological compromise. Another key issue is that time to surgery should be as soon as possible to ensure the best outcome.

7.10.3.5 Inflammatory

A 40-year-old female patient presented with a few weeks of back pain and 4 days of right leg radicular pain. She reported a 5 kg weight loss over several months. She was systemically well with no fevers. No previous significant past medical history was noted. On initial examination, she had right lower limb weakness in the L2/3 myotomes, but intact distally. Bilateral hyperreflexia with upgoing plantar reflexes. No bowel or bladder disturbance initially. She proceeded to MRI of whole spine. This demonstrated extensive multilevel spondylodiscitis with multiple abscesses. There was almost complete destruction of the T5 vertebrae with associated kyphosis. There was a collection at the T4-6 level with cord compression. A similar picture was evident around T12

Fig. 7.30 Post-operative MRI imaging showing cord signal change
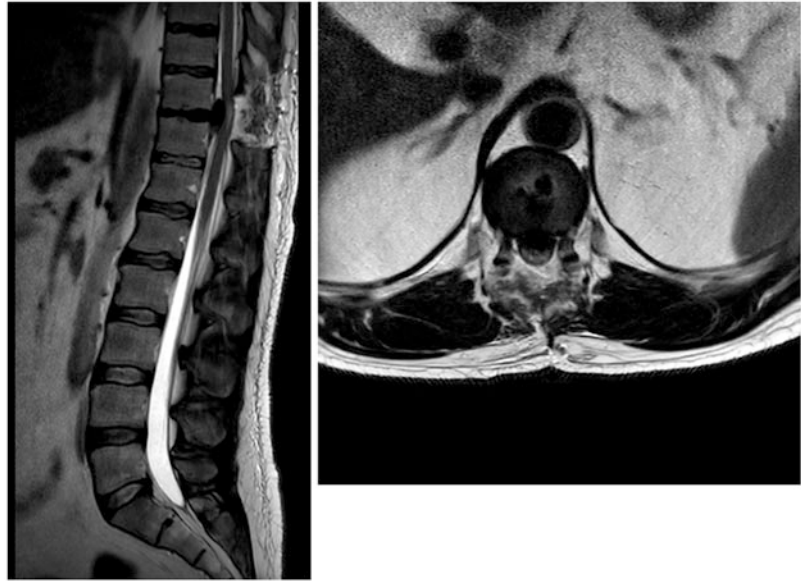
and L3/4 with bony destruction and ring enhancing collections (Fig. 7.34).

Following MRI, the likely diagnosis was felt to be tuberculous spondylodiscitis with abscess formation. The patient was immediately commenced on an antimicrobial regime to treat TB and transferred to the spinal unit for intervention.

Fig. 7.31 Intraoperative imaging demonstrating thoracic cage

Following transfer, the patient developed rapid, progressive deterioration, with complete paralysis of the lower limb. Her sensory level was at T7. Her power was 2/5 bilaterally in L2-4 and 1/5 in L5-S1. She had been in urinary retention and was catheterised. She proceeded to theatre for posterior decompression and stabilisation T2 to L2 (Fig. 7.35). Such a significant stabilisation was required due to the significant bony destruction and compression of the spinal cord. A large volume of pus was evacuated and these samples confirmed the diagnosis of TB. Overall spinal alignment was considerably improved with the correction of the previous kyphosis.

Post-operatively she remained systemically well. She had extensive input from infectious diseases, who monitored her TB therapy. She completed a period of rehabilitation in the spinal injuries unit where some improvements were made. She was continent of bowel and bladder. She was able to mobilise short distances with a rollator as power improved.

This patient had extremely extensive tuberculous spondylodiscitis on initial imaging. She had a very successful decompression with copious pus drained and a stable fixation performed. This highlights TB as a highly aggressive

Fig. 7.32 Post-operative sagittal and axial MRI 1 week following surgery

Fig. 7.33 Final post-operative AP and lateral radiographs
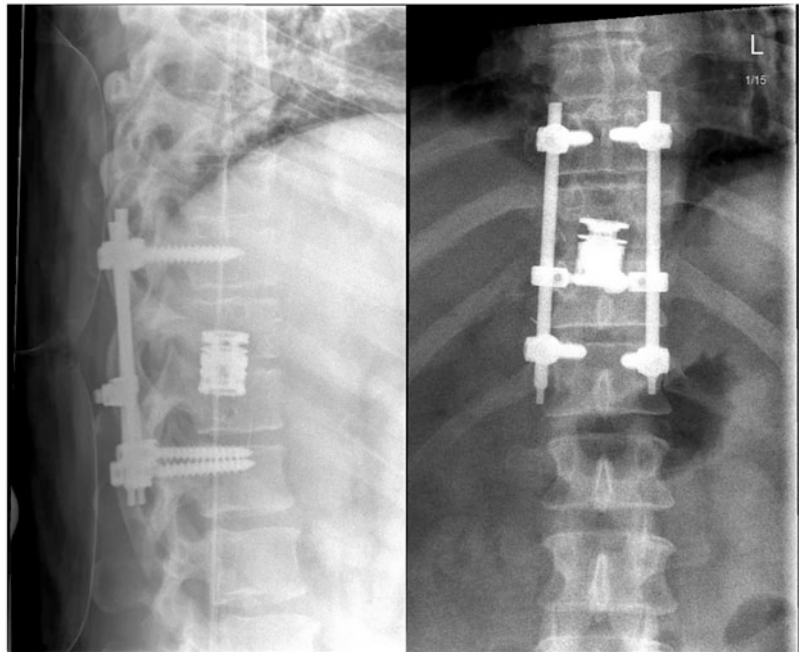
pathogen, and an important one to consider. This was a complex case which required input from the whole multidisciplinary team, including spinal surgeons, infectious diseases physicians and the specialist rehabilitation team. This case highlights the need for emergency surgical decompression with neurological compromise, as this patient had complete lower limb paralysis pre-operatively and is now able to mobilise.

Fig. 7.34 Initial Whole Spine MRI Sagittal and axial cut at T12
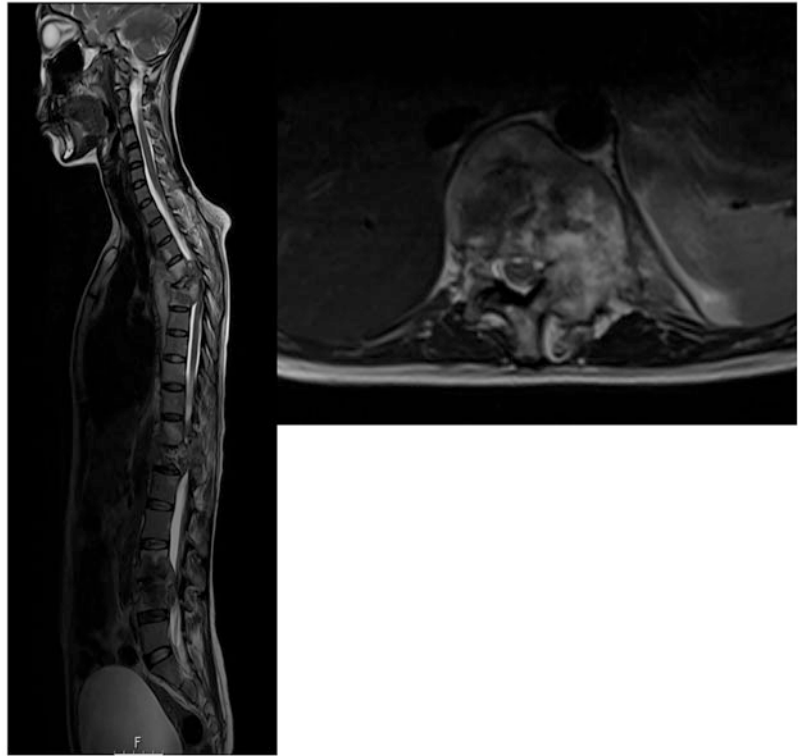
Fig. 7.35 Post-operative AP and lateral radiographs
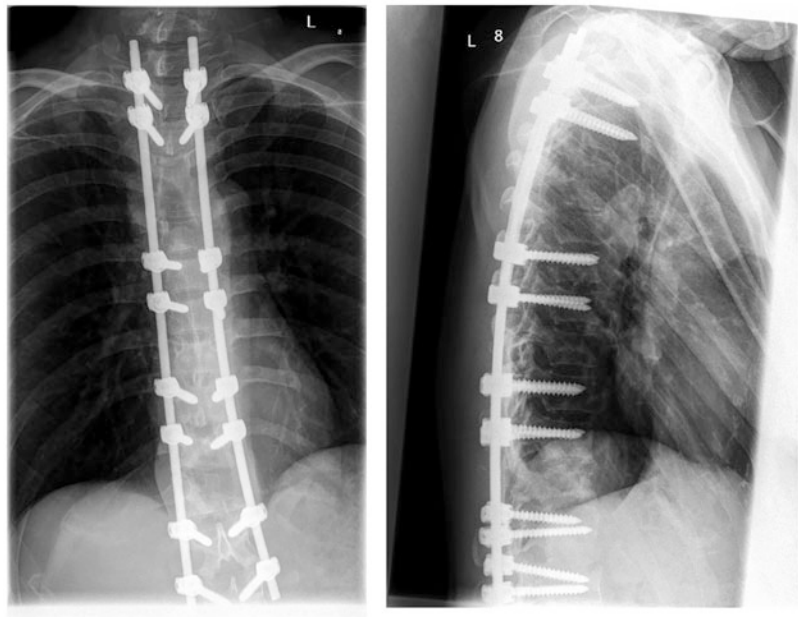
7.11   Conclusion

Visualisation of the human spine allows us to better understand and manage patients with spinal pathology. In this chapter, basic visualisation techniques were discussed including plain radiographs, as well as more modern and complex modalities such as the MRI advance of zero ET and intraoperative CT using the O-arm. A sound knowledge of anatomy and spinal biomechanics is vital to truly comprehend the 3D spine, and this chapter discusses the basic aspects of these. 3D printing can be used to enhance spinal surgery in many ways, including improved pre-operative planning, use in intraoperative templating and for improved surgical education. Navigation and robotic surgery allow surgeons to visualise the human spine in real-time 3D, therefore allowing improved screw positioning and intraoperative feedback. This development of human–computer interaction has allowed higher levels of surgical accuracy, and therefore overall improved surgical outcomes. There is a continuous development of new technologies, such as robotics and virtual reality, which will only improve patient care in the future.

References

Alluri RK, Sivaganesan A, Vaishnav AS, Qureshi SA (2021) Robotic guided minimally invasive spine surgery. Minimally invasive spinal fusion. IntechOpen, London

Baumrind S (2011) The road to three-dimensional imaging in orthodontics. Seminars in orthodontics. Elsevier, New York, pp 2–12

Berger A (2002) Magnetic resonance imaging. BMJ 324: 35

Biswas D, Bible JE, Whang PG, Simpson AK, Grauer JN (2008) Sterility of C-arm fluoroscopy during spinal surgery. Spine 33:1913–1917

Cawley D, Dhokia R, Sales J, Darwish N, Molloy S (2020) Ten techniques for improving navigated spinal surgery. Bone Joint J 102:371–375

Coley BD (2013) Caffey's pediatric diagnostic imaging e-book. Elsevier Health Sciences, New York

Dasarju VK, Sree S, Kikkeri MS, Shireesha B, Pallavi N, Kumar CS (2020) Magnetic resonance imaging in spinal tumors, vol 5. IJCMSR

Denis F (1983) The three column spine and its significance in the classification of acute thoracolumbar spinal injuries. Spine 8:817–831

Garroway AN, Grannell PK, Mansfield P (1974) Image formation in NMR by a selective irradiative process. J Phys C Solid State Phys 7:L457

Giunta CJ, Mainz VV (2020) Discovery of nuclear magnetic resonance: Rabi, Purcell, and Bloch. Pioneers of magnetic resonance. ACS Publications, Washington, DC

Holdsworth F (1963) Fractures, dislocations, and fracture-dislocations of the spine. J Bone Joint Surg Am 45:6–20

Holly LT, Kelly DF, Counelis GJ, Blinman T, McArthur DL, Cryer HG (2002) Cervical spine trauma associated with moderate and severe head injury: incidence, risk factors, and injury characteristics. J Neurosurg 96:285–291

Hounsfield GN (1980) Computed medical imaging. Science 210:22–28

Hull CW (1986) Apparatus for production of three-dimensional objects by stereolithography. Google Patents

Jimenez RR, Deguzman MA, Shiran S, Karrellas A, Lorenzo RL (2008) CT versus plain radiographs for evaluation of c-spine injury in young children: do benefits outweigh risks? Pediatr Radiol 38:635–644

Kamalian S, Lev MH, Gupta R (2016) Chapter 1 - Computed tomography imaging and angiography – principles. In: Masdeu JC, González RG (eds) Handbook of clinical neurology. Elsevier, New York

Kelley SP, Ashford RU, Rao AS, Dickson RA (2007) Primary bone tumours of the spine: a 42-year survey from the Leeds regional Bone Tumour Registry. Eur Spine J 16:405–409

Khanna AR, Yanamadala V, Coumans JV (2016) Effect of intraoperative navigation on operative time in 1-level lumbar fusion surgery. J Clin Neurosci 32:72–76

Kumagai G, Wada K, Tanaka S, Asari T, Nitobe Y, Ishibashi Y (2022) Association between intraoperative computed tomography navigation system and incidence of surgical site infection in patients with spinal surgeries: a retrospective analysis. J Orthop Surg Res 17:52

Lauterbur PC (1973) Image formation by induced local interactions: examples employing nuclear magnetic resonance. Nature 242:190–191

Ljungberg E, Damestani NL, Wood TC, Lythgoe DJ, Zelaya F, Williams SCR, Solana AB, Barker GJ, Wiesinger F (2021) Silent zero TE MR neuroimaging: current state-of-the-art and future directions. Prog Nucl Magn Reson Spectrosc 123:73–93

Lukasiewicz AM, Bohl DD, Varthi AG, Basques BA, Webb ML, Samuel AM, Grauer JN (2016) Spinal fracture in patients with ankylosing spondylitis: cohort definition, distribution of injuries, and hospital outcomes. Spine (Phila Pa 1976) 41:191–196

Maier A, Steidl S, Christlein V, Hornegger J (2018) Medical imaging systems: an introductory guide. Springer, New York

NICE, National Institute for Health and Care Excellence (2008) Metastatic spinal cord compression in adults: risk assessment, diagnosis and management. Clinical guideline [CG75]

NICE, National Institute for Health and Care Excellence (2014) Head injury quality standard [QS74]

Nolte LP, Visarius H, Arm E, Langlotz F, Schwarzenbach O, Zamorano L (1995) Computer-aided fixation of spinal implants. J Image Guid Surg 1:88–93

Ojodu I, Ogunsemoyin A, Hopp S, Pohlemann T, Ige O, Akinola O (2018) C-arm fluoroscopy in orthopaedic surgical practice. Eur J Orthop Surg Traumatol 28: 1563–1568

Pally E, Kreder HJ (2013) Survey of terminology used for the intraoperative direction of C-arm fluoroscopy. Can J Surg 56:109

Patel A, James S, Davies A, Botchu R (2015) Spinal imaging update: an introduction to techniques for advanced MRI. Bone Joint J 97:1683–1692

Rontgen WC (1896) On a new kind of rays. Nature 53: 274–276

Röntgen WC (1896) On a new kind of rays. Science 3: 227–231

SBNS (2018) Standards of care for investigation and management of cauda equina syndrome

Sheha ED, Gandhi SD, Colman MW (2019) 3D printing in spine surgery. Ann Transl Med 7

Stimson LA (1899) A practical treatise on fractures and dislocations. Lea & Febiger

Svensson H, Olofsson E, Karlsson J, Hansson T, Olsson L-E (2016) A painful, never ending story: older women's experiences of living with an osteoporotic vertebral compression fracture. Osteoporos Int 27: 1729–1736

Tang J, Zhu Z, Sui T, Kong D, Cao X (2014) Position and complications of pedicle screw insertion with or without image-navigation techniques in the thoracolumbar spine: a meta-analysis of comparative studies. J Biomed Res 28:228–239

Vu C, Gendelberg D (2020) Classifications in brief: AO thoracolumbar classification system. Clin Orthop Relat Res 478:434

Winans J (2018) Melville's Dr. Raymond Damadian, Father of the MRI. Long Island Press [Online]. https://www.longislandpress.com/2018/01/08/melvilles-dr-raymond-damadian-father-of-the-mri/

Young IR (2004) Significant events in the development of MRI. J Magn Reson Imaging 20:183–186

Part III

Anatomy Education

Visualization in Anatomy Education

8

Apurba Patra, Nagavalli Basavanna Pushpa,
and Kumar Satish Ravi

Abstract

In the post-pandemic era, one of the significant challenges for anatomy teachers is to reciprocate the experience of practical exposure while teaching the subject to undergraduates. These challenges span from conducting cadaveric dissections to handling real human bones, museum specimens, and tissue sections in the histology lab. Such exposures help the instructors to develop interactive communication with their fellow students and thus help to enhance communication skills among them. Recently, anatomy teachers all over the world started using cutting-edge educational technologies to make teaching-learning experiences for students more engaging, interesting, and interactive. Utilizing such cutting-edge educational technologies was an "option" prior to the pandemic, but the pandemic has significantly altered the situation. What was previously an "option" is now a "compulsion." Despite the fact that the majority of medical schools have resumed their regular on-campus classes, body donation and the availability of cadavers remain extremely limited, resulting in a deadlock. Anatomy teachers must incorporate cutting-edge educational technologies into their teaching and learning activities to make the subject more visual. In this chapter, we have attempted to discuss various new technologies which can provide a near-realistic perception of anatomical structures as a complementary tool for dissection/cadaver, various visualization techniques currently available and explore their importance as a pedagogic alternative in learning anatomy. We also discussed the recent advancement in visualization techniques and the pros and cons of technology-based visualization. This chapter identifies the limitations of technology-based visualization as a supplement and discusses effective utilization as an adjunct to the conventional pedagogical approaches to undergraduate anatomy education.

A. Patra
Department of Anatomy, All India Institute of Medical Sciences, Bathinda, Bathinda, Punjab, India

N. B. Pushpa
Department of Anatomy, JSS Medical College, JSSAHER, Mysore, Karnataka, India

K. S. Ravi (✉)
Department of Anatomy, All India Institute of Medical Sciences, Rishikesh, Rishikesh, Uttarakhand, India

8.1 Introduction

Human anatomy is a fundamental subject in medical education. A basic understanding of the bodily structure and architecture of humans is a

must to become a competent physician. Furthermore, sound knowledge of regional anatomy is necessary to know the disease process, gain surgical skills and interpret radiological imaging. Learning anatomy entails the study of body tissue and organ system and appreciating their 3D orientation (Basavanna et al. 2022). Although the learning modality (visual, auditory, reading, and kinaesthetic) preference of the student has to be considered while delivering the concepts, it is not a hard and fast rule to stick to it. Moreover, anatomy learning is not limited to understanding the 3D orientation of the organ system but also understanding the complex dynamics of development, the microstructure of tissues, and analyzing and interpreting radiology images (Hall 2016). The potential to interpret 3D anatomical features in 2D cross-sectional text or pictures can be troublesome for undergraduate students (Keenan and Ben Awadh 2019).

Presently, the main impetus behind incorporating technology-based learning in the ongoing curriculum is to enhance undergraduate medical students' learning of clinically oriented anatomy, improvement in skill coordination, team training, and enhancement of perceptual variation (Guze 2015). Here, we will describe various visualization techniques currently available and explore their importance as a pedagogic alternative in learning anatomy. Following this, we will discuss the recent advancement in visualization techniques. Lastly, we wish to briefly debate the merits and demerits of technology-based visualization and identify their limitations as a supplement and effective tool to utilize as an adjunct to the conventional pedagogical approaches to undergraduate anatomy education.

8.1.1 Changing Scenario in Anatomy Education

For decades, anatomy has been taught and learned through lectures and textbooks with 2D or line diagrams. Cadaveric dissection is the most admired and widespread way of studying anatomy, which enables us to visualize structures in their three-dimensional form with spatial

relationships. Many studies have concluded that cadaveric dissection is the only 3D experience students receive in their anatomy learning. The limited exposure to 3D learning increases the cognitive burden on students since they struggle to translate the 2D experience into a 3D experience (Guillot et al. 2007). Also, observation and visualization are essential components of learning anatomy (Jasani and Saks 2013). Not only gross anatomy but understanding developmental anatomy/embryology and complex dynamics is difficult with available handmade models (Ruiz et al. 2009). Over recent years, anatomy teaching has been moving from conventional cadaver dissection to virtual cadavers, 3D printed specimens, and computed 3D body systems (Sharma and Kumar 2021). The virtual dissection table utilizes simulation technology to offer a realistic 3D visualization of the anatomical details of a virtual cadaver. The most significant advantage of a virtual cadaver is that students can "do-redo-repeat" dissection. This can significantly aid most medical schools which do not have access to donors due to the pandemic, and virtual dissectors can help to compensate for the deficit (Ravi 2020). Most medical schools, which used almost no technology-based medical education applications in the pre-pandemic era, are now widely adopting these tools to effectively deliver anatomy knowledge.

8.1.2 Traditional 3D Visualization in Anatomy and Its Limitations

The effectiveness and applicability of teaching depends on the optimal availability of study material. In traditional pedagogy, cadaver dissections, real bones, skeletons, museum specimens, and handmade clay models have always remained the primary sources of learning 3D anatomy. Although all of these modalities are proven ways of learning anatomy, they have their own limitations. The lack of cadavers and the ethics associated with their acquisition discourage the administration of some medical schools from continuing with cadaveric dissection. Very recently, the pandemic has shown us how

important it is for medical schools to be prepared with suitable alternatives. Real human bones and articulated skeletons are a good resource for studying musculoskeletal anatomy and their spatial relationships, but less availability and enormous cost make their acquisition problematic. An essential part of teaching anatomy is the use of high-quality human anatomical specimens that can demonstrate the topographical relationships of individual anatomical structures. However, long-term use of these real human specimens leads to their degradation, which reduces the quality of teaching. Handmade clay models depicting different stages of human development are also a very good resource for understanding the dynamic events of embryogenesis. However, the production of these models requires human precision, and their fragility also leads to degradation, limiting the quality of teaching. Students also use anatomical literature, scripts, illustrations, and atlases. However, anatomical atlases, which are indispensable in learning anatomy, are quite expensive for students. This accounts for the emerging use of 3D interactive anatomy models as significant alternative study tools for students. These tools help them to correctly interrogate and understand the really intricate topographical and functional relationships of anatomical structures (Brazina et al. 2014). It is indeed of great concern that students have opined that they have acquired a lack of knowledge of anatomy despite having good quality specimens supported by various teaching methods (Dev et al. 2002; Basavanna et al. 2022).

8.2 Potential Technological Tools of Visualization in the Teaching of Anatomy

With this background, we would like to present possible solutions for supporting education through various interactive applications. In particular, newer applications such as 3D printing, computerized learning management systems (LMS), virtual classrooms, artificial intelligence, cloud technology, virtual dissection, simulation,

radiological imaging, immersive technology, web-based learning, and interactive 3D computer graphics, etc. (Owolabi and Bekele 2021). The 3D approach provides students with an advanced way to work with scanned images of human tissues and organs using 3D computer simulation. Interactive 3D models were developed with the appropriate modeling tool for research purposes. Typically, this period is a transition to a visualization and simulation environment created to solve a specific problem or cope with the global learning environment of current 3D visual tools (Fig. 8.1).

8.2.1 3D Printing in Anatomy

Three-dimensional printing is a technique of creating a physical object using a 3D computer model. Here, printed materials are layered on top of each other using computer control to produce an object/pattern that matches the real thing. Figure 8.2 represents a flow chart showing the methodology of developing 3D printed models from a patient CT/MRI. It is another newer modality to create a 3D model of dissected specimens so that the complex architecture of any tissue can be made accessible to students in a more comprehensive way. 3D printing is an impressive tool for creating synthetic models of organs and structures. It is possible to create models that students can explore, interact with, and learn from in a group. 3D printing is very useful for both visual and kinaesthetic learners. It can reduce the time spent on planning and designing models (Abou Hashem et al. 2015; Sharma and Kumar 2021). Other advantages include user-friendly or easy creation of geometric parts with added complexity, replication of models in large numbers or easy prototyping, cost-effectiveness (no molds required), fully customizable, creation of parts with specific properties, accuracy (computer-aided design), no-use of formalin, no human or animal tissues are used, so there are no ethical concerns. Apart from that, creating models with anomalies to arouse interest in applied anatomy and clinical cases (Ye et al. 2020). There were also several disadvantages, including
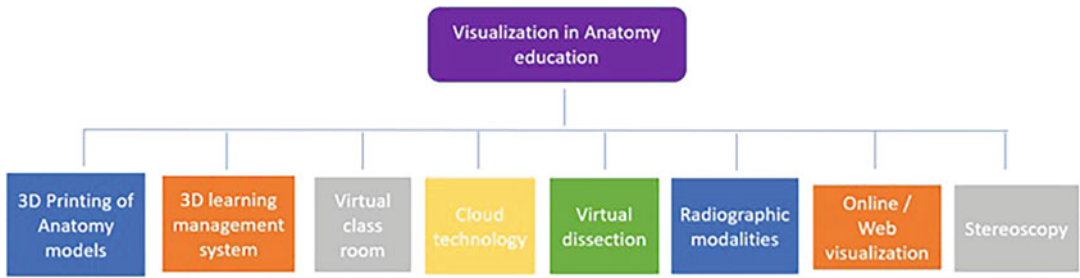
Fig. 8.1 Represents a flow chart listing newer tools/techniques for visualization in anatomy other than cadaveric dissection

fragility as the parts are assembled layer over layer, which decreases the strength by 10–50%, more cost at high volume, post-processing requirements such as grinding or smoothing to create the desired finish, and heat treatment to achieve specific material properties or final processing.

Role of 3D Printing Anatomy Teaching

Amongst the various teaching aids available, dissection is the elite and most effective teaching mode. The unavailability of cadaver dissection has resulted in hindrances in anatomy education for students (Kerby et al. 2011). The complex architecture of organs (liver) or small bones (ear ossicles) may not be clearly visible during dissection, and students might find difficulty understanding them. 3D printed models of such structures can be of great help. The complex architecture of extraocular muscles with respect to the eyeball is quite difficult to understand for medical students; hence a 3D printed model of such a structure aids students in understanding the system effectively (Fig. 8.3). Moreover, 3DP of organs/bones is a cost-effective way that provides a haptic study for better understanding (Kong et al. 2016).

3D printed models of the skull, transverse sections of the brain, orbital anatomy, and cardiovascular development (Fig. 8.3) can be used to teach complex anatomy of difficult regions and different surgical procedures pertaining to these

Fig. 8.2 Flow chart showing the methodology of developing 3D printed models from Patient CT/MRI
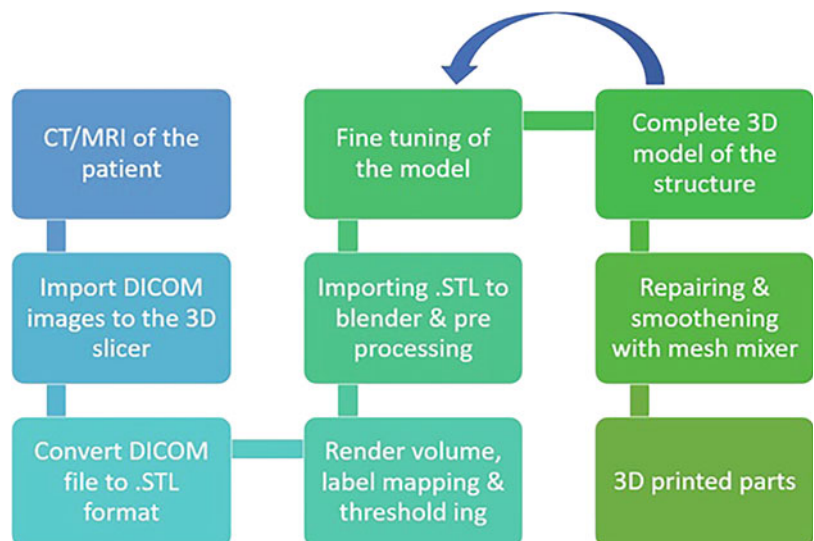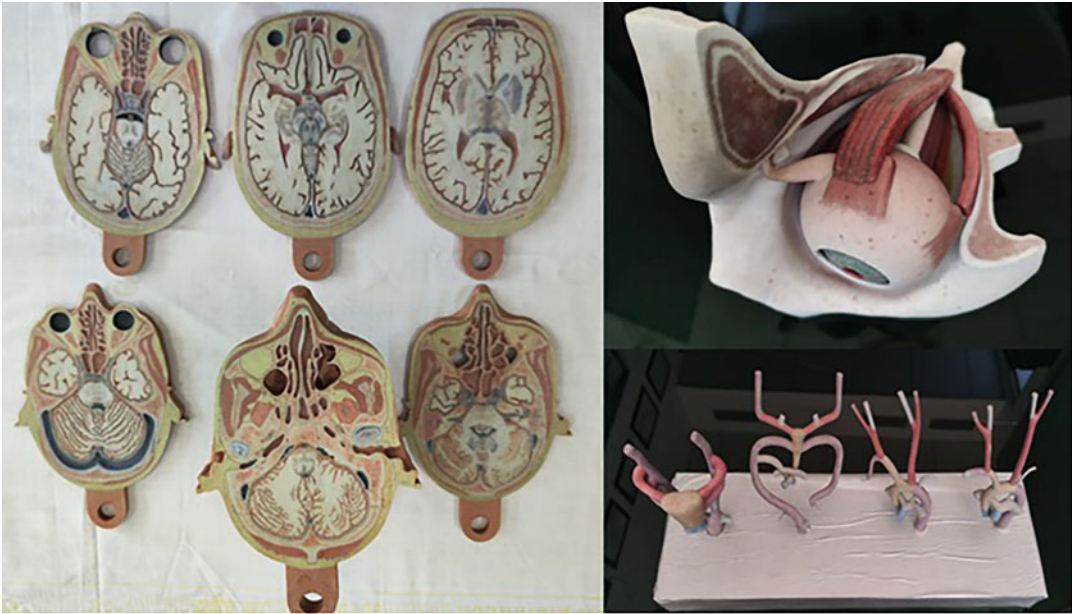
Fig. 8.3 3D printing models of different organs (owned by authors for copyright)

regions. Mainly related to the heart, cardiovascular 3D printing augments the diagnostic work-up of complex congenital heart defects and assists in planning surgical and interventional procedures.

8.2.2 3D Learning Management System

Currently, LMS offers limited access for teachers and students to design teaching and learning activities based on experience and collaboration. Integrating two environments (LMS and 3D) is not the only method to improve learning; this combination can enhance students' independent learning skills (Yasar and Adiguzel 2010). 3D LMS Software provides students with interactive anatomy resources. This software enables users with an interactive way to visualize, appreciate, dissect, and study real-life examples of human anatomy on their computer screens. Below we explain the student and Instructor's 3D views.

Student view:

Students can download the 3D anatomy software directly to their PC/laptop and access 3D anatomy resources anytime, anywhere. 3D

Anatomical Visualization uses CT/MRI scans from real patients to develop interactive 3D visualizations that depict realistic patient anatomy. The screen's pan and zoom provisions allow students to visualize and study any anatomical structures with their 3D spatial relationships. Students can peel back layers of tissue and explore through tissue and color modes to appreciate and learn each structure in 3D.

Instructors' View:

With the help of interactive 3D visualizations, teachers can enhance less engaging lecture materials to make them more interesting so that students can better understand anatomical concepts before entering the dissection lab. Instructor features in 3D anatomy software make it easy to develop engaging and real anatomical material for the lecture. For example, using an online portal, instructors can easily assign quizzes and homework to the students and track their performance with automated grading. 3D visualization scans reconstructed from real CT/MRI scans can aid in student interaction, dissection, and teaching. In addition, teachers can mark and annotate specific anatomical structures/including

additional content such as images or text from the reading material.

The multimodal role of 3D LMS in the transformation of anatomy education:

3D LMS has enormous potential to make anatomy visible. For this, we need to incorporate and implement it in the ongoing curriculum using three formats as suggested below:

Inside the lecture hall: Learning objectives and course materials can be presented to students with the help of the lecturer's version of the software. Depending on instructor preference, this can be completed before the session and incorporated into PowerPoint videos/slides or demonstrated live in front of students with a multimedia projector.

Inside the Dissection Lab: Students can work individually/in small groups to complete the virtual dissection, which is part of the active learning modules. Every lab module could include step-by-step instructions for the students to complete a virtual autopsy.

At Home: Students can be assigned homework and apply their classroom and lab knowledge to answer interactive quizzes provided in the assessment modules. In addition, several educational programs provide ungraded review modules to help students prepare for exams.

3D LMS provides a new range of learning opportunities. The nature of the environment provided is generative, enabling users to explore and interact with an already existing 3D environment and extend that experience by creating their own study materials (Kluge and Riley 2008).

Elsevier's Complete 3D Anatomy tutorial was one of the tools which helped teach anatomy during the pandemic. The software has voice recording features that allow video creation using dynamic 3D representations to design video lectures linked to a learning management system (LMS) or directly through the software platform. In addition, this 3D software also offers a kinesthetic advantage based on the VARK learning theory (Othmana and Amiruddinb 2010; Bhagat et al. 2015; Mozaffari et al. 2020).

8.2.3 Virtual Classroom

A virtual classroom (VC) is a video conferencing tool in which instructors/teachers and participants engage using learning material. The difference between VC and other video conferencing tools is that VCs provide add-on features necessary for a learning environment. This platform aids in making learning an interactive and engaging process in a controlled environment that goes beyond the classroom. Instructors can access the classroom prior to the session to prepare study material. This study content, as well as the recording of the session, is available after the class for reference by both instructors and participants. Participants can join the virtual classroom platforms using any device with an internet connection. This type of flexibility allows participants to learn the content anywhere in the world. Another great benefit of a virtual classroom is that it makes it easy to track student progress. Instructors can collect data such as class attendance and student activity. They can track participant progress through online surveys and analytics, identify areas of difficulty, and use visual tools to facilitate learning challenges for participants. Finally, many virtual classroom platforms can be integrated into an institution's existing Learning Management System (LMS). Advanced platforms aid Learning Tools Interoperability (LTI) so that the virtual classroom system and LMS can communicate with each other, making the whole perspective more effective. Current techniques such as smart boards to draw diagrams, video presentations with hyperlinks (Osmosis videos (Haynes et al. 2014; Guven et al. 2020) and ScholarRx videos (Le and Prober 2018)) may be incorporated through a learning management system (LMS), and 3D images are more attractive and make students active. The LMS provides its students with lecture broadcasts, allowing them to visit a "virtual classroom" anywhere, anytime, and track student activities, progress, and compliance (Owolabi and Bekele 2021). These information technologies are even more important to complete the Anatomy E-book curriculum on smartphones,

laptops, or tablets; they are easily accessible "mobile libraries" that allow students to consult them even between lectures.

8.2.4 Cloud Technology/Educational Videos

Cloud technology (CT) in medical education treats students and administrators equally. CT allows students to access homework anywhere with internet access, allows teachers to upload learning materials instantly, and to collaborate with each other easily, saving money on data storage. It gives students the opportunity to live chat and share knowledge on a specific topic and, therefore, can be used in a new educational model. In this technique, students watch the lecture in advance, and this allows for more detailed and engaging discussions during class. Additionally, group work and analytical activities can take place in the classroom. The flipped classroom helps improve learning outcomes, not only in terms of student performance but also in internalizing information for better results (Hurtubise et al. 2015; Hew and Lo 2018).

CT-based tools have been gaining popularity over the decades, but the pandemic has caused a paradigm shift in its current acceptability as a visualization technique in the teaching of anatomy. Technologies based on CT are one of the demanding and actively developing areas of the world of modern information technology. In the educational process, the use of CT is becoming more popular and opens up many opportunities for students, teachers, and educational institutions. Below are the main domains of cloud technology in teaching anatomy:

Nowadays, mobile devices dominate the technology world and have become an essential tool in learning. Running a full-scale 3D human body directly from a smartphone or tablet for learning purposes, hospital practice and even for direct guidance of medical procedures would become a trivial method. However, it is still quite tricky due to software and hardware (Gopalakrishnakone et al. 2010).

Online Cloud-Based Mobile Enabled 3D Human Body E-Learning Solution:

This is a platform that can render a complex 3D human body using the power of cloud computing environments. The model uses adaptive technologies to display dynamic 3D content on any kind of modern device, from tablets to smartphones and notebooks. The atlas contains a detailed and accurate representation of the human anatomy and an interesting, unique feature: real-time modification of body parts directly related to an associated disease.

Cloud computing environment: The functionalities of this E-learning solution is achieved by using the latest technologies for advanced browser-based 3D modeling (for a precise view of the components of the human body) combined with the outstanding power of Windows Azure cloud computing services to ensure prompt and efficient interaction through the application.

The most important aspect of this technology is Blob Storage. After exporting and adding the parts of the body to the app (3D models), each part is converted into a blob, each containing a small piece of the human body. This technique gets benefitted from CDN (Content Delivery Network), which allows the data to be sent from multiple locations or the closest and most reliable location to the user.

Since the system is cloud-based, it has "unlimited" processing power. This feature not only helps to convert the 3D object into a blob and vice-versa but also does a small pre-processing phase by converting the classic 3D object to WebGL (Web Graphics Library) 3D object server side so that a lot of the processing power is moved from client side to server side, which allows the models to be seen on low-performance devices.

Another important aspect that makes this E-learning unique is the usage of object-oriented databases. This way, the user can get benefitted from the elasticity of cloud-based databases to map all the 3D features (color, size, neighbors, status, etc.). Mapping can be done not just inside 3D objects themselves but directly into a database and from there to the app. So, whenever any editing is done to a 3D object feature, it will

also be stored in the database. They are not editing the object itself but only changing the info in the database (Butean et al. 2014).

The SaaS (Software as a service) model is considered one of the biggest advantages of cloud-based computing. It is common for software applications to be available to students for a low fee or for free, making education accessible to most students. Textbooks recommended by universities are often expensive and sometimes outpace another element of medical education, including tuition. As a result, many students refrain from purchasing them. Cloud-based textbooks are one solution to this problem. Digital books are usually cheaper; thus, students with lower incomes can gain access to high-quality education. The implementation of cloud technologies removes the financial inequalities between students who may exist in the same educational environment.

Cloud technologies make learning a simple and fun experience for participants on both sides of the learning process. Recently, during the COVID pandemic, students and teachers have gained access to this technology for seamless continuation of anatomy and other curricula and have greatly appreciated its easy accessibility, time and money savings, instant feedback, valuable information, and inexpensive textbooks.

8.2.5 Virtual Dissection

Over the past decade, the teaching of anatomy has gradually shifted from wet lab to virtual dissection, pre-dissected and plasticized specimens, and virtual 3D body systems. The virtual dissection table utilizes simulation technology to deliver a realistic visualization of the 3D anatomical details of a virtual cadaver. Unlike cadavers, students can "do-return-repeat" dissection multiple times. The Synchronized Multiple Visualizer System is software for teaching anatomy and physiology, including certain aspects of histology, comparative anatomy, embryology, and pathology (Owolabi and Bekele 2021). The virtual dissection table is a commercial product of Anatomage (a USA-based company) (Fig. 8.4). This virtual

cadaver table can serve different purposes based on the student's needs and the user's expertise. These uses may include virtual dissection, virtual 3D atlas, teaching aids, and virtual simulators of human body anatomy and functions (García et al. 2018).

8.2.6 Radiographic Modalities

The use of visualization technologies in the teaching of anatomy should not be restricted to the mere demonstration of anatomical images for a more detailed, interactive, or accessible format (Bajka 2004). Identification of anatomical structures in clinical images is a professional requirement for disease diagnosis and treatment. Thus, the use of imaging in the medical curriculum should also focus on preparing future doctors to use these technologies appropriately in their future practice. In this regard, an effective approach to integrating radiology teaching into anatomy teaching can be aided by the use of technology-assisted visualization (Webb 2013).

Computed tomography (CT) and magnetic resonance imaging (MRI) are used extensively in the majority of anatomy courses to understand better the various clinical conditions discussed in anatomy sessions (Mavrych 2016). Recently, medical technology has provided synthetic cadavers with organs equipped with an ultrasound probe inside for better visualization. The use of endoscopy and colonoscopy to visualize the internal anatomy of the intestine can make the topic particularly interesting and engaging for students (Patra et al. 2022).

8.2.7 Online or Web Screen Visualization

Distance online learning and portable networking devices are becoming an essential component of the learning environment in anatomy education, impacting the design and reshaping of the anatomy curriculum. Some lectures are delivered online through systems such as Zoom meetings, Go - to the webinar, Google classrooms or

Fig. 8.4 Anatomy Professor teaching students using virtual dissection table (this is from our medical school, copyright owned by us and permission obtained from students)

Microsoft Teams, etc. These new communication and information modalities can be used to improve teaching and learning experiences. They have the ability to facilitate student learning and problem-solving potential, allowing for better integration of the didactic classroom experience and smoother clinical practice. Technologies can merge a large amount of factual information in digitized form to make conventional didactic lectures more interesting (Mavrych 2016).

8.2.8 3D Stereoscopy

Stereoscopy refers to increasing or creating the illusion of depth using binocular vision or a stereoscope. An advanced stereoscope allows viewers to perceive three-dimensional depth in two-dimensional images (Holliman 2005). It

was Daniel John Cunningham, a Scottish anatomist, who first used stereoscopy in the teaching of anatomy. Stereoscopic 3D instructional videos are available and affordable via smartphone, a complementary tool that has proven more beneficial than 2D videos in improving students' knowledge of anatomical relationships and reasoning. The most challenging aspect of learning anatomy is the correlation between the 3D complexity of a structure and its anatomy. This can be better achieved by using 3D videos of autopsies or surgeries. The anatomy of the brain is complicated to learn. As their anatomical structures are numerous and assembled in a complex three-dimensional (3D) architecture, classical schematic drawing or two-dimensional (2D) photography has proven difficult in providing a simple, clear, and accurate message. Advances in photography and computer science

led to the development of stereoscopic 3D visualization, first for entertainment and then for education. Stereoscopic 3D teaching of neuroanatomy has sparked enthusiasm for digital technology among medical students. It could improve their anatomical knowledge and test results, as well as their clinical competence. Depending on the institute's possibilities and the teachers' commitment, this new modality should also be extended to other anatomical disciplines. However, its implantation requires trained faculties and its impact on clinical competence needs to be objectively assessed (Jacquesson et al. 2020). Incorporating 3D videos as supplementary teaching in the curriculum could enhance students' knowledge of anatomical relationships and reasoning. (Bernard et al. 2020).

8.2.9 Interactive 3D Computer Graphics (3DCG) Model

Medical students frequently find it difficult to conceptualize 3D anatomical structures, such as bone alignment, spatial muscle anatomy, and complex movements, from 2D images (Battulga et al. 2012). Although cadaveric dissection allows haptic understanding of 3D anatomical structures, it is expensive and time-consuming (McLachlan and Patten 2006). In addition, the time allocated to complete the anatomy curriculum decreases year by year (Cottam 1999; Drake et al. 2009), leading to increased cognitive load and hindering the learning of anatomy for students with poor spatial skills (Garg et al. 2001; McLachlan et al. 2004; Levinson et al. 2007; Huk 2006). Thus, the current trend is to achieve anatomical understanding in a short period by incorporating innovative educational technologies in anatomical education. Animated and interactive three-dimensional computer graphics (3DCG) models are a relatively new technology that can approximate human anatomy and movement. 3DCG models have shown promise in achieving a spatial understanding of 3D anatomy from 2D images (Fig. 8.5) and text and in overcoming many of these learning tasks. According to Mayer's cognitive theory of multimedia learning, students learn best with both

words and pictures in an electronic learning environment (Mayer 2009). 3DCG visually conveys semi-real information to students, allowing them to easily grasp the content. In addition, the interactive 3DCG content also improves students' cognitive abilities.

Several institutions have developed 3DCG animation and interactive 3DCG (Silén et al. 2008). Kobayashi et al. reported that it was much easier and more accurate to explain the details of surgical procedures using 3DCG animation than 2D illustration (Kobayashi et al. 2006). In addition, methods have been developed to allow users to create highly specialized 3DCG content on the web. The use of 3DCG models has benefits over traditional methods of teaching anatomy; however, their development and adoption are time-consuming. Therefore, new educational methods of teaching information and communication technologies are needed.

8.3 Recent Advances in Visualization

8.3.1 Anatomy Studio

3D reconstruction from anatomical sections allows anatomists to develop 3D representations of real anatomical structures by tracing organs from cryosection sequences. However, conventional user interfaces depend on a single user experience to develop content for educational or training purposes. Anatomy Studio, a mixed reality (MR) tool for virtual dissection through augmented three-dimensional reconstruction (3DR), combines tablet drawing with touch and transparent head-mounted displays with MR-based visualization to perform 3DR of anatomical structures. This is a new interactive technique designed to support spatial understanding and speed up manual segmentation. Using in-air interactions and interactive surfaces, instructors can easily access the cryosection and edit contours while watching other users' contributions. A user study involving experienced instructors and medical professionals conducted in actual working sessions shows that Anatomy

Fig. 8.5 Description of structure and outcome with local coordination (assembled 3DCG animated model from 2D illustrations)
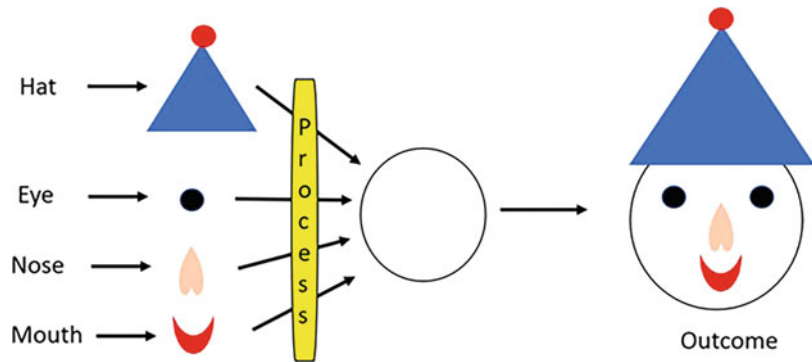
Studio is suitable and beneficial for 3D reconstruction. The results suggest that Anatomy Studio supports close-knit collaboration and group discussion to gain deeper insights. 3D visualization provides enhanced perceptual interaction with Anatomy Studio using in-air gesture collaboration that shows real-time contour changes made by others, thus facilitating communication. The anatomical study includes a drawing table, and the user is equipped with a tablet, a stylus, and a transparent display mounted on the head. Using a hand gesture, the user can build a 3D virtual model on the MR (mixed reality) dissection table (Zorzal et al. 2019).

8.3.2 Artificial Intelligence/Humanoid Robots

Artificial intelligence (AI) refers to the capacity of a computer/robot to perform human-like tasks with respect to cognition (Russell and Norvig 2003). An intelligent system has the best chance of achieving this goal, as it is aware of its surroundings and can act appropriately. This was aptly called as "AI," to describe automated computers that imitate human "cognitive" activities like "learning" and "problem-solving." Our daily lives are surrounded and influenced by a wide range of AI applications, including self-driving cars to humanoid robots, human speech comprehension applications (such as Siri and Alexa), suggestion tools (such as Vimeo, Facebook, and iTunes), sophisticated electronic databases (such as Google), and suggestion tools

(Poole et al. 1998; Asghar et al. 2022). In recent days, the use of Robots to perform different surgeries is becoming popular. Humanoid robots have recently been used as caregivers in many hospitals to protect doctors and nurses from the pandemic. Although many patient care services can be handled by robotics, including screening, disinfection, surgery, telehealth, and logistics, their role in medical education and academia is unclear (Shen et al. 2021; Asghar et al. 2022).

Exemplification and the capacity to integrate social interaction into the learning environment are fundamental qualities of educational robots that guide in viable learning among students. Significant progress has been made in the creation of such a robot with a musculoskeletal system that is comparable to that of a human. Aldebaran Robotics created the autonomous, programmable humanoid robot NAO for use in educational and research settings to map humanoid movement onto a reinforcement learning task (García and Shafie 2020; Asghar et al. 2022) These robots are more beneficial than computer software or other educational aids in many instructional goals because they can mimic human responses (Tuna and Tuna 2019). They are so well-equipped with cutting-edge information and original teaching methods. Humanoid robots can also be trained to know exactly what each student needs to know, which could help with customized instruction. In light of the numerous possibilities that humanoid robots can provide, we have attempted to investigate their current use in education, their potential roles and functions in the

instructional delivery of Anatomy, and the challenges in this domain.

The Role of a Robotic Assistant in the Era of Virtual Anatomy

The conventional, century-old method of teaching and learning anatomy is human cadaveric dissection. If the organ is too small to dissect or difficult to visualize, like the pituitary, prostate, and adrenal glands, it is difficult for the anatomist to reach it. While robotic dissection with expanded vision has enabled the display of intricate anatomical structures. According to Dal Moro (2018), a robotic dissection is a team approach that involves a robotic assistant at the corpse and an anatomist at the console. With a magnified three-dimensional (3D) view and more advanced wrist-hand movements than human assistance, a robotic assistant might, for instance, handle delicate tissue. Using 3D eyeglasses, a 3D view of the dissected can be seen as a byproduct of robotic dissection and with the assistance of a large 3D monitor (Zhang et al. 2019).

Additionally, during the dissection, the clinical or surgical anatomy could be explained. As a result, residents and medical students could benefit greatly from robotic dissection as a teaching tool. Hence robotic dissection could be an effective education program that can be developed and tested. A computer-simulated environment is provided by virtual reality simulators to enhance one's ability to dissect. Computer connections are necessary for both tactile dissection and virtual reality simulators; Consequently, they will continue to grow simultaneously. Students will undoubtedly be able to develop their surgical skills right from the start of their medical training if cadaveric dissection is performed using surgical robots.

8.3.3   High Fidelity Simulation

High Fidelity Simulation uses sophisticated mannequins in simulated patient environments. It is also called a human patient simulator or high-fidelity simulator. This method uses computers to control full-body mannequins that

are programmed to provide realistic physiological responses to student actions. Normally, these mannequins can demonstrate physiological and pathophysiological processes and respond to interventions, making them very useful for teaching complex phenomena and integrating multiple dimensions of basic medical science into individual sessions. For example, mannequins can sleep and wake up, breathe and talk, and are also capable of giving birth, bleeding, and vomiting. They can be utilized to learn and manipulate almost all significant vital and physiological signs such as pulse, heart rate, EKG, and more. All these features allowed students to better present structures, functions, symptoms, and medical skills (Lewis et al. 2012).

8.3.4   Immersion or Haptic Technology

This technology refers to tactile-based feedback technology, where the sense of touch is applied by applying motion to the user's fingertips. Virtual Reality (VR), Augmented Reality (AR), as well as other recent technologies provide a unique scenario (Motaharifar et al. 2021). AR has a variety of approaches for teaching health professionals of all ages. Students of different levels can benefit from computer-generated simulations. With Human–Computer Interface (HCI), students can engage and experience virtual environments. They differ in terms of fidelity, immersion, and interactivity. Immersive high-definition visual inputs create accurate digital representations of the real anatomical structures in virtual reality. Head-mounted displays (VR headsets), motion sensors, controllers, keyboards, and speech recognition software are used to interact with the virtual world. In contrast, AR superimposes computer-generated stimuli on real-world environments/objects, such as computer-generated anatomical structures superimposed on a mannequin (Othmana and Amiruddinb 2010). Alternate reality platforms provide an alternate world where users can engage with the story and influence it by making choices. Participants interact with the virtual
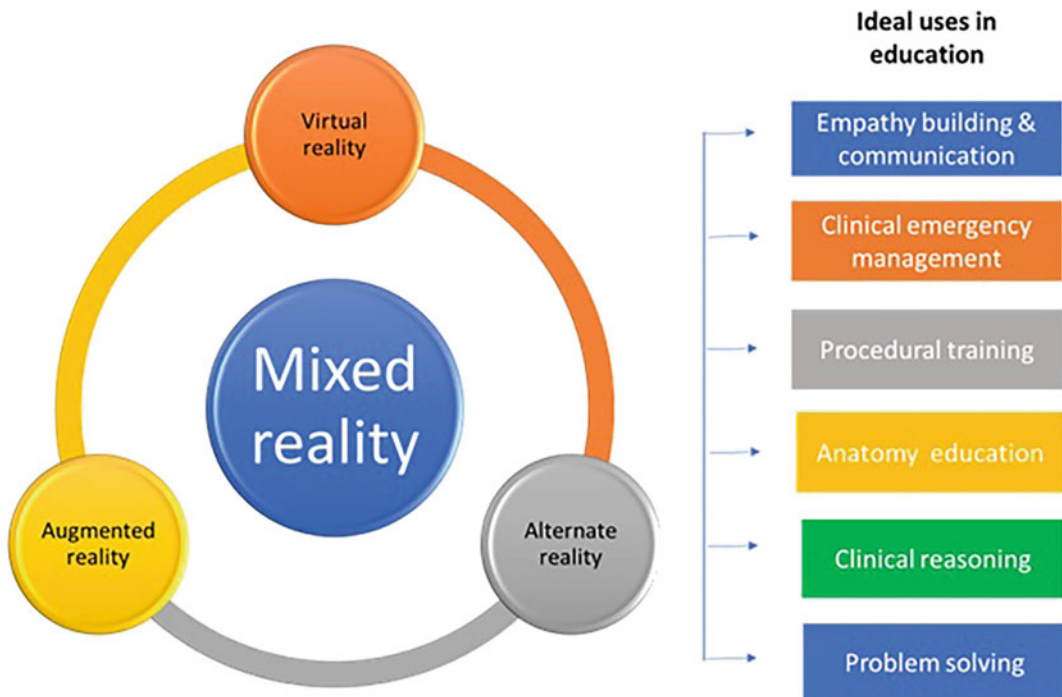
Fig. 8.6 Recent advances in visualization and its possible uses

environment using real-world technology in alternate reality simulations, like interfacing with patient data using electronic health record simulations. Although the forms exist on an overlapping continuum often characterized as "mixed reality," the degree of immersion in the virtual environment distinguishes VR from AR and alternate reality (Fig. 8.6).

8.4   Further Thoughts and Recommendations

8.4.1   Merits and Demerits of Using 3D Visualizations

Undoubtedly, the visualization of anatomy and related basic medical subjects could be improved through strategic adjustments, media, and technology (Owolabi and Bekele 2021). The pandemic provided insight into the advantages and disadvantages of these technologies and innovations. The continued integration of technology into anatomy education is certainly necessary to improve learning outcomes and address the cognitive load related to the volume of anatomy education and training (Gaur et al. 2020). Traditional teaching practice such as cadaver dissection is almost synonymous with teaching anatomy. However, if the lack of corpses continues, it would be impractical to stop or continue teaching anatomy with a limited number of cadavers. Thus, technology remains a reliable way to ensure that students do not suffer from deficiencies. Therefore, judicious use of technology and creative adaptations is necessary to ensure the timely, efficient and effective provision of anatomical education despite the limitations that have developed during or even after the pandemic (Saverino 2020). For example, it is also evident in the United Kingdom that such adjustments are being made with evidence of success (Longhurst et al. 2020).

8.4.2 Limitations

It is essential to note that despite the enormous advantages presented by the adoption of technology that has empowered constant realization, there have been various constraints for the same. These restrictions incorporate unfeasible visual techniques, discriminatory access, cost viability, and absence of preparation among anatomy educators. The objective of all educational innovation or technology is to develop learning further, yet we have shown that adding dynamic simulation affects the people who likely need it most: students with somewhat poor spatial capacity. Bodies provide real-time learning for medical students, while virtual cadavers provide a realistic visualization of 3D anatomical detail. Post-mortem training or procedure imparts in youthful personalities the qualities of empathy, professionalism, ethics, and confidentiality. Learning anatomy through virtual dissection is unrealistic (Basavanna et al. 2022). Accordingly, virtual modalities can be utilized as an adjunct to envision the anatomy of complicated structures (middle ear cavity or ethmoid cavity).

8.5 Concluding Statements/Take-Home Message

Anatomy education and teaching medicine as a profession was never designed to be fully virtual. However, the use of technology-based online pedagogies (3D learning management system, anatomy studio, virtual classroom, medical simulations, virtual cadavers, 3D stereoscopy, etc.) has been proven to play a pivotal role in the successful completion of the Anatomy curriculum. As discussed, there are a plethora of technologies that aid in learning anatomy. Policymakers need to think critically about how to amalgamate medical informatics and conventional pedagogical approach to timely reform anatomy education. Interactive 3D visualization technologies have undoubtedly made the subject of Anatomy extremely visual. Consequently,

anatomy, conventionally a teacher-centric subject, is gradually becoming learner-centric with the use of readily available online pedagogies, and rightly so. There is no harm in using readily available study materials available online, but the content available should not be trusted blindly but rather be cross-checked; this is the role of conventional textbooks and teachers. Last but not the least, we should always remember that the finest way to teach and learn modern Anatomy is by blending conventional pedagogy with multimodal system-based approaches to complement one another.

References

Abou Hashem Y, Dayal M, Savanah S (2015) The application of 3D printing in anatomy education. Med Educ Online 20(1):29847

Asghar A, Patra A, Ravi KS (2022) The potential scope of a humanoid robot in anatomy education: a review of a unique proposal. Surg Radiol Anat 44:1309–1317. https://doi.org/10.1007/s00276-022-03020-8

Bajka M, Manestar M, Hug J, Székely G, Haller U, Groscurth P (2004) Detailed anatomy of the abdomen and pelvis of the visible human female. Clin Anat: Off J Am Assoc Clin Anat Br Assoc Clin Anat 17(3):252–260

Basavanna PN, Ravishankar MV, Arora D (2022) Anatomy lives in the dissection hall: post-Covid-19 perception of students. Anat Sci Educ 15(1):83–85

Battulga B, Konishi T, Tamura Y, Moriguchi H (2012) The effectiveness of an interactive 3-dimensional computer graphics model for medical education. Interact J Med Res 1(2):e2

Bernard F, Richard P, Kahn A, Fournier HD (2020) Does 3D stereoscopy support anatomical education? Surg Radiol Anat 42(7):843–852

Bhagat A, Vyas R, Singh T (2015) Students' awareness of learning styles and their perceptions to a mixed method approach for learning. Int J Appl Basic Med Res 5 (Suppl 1):S58–S65

Brazina D, Fojtik R, Rombova Z (2014) 3D visualization in teaching anatomy. Procedia Soc Behav Sci 143: 367–371

Butean VA, Moldoveanu A, Ovreiu E, Morar A, Egner A (2014) An online cloud based Mobile enabled 3D human body E-learning solution. In The 10th international scientific conference eLearning and software for education, Bucharest

Cottam WW (1999) Adequacy of medical school gross anatomy education as perceived by certain postgraduate residency programs and anatomy course directors. Clin Anat 12(1):55–65

Dal Moro F (2018) How robotic surgery is changing our understanding of anatomy. Arab J Urol 16:297–301

Dev P, Montgomery K, Senger S, Leroy Heinrichs W, Srivastava S, Waldron K (2002) Simulated medical learning environments on the internet. J Am Med Inf Assoc 9:437–447

Drake RL, McBride JM, Lachman N, Pawlina W (2009) Medical education in the anatomical sciences: the winds of change continue to blow. Anat Sci Educ 2(6):253–259

García J, Shafie D (2020) Teaching a humanoid robot to walk faster through safe reinforcement learning. Eng Appl Artif Intell 88:103–160

García MJ, Dankloff MC, Aguado HS (2018) Possibilities for the use of anatomage (the anatomical real body-size table) for teaching and learning anatomy with the students. Biomed J Sci Tech Res 4(4):94

Garg AX, Norman G, Sperotable L (2001) How medical students learn spatial anatomy. Lancet 357(9253):363–364

Gaur U, Majumder MAA, Sa B, Sarkar S, Williams A, Singh K (2020) Challenges and opportunities of pre-clinical medical education: COVID-19 crisis and beyond. SN Compr Clin Med 2020(2):1992–1997

Gopalakrishnakone P, Jianfeng L, Sun GP, Abeykoon Fernando AON, Cheok ADA (2010) Multimodal virtual anatomy learning tool for medical education. In: Entertainment for education, digital techniques and systems LNCS 6249. Springer, Berlin, pp 278–287

Guillot A, Champely S, Batier C, Thiriet P, Collet C (2007) Relationship between spatial abilities, mental rotation and functional anatomy learning. Adv Health Sci Educ 12:491–507

Guven T, Geraci C, Green J (2020) Learning through osmosis: a global Wikipedia editing course for medical students. MedEdPublish 9(1):109

Guze PA (2015) Using technology to meet the challenges of medical education. Trans Am Clin Climatol Assoc 126:260–270

Hall E (2016) The tenacity of learning styles: a response to Lodge, Hansen, and Cottrell. Learn Res Pract 2:18–26

Haynes MR, Gaglani SM, Wilcox MV, Mitchell T, DeLeon V, Goldberg H (2014) Learning through osmosis: a collaborative platform for medical education. Innov Global Med Health Educ 2014(1):2

Hew KF, Lo CK (2018) Flipped classroom improves student learning in health professions education: a meta-analysis. BMC Med Educ 18(1):38

Holliman N (2005) 3D display systems. The handbook of optoelectronics. Institute of Physics Press, London

Huk T (2006) Who benefits from learning with 3D models? The case of spatial ability. J Comput Assist Learn 22:392–404

Hurtubise L, Hall E, Sheridan L, Han H (2015) The flipped classroom in medical education: engaging students to build competency. J Med Educ Curricular Dev 2:35–43

Jacquesson T, Simon E, Dauleac C, Margueron L, Robinson P, Mertens P (2020) Stereoscopic three-dimensional visualization: interest for neuroanatomy teaching in medical school. Surg Radiol Anat 42:719–727. https://doi.org/10.1007/s00276-020-02442-6

Jasani SK, Saks NS (2013) Utilizing visual art to enhance the clinical observation skills of medical students. Med Teach 35:e1327–e1331

Keenan ID, Ben Awadh A (2019) Integrating 3D visualisation technologies in undergraduate anatomy education. Adv Exp Med Biol 1120:39–53

Kerby J, Shukur ZN, Shalhoub J (2011) The relationships between learning outcomes and methods of teaching anatomy as perceived by medical students. Clin Anat 24(4):489–497

Kluge S, Riley L (2008) Teaching in virtual worlds: opportunities and challenges. IISIT 5:127–135

Kobayashi M, Nakajima T, Mori A, Tanaka D, Fujino T, Chiyokura H (2006) Three-dimensional computer graphics for surgical procedure learning: web three-dimensional application for cleft lip repair. Cleft Palate Craniofac J 43(3):266–271

Kong X, Nie L, Zhang H, Wang Z, Ye Q, Tang L, Li J, Huang W (2016) Do three-dimensional visualization and three-dimensional printing improve hepatic segment anatomy teaching? A randomized controlled study. J Surg Educ 73(2):264–269

Le TT, Prober CG (2018) A proposal for a shared medical school curricular ecosystem. Acad Med 2018(93):1125–1128

Levinson AJ, Weaver B, Garside S, McGinn H, Norman GR (2007) Virtual reality and brain anatomy: a randomised trial of e-learning instructional designs. Med Educ 41(5):495–501

Lewis R, Strachan A, Smith MM (2012) Is high fidelity simulation the most effective method for the development of non-technical skills in nursing? A review of the current evidence. Open Nurs J 6:82–89

Longhurst GJ, Stone DM, Dulohery K, Scully D, Campbell T, Smith CF (2020) Strength, weakness, opportunity, threat (SWOT) analysis of the adaptations to anatomical education in the United Kingdom and Republic of Ireland in response to the Covid-19 pandemic. Anat Sci Educ 13(3):301–311

Mavrych V (2016) Modern trends in clinical anatomy teaching. MOJ Anat Physiol 2(1):20–21

Mayer RE (2009) Multimedia learning, 2nd edn. Cambridge University Press, Cambridge

McLachlan JC, Patten D (2006) Anatomy teaching: ghosts of the past, present and future. Med Educ 40(3):243–253

McLachlan JC, Bligh J, Bradley P, Searle J (2004) Teaching anatomy without cadavers. Med Educ 38(4):418–424

Motaharifar M, Norouzzadeh A, Abdi P, Iranfar A, Lotfi F, Moshiri B, Lashay A, Mohammadi SF, Taghirad HD (2021) Applications of haptic technology, virtual reality, and artificial intelligence in medical training during the COVID-19 pandemic. Front Robot AI 8:612949

Mozaffari HR, Janatolmakan M, Sharifi R, Ghandinejad F, Andayeshgar B, Khatony A (2020) The relationship between the VARK learning styles and academic achievement in dental students. Adv Med Educ Pract 11:15–19

Othmana N, Amiruddinb MH (2010) International conference on learner diversity different perspectives of learning styles from VARK model. Procedia Soc Behav Sci 7(C):652–660

Owolabi J, Bekele A (2021) Implementation of innovative educational technologies in teaching of anatomy and basic medical sciences during the COVID-19 pandemic in a developing country: the COVID-19 silver lining? Adv Med Educ Pract 12:619–625

Patra A, Asghar A, Chaudhary P, Ravi KS (2022) Integration of innovative educational technologies in anatomy teaching: new normal in anatomy education. Surg Radiol Anat 44(1):25–32

Poole DL, Mackworth AK, Goebel R (1998) Computational intelligence: a logical approach. Oxford University Press, New York, p 558

Ravi KS (2020) Dead body management in times of Covid-19 and its potential impact on the availability of cadavers for medical education in India. Anat Sci Educ 13(3):316–317

Ruiz JG, Cook DA, Levinson AJ (2009) Computer animations in medical education: a critical literature review. Med Educ 43:838–846

Russell SJ, Norvig P (2003) Artificial intelligence: a modern approach, 2nd edn. Prentice Hall, Upper Saddle River, NJ, p 1080

Saverino D (2020) Teaching anatomy at the time of COVID-19. Clin Anat 23616

Sharma A, Kumar A (2021) Evolving trends in anatomy: a global perspective. Indian J Clin Anat Physiol 8(3): 159–161

Shen Y, Guo D, Long F et al (2021) Robots under COVID-19 pandemic: a comprehensive survey. IEEE Access 9:1590–1615

Silén C, Wirell S, Kvist J, Nylander E, Smedby O (2008) Advanced 3D visualization in student-centred medical education. Med Teach 30(5):e115–e124

Tuna A, Tuna G (2019) The use of humanoid robots with multilingual interaction skills in teaching a foreign language: opportunities, research challenges and future research directions. CEPS J 9:95–115

Webb AL, Choi S (2013) Interactive radiological anatomy eLearning solution for first year medical students: development, integration, and impact on learning. Anat Sci Educ 7(5):350–360. https://doi.org/10.1002/ase.1428

Yasar O, Adiguzel T (2010) A working successor of learning management systems: SLOODLE. Procedia Soc Behav Sci 2(2):5682–5685

Ye Z, Dun A, Jiang H (2020) The role of 3D printed models in the teaching of human anatomy: a systematic review and meta-analysis. BMC Med Educ 20:335

Zhang X, Yang J, Chen N et al (2019) Modeling and simulation of an anatomy teaching system. Vis Comput Ind Biomed Art 2:8

Zorzal E, Sousa M, Mendes D, Anjos R, Medeiros D, Paulo SF et al (2019) Anatomy studio: a tool for virtual dissection through augmented 3D reconstruction. Comput Graph 85:74–84

Visualizing Anatomy in Dental Morphology Education

9

Tamara Vagg, Andre Toulouse, Conor O'Mahony, and Mutahira Lone

Abstract

Tooth morphology is a foundation course for all dental healthcare students including dentists, dental hygiene, dental therapy, and dental nursing students. This chapter explores the conventional and innovative teaching methods to deliver tooth morphology educational modules. The teaching tools are explored with a 2D and 3D lens, with a particular focus on visualization, student understanding, and engagement. Traditional methods of teaching tooth morphology must be complemented with innovative pedagogical approaches in order to maintain student's attention and accommodate their diverse learning methods. Teaching 3D anatomy enables students to visualize and spatially comprehend the link between various anatomical components. Online tests and quizzes motivate students and are also beneficial in preparing students for exams. Online self-examinations offering visualization with 3D teeth enable students to evaluate their knowledge and offers immediate feedback, which aids in the long-term retention of information. These tools can be as efficient as other teaching methods, allowing the students to study at their own pace and with repetition. The authors conclude that blended and innovative teaching methods should supplement student learning and not replace, traditional face-to-face educational methods.

9.1 Background

Anatomy is a core module that provides a strong foundation in all healthcare programs including the undergraduate and postgraduate dental curriculum (Sugand et al. 2010; Abdalla 2020; McHanwell and Matthan 2020). Prior to patient examination, diagnosis, and clinical treatment, a thorough grasp of anatomy is required (Abdel Meguid et al. 2017; McHanwell and Matthan 2020; Reddy and Pathak 2021; Fonseca et al. 2022). Vesalius' traditional method of

T. Vagg
Cork Adult CF Centre, Cork University Hospital, University College Cork, Wilton, Cork, Republic of Ireland

School of Computer Science and Information Technology, University College Cork, Cork, Republic of Ireland

HRB Clinical Research Facility Cork, University College Cork, Cork, Republic of Ireland
e-mail: tamara.vagg@ucc.ie

A. Toulouse · C. O'Mahony · M. Lone (✉)
Department of Anatomy and Neuroscience, University College Cork, Cork, Republic of Ireland
e-mail: A.Toulouse@ucc.ie; conoromahony@ucc.ie; m.lone@ucc.ie

teaching anatomy via dissection has evolved with an emphasis on didactic lectures but now also includes digital education, e-learning, and a broad variety of 3D models (Nagasawa et al. 2010; Salajan et al. 2015; Lone et al. 2018) as the current generation of students are increasingly using devices like computers/laptops and cell phones for their academic needs (Khatoon et al. 2014). Additionally, visualization has been found to be particularly vital for student comprehension as well as the development of psychomotor abilities, which are particularly important for a dental student (Fonseca et al. 2022).

The term "dental student" has evolved over time to include not just those pursuing a dental science degree (bachelor's or doctorate, depending on the region), but also those pursuing degrees in dental hygiene, dental therapy, or dental nursing (Bakr et al. 2016; McHanwell and Matthan 2020). As they begin their respective degree, these students will treat patients by performing oral examinations, dental scaling, restorations, and small surgeries; thus, in order to promote safe clinical practice, anatomical knowledge is a crucial part of their early training (McHanwell and Matthan 2020). General gross anatomy, embryology, neuroanatomy, histology, and oral anatomy (including tooth morphology) are among the anatomical topics that are typically covered in the first 2 years of a dental study program (McHanwell et al. 2007; Gould et al. 2014; McHanwell and Matthan 2020; Chow and Sharmin 2021), with a core anatomy curriculum published by the Association for Dental Education in Europe (ADEE) (ADEE 2016; Best et al. 2016). Dental students need to cover certain anatomical topics in more detail than other healthcare students including the anatomical structures of the oral cavity, major and minor salivary glands, maxilla, mandible, nerve supply to the teeth, floor of the oral cavity, and the lymphatic drainage of the head and neck to name a few (Guttmann et al. 2003; ADEE 2016). There is a shortage of qualified dental anatomy staff available to teach anatomy to dental students, especially those who can emphasize the dental relevance of the anatomical structures (McHanwell 2015). Furthermore, horizontal and

vertical integration of anatomy into the dental curriculum is recommended, which is extremely relevant in the clinical years (Manogue et al. 2011; McHanwell and Matthan 2020).

Courses in dental anatomy are normally taught as either separate modules or as an integrated anatomy module (Guttmann et al. 2003). Co-teaching, in which students of different dental specialties learn alongside one another, is another strategy that has been proposed as a means of enhancing students' capacities in the areas of communication and teamwork in preparation for the students' future roles as members of the dental care team (Bakr et al. 2016; Amin et al. 2017; McHanwell and Matthan 2020).

In the following sections of this chapter, the conventional and innovative teaching tools used for tooth morphology will be discussed with a focus on instructional tools employed with visualization at its core.

9.2 Tooth Morphology

Tooth morphology is the study of the morphological features of the permanent and deciduous dentitions (Obrez et al. 2011). Dental students including dental hygienists, dental nurses, and dental technicians must be familiar with tooth morphology including the visualization and understanding the 3D aspects of different teeth for clinical and lab work (Obrez et al. 2011; Abu Eid et al. 2013; Bakr et al. 2016; Risnes et al. 2019). The tooth morphology module is usually delivered in the first 2 years of the dental degree (Lone et al. 2018) with its application in the subsequent years. This often leads to a loss of knowledge called "decontextualized technique learning" (Magne 2015). The teaching of tooth morphology has always been an important but difficult aspect (Wang et al. 2020) with various teaching aids available to assist student learning and understanding. Tooth anatomy and identification is not only important for the clinical treatment and restoration of teeth but also for the identification of dental anomalies, dental variations, and pathologies commonly seen in clinical practice (Bakr et al. 2016). In the next
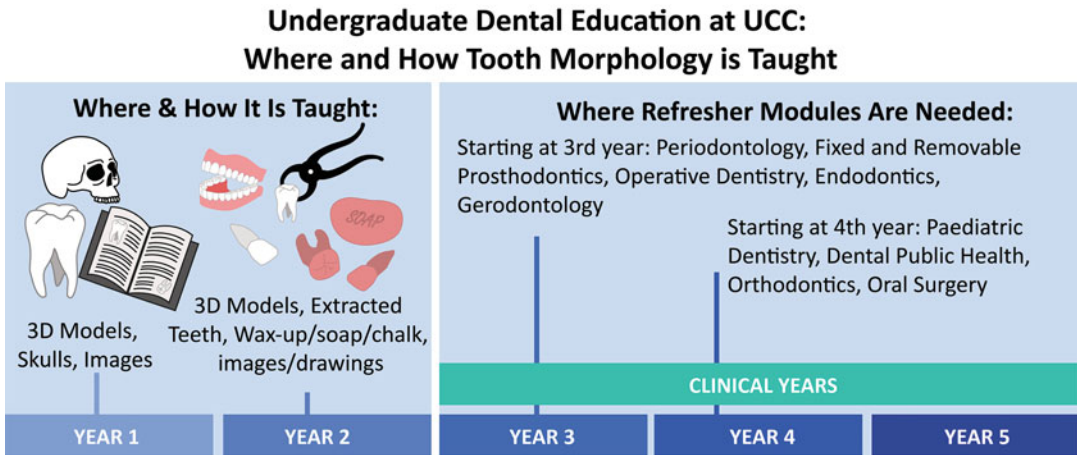
Fig. 9.1 Timeline showing the 5-year curriculum at University College Cork (UCC). Tooth morphology is taught in years 1 and 2 with vertical integration needed in the following years (years 3–5)

section, the authors will discuss the visualization offered by conventional (2D and 3D) methods for teaching tooth morphology.

9.3   Conventional Methods of Teaching Tooth Morphology Which Offer Visualization

Modalities used for teaching tooth morphology include a variety of approaches, such as lectures supplemented with prosected material, anatomical models, and extracted teeth (Lone et al. 2018) (Fig. 9.1). As this chapter focuses on visualization offered by each teaching method, the teaching modalities are further subdivided into 2D and 3D teaching methods.

9.4   2D Teaching Methods

9.4.1   Lectures

Didactic lectures utilizing PowerPoint (Shigli et al. 2016) are often the preferred medium for teaching dental anatomy (Johnson et al. 2012; Schonwetter et al. 2016; Lone et al. 2018). Dental

anatomy is a topic that easily lends itself to being taught in this style since it is so readily supported by visual media. Furthermore, viewing multiple two-dimensional representations of the same structure may help to create a 3D mental image. Anatomy didactic lectures can be supplemented with other teaching modalities to offer multiple entry points and provide multimodal and holistic teaching, as will be discussed in the following section; however, when used on its own, this mode of instruction can assist students in developing mental images of the structures.

During the recent pandemic, online lectures and webinars substituted the didactic lecture content in dental schools globally (Goodacre et al. 2021; Lone et al. 2021). As we return back to face-to-face teaching, the lecture recordings would be a helpful student resouce as a review tool to explain certain points for visual learners as well as for auditory learners. According to Bacro et al. (2013), there is substantial association between grades for students with a preference for auditory learning and frequent viewings of lecture recordings. The authors hypothesize that auditory learners would greatly benefit from having access to recorded lectures (Bacro et al. 2013).

9.4.2 Flash Cards

Flash cards offer a 2D representation of tooth anatomy which aids visualization and allows for multiple viewings according to user suitability. These flash cards are readily available in textbooks (Nelson 2014; Wignall 2014; Fehrenbach 2015), provide a detailed description of the features of the teeth, promote student learning, and facilitate a transfer of knowledge from 2D to 3D (Bryson 2012). Flash cards can also be offered to dental students as case-based studies in the clinical years (Al-Rawi et al. 2015; McAndrew et al. 2016; Toyohiro et al. 2021).

9.5 3D Teaching Methods

9.5.1 Dissection- and Prosection-Based Teaching

An ongoing debate exists about whether dissection or prosection-based practical sessions are the superior approaches for teaching anatomy. Both dissection sessions and prosections give visual cues and aid dental students in gaining a better understanding of the head and neck region, particularly the teeth in occlusion and their relationship to the surrounding anatomical structures in the oral cavity. Prosection-based instruction is often favored by students themselves (Abdel Meguid et al. 2017). Snelling et al. (2003) conducted a poll of dental students and the students rated tutorials, prosections, and textbooks as excellent anatomy learning tools (Snelling et al. 2003).

Redwood and Townsend (2011) state that dental students' interest in pursuing a dental surgical career may explain why they choose prosection over dissection as the preferred learning method. Regardless of the reasons stated above, prosections and dissection sessions should remain a core teaching component of the dental curriculum since it aids student development into clinicians, with the cadaver as their first teaching patient, and also provides 3D understanding and visualization of the anatomical relationship of the teeth and other anatomical structures in the oral cavity (Redwood and Townsend 2011).

9.5.2 Anatomical Models

Teaching tooth morphology commonly employs the use of plastic or resin-based anatomical models (Lone et al. 2018). The models are easily available, convenient to use and store and have a long shelf life (Abu Eid et al. 2013). Students, themselves, appreciate the 3D teaching offered by plastic models and use it routinely to supplement their learning (Abu Eid et al. 2013; Abdel Meguid et al. 2017).

Tooth morphology taught with the use of high-quality commercial replicas with color-coding or numbering of certain tooth characteristics has visually emphasized the differentiation of tooth characteristics, further aiding student understanding (Abu Eid et al. 2013). However, one disadvantage is that all the plastic teeth are identical and do not show normal anatomical variations or anomalies (Obrez et al. 2011).

9.5.3 Extracted/Plastic Teeth

Historically, extracted teeth are the most popular teaching aid for studying dental morphology and identifying tooth characteristics (Mitov et al. 2010). According to research by Abu Eid et al. (2013), students prefer to study dental morphology using extracted teeth (Abu Eid et al. 2013). However, there are various drawbacks for teaching with extracted teeth including obtaining a sufficient number of hygienic and healthy, non-carious, unworn extracted teeth with ethical and informed consent (Cantín et al. 2015).

In most countries, improvements in oral health care have led to a decline in the number of tooth extractions (Muller et al. 2007; Dietrich et al. 2015), posing a further challenge for the procurement of healthy extracted teeth for educational purposes (Obrez et al. 2011). Innovative teaching methods are currently being incorporated into the teaching of tooth morphology (Nagasawa et al.

2010; Cantín et al. 2015; Lone et al. 2021) in order to provide visualization and 3D comprehension of the dental morphological anatomy (Mitov et al. 2010; Allen et al. 2015). However, extracted teeth are still preferred for learning tooth morphology and also for examinations (Suh et al. 2022).

9.5.4 Carving Teeth

Carving tooth models from various media, such as wax, chalk, or soap (Mitov et al. 2010; Lone et al. 2018), has helped facilitate the learning of comprehensive dental morphology (Obrez et al. 2011). This method utilizes visualization and haptic touch to provide the development of fine motor skills along with morphological knowledge, which is a prerequisite for reconstructing lost or damaged tooth structure during various dental treatments (Abu Eid et al. 2013; Lam et al. 2015; Goodacre et al. 2021). A study done in 2013 introduced wax tooth carving practical sessions for first-year graduate dentistry students with more than 80% of the students claiming that the carving assignments improved their manual dexterity along with their understanding and ability to visualize the 3D architecture of the teeth (Abu Eid et al. 2013).

More recently, Abdalla (2020) supplemented dental carving exercises with clinical-based teaching and also digital learning to improve student satisfaction and student performance. Introducing clinical scenarios allowed students to see the relevance and application of tooth anatomy in their clinical practice and careers. The digital teaching introduced for the tooth morphology module linked directly to the digital software used in dental practices and hence allowed the dental students to link their pre-clinical haptic exercises to digital uses and clinical applications (Abdalla 2020). At-home waxing exercises (Goodacre et al. 2021) and 3D tooth models (Lone et al. 2021) were also found to be effective for teaching students the didactic aspects of various teeth during the recent COVID-19 pandemic. However, the students expressed an interest in returning to campus for these tooth morphology modules.

There appears to be a debate about the benefits of dental carving exercises and whether they should be retained or introduced/reintroduced in the tooth morphology module (Conte et al. 2021). Goodacre et al. (2021) favors the carving sessions for the students as it not only enhances their detailed tooth morphology knowledge but also introduces 3D spatial understanding of the tooth along with detailed hand manipulation of dental instruments, which will all be relevant skills needed in the dental care of the patients (Goodacre et al. 2021).

While the sections above discuss the various teaching methods, self-assessment with mock quizzes or spots can also be used to enhance student learning and motivate them. The next section discusses how this has been implemented for tooth morphology teaching.

9.5.5 Formative "Spotter" Examination

Self-assessment tools have been found to enhance student learning with better results and motivation (Lone et al. 2019). *Tooth morphology*, a computer-based learning program for tooth morphology showed promising results with improved student learning (Bogacki et al. 2004). The majority of dental schools evaluate tooth morphology formally as part of an objective structured practical examination or formative spot examination which consists of stations where students are asked to identify extracted or plastic teeth and chart them in an appropriate notation system and answer a clinically or developmentally related question (Abu Eid et al. 2013; Lone et al. 2019).

9.5.6 Innovative Visual Methods for Teaching Tooth Morphology to Dental Students

Dental students require detailed knowledge of the morphology of the permanent and deciduous teeth. Technology has been used successfully in

pre-clinical and clinical dental teaching (Suh et al. 2022). The challenge for educators is to provide a framework so that students are offered a learning environment that includes all different types of learners. Providing the students the opportunity to learn both online and in-person, gives all the learners a chance to get a better understanding of the best way for them to learn. In the last few years changes in the anatomy curriculum along with the recent COVID-19 pandemic (Drake and Pawlina 2014; McBride and Drake 2018; Longhurst et al. 2020; Dulohery et al. 2021) resulted in reduced course hours for anatomy. This led to an increase in the use of adjunctive tools and self-directed learning which have been demonstrated to be efficient as teaching resources while also being easily accessible for students (Tam et al. 2009; Yeung et al. 2011; Goodacre et al. 2021; Lone et al. 2021). Medical students are routinely utilizing newly created and tested instructional strategies (Rizzolo and Stewart 2006; Johnson et al. 2012) which have also been incorporated into the dental curriculum (Maggio et al. 2012). In addition to this, a survey conducted by Lone et al. (2018) investigating the tooth morphology teaching methods employed within the United Kingdom and Ireland, found that minimum time is dedicated to the delivery of tooth morphology resulting in a greater emphasis on students' self-directed learning. The authors also conclude that Computer Aided Learning (CAL) systems and tools could assist in acquiring and sustaining tooth morphology learning (Lone et al. 2018). Furthermore, since dental students use the latest electronic learning devices, these CAL systems and online tools for self-directed dental education are easily accessible (Redwood and Townsend 2011). Indeed, a study conducted at the School of Dentistry, University of Birmingham found that dental students preferred devices like laptops and smartphones for studying and self-testing their knowledge (Khatoon et al. 2014). What follows is a review of the current literature, exploring the use of innovative tools offering visualization to teach tooth morphology to dental students.

9.5.7 Animations and Multimedia Learning Resources

The use of graphics and visual information enhances understanding, retention, and recall of a theory or notion (Tversky et al. 2002). Teaching modalities using both static images (such as pictures and diagrams) and dynamic images (such as videos and animations) are essential in stimulating and creating an enhanced environment for teaching and learning (Wilson 2015). Animations serve two functions in an educational context: affective and cognitive. The affective component of an animation keeps the viewers' attention, while also working as a motivational tool. On the other hand, the cognitive component of animation is associated with comprehension (Lowe 2004). Regardless of the results obtained, students have expressed enthusiasm toward the use of technology-based courses or modules within the curriculum (Kesner and Linzey 2005; Vuchkova et al. 2012).

Animation and various multimedia learning tools have been developed for dental students to teach topics like cranial nerves (Richardson-Hatcher et al. 2014; Lone et al. 2017) (Fig. 9.2), temporomandibular joint and dental anesthesia (Guttmann 2000) and the 3D morphology of the teeth (Lone et al. 2019). According to Mitov et al. (2010), their 3D animated tooth software proved effective and enjoyable for learning tooth morphology (Mitov et al. 2010).

Bogacki et al. (2004) conducted a randomized controlled trial assessing the efficacy of "Tooth Morphology," an interactive CAL course with lectures containing text, illustrations and 3D graphics, against traditional lectures for teaching tooth morphology (Bogacki et al. 2004). For a cohort of first-year dental students at Virginia Commonwealth University, the results found that "Tooth Morphology" was statistically equal to traditional teaching lectures. These discoveries have resulted in the substitution of conventional lectures with a mix of "Tooth Morphology" and interactive classroom discussions since this new format was deemed to be more interactive and gave students active control over the time and
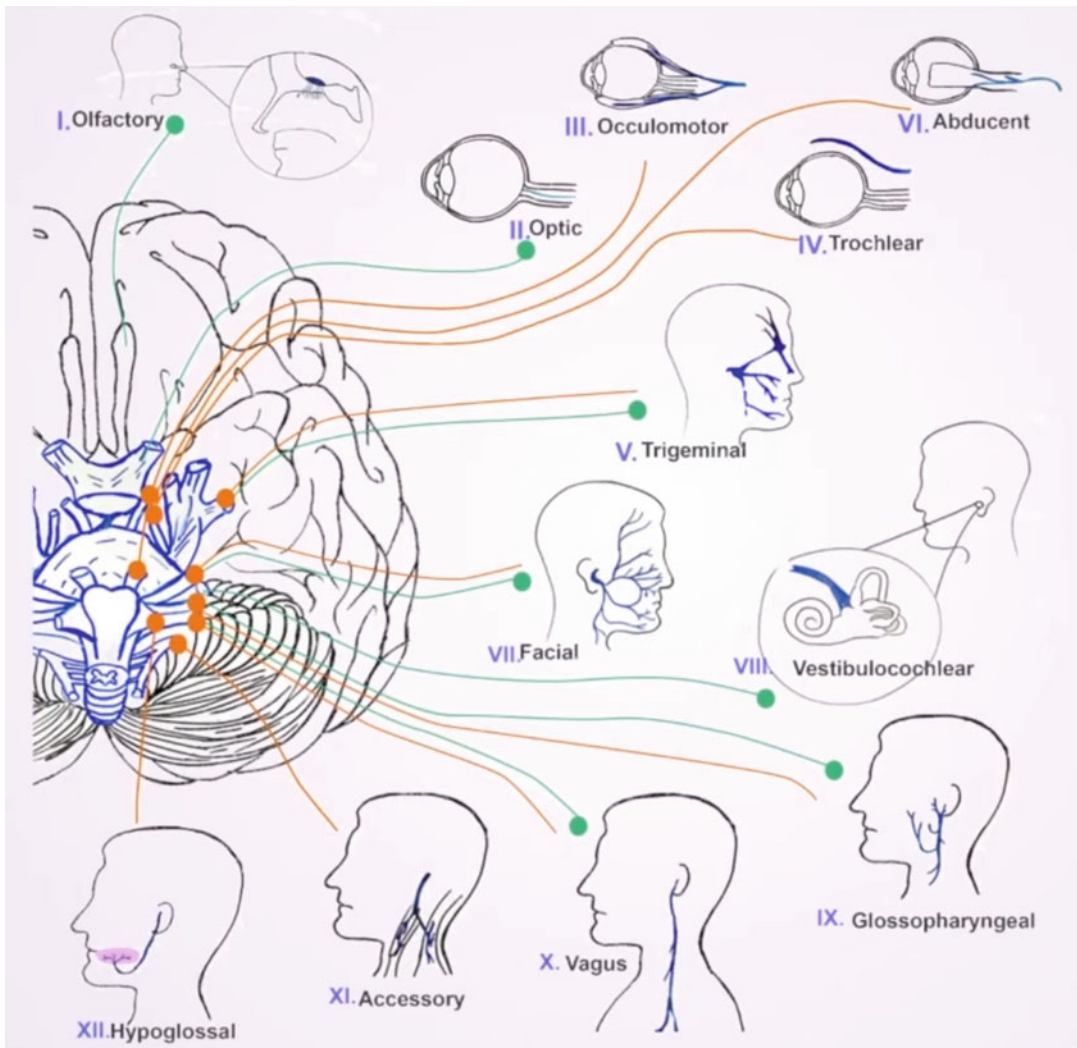
Fig. 9.2 Screenshot of the cranial nerve animation showing the 12 pairs of cranial nerves with individual functions. Sensory supply is demonstrated in green whereas motor supply is shown in orange

pace of their learning. It also increased chances for teachers to connect with the students, provide assistance and emphasize the clinical importance of tooth morphology (Bogacki et al. 2004).

Students' use of a DVD-based interactive tooth atlas was studied by Wright and Hendricson (2010). The atlas included photographic, radiographic, and CT scan images of all the teeth and was offered to the dental students in the first three years of their degrees at the University of Texas Health Center, San Antonio. Before performing

surgical procedures like periapical and implant surgeries these atlases could be reviewed to analyze the anatomy of various teeth and their relationship to the surrounding hard and soft tissues. Only 14% of dental students downloaded the atlas. However, once students were informed that atlas-based questions would be featured on the exam the uptake of the atlas increased to 43% of students (Wright and Hendricson 2010). In addition, the authors of the study determined that the atlas was mostly used by third-year dental

students, presumably because they were involved with the clinical rotations and could comprehend the clinical significance of the anatomical information available in the resource (Wright and Hendricson 2010).

In the aforementioned examples, the animations and multimedia learning resources were limited in terms of their interaction capabilities and accessibility to students, which is reflective of Information Communication Technologies (ICT) for that time. However, since then, innovative visualization methods have continued to advance, with the emergence of a new cycle of interactive 3D programs capable of virtual/augmented/mixed realities and even delivery through web platforms. The proceeding sub-sections will explore how these innovations have been utilized for dental/tooth morphology.

## 9.5.8 3D Models, 3D Animations and Interactive 3D

There are numerous benefits for employing novel teaching tools, such as simultaneous visualization of material by multiple students and the application of teaching and clinical training concurrently (Nagasawa et al. 2010). Continuous improvements in technology over the years have led to the development of 3D teaching tools for dental students such as interactive 3D tooth (de Boer et al. 2015) or 3D tooth atlases (Salajan and Mount 2008; Nagasawa et al. 2010; Wright and Hendricson 2010; Salajan et al. 2015; Suh et al. 2022), including the development of an tooth atlas using micro CT scanning (Nagasawa et al. 2010; Cantín et al. 2015; Koopaie and Kolahdouz 2016), and 3D visualization of the internal tooth structure (Salajan et al. 2015). Atlases have been provided to students via CD/DVD (Wright and Hendricson 2010) or more recently, via web-based or online delivery (Salajan et al. 2015). Also, the use of other 3D delivery solutions/software such as Computer-Aided Design (CAD) and Computer-Aided Manufacturing (CAM) technology aided student performance in wax-up and restoration of teeth (Douglas et al. 2014). Furthermore, tooth morphology may be taught in a safe and cost-effective manner using 3D scanning of extracted teeth (Elgreatly and Mahrous 2020).

Mitov et al. (2010) introduced a 3D tool via web-based CAL software "MorphoDent" to dental students in their second year of study at the University of Saarland in Homburg, Germany. Scanners were utilized to build 3D models of extracted teeth which were previously used for the teaching tooth morphology. Students were provided with the teaching tool two weeks before examination in order to evaluate their perception about the efficacy of the 3D teaching tool. 3D tooth models were also examined, in addition to the standard examination using extracted teeth. Data gathered shows that while students liked learning with MorphoDent, no significant statistical difference was seen between the outcome of the two examination scores (Mitov et al. 2010). However, Lone et al. (2018) developed an interactive 3D tooth morphology quiz and evaluated its effects on dental education via a cross-over study designed to compare the novel system with traditional teaching methods. Students who used the 3D tooth morphology quiz felt the system was intuitive and aided in their understanding of tooth morphology. The results of the study found that student groups with access to the 3D tooth morphology quiz performed significantly better than previous years. The authors conclude that the 3D tooth morphology quiz is a useful adjunct for dental anatomical education (Lone et al. 2019) (Fig. 9.3).

Magne (2015) revised and implemented a significant update of the dental morphology and occlusion module at Herman Ostrow School of Dentistry in the University of Southern California by introducing 2D, 3D, and 4D principles for learning essential practical and clinical skills. Initially, his method focused on 2D tooth drawings, proceeded by partial or full 3D wax-ups of teeth. 4D was utilized by layering acrylic and resin restorations simulating the different layers of the internal structure of the tooth, namely enamel, and dentine. Increased student engagement along with staff satisfaction was reported with the modified program (Magne 2015).
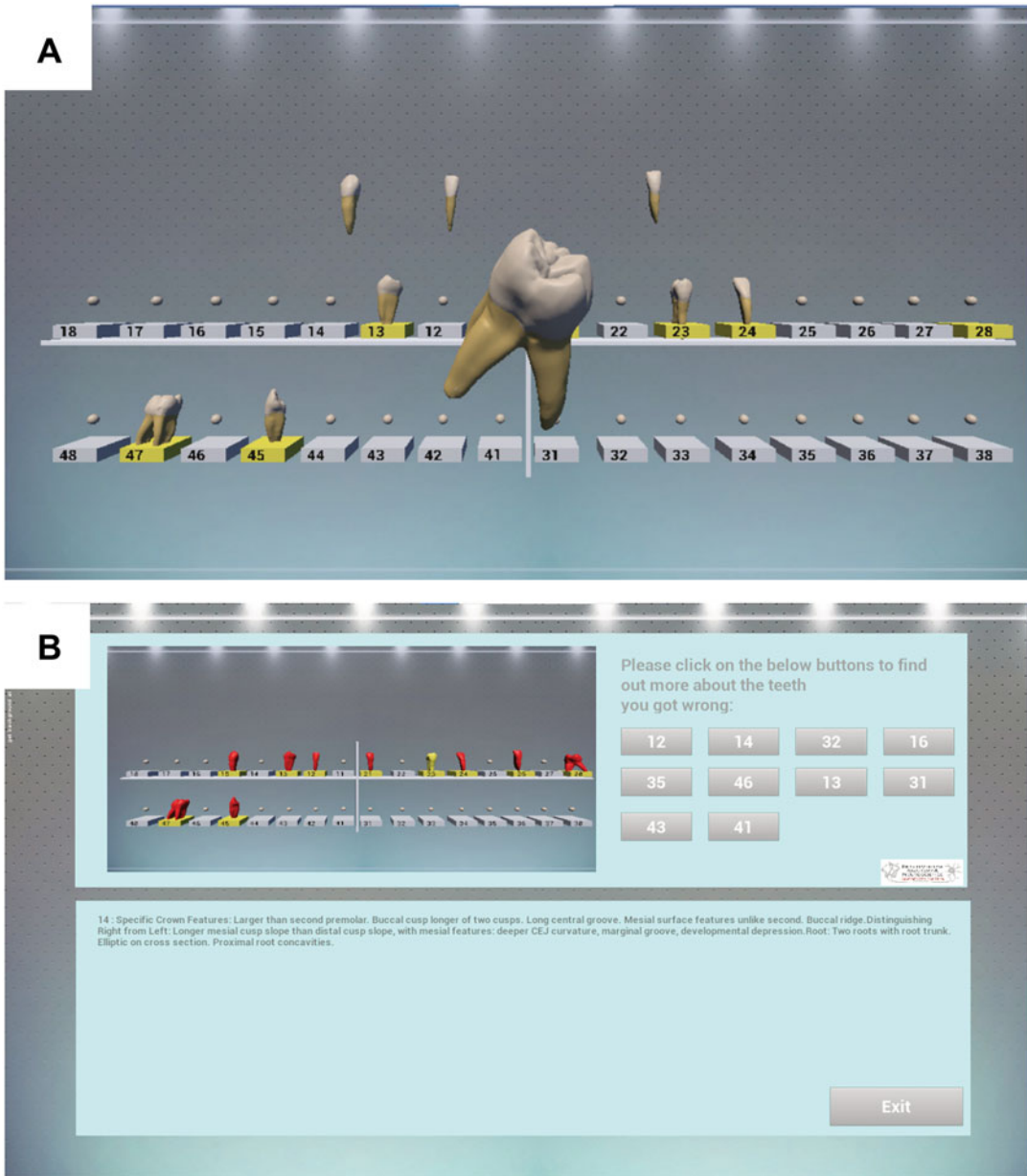
Fig. 9.3 Tooth morphology quiz (TMQ). (**a**) Active quiz screen showing Fédération Dentaire Internationale (FDI) notation placements of the teeth along with a 3D rotating image of selected tooth. (**b**) Results of the TMQ with feedback screen. Selecting an incorrect answer will highlight it in yellow with relevant feedback on identification features provided

Extracted teeth, as discussed before, are routinely used for studying the morphology of the teeth. Game-based learning and gamification has also been applied for the teaching of tooth morphology using extracted teeth, with results showing it to be cost-effective, student-friendly, and providing 3D understanding for all the learners (Risnes et al. 2019).

As part of a dental anatomy module redesign at the University of Kentucky College of Dentistry, Abdalla (2020) incorporated a 3D dental software program ("Tooth Explorer"), designed to teach oral anatomy and tooth morphology. The software was employed during lectures on a second screen where a 3D view of the tooth was displayed, illustrating anatomical landmarks and unique features. The authors report that the redesigned module as a whole, including the use of "Tooth Explorer" 3D visualization, was highly appreciated and rated by students (Abdalla 2020).

9.5.9 Virtual and Augmented Reality

Digital applications are widely used in all areas of dental education (Roy et al. 2017; Murbay et al. 2020). In addition to 3D, computer simulations are showing promising results. Virtual Reality (VR) is defined as a computer-generated recreation of a world or scenario where the user experiences the virtual world personally via simulation in real time (Joda et al. 2019).

Augmented Reality (AR) on the other hand is defined as a system that superimposes virtual objects onto the physical world (Bölek et al. 2021). In a recent review published by Zitzmann et al. exploring digital technology in dentistry education, the authors conclude that VR and AR will play a dominant role in dental education in the future (Zitzmann et al. 2020). An example of VR being used for dental morphology education is presented by Liebermann et al. who developed an interactive VR teaching environment that utilizes a HTC Vive Pro headset (Liebermann and Erdelt 2020). Within this environment dental students were presented with a labeled 3D model of the jaw with teeth and had the facility to select individual teeth that could then be manipulated via scaling, rotating, and moving. Additional images, text, and audio were also available within the environment to further reinforce the educational content. The authors evaluated their VR system with 63 pre-clinical dentistry students via a custom survey and found that the majority of participants felt they understood dental morphology better than when compared to traditional textbook teaching (34.9% selecting "Much Better," and 57.1% Selecting "Better"). The authors also found that students were willing to purchase VR equipment privately to support their learning, and that haptic and auditive elements were evaluated more highly than just visual (Liebermann and Erdelt 2020).

In the previous VR example, a specialized VR headset was required to facilitate the delivery of the educational content. However, as the potential for VR and AR continue to grow, specialized headsets are becoming cheaper, and VR/AR environments can now be delivered via smartphone applications. Juan et al. demonstrate such an example whereby they developed an AR smartphone app to support dental morphology education (Juan et al. 2016). The AR app accesses the smartphone camera which allows the student to focus on a printed 2D image of a jaw, the app then detects the image and displays a 3D model of the jaw with teeth over the image. The student can then choose a specific tooth to view in isolation which can be further explored by scaling or manipulating the camera location. There are additional learning aids within the app that overlays all morphological details. The AR app was then evaluated with undergraduate students, postgraduate students, and academic staff, and demonstrated that the app was effective in knowledge transmission and for reinforcing acquired knowledge (Juan et al. 2016). Furthermore, Haji et al. (2021) conclude within their review of AR for dental education that the benefits of AR and VR for dental education are evident and can further provide access to quality educational interactions with an overall lowered cost to training (Haji et al. 2021).

The combination of VR and AR is referred to as Mixed Reality (MR), and despite its perceived advantages in other dentistry applications, it has yet to be used specifically for dental/tooth morphology education (Monterubbianesi et al. 2022).

9.5.10 The Web as a Learning Technology

Harnessing the power of the web as a learning technology is not a new or novel method; however, the increasing capabilities of the modern web continue to support innovations in the delivery of the educational content. Early web applications were limited and were mostly refined to the display of text, images, audio and video files. However, advances in web technology (namely HTML5) have allowed for the integration of interactive 3D, VR, and AR making it a powerful CAL system. As regarded by Zitzmann et al., the possibilities of e-Learning can create meaningful and enjoyable learning experiences that are accessible anytime for dental students (Zitzmann et al. 2020). However, researchers and developers within this space often disagree on domain definitions, as in other areas of technology/multimedia, as the potential and power of the technology evolves, so too does its definition (Moore et al. 2011), often narrowing or broadening the definition scope. For example, "E-Learning" is considered by some researchers as strictly web-based education, whereas others include offline computer-assisted teaching aids such as CDs/DVDs (Moore et al. 2011). For the purpose of the below sub-sections, we refer to the e-learning definition as the explicit use of the web as a learning technology.

9.5.11 E-Learning

E-learning has several benefits: access to a greater variety of learning materials, flexible learning environment with control over the pace and accessibility of learning, more adaptive than traditional teaching methods alone and offering increased visualization. Additionally, it offers educators with an easily updatable multimedia platform for interactive teaching and improved cognitive skills (Salajan et al. 2009; Wright and Hendricson 2010; Maggio et al. 2012; Arevalo et al. 2013; Patil et al. 2015; Chavarria-Bolaños et al. 2020; Movchun et al. 2021).

The introduction of e-learning into the dentistal curriculum has been assisted by technological advances (Mitov et al. 2010; Manogue et al. 2011) and students choosing to study with various online resources (Abu Eid et al. 2013). Blended learning techniques are beneficial for students with different learning styles and have demonstrated to produce better results (Pereira et al. 2007) along with increased student satisfaction (Reissmann et al. 2015) and enhanced communication between students and teachers (Wright and Hendricson 2010).

However, the use of e-Learning for tooth morphology education does not need to strictly use online systems. Goodacre et al. (2021) demonstrate this through their combination of online webinars with at-home wax-up of teeth. Over the course of three weeks, students were required to attend 11 webinars and complete five waxing projects through images and videos available via the online 3D tooth atlas. It was concluded that this novel approach yielded very good results from the students and that they effectively learned the didactic aspects required for tooth morphology; however, most of the students preferred face-to-face lectures and lab sessions for learning tooth morphology (Goodacre et al. 2021).

9.5.12 Learning Management System (LMS)

Learning Management Systems (LMS) are virtual learning environments that can simulate face-to-face learning and also allow for the sharing, management, and automation of educational resources (de Oliveira et al. 2016). Commonly used LMSs include Blackboard (2022), Moodle (2022), and Canvas (2022).

These systems have been utilized for the delivery of educational materials for a number of years; however, as these systems are further developed, their potential use for the delivery of educational materials increases. This was further exemplified during the COVID-19 pandemic where social distancing regulations drove the need for virtual and remote learning. Some
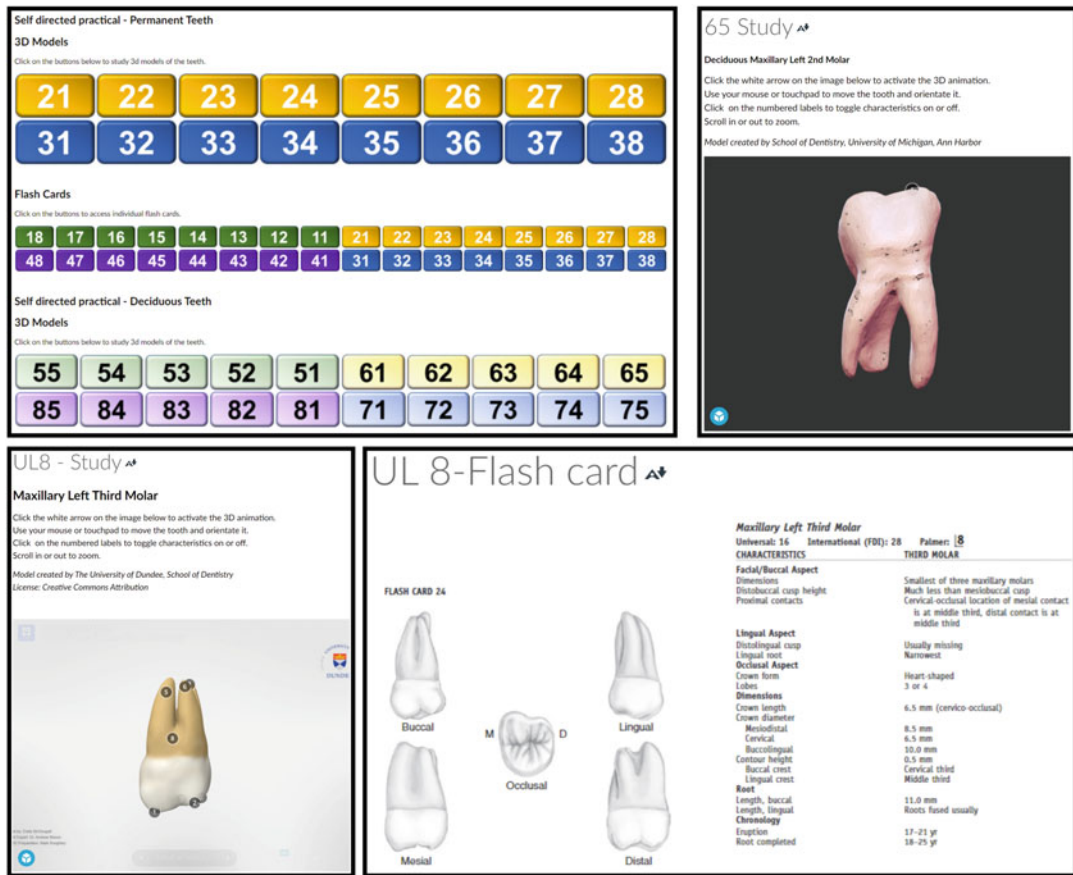
Fig. 9.4 Study tools provided for the Tooth morphology module during the COVID pandemic. FDI grids accessing 3D models for permanent and deciduous dentition and 2D flash cards. The models included were from the SketchFab™ website and were prepared by the University of Dundee (permanent dentition) and the University of Michigan (deciduous dentition). The 2D flash cards for permanent dentition were obtained from Wheeler's Dental Anatomy

researchers considered the imposed necessity as an enormous opportunity for dental educators to move toward and fully harness LMSs for dental teaching/learning experiences (Chavarria-Bolaños et al. 2020). This can be seen in the work of Lone et al. (2021) who developed an interactive tooth morphology module via the Canvas LMS. This module included video recordings of lectures, lecture notes, links to live sessions, and an interactive Fédération Dentaire Internationale (FDI) grid, whereby students could click on each of the notations and be brought to either a 2D flashcard or interactive 3D model of the selected tooth. The authors conclude that the course was a feasible solution during the pandemic as student results for that year were in line with previous years (Lone et al. 2021) (Fig. 9.4).

9.5.13 Social Media

Social Media Platforms (SMP) are websites and applications originally developed to allow users to connect and share information and content with each other in a social context, via text, image, and video posts (Kurian et al. 2022). However, the ubiquity and usability of such platforms has led to

their widespread usage in education as tools to facilitate teaching, learning, communication, and collaboration (Mcandrew and Johnston 2012).

The advent of SMPs during the 2000s and their subsequent use in dental education includes social networking sites such as Facebook and Twitter (Arnett et al. 2013; Siqueira et al. 2021) video sharing sites such as YouTube (Knösel et al. 2011; Mukhopadhyay et al. 2014), information repositories such as "wikis" (Salajan and Mount 2012), audio/podcasting platforms such as iTunes (Jham et al. 2008) and blogging platforms such as WordPress (Mcandrew and Johnston 2012). In more recent years, the development of newer SMPs and their popularity with the "social media" generation of students, along with increased availability of internet and smartphones, has led to a further increase in the use of SMPs in dental education (Rajeh et al. 2021; Kurian et al. 2022). This includes platforms such as photo- and video-sharing social networking sites such as Instagram, Snapchat, and TikTok (Nguyen et al. 2021; Rajeh et al. 2021), as well as social messaging app like WhatsApp (Martins et al. 2022).

The usage of SMPs within dental education is varied and often echoes the original purpose of these platforms for social connection and communication. For example, Siqueira et al. (2021) used Facebook groups as a forum for peer-to-peer discussion regarding course content and also for communication between faculty and students, which they found to lead to increased engagement (Siqueira et al. 2021). Similarly, in a scoping review on the use of WhatsApp in dental education, Martins et al. (2022) concluded that the app is a useful tool for exposing students to information and also for communication between students and teachers (Martins et al. 2022). Furthermore, the visual aspect of these platforms, which allow the creation and sharing of content and resources such as images, illustrations, animations, and videos, can facilitate methods of student learning as previously described in sections on both conventional and innovative visual methods for teaching tooth morphology.

YouTube is one of the more popular SMPs utilized by dental students (Burns et al. 2020). with a large number of dental education videos publicly available (Knösel et al. 2011). As part of a tooth morphology module redesign, Abdalla (2020) integrated YouTube videos into the digital delivery of the new module to host videos of recorded lectures and detailed demonstrations of tooth morphology waxing. The authors note that recording this content and making it available to students has an advantage over live demonstrations since the videos can be replayed and watched at the students' own pace (Abdalla 2020). As well as standard videos, YouTube is now capable of hosting interactive 3D animations and videos for use on smartphone VR devices, and it has the potential to be further integrated into dental morphology education as an accessible VR system. However, YouTube must be used or recommended to medical and dental students with extreme caution (Bosslet 2011) in order to guarantee the accuracy of content and reliability of writers/content creators (Knosel et al. 2011; Mukhopadhyay et al. 2014).

A survey by Nguyen et al. (2021) at two dental institutions in the USA found that students felt Instagram was a useful tool for reinforcing tooth morphology content as well as encouraging further engagement with the material outside of class (Nguyen et al. 2021). In this study, the education content consisted of faculty-curated private Instagram accounts which posted images, videos, practice questions, and quizzes (Nguyen et al. 2021). However, there are also a large number of public Instagram accounts focusing on dental anatomy content, although (similar to YouTube) a potential drawback to these public accounts is lack of quality control and ensuring information is correct (Douglas et al. 2019). Nevertheless, the visual nature of the image- and video-sharing features of Instagram and other SMPs seem to be a good fit to the teaching of visually-focused fields such as dental anatomy and tooth morphology (Douglas et al. 2019; Nguyen et al. 2021).

9.6   Digital Teaching: Some Points to Ponder!

In the preceding sections, we examined the conventional teaching of tooth morphology and the use of visualization, as well as changes in digital education that offer visualization to their learners. There are, however, a few crucial factors to consider before e-learning is implemented and digital changes are made to a curriculum.

Before giving the final takeaway message, the authors of this chapter will outline and explore several crucial and fundamental factors that need to be considered for digital and online education.

9.6.1   The Digital Divide

ICT (Information and Communication Technology) is changing how dental morphology is visualized, as well as education in general, as was previously stated. However, with these advancements and potential implementations of ICT in the Dental Curricula comes a "Digital Divide" with a global disparity noticed, with some institutes reporting high (Hamissi et al. 2013) and low (Postma et al. 2020) dental student ICT. This gap or Digital Divide is frequently used in the context of education to describe the disparities in access to technology (hardware, software, and the internet) imposed by a variety of reasons, including social, economic, and geographic ones (Baig et al. 2019). In order to prevent these students from becoming "digitally excluded," some universities attempt to provide their students with help such as equipment loan, minor financing awards, and accessible labs/study facilities. However, this provision also applies to other factors, such as training access and familiarity with digital literacy abilities for the students (the "digi divide") (Salajan et al. 2010). As a result, teachers using cutting-edge digital learning tools should make sure that their pupils have access to all required resources (technology,

the internet, etc.), including digital training (Khatoon et al. 2019).

9.6.2   Accreditation of Digital Technology in Education

Different LMS and CAL systems have been used to facilitate remote learning in various elements of dental education that required visualization during the COVID-19 pandemic (Azab and Aboalshamat 2021; Lone et al. 2021). The asynchronous tools, however, may be utilized less frequently or even abandoned altogether (Crome et al. 2021) as we transition toward a post-COVID setting and synchronous face-to-face/traditional approaches are once again viable. But there are still circumstances where these LMS and CALs for remote learning might be useful, such as during a new pandemic, a virus outbreak, to support students who are susceptible/high risk/unable to attend due to bereavement/sickness, and during natural disasters like storms and flooding (Longhurst et al. 2020; Mishall et al. 2022; Nassar and Rajeh 2022). Therefore, it is strongly advised that researchers and educators continue to think about these technologies in order to promote independent or distant learning (perhaps using a blended/hybrid method), especially in developing countries (Baig et al. 2019).

9.6.3   Suggested Recommendations for Educators to Implement Novel Visualization Tools

Academics and educators are finding it challenging to offer time to update tooth morphology (especially in senior clinical years), where it is most needed, due to operational challenges imposed by the growth in dental student numbers, decrease in healthy extracted teeth which can be used for teaching, and reduction in teaching hours. Therefore, putting in place cutting-edge

visualization technologies to assist self-directed revision might aid in resolving these problems.

9.6.4 Educators to Offer Multiple Modes of Representation

In order to enable learning for all the learners in a single environment, the Center of Applied Special Technology (CAST) in the United States developed the educational framework known as Universal Design for Learning (UDL) (About Universal Design for Learning 2022). Educators can utilize this educational framework's three guiding principles and 31 checkpoints while creating the learning outcomes of their modules/curriculum and also executing the delivery of the teaching for the module. UDL offers flexible instruction and seeks to engage and inspire all students. Various methods of representation, numerous means of action and expression, and multiple ways of interaction and engagement are among the three fundamental tenets of UDL.

Tooth morphology is a basic science subject with numerous applications in the clinical years for dental healthcare professionals. Therefore, it is crucial to make sure that dental students retain, recall, and comprehend the morphological properties of all the teeth rather than acquiring information by rote. We can develop resourceful and informed learners by putting the UDL multiple means of representation principles into practice and allowing dental students to visualize the tooth morphology using a variety of teaching tools like extracted teeth, plastic teeth, 3D teeth, 2D flash cards, and lecture recordings. The flipped classroom model has been successfully implemented in medical and dental education and shows promising results in the dental anatomy classroom by empowering the students to improve their cognitive and psychomotor abilities while the teacher promotes and supports their learning (Chutinan et al. 2018; Kellesarian 2018).

9.6.5 Educators to Be Involved in the Development/Selection of Teaching Tools

Additionally, participating actively in the creation and assessment of digital tools is advised for educators interested in integrating digital technology into the teaching of dental morphology. This can take the form of actively examining the open-source information that is currently accessible and advising students on accurate and appropriate tools, or it can take the form of creating/collaborating on the creation of a new visualization resource.

9.7 Individualizing the Process with One University's Example: Tooth Morphology Module Teaching at University College Cork

At University College Cork, students can enter the Bachelor of Dental Surgery (BDS) program through two different routes, either direct BDS entry after finishing secondary education, or a graduate entry program, where mature students with a third-level biological sciences degree can apply (BDSG). The BDS degree is a 5-year program whereas the BDSG degree is a condensed 4-year program. The tooth morphology course is taught in the second and fourth semesters of the dental degrees (BDSG and BDS respectively) and includes 15 hours of face-to-face interactive lectures and 12 hours of practical laboratory hours with ~2.5 contact hours per week. The teaching is supported by the university's LMS Canvas allowing student's access to lecture/practical handout, learning recordings, online resources, along with any communication about the teaching. The practical sessions are held in the laboratory where students are offered hands-on approach to learning with a wide range of
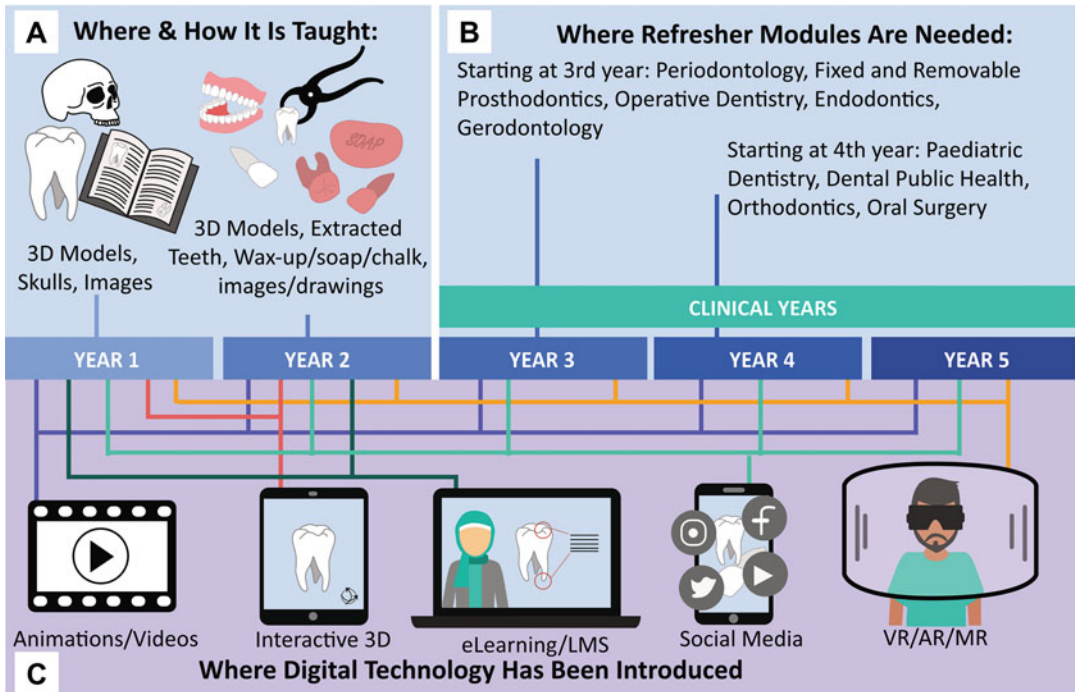
Fig. 9.5 Timeline showing the tooth morphology teaching in the 5-year curriculum at University College Cork. (**a**) Year 1 and Year 2 of the dental curriculum, where tooth morphology is taught with various teaching tools. (**b**) Year 3, 4, and 5, where clinical dental modules need the vertical integration of tooth morphology. (**c**) Inclusion of digital technologies to allow tooth morphology revision throughout the dental curriculum

teaching tools such as extracted human teeth, high-quality plastic replica teeth set, online 3D tooth morphology quiz, and a self-assessment opportunity with extracted teeth. Students are offered self-directed learning to study the dental morphological features of permanent and deciduous teeth with a lecturer facilitating the learning process (Lone et al. 2019). The recommended supporting textbook and atlas are *Wheeler's Dental Anatomy Physiology and Occlusion* (Nelson 2014) and *Illustrated Dental Embryology, Histology and Anatomy* (Fehrenbach 2016).

Assessment for this module has two elements, a formative spot examination and an end-of-module examination. The formative spot exam is a timed exam held in the lab with various stations having extracted human permanent and deciduous teeth which the students are asked to identify and also chart its notation using either the Fédération Dentaire Internationale (FDI) or Palmer

notation system. Each station is timed for one minute. The end of the module examination consists of essay and multiple-choice questions and is 1.5 hours in duration.

In the diagram below the authors have demonstrated the various teaching aids used in the first 2 years of the dental curriculum to teach tooth morphology. It has also been demonstrated where the revision of tooth morphology can be employed in the clinical years and which clinical specialities it could be helpful for, thus showing vertical integration of tooth morphology (Fig. 9.5).

9.8 Best Practice Moving Forward

The best way to teach tooth morphology's fundamental concepts is through conventional lectures and practical sessions supported by a variety of

cutting-edge auxiliary teaching tools. Therefore, moving ahead, a blended/hybrid teaching paradigm should be used. These cutting-edge digital tools must be introduced in order to supplement dental students' learning. These tools work best when used in conjunction with traditional teaching techniques like lectures and labs. Numerous readily available supplemental teaching methods like online tools, and software programs may be helpful in grasping certain components of the curriculum, however they cannot replace direct visual and tactile contact with extracted teeth since in situ teeth are the ones that the students treat primarily in clinical settings (Risnes et al. 2019). Offering multiple teaching pedagogies will ensure active student engagement in the learning process. Futhermore, these digital tools can be easily used in the clinical years to allow for vertical integration of tooth morphology within the dental currciulum.

References

'Blackboard' (2022) Blackboard Inc, Washington, DC. https://www.blackboard.com/en-eu/teaching-learning/learning-management/blackboard-learn

'Moodle' (2022) Moodle. West Perth, Western Australia. https://moodle.org

Abdalla R (2020) Teaching dental anatomy & morphology: an updated clinical- & digital-based learning module. Eur J Dent Educ 24(4):650–659. https://doi.org/10.1111/eje.12552

Abdel Meguid E, Aly A, Allen W (2017) Dental students' perceptions of effective anatomy teaching. Literacy Inf Comput Educ J 8(2):2562–2569. https://doi.org/10.20533/licej.2040.2589.2017.0339

About Universal Design for Learning (2022) CAST. https://www.cast.org/impact/universal-design-for-learning-udl. Accessed 25 July 2022

Abu Eid R et al (2013) Self-directed study and carving tooth models for learning tooth morphology: perceptions of students at the University of Aberdeen, Scotland. J Dent Educ 77(9):1147–1153. http://www.jdentaled.org/content/77/9/1147.full.pdf

ADEE (2016) SIGT-02: 'Biomedical sciences in dentistry: developing a contemporary Core curriculum'. Association for Dental Education in Europe (Outcome of ADEE SIG's 2013-2016)

Allen LK, Bhattacharyya S, Wilson TD (2015) Development of an interactive anatomical three-dimensional eye model. Anat Sci Educ 8(3):275–282. https://doi.org/10.1002/ase.1487

Al-Rawi W, Easterling L, Edwards PC (2015) Development of a Mobile device optimized cross platform-compatible Oral pathology and radiology spaced repetition system for dental education. J Dent Educ 79(4):439–447. https://doi.org/10.1002/j.0022-0337.2015.79.4.tb05902.x

Amin M et al (2017) Dental students' perceptions of learning value in PBL groups with medical and dental students together versus dental students alone. J Dent Educ 81(1):65–74. http://www.jdentaled.org/content/81/1/65.long

Arevalo C et al (2013) Framework for E-learning assessment in dental education: a global model for the future. J Dent Educ 77:564–575. https://doi.org/10.1002/j.0022-0337.2013.77.5.tb05504.x

Arnett MR, Loewen JM, Romito LM (2013) Use of social media by dental educators. J Dent Educ 77(11):1402–1412. https://doi.org/10.1002/j.0022-0337.2013.77.11.tb05616.x

Azab E, Aboalshamat K (2021) Attitudes, barriers, and experiences regarding E-learning and dental education during COVID-19 pandemic. Open Dent J 15:464–472. https://doi.org/10.2174/1874210602115010464

Bacro TR, Gebregziabher M, Ariail J (2013) Lecture recording system in anatomy: possible benefit to auditory learners. Anat Sci Educ 6(6):376–384. https://doi.org/10.1002/ase.1351

Baig QA, Abbas Zaidi SJ, Alam BF (2019) Perceptions of dental faculty and students of E-learning and its application in a public sector Dental College in Karachi, Pakistan. J Pak Med Assoc 69(9):1320–1325. PMID: 31511718

Bakr MM, Thompson CM, Massadiq M (2016) Anatomical sciences: a foundation for a solid learning experience in dental technology and dental prosthetics. Anat Sci Educ. https://doi.org/10.1002/ase.1650

Best L et al (2016) Reaching consensus on essential biomedical science learning objectives in a dental curriculum. J Dent Educ 80(4):422–429. http://www.jdentaled.org/content/80/4/422.full.pdf

Bogacki R, Best A, Abbey L (2004) Equivalence study of a dental anatomy computer-assisted learning program. J Dent Educ 68:867–871. https://doi.org/10.1002/j.0022-0337.2004.68.8.tb03836.x

Bölek KA, De Jong G, Henssen D (2021) The effectiveness of the use of augmented reality in anatomy education: a systematic review and meta-analysis. Sci Rep 11(1):1–10. https://doi.org/10.1038/s41598-021-94721-4

Bosslet GT (2011) Commentary: the good, the bad, and the ugly of social media. Acad Emerg Med 18(11):1221–1222. https://doi.org/10.1111/j.1553-2712.2011.01197.x

Bryson D (2012) Using flashcards to support your learning. J Vis Commun Med 35(1):25–29. https://doi.org/10.3109/17453054.2012.655720

Burns LE et al (2020) YouTube use among dental students for learning clinical procedures: A multi-institutional

study. J Dent Educ 84(10):1151–1158. https://doi.org/10.1002/jdd.12240

Cantín M, Muñoz M, Olate S (2015) Generation of 3D tooth models based on three-dimensional scanning to study the morphology of permanent teeth. Int J Morphol 33(2):782–787. https://doi.org/10.4067/S0717-95022015000200057

'Canvas' (2022) Instructure. Salt Lake City, UT. https://www.instructure.com

Chavarria-Bolaños D et al (2020) E-learning in dental schools in the times of COVID-19: a review and analysis of an educational resource in times of the COVID-19 pandemic. Odovtos Int J Dent Sci:207–224. https://doi.org/10.15517/ijds.2020.41813

Chow AK, Sharmin N (2021) Developing an interactive computer program for integrated dental education. Healthc Inform Res 27(4):335–340. https://doi.org/10.4258/hir.2021.27.4.335

Chutinan S, Riedy CA, Park SE (2018) Student performance in a flipped classroom dental anatomy course. Eur J Dent Educ 22(3):e343–e349. https://doi.org/10.1111/eje.12300

Conte DB et al (2021) Educational interventions to improve dental anatomy carving ability of dental students: a systematic review. Anat Sci Educ 14(1):99–109. https://doi.org/10.1002/ase.2004

Crome M et al (2021) Synchronous vs. asynchronous education: questionnaire-based survey in dental medicine during the COVID-19 pandemic**. Dtsch Zahnarztl Z. https://doi.org/10.3238/dzz-int.2021.0025

de Boer IR et al (2015) Evaluation of the appreciation of virtual teeth with and without pathology. Eur J Dent Educ 19(2):87–94. https://doi.org/10.1111/eje.12108

de Oliveira PC, de Cunha CJC, Nakayama MK (2016) Learning management systems (LMS) and e-learning management: an integrative review and research agenda. JISTEM 13:157–180. https://doi.org/10.4301/s1807-17752016000200001

Dietrich T et al (2015) Smoking, smoking cessation, and risk of tooth loss: the EPIC-Potsdam study. J Dent Res 94(10):1369–1375. https://doi.org/10.1177/0022034515598961

Douglas RD, Hopp CD, Augustin MA (2014) Dental students' preferences and performance in crown design: conventional wax-added versus CAD. J Dent Educ 78(12):1663–1672. http://www.jdentaled.org/content/78/12/1663.full.pdf

Douglas NKM et al (2019) Reviewing the role of Instagram in education: can a photo sharing application deliver benefits to medical and dental anatomy education? Med Sci Educ 29(4):1117–1128. https://doi.org/10.1007/s40670-019-00767-5

Drake RL, Pawlina W (2014) Multimodal education in anatomy: the perfect opportunity. Anat Sci Educ 7(1):1–2. https://doi.org/10.1002/ase.1426

Dulohery K et al (2021) Emerging from emergency pandemic pedagogy: a survey of anatomical educators in the United Kingdom and Ireland. Clin Anat 34(6):948–960. https://doi.org/10.1002/ca.23758

Elgreatly A, Mahrous A (2020) Enhancing student learning in dental anatomy by using virtual three-dimensional models. J Prosthodont 29(3):269–271. https://doi.org/10.1111/jopr.13152

Fehrenbach MJ (2015) Student workbook for illustrated dental embryology, histology and anatomy-E-book, 4th edn. Elsevier Health Sciences

Fehrenbach MJ (2016) Illustrated dental embryology, histology, and anatomy - E-book. Elsevier Health Sciences. https://books.google.ie/books?id=iy9TBwAAQBAJ&printsec=frontcover&dq=Illustrated+Dental+Embryology,+Histology+and+Anatomy%E2%80%99+student+workbook&hl=en&sa=X&redir_esc=y#v=onepage&q=Illustrated%20Dental%20Embryology%2C%20Histology%20and%20Anatomy%E2%80%99%20student%20workbook&f=false

Fonseca A et al (2022) Effect of dental course cycle on anatomical knowledge and dental carving ability of dental students. Anat Sci Educ 15(2):352–359. https://doi.org/10.1002/ase.2078

Goodacre CJ et al (2021) An educational experiment resulting from COVID-19: the use of at-home waxing and webinars for teaching a 3-week intensive course in tooth morphology to first year dental students. J Prosthodont 30(3):202–209. https://doi.org/10.1111/jopr.13295

Gould D et al (2014) How neuroscience is taught to North American dental students: results of the basic science survey series. J Dent Educ 78:437–444. https://doi.org/10.1002/j.0022-0337.2014.78.3.tb05693.x

Guttmann GD (2000) Animating functional anatomy for the web. Anat Rec 261(2):57–63. https://doi.org/10.1002/(SICI)1097-0185(20000415)261:2<57::AID-AR3>3.0.CO;2-R

Guttmann GD, Ma TP, MacPherson BR (2003) Making gross anatomy relevant to dental students. J Dent Educ 67(3):355–358. http://www.jdentaled.org/content/67/3/355.full.pdf

Haji Z et al (2021) Augmented reality in clinical dental training and education. JPMA J Pak Med Assoc 71(1):S42. PMID: 33582722

Hamissi J, Gholami S, Hamissi H (2013) The emerging role of computer literacy in improving the performance of dental students. Int J Collab Res Internal Med Public Health 5

Jham BC et al (2008) Joining the podcast revolution. J Dent Educ 72(3):278–281. https://doi.org/10.1002/j.0022-0337.2008.72.3.tb04493.x

Joda T et al (2019) Augmented and virtual reality in dental medicine: a systematic review. Comput Biol Med 108:93–100. https://doi.org/10.1016/j.compbiomed.2019.03.012

Johnson EO, Charchanti AV, Troupis TG (2012) Modernization of an anatomy class: from conceptualization to implementation. A case for integrated multimodal-multidisciplinary teaching'. Anat Sci Educ 5(6):354–366. https://doi.org/10.1002/ase.1296

Juan M et al (2016) A mobile augmented reality system for the learning of dental morphology. Digit Educ Rev 30:234–247

Kellesarian SV (2018) Flipping the dental anatomy classroom. Dent J 6(3). https://doi.org/10.3390/dj6030023

Kesner MH, Linzey AV (2005) Can computer-based visual-spatial aids lead to increased student performance in anatomy & physiology? Am Biol Teach 67(4):206–212. https://doi.org/10.2307/4451824

Khatoon B, Hill KB, Walmsley AD (2014) Dental students' uptake of mobile technologies. Br Dent J 216(12):669–673. https://doi.org/10.1038/sj.bdj.2014.523

Khatoon B, Hill K, Walmsley AD (2019) Mobile learning in dentistry: challenges and opportunities. Br Dent J 227(4):298–304. https://doi.org/10.1038/s41415-019-0615-x

Knösel M, Jung K, Bleckmann A (2011) YouTube, dentistry, and dental education. J Dent Educ 75(12):1558–1568. https://doi.org/10.1002/j.0022-0337.2011.75.12.tb05215.x

Knosel M, Jung K, Bleckmann A (2011) YouTube, dentistry, and dental education. J Dent Educ 75(12):1558–1568. http://www.jdentaled.org/content/75/12/1558.full.pdf

Koopaie M, Kolahdouz S (2016) Three-dimensional simulation of human teeth and its application in dental education and research. Med J Islam Repub Iran 30:461–461

Kurian N et al (2022) Influence of social media platforms in dental education and clinical practice: a cross-sectional survey among dental trainees and professionals. J Dent Educ. https://doi.org/10.1002/jdd.12914

Lam MT et al (2015) Evaluation of an innovative digital assessment tool in dental anatomy. J Contemp Dent Pract 16(5):366–371

Liebermann A, Erdelt K (2020) Virtual education: dental morphologies in a virtual teaching environment. J Dent Educ 84(10):1143–1150. Available at: 10/gqjtzz

Lone M et al (2017) Evaluation of an animation tool developed to supplement dental student study of the cranial nerves. Eur J Dent Educ 22(3):e427–e437. https://doi.org/10.1111/eje.12321

Lone M et al (2018) A survey of tooth morphology teaching methods employed in the United Kingdom and Ireland. Eur J Dent Educ 22:e438. https://doi.org/10.1111/eje.12322

Lone M et al (2019) Development and assessment of a three-dimensional tooth morphology quiz for dental students. Anat Sci Educ 12(3):284–299. https://doi.org/10.1002/ase.1815

Lone M, Mohamed MAA, Toulouse A (2021) Development of an online tooth morphology course in response to COVID-19 restrictions. J Dent Educ 85(S3):1946–1948. https://doi.org/10.1002/jdd.12643

Longhurst GJ et al (2020) Strength, weakness, opportunity, threat (SWOT) analysis of the adaptations to anatomical education in the United Kingdom and Republic of Ireland in response to the Covid-19 pandemic. Anat Sci Educ 13(3):301–311. https://doi.org/10.1002/ase.1967

Lowe RK (2004) Animation and learning: value for money. Curtin University, Bentley, WA, pp 558–561

Maggio MP, Hariton-Gross K, Gluch J (2012) The use of independent, interactive media for education in dental morphology. J Dent Educ 76(11):1497–1511. http://www.jdentaled.org/content/76/11/1497.full.pdf

Magne P (2015) A new approach to the learning of dental morphology, function, and esthetics: the "2D-3D-4D" concept. Int J Esthet Dent 10(1):32–47

Manogue M et al (2011) Curriculum structure, content, learning and assessment in European undergraduate dental education - update 2010. Eur J Dent Educ 15(3):133–141. https://doi.org/10.1111/j.1600-0579.2011.00699.x

Martins JCS et al (2022) Use of WhatsApp in dental education: a scoping review. Med Sci Educ 32(2):561–567. https://doi.org/10.1007/s40670-022-01520-1

Mcandrew M, Johnston A (2012) The role of social Media in Dental Education. J Dent Educ 76:1474–1481. https://doi.org/10.1002/j.0022-0337.2012.76.11.tb05409.x

McAndrew M et al (2016) Dental student study strategies: are self-testing and scheduling related to academic performance? J Dent Educ 80(5):542–552

McBride JM, Drake RL (2018) National survey on anatomical sciences in medical education. Anat Sci Educ 11(1):7–14. https://doi.org/10.1002/ase.1760

McHanwell S (2015) Teaching anatomical sciences to dental students. In: Chan LK, Pawlina W (eds) Teaching anatomy: a practical guide, 1st edn. Springer, New York, pp 353–361

McHanwell S, Matthan J (2020) Teaching anatomical sciences to dental students. In: Chan LK, Pawlina W (eds) Teaching anatomy: a practical guide. Springer, Cham, pp 495–507. https://doi.org/10.1007/978-3-030-43283-6_48

McHanwell S et al (2007) Adding 'common sense' to 'the need to know' in anatomy teaching. J Anat 210(5):615–616

Mishall PL et al (2022) Transition to effective online anatomical sciences teaching and assessments in the pandemic era of COVID-19 should be evidence-based. Med Sci Educ 32(1):247–254. https://doi.org/10.1007/s40670-021-01435-3

Mitov G et al (2010) Introducing and evaluating MorphoDent, a web-based learning program in dental morphology. J Dent Educ 74(10):1133–1139. https://doi.org/10.1002/j.0022-0337.2010.74.10.tb04968.x

Monterubbianesi R et al (2022) Augmented, virtual and mixed reality in dentistry: a narrative review on the existing platforms and future challenges. Appl Sci 12(2):877

Moore JL, Dickson-Deane C, Galyen K (2011) e-Learning, online learning, and distance learning environments: are they the same? Internet High Educ 14(2):129–135

Movchun V, Lushkov R, Pronkin N (2021) Prediction of individual learning style in e-learning systems: opportunities and limitations in dental education.

Educ Inf Technol 26:1–15. https://doi.org/10.1007/s10639-020-10372-4

Mukhopadhyay S, Kruger E, Tennant M (2014) YouTube: A new way of supplementing traditional methods in dental education. J Dent Educ 78(11):1568–1571. https://doi.org/10.1002/j.0022-0337.2014.78.11.tb05833.x

Muller F, Naharro M, Carlsson GE (2007) What are the prevalence and incidence of tooth loss in the adult and elderly population in Europe? Clin Oral Implants Res 18(Suppl 3):2–14. https://doi.org/10.1111/j.1600-0501.2007.01459.x

Murbay S et al (2020) Evaluation of the introduction of a dental virtual simulator on the performance of undergraduate dental students in the pre-clinical operative dentistry course. Eur J Dent Educ 24(1):5–16. https://doi.org/10.1111/eje.12453

Nagasawa S et al (2010) Construction of database for three-dimensional human tooth models and its ability for education and research--carious tooth models'. Dent Mater J 29(2):132–137. https://www.jstage.jst.go.jp/article/dmj/29/2/29_2009-013/_pdf

Nassar AA, Rajeh MT (2022) Blackboard in dental education: educators' perspectives during the COVID-19 pandemic: A qualitative study. Adv Med Educ Pract 13:629–639. https://doi.org/10.2147/AMEP.S367221

Nelson SJ (2014) Wheeler's dental anatomy, physiology and occlusion - E-Book. Elsevier Health Sciences. https://books.google.ie/books?id=BM5sBQAAQBAJ

Nguyen VH, Lyden ER, Yoachim SD (2021) Using Instagram as a tool to enhance anatomy learning at two US dental schools. J Dent Educ 85(9):1525–1535. https://doi.org/10.1002/jdd.12631

Obrez A et al (2011) Teaching clinically relevant dental anatomy in the dental curriculum: description and assessment of an innovative module. J Dent Educ 6:797–804. http://www.jdentaled.org/content/75/6/797.full.pdf

Patil S et al (2015) Knowledge, attitude and practice of tooth morphology among dental students. J Adv Clin Res Insights 2:124–130. https://doi.org/10.15713/ins.jcri.60

Pereira JA et al (2007) Effectiveness of using blended learning strategies for teaching and learning human anatomy. Med Educ 41(2):189–195. https://doi.org/10.1111/j.1365-2929.2006.02672.x

Postma TC et al (2020) The "digital access divide" at a South African dental school - a cross-sectional study - part 1. South Afr Dent J 75(7):373–376. https://doi.org/10.17159/2519-0105/2020/v75no7a4

Rajeh MT et al (2021) Social media as a learning tool: dental students' perspectives. J Dent Educ 85(4):513–520. https://doi.org/10.1002/jdd.12478

Reddy R, Pathak L (2021) Curriculum integration for medical and dental students. J Univ College Med Sci 9(01):82–86. https://doi.org/10.3126/jucms.v9i01.37989

Redwood CJ, Townsend GC (2011) The dead center of the dental curriculum: changing attitudes of dental students during dissection. J Dent Educ 75(10):1333–1344. https://doi.org/10.1002/j.0022-0337.2011.75.10.tb05179.x

Reissmann DR et al (2015) A model of blended learning in a preclinical course in prosthetic dentistry. J Dent Educ 79(2):157–165. http://www.jdentaled.org/content/79/2/157.full.pdf

Richardson-Hatcher A, Hazzard M, Ramirez-Yanez G (2014) The cranial nerve skywalk: A 3D tutorial of cranial nerves in a virtual platform. Anat Sci Educ 7(6):469–478. https://doi.org/10.1002/ase.1445

Risnes S et al (2019) Tooth identification puzzle: a method of teaching and learning tooth morphology. Eur J Dent Educ 23(1):62–67. https://doi.org/10.1111/eje.12403

Rizzolo LJ, Stewart WB (2006) Should we continue teaching anatomy by dissection when . . .? Anat Rec B New Anat 289(6):215–218. https://doi.org/10.1002/ar.b.20117

Roy E, Bakr MM, George R (2017) The need for virtual reality simulators in dental education: a review. Saudi Dent J 29(2):41–47. https://doi.org/10.1016/j.sdentj.2017.02.001

Salajan FD, Mount GJ (2008) University of Toronto's dental school shows "new teeth": moving towards online instruction. J Dent Educ 72(5):532–542. https://doi.org/10.1002/j.0022-0337.2008.72.5.tb04517.x

Salajan FD, Mount GJ (2012) Leveraging the power of web 2.0 tools: a Wiki platform as a multimedia teaching and learning environment in dental education. J Dent Educ 76(4):427–436. https://doi.org/10.1002/j.0022-0337.2012.76.4.tb05274.x

Salajan FD et al (2009) Learning with web-based interactive objects: an investigation into student perceptions of effectiveness. Comput Educ 53(3):632–643. https://doi.org/10.1016/j.compedu.2009.04.006

Salajan FD, Schönwetter DJ, Cleghorn BM (2010) Student and faculty inter-generational digital divide: fact or fiction? Comput Educ 55:1393–1403. https://doi.org/10.1016/j.compedu.2010.06.017

Salajan FD, Mount GJ, Prakki A (2015) An assessment of students' perceptions of learning benefits stemming from the design and instructional use of a Web3D atlas. Electron J e-Learning 13(2):120–137

Schonwetter DJ et al (2016) Assessing the impact of voice-over screen-captured presentations delivered online on dental students' learning. J Dent Educ 80(2):141–148. http://www.jdentaled.org/content/80/2/141.full.pdf

Shigli K et al (2016) Use of PowerPoint presentation as a teaching tool for undergraduate students in the subject of gerodontology. J Indian Prosthodont Soc 16(2):187–192. https://doi.org/10.4103/0972-4052.167940

Siqueira MF, Saeed SG, Siqueira WL (2021) Using Facebook to increase student engagement. J Dent Educ 85(S3):2028–2029. https://doi.org/10.1002/jdd.12531

Snelling J, Sahai A, Ellis H (2003) Attitudes of medical and dental students to dissection. Clin Anat 16(2):165–172. https://doi.org/10.1002/ca.10113

Sugand K, Abrahams P, Khurana A (2010) The anatomy of anatomy: a review for its modernization. Anat Sci Educ 3(2):83–93. https://doi.org/10.1002/ase.139

Suh E et al (2022) The effectiveness of a 3D virtual tooth identification test as an assessment tool for a dental anatomy course. Eur J Dent Educ 26(2):232–238. https://doi.org/10.1111/eje.12691

Tam M et al (2009) Is learning anatomy facilitated by computer-aided learning? A review of the literature. Med Teach 31(9):e393–e396. https://doi.org/10.1080/01421590802650092

Toyohiro K et al (2021) Development of flash cards to teach about lesions in the jaws and maxillary sinuses. Oral Radiol 37(2):231–235. https://doi.org/10.1007/s11282-020-00435-0

Tversky B, Morrison JB, Betrancourt M (2002) Animation: can it facilitate? Int J Hum-Comput St 57(4):247–262. https://doi.org/10.1006/ijhc.2002.1017

Vuchkova J, Maybury T, Farah CS (2012) Digital interactive learning of oral radiographic anatomy. Eur J Dent Educ 16(1):e79–e87. https://doi.org/10.1111/j.1600-0579.2011.00679.x

Wang H et al (2020) The effect of 3D-printed plastic teeth on scores in a tooth morphology course in a Chinese university. BMC Med Educ 20(1):469. https://doi.org/10.1186/s12909-020-02390-0

Wignall R (2014) Book review: anatomy of orofacial structures: a comprehensive approach, 7th edition. Br Dent J 217(4):166–166. https://doi.org/10.1038/sj.bdj.2014.723

Wilson T (2015) Role of image and cognitive load in anatomical multimedia. In: Chan LK, Pawlina W (eds) Teaching anatomy: a practical guide, 1st edn. New York, NY, Springer, pp 237–246

Wright EF, Hendricson WD (2010) Evaluation of a 3-D interactive tooth atlas by dental students in dental anatomy and endodontics courses. J Dent Educ 74(2):110–122. https://doi.org/10.1002/j.0022-0337.2010.74.2.tb04860.x

Yeung JC, Fung K, Wilson TD (2011) Development of a computer-assisted cranial nerve simulation from the visible human dataset. Anat Sci Educ 4(2):92–97. https://doi.org/10.1002/ase.190

Zitzmann NU et al (2020) Digital undergraduate education in dentistry: a systematic review. Int J Environ Res Public Health 17(9). https://doi.org/10.3390/ijerph17093269

Flashcards: The Preferred Online Game-Based Study Tool Self-Selected by Students to Review Medical Histology Image Content

10

Priti L. Mishall , William Burton, and Michael Risley

Abstract

Medical students use several supplementary digital resources to support learning. Majority of these supplementary resources enhance learning by recall and repetition. A few examples of these resources are concept maps, flashcards (FCs), and self-testing tools. Traditionally, paper-based FCs are used in higher education. The concept of paper-based FCs is extended to the digital world in the form of electronic/web-based FCs. The use of electronic/digital flashcards has been reported to review course material in the medical school curriculum. Some of the medical school coursework requires students to acquire visual skills, for example, histology and pathology. Students, who do not have prior knowledge of the basic content on histology and pathology struggle to identify microscopic tissues and

organs. Therefore, students look for other supplementary resources to support visual learning. Digital resources like Anki, Quizlet, and Osmosis provide study tools that support visual skills. A review of the literature revealed only a few publications pertaining to the use of digital testing tools for histology education in medical school curriculum. In the medical histology course at the Albert Einstein College of Medicine (Einstein), Bronx, NY, first-year medical students used a game-based platform (Quizlet) to review image-based histology course content in the form of four Quizlet study sets. Students chose from six Quizlet study tools (Flashcards, Learn, Speller, Test, Match, and Race/Gravity) to review the image-based course material and test their knowledge on accurate identification of histological images. The data on student usage of study tools was tracked and analyzed for 4 years (Graduating Classes of 2018 to 2021) to calculate: the total usage of the game-based study tools (Flashcards, Learn, Speller, Test, Match, and Race/Gravity) over the period of 4 years, total percent usage over 4 years of each game-based study tools (Flashcards, Learn, Speller, Test, Match, and Race/Gravity) in each of the four Quizlet study sets and to identify the preferred game-based study tool. The data showed a consistent year-on-year increase in usage of game-based study tools by 50% ($M = 445$ in 2018 compared to $M = 849$ in 2021). For the four Quizlet study

P. L. Mishall (✉)
Departments of Pathology & Ophthalmology and Visual Sciences, Albert Einstein College of Medicine, Bronx, NY, USA
e-mail: priti.mishall@einsteinmed.edu

W. Burton
Department of Family and Social Medicine, Albert Einstein College of Medicine, Bronx, NY, USA

M. Risley
Department of Developmental & Molecular Biology, Albert Einstein College of Medicine, Bronx, NY, USA

sets the percent usage of each study tool Flashcards, Learn, Test, Match, Gravity, and Speller was tracked and combined across the four academic years. It was found that Flashcards were used significantly more frequently than any other tool and this was followed by Learn, Test, Match, Gravity, and Speller ($p < 0.0001$ using chi-square). The study concludes that flashcards are the preferred study tool used by students to acquire visual skills for identifying histological images and could be incorporated when designing online study tools.

10.1 Introduction

Web-based self-testing resources are used by students to improve recall and repetition.

Several online formative assessment tools are available in the market like Anki, Quizlet, Study Blue, and CRAM. These self-assessment resources do not count toward students' grades, hence ideal for formative assessments. These formative assessments support multiple opportunities to relearn and receive feedback and prepare well for the summative assessments that count toward the student grades. The self-testing tools are based on the educational principles of spaced repetition and spacing. Additionally, these self-assessment tools have an intrinsic ability to self-test student knowledge and provide students feedback on their performance to promote self-directed and independent learning. These self-assessment tools are used in medical school coursework, especially for visually demanding subjects like histology or pathology. These self-testing tools eventually become an integral part of the hidden curriculum (Vogelsang et al. 2018) Students who do not have prior exposure to this new material use supplementary resources to develop visual skills that

allow for repeated reviews to develop visual accuracy to identify microscopic images.

This chapter explores the use of an online game-based study tool Quizlet by first-year medical students. Students used Quizlet as a supplementary resource to review histology image sets. This game-based online platform allows students to hone their ability to identify a wide range of histology images. Students used the Quizlet platform to repeatedly review image sets until students were confident in correctly identifying the images. This study does not have a control and experimental group and the study does not measure the impact of the use of resources on knowledge gain and retention. The study focuses on the usage of study tools for 4 years (Graduating Classes of 2018 to 2021) to calculate: the total usage of the game-based study tools (Flashcards, Learn, Speller, Test, Match, and Race/Gravity) for 4 years, total percent usage of game-based study tools (Flashcards, Learn, Speller, Test, Match, and Race/Gravity) in each of the four Quizlet study sets over 4 years and finally to identify the preferred game-based study tool.

10.1.1 Learning Resources that Support Knowledge Retrieval

Formative assessment is critical for learning. Frequent review of the course content by repetition and recapitulation supports successful knowledge retrieval (Jurjus et al. 2014, 2016; Routt et al. 2015; Taveira-Gomes et al. 2015; Sun et al. 2021; Tsai et al. 2021). Several resources are used by students to enhance learning, for example, notes (Back et al. 2016; Luo et al. 2016; McAndrew et al. 2016; Trelease 2016; Javaid et al. 2018), drawings (Bell and Evans 2014; Gheysens et al. 2017; Greene 2018; Shapiro et al. 2020), concept maps (Muirhead 2006; Demirdover et al. 2008; Karpicke and Blunt 2011; Thomas et al. 2016; Chen and Allen 2017), and Flashcards (Abramson et al. 2002; Reilly 2011; Golding et al. 2012; Al-Rawi et al.

2015; Deng et al. 2015). Historically, the frequency of repetition and timing of repetition has been a matter of research for centuries. Ebbinghaus described in 1800 that it is easier to remember information when it is studied multiple times over a long-time span rather than studied once or a few times in a short time span (Ebbinghaus 1913; Al-Rawi et al. 2015). This principle is applied to study tools like Flashcards. For example, a company called SuperMemo, a commercial Flashcard program implemented spaced repetition by keeping track of the ideal time to review material, optimized based on the performance of the user (Al-Rawi et al. 2015). In the last two decades, students are using numerous online platforms to review/self-test study material to supplement their learning. There are several benefits of online learning platforms:

(a) Learners have the flexibility to use the tools anywhere and everywhere.
(b) The platform usually automatically randomizes the content before the test. This ensures that students are learning the material and not simply the alphabetical order of the content.
(c) The online quizzing platforms allow students to self-assess their learning. Students receive immediate feedback on the progress of learning. This allows students to monitor and modify their learning.
(d) The online learning platform is a self-testing device that supplements self-directed learning.
(e) The online learning platform provides an opportunity for interactivity. Interactivity is achieved by providing learners with opportunities for repetition and self-assessment through immediate feedback (Reilly 2011)
(f) The online learning platform supports retrieval-based practice (Deng et al. 2015) and spaced repetition (Al-Rawi et al. 2015; Deng et al. 2015)
(g) The online learning platform promotes repetition and active learning (Chariker et al. 2011; Reilly 2011)

10.1.2 Supplementary Learning Resources and Educational Principles

Generation Z students use a number of online supplementary resources like Socrative, Kahoot, Quizizz, Quizlet, Quizalize, Mentimeter, Blooket, Riddle, and Brainscape (Kharbach 2022). These supplementary resources become integral components of the hidden curriculum (Hafferty 1998). The learning content of majority of these supplementary resources is student-generated and not always vetted for content accuracy by the expert faculty. The popularity of a self-directed supplementary resource is based on the ability of resources to allow students to self-test (Abramson et al. 2002; Kornell and Son 2009; McAndrew et al. 2016), spaced repetition (Kerfoot et al. 2007; Deng et al. 2015; Lu et al. 2021; Hart-Matyas et al. 2019), and interactivity (Sweller 1994; Betrancourt 2005; Kirschner 2002; Back et al. 2016; Holland et al. 2016). Spaced repetition allows learners to remember information when it is done multiple times over a long time span rather than studying once or few times in a short time span (Fig. 10.1). Interactivity refers to the process of a user utilizing input devices to activate technology to elicit some type of visual or audio response (Sims 1997). It is found that interactivity plays a key role in knowledge acquisition and development of cognitive skills (Friedman 1996; Sims 1997; McLean 2001; Patel et al. 2006).

10.1.3 Use of Digital Platforms for Histology and Pathology Teaching

Histology and Pathology courses report the use of several online instructional programs to support students' visual learning in the coursework. Hoffman et al. (1992) developed "PathPics" to help students process the large volume of visual information and then use a quiz mode to assess their mastery of material (Hoffman et al. 1992). Some universities have made Virtual slides online
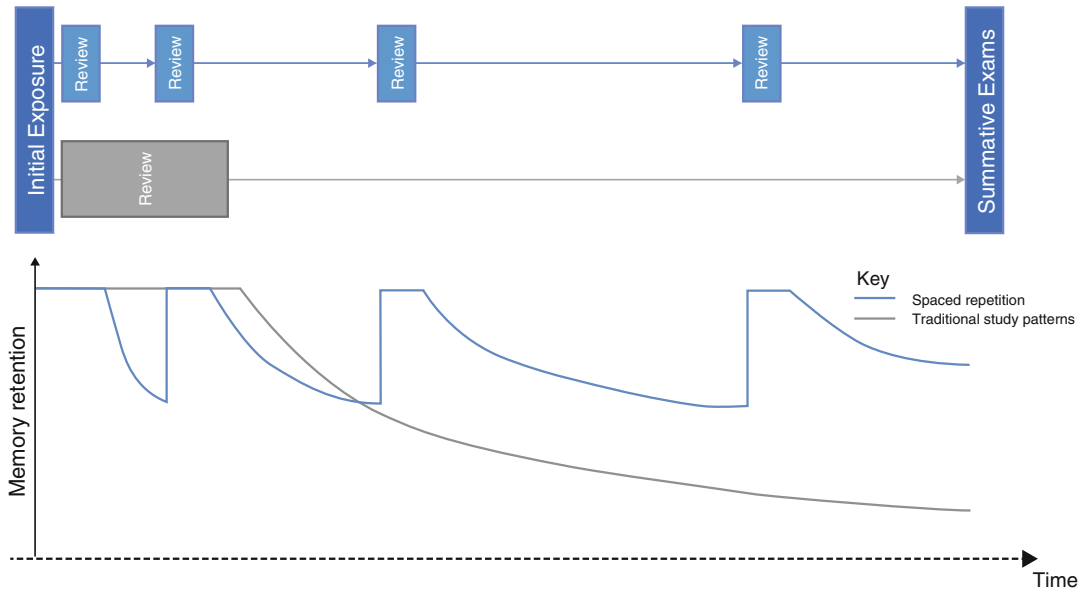
Fig. 10.1 Comparison of exposures to knowledge with spaced repetition and traditional techniques. This diagram illustrates the early focus of traditional learning techniques on amassing practice, which creates an initially strong memory that ultimately decays without further revision.

By comparison, spaced repetition is known to effectively distribute meaningful practice across time to reinforce learning and slow the decay of memory, promoting long-term retention. "From Jape et al. (2022), originally published under CC BY 4.0"

for students and faculty to view (http://www.path.uiowa.edu/virtualslidebox/). Campos-Sanchez et al. (2014) describe the use of a video as an audiovisual learning notebook as a self-learning tool in histology (Campos-Sanchez et al. 2014). Michigan's "eHistology—A SecondLook Series" published a self-evaluation tool by students, who want to test their level of preparedness before taking quizzes and examinations (Hortsch 2013). Another study describes the student preferences for an e-learning resource SecondLook TM as a self-review histology tool. The study compared three interfaces, PowerPoint files, an online website, and a mobile application, and concluded that "Convenience," "larger screen," and "easy to use" PowerPoint files were the most popular (Bringman-Rodenbarger and Hortsch 2020). A couple of others report institute-specific histology resources in the form of images and accompanying quizzes (Brelje and Sorenson 2014; Lisa and Oana 2022). Additionally, student-generated and self-directed image-based self-testing resources (for example, Anki

and Quizlet) are in demand to acquire visual identification skills in histology and pathology. Anki decks present the image-based content in only one testing mode that is as digital flashcards (Lu et al. 2021). On the other hand, the Quizlet game-based platform presents learners with six different testing modes (Flashcards, Learn, Test, Match, Gravity, and Speller) to self-test the image-based content.

10.1.4 Rationale for a Study in Histology Education on Student Usage of Various Study Tools Offered by an Online Web-Based Platform Quizlet

The study of medical histology requires the integration of structure with physiology and pathology. Structure is mostly at the light and electron microscope levels. Thus, medical students are expected to gain mastery in identifying tissues

and organs by recognizing their salient features. Most medical students have little prior exposure or no exposure to microscopic image-based learning. Students are trained to recognize normal and abnormal structure on digitized histological slides. These digitized images represent light or electron microscopic views of the structures.

Many times, students fail to identify the organs or tissues correctly due to struggles with developing appropriate visual cues. The goal of histology courses is to ensure that students confidently identify organs and tissues by visualizing their light and electron microscopic images. Students in the histology course are trained to identify hematoxylin and eosin (H&E) stained normal histological tissues using visual cues. For example, students learn to recognize the duodenum by identifying the branched tubuloalveolar Brunner's glands in the submucosa or differentiate a bronchus from a bronchiole by recognizing a ring of hyaline cartilage in a bronchus compared to the absence of cartilage in a bronchiole. First-year medical students perceive learning and recall of these varied microscopic images as very challenging (Garcia 2019). Therefore, students demand resources that aid the development of visual skills, especially a resource designed to present microscopic images and test their ability to correctly identify the image. Preferably, the resource could repeatedly present diverse visual images until the student gains confidence in correctly identifying the microscopic tissue in the image. Hence, online supplementary study resources become critical because these resources allow students for repeated review of microscopic images in a self-paced manner. Histology @Yale is a well-designed web-based open lab resource that has images with multiple-choice questions; however, this resource is not accompanied by gaming study tools (Takizawa 2011). To review the existing published articles a PubMed and MedEdPortal search using the term "image-based quiz tools for histology education" yielded zero and seven results, respectively. The inclusion criteria were preclerkship histology education, quizzing tools, e-learning, and self-assessments. In the MedEdPortal, six articles were excluded because of their focus on anatomy and dermatology education. Only one histopathology e-learning histology tutorial on lymph node fit the inclusion criteria. The authors of the article used PowerPoint features to ask quizzes but did not use an online quizzing platform (Soma 2016). None of these studies compared the use of different study tools' effectiveness for self-assessment in histology. Also, there is little data as to which quizzing tool would be preferred by students.

In the current study, students used the supplementary resource on the Quizlet platform to review histology image-based study sets that provided more complete coverage of topics included in the course, met diverse needs of student's example Visual, Aural and Read/Write, and used current, relevant technology/computer-assisted learning (CAL) that further engaged interactive independent self-directed learning. Additionally, the Quizlet program allowed to track learner usage of the application. However, none of the published literature reports on the total usage of Quizlet study tools and the preferred study tool self-selected by the learners.

10.2 Aims

First-year medical students at Albert Einstein College of Medicine (Einstein) used six game-based study tools namely Flashcards, Learn, Test, Match, Gravity, and Speller offered by the Quizlet platform to learn both light and electron microscopy histology images. The goal of the study was to determine the student usage of the six game-based study tools to study image-based histology study sets on the Quizlet platform. The study aimed to investigate the usage of study tools for 4 years (Graduating Classes of 2018 to 2021) to calculate: the total usage of the game-based study tools (Flashcards, Learn, Speller, Test, Match, and Race/Gravity), total percent usage of each game-based study tool (Flashcards, Learn, Speller, Test, Match, and Race/Gravity) for each of the four Quizlet study sets and finally to identify the preferred game-based study tool.

10.3 Methods

10.3.1 Participant Recruitment

First-year medical students for the Class 2018 ($n = 169$), 2019 ($n = 172$), 2020 ($n = 169$), and 2021 ($n = 168$) participated in the anonymous retrospective study. The demographic data for this larger cohort of students over a period of 4 years is similar. The study does not compare between the gender differences or education or prior knowledge of the participants. This was a retrospective study approved by the institutional review board of Einstein. All the participants were deidentified.

10.3.2 Steps in Creation of Study Sets

Quizlet is an online platform that allows students and teachers to create customized sets of learning materials. Learners can review this study material using eight different interactive study tools namely Flashcards, Learn, Write, Spell, Test, Match, and Gravity and Live. At Einstein students did not use two study tools, namely Write and Live. The study tool Write asked students to type the name of the histological tissue and the study tool Live allowed students to compete live with students in another team in the classroom setting. Note that the updated Quizlet website in 2022 offers a fewer number of study tools.

Considering student demand for a learning resource in the first-year medical histology course at Einstein, Bronx, NY the authors assessed various online quizzing platforms and decided to use Quizlet because of its ease to upload histological images and its relatively cheap annual subscription rate and ability to maintain the privacy of institutionally copyrighted content.

The authors used the online gaming platform Quizlet to create four image-based histology practice sets. Most of the study sets on the Quizlet website are free for all registered users. In the current study, the authors purchased the annual subscription-based Quizlet for teacher's services

($34.99). This service enabled faculty to track student usage of study tools and provided students with an advertisement-free study experience. The four-histology image-based study sets were created. Here are the steps to create the image-based library. First, the correct name of the microscopic tissue was typed, and the corresponding icon of the microscopic image was uploaded. These microscopic tissue images were selected from a diverse library of light or electron microscopic images. The left column shows the text, and the right column shows the corresponding histological image (Fig. 10.2).

Four Quizlet study sets were created. Students used the study sets as a supplementary study resource as the histology course progressed.

1. Quizlet 1: Cell structure and organelles, Epithelium, Connective tissue, Bone, and Cartilage
2. Quizlet 2: Muscle, Nervous system, Blood, and Lymphatic tissue
3. Quizlet 3: Skin, Digestive, and Endocrine
4. Quizlet 4: Respiratory, Urinary, Male and Female Reproductive systems
   The number of histological images in each study set and class is listed in Table 10.1.

The study sets were placed in a password-protected Class folder on the website to prevent tampering or inaccuracies. Only course faculty and the Quizlet creator had access to the Class folders and ability to alter the image-based study sets. A specific Class link to the Quizlet website was posted on the learning management system. Students used the link to sign up for a free account on Quizlet.com. After students created an account, an auto-generated email request from the student account was sent to the course faculty administrator. Upon the administrator accepting the request, the student received access to the specific Class study sets. This mechanism ensured that only registered students received access to the institutionally copy-righted histological images in the study sets. After gaining access to the specific Class study sets, students had the flexibility to pick any or all the online study tools to review image-based microscopic tissues and hone their tissue identification skills.
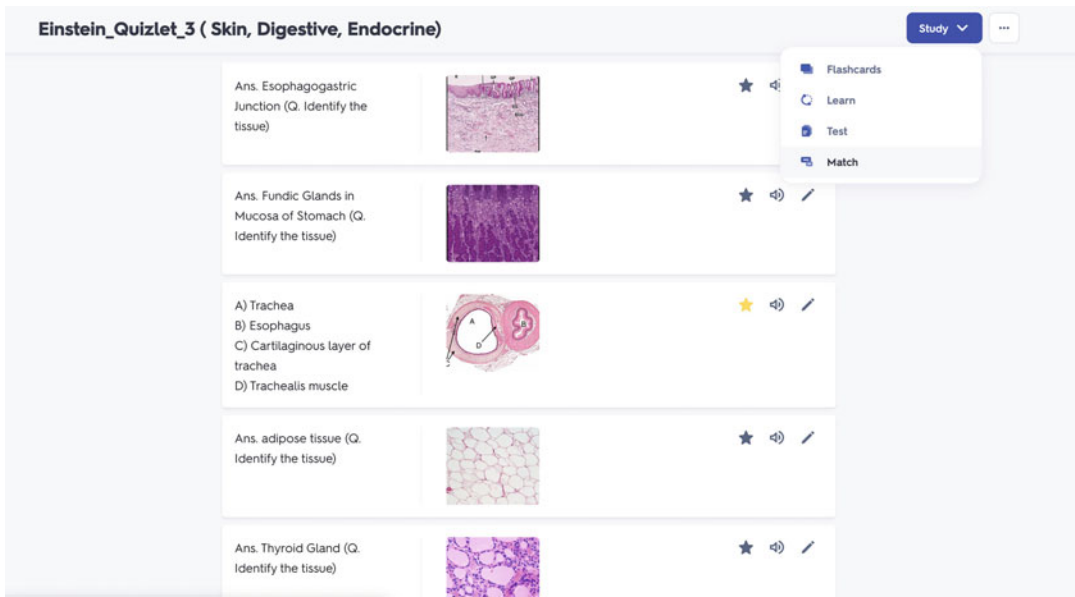
Fig. 10.2 Shows Quizlet 3 study set. The upper part of the study set shows the title of the study set. The top right corner displays the study tools offered to learners to self-select. Then there are two columns. The left column shows the correct name of the histological image, and the right column shows the corresponding histological image. This data of diverse images from light and electron microscopy is saved in the library

Students used the Quizlet platform as a supplementary learning resource on a voluntary basis. The authors did not restrict students from creating their own study sets or use existing histology study sets that were freely available. Faculty did not track the names of individual students to maintain anonymity. Students freely choose any of the study tools offered by the Quizlet website to practice identification of the microscopic images. Below is an overview of all study tools:

The study tool Flashcards tests students' knowledge by presenting a microscopic image on the screen. Students use the space bar on the screen to flip the flashcard and read the correct answer. Students could also use the left and right arrow keys to move between cards (Fig. 10.3a, b).

The study tool Learn tests students' knowledge of image identification by tracking which images the student correctly identified and what images the student did not correctly identify; the software then retests them of their mistakes.

The study tool Test provides customized practice tests on any study set by generating a random test by using images from the study sets and presenting the image identification in multiple format examples including matches, MCQs, and true/false.

Table 10.1 The column on the left lists the number of Quizlet Study Sets and the column on the right shows the number of images in each study set for the Class of 2018 and Classes 2019–2023

Study set	Number of images in each study set	
	Class 2018	Class 2019–Class 2021
Quizlet 1	74	53
Quizlet 2	85	85
Quizlet 3	56	56
Quizlet 4	44	44
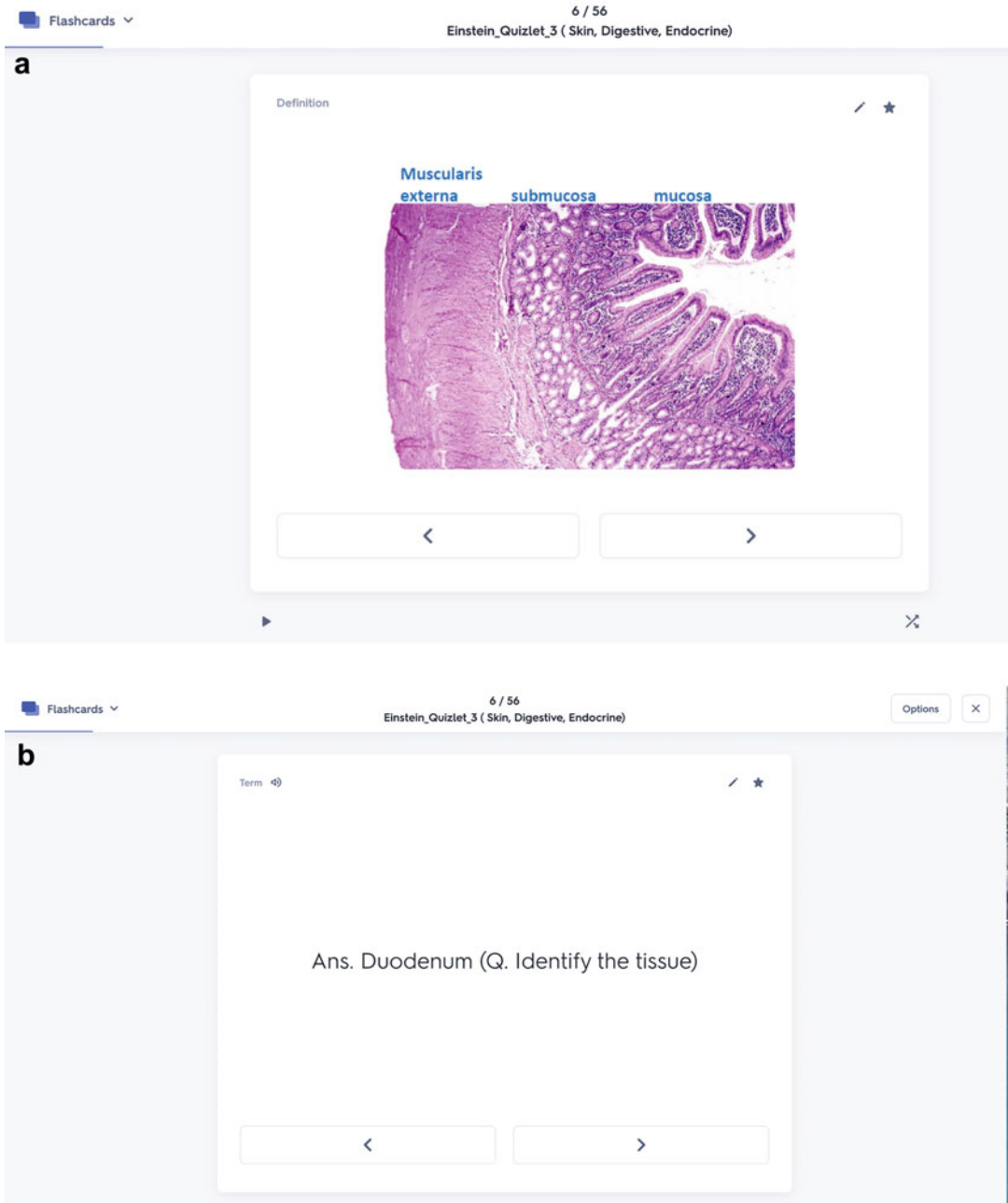
Fig. 10.3 (**a**) Study tool Flashcard. The screen shows an H&E-stained histological image. (**b**) Study tool Flashcard (flipped). The screen shows the correct answer for (**a**)

The study tool Match presents on the screen a random display of histology images and the correct answers. The study tool Match challenges the student to drag the correct answer and drop it to the correct image by using the computer mouse. The study tool Match additionally allows students

to compete with friends and attempt to beat the current record. This activity encourages students to achieve accuracy in image identification in the minimum amount of time (https://quizlet.com/en-gb/help) (Fig. 10.4).

The study tool Gravity is like the classic space invaders game where students try to prevent an object, in this case an asteroid, from reaching the earth by correctly entering the corresponding name of the histological image in the text box.

The current study explores and discusses the use of six study tools namely Flashcards, Learn, Spell, Test, Match, and Gravity. At Albert Einstein College of Medicine, students used Quizlet as a supplementary learning resource wherein students self-selected one or more of these study tools to review the image content to prepare for their formative assessments. The Quizlet resource stored a library of histological images aligned to the formative assessment quiz topics in the course.

Data Analysis

Statistical analysis was performed using Chi-square tests. Statistical analyses and interpretation of data were conducted using the SPSS statistical package, version 20 (IBM Corp, Armonk, NY). This retrospective study was approved by the institutional review board of Einstein.

Data Protection

In this retrospective study, the data collection was totally anonymous; no specific information which may lead to the identification of an individual was released. Concerning the course evaluation questionnaire, participants may choose to skip any question they did not want to answer. Appropriate data security procedures and precautions were adopted so that data obtained were kept secured in a password-protected computer with access only by the researchers.

At the end of the histology course, each year quantitative and qualitative data was collected. The quantitative data collection focused on student use of each study tool. Also, students rated the overall Quizlet experience using the Likert scale (1–4). The qualitative data collection was in form of student comments on the overall Quizlet experience. The data was collected for the following four Classes (Class 2018, 2019, 2020, and 2021). Statistical analyses were performed, and p-values were calculated. The statistical test used was a Chi-square homogeneity of variance test.

Results

1. The overall usage of the game-based study tools Over the 4-year period.
   The mean logins (M) on the Quizlet website for the four Classes was as follows: Class of 2018 ($M = 445$); Class 2019 ($M = 650$); Class of 2020 ($M = 955$); and Class of 2021 ($M = 849$), respectively (Fig. 10.5).
2. The percent usage of the study tools for each Quizlet study set ($n = 4$) over the 4-year period
   For the four Quizlet study sets 1, 2, 3, and 4, the percent usage of each study tool Flashcards, Learn, Test, Match, Gravity, and Speller was tracked and combined across the four academic years. It was found that Flashcards were used significantly more frequently used than any other tool and this was followed by Learn, Test, Match, Gravity, and Speller ($p < 0.0001$ using chi-square) (Fig. 10.6).
3. Identify the preferred study tool self-selected by learners to review the histology image-based content.
   It was also found that the students' use of Flashcards was significantly greater compared to their use of all other study tools combined (Fig. 10.7). This was true for academic years 2018 ($p = 0.004$), 2019 ($p < 0.0001$), 2020 ($p = 0.007$), and 2021 ($p < 0.0001$).
4. Student perception on the use of the Quizlet to learn histology
   In the course evaluations, students' response to the Quizlet experience for the three graduation classes were collected, except for the Class of 2020. Students responded to the statement "The online Quizlet study tool aided my self-
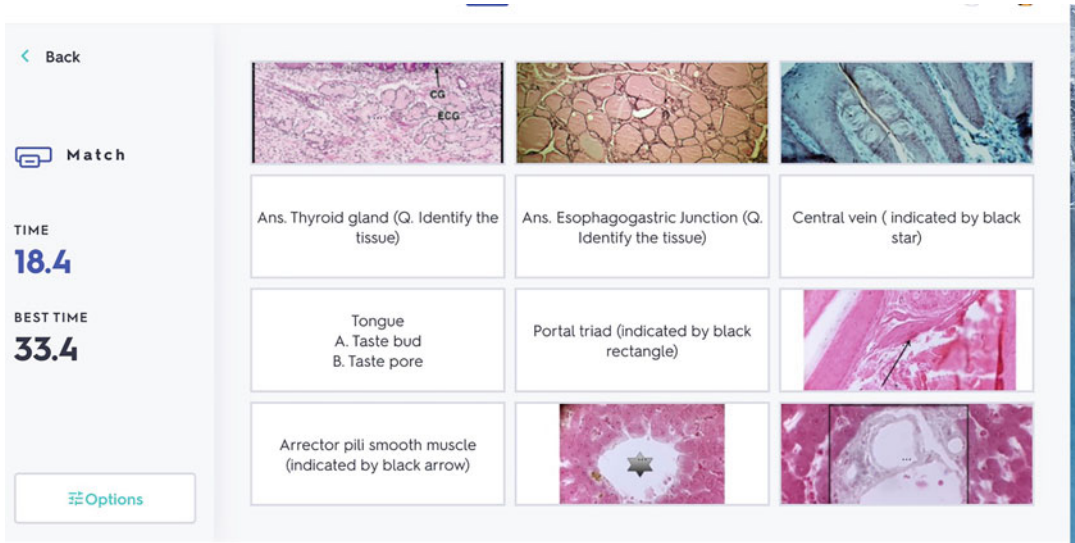
Fig. 10.4 Shows the study tool Match. The screen presents a random display of histology images and the correct answers. The student is required to drag the correct answer to the corresponding histological image or vice versa

assessment in studying histology." The ratings were as follows graduating class 2018 (3.86/5), 2019 (3.3/4), and 2021 (3.5/4). The course was evaluated out of 4 for all years except 2018. The qualitative data was analyzed, and themes were identified; comments and recommendations are in Table 10.2.
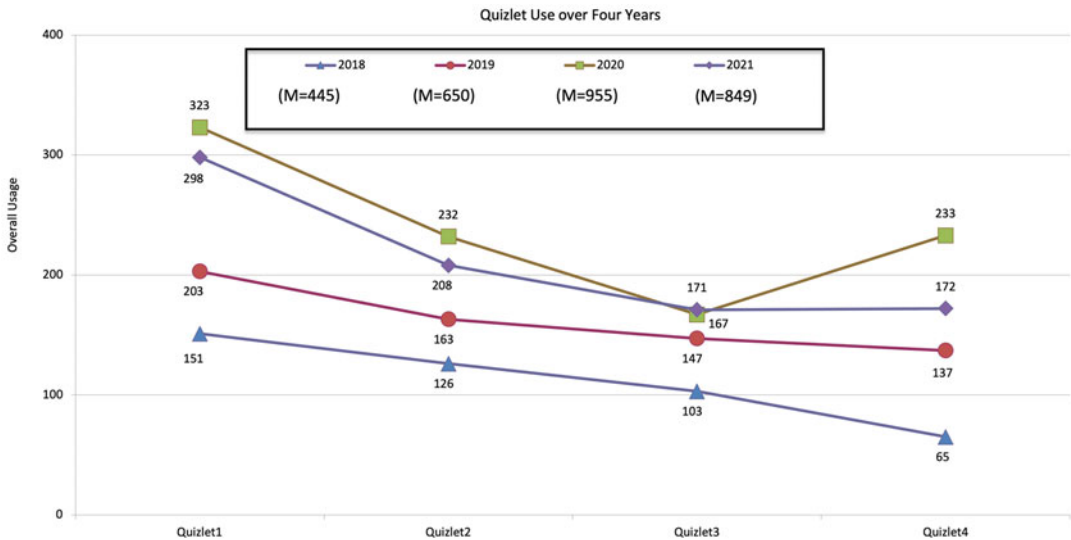

Fig. 10.5 The use of Quizlet tended to increase over the 4 years of the study, though use tended to decline within each year. The x-axis shows the Quizlet study sets and the y-axis shows total student usage (M = mean log-ins on the Quizlet website)

Study Tool Preference by Quizlet
(Combined across Four Academic Years)
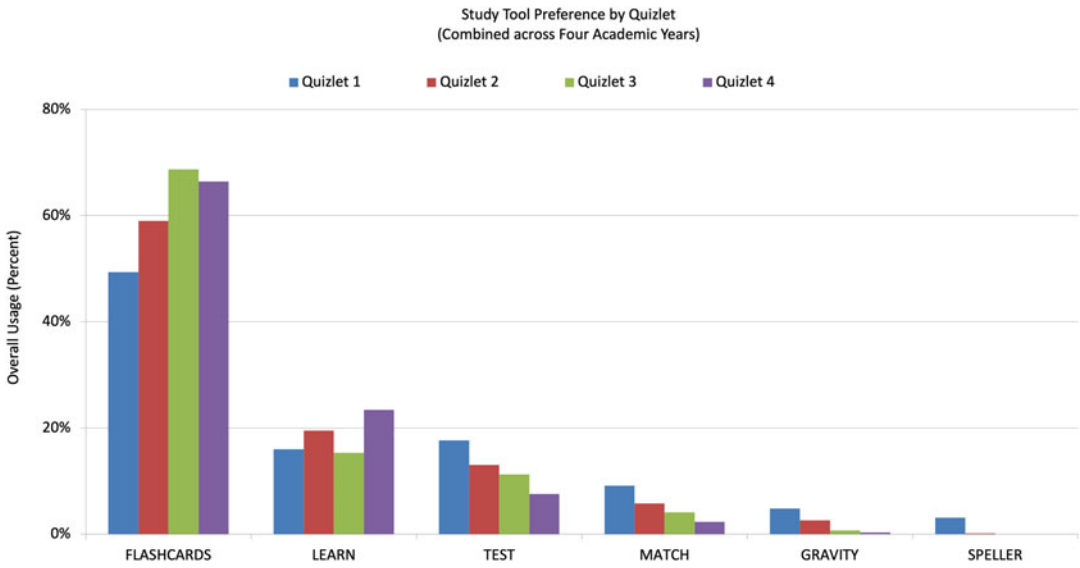
Fig. 10.6 Flashcards were the most popular study tools. The *x*-axis shows the different study tools while the *y*-axis indicates the percent use of each study tool. Flashcard use increased from Quizlet 1–3 as the course progressed and remained high for Quizlet 4. It was revealed that within the 4 Quizlet study sets, Quizlet 3 reflected the maximum use of the Flashcards study tool (70% of usage across all six study tools)

Flashcard Preference vs. All Other Tools Combined
(by Quizlet)
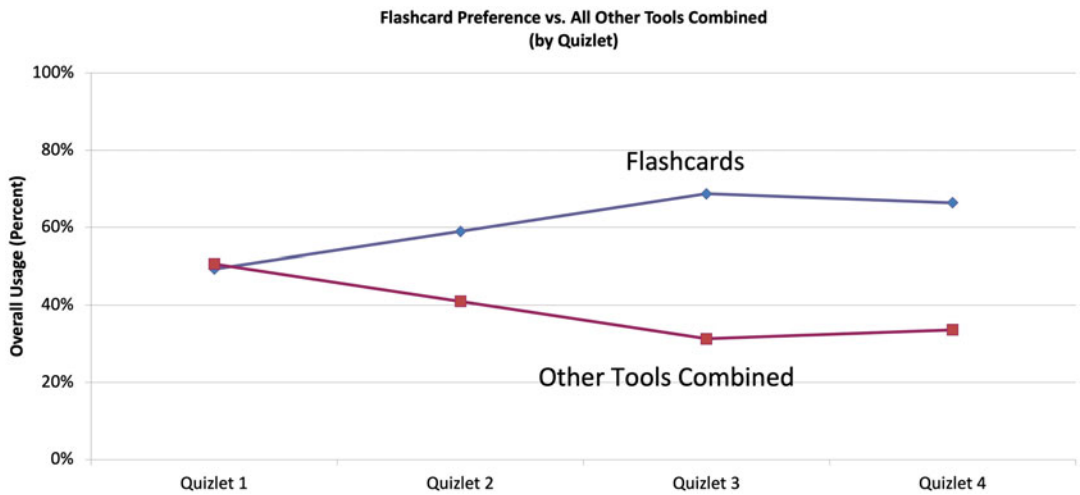
Fig. 10.7 Flashcards became the preferred study tool over all other Study Tools combined. The *x*-axis shows the Quizlet study sets. The *y*-axis shows percent usage of study tools

Table 10.2 Qualitative data in form of Student feedback to the question "The online Quizlet study tool aided my self-assessment in studying histology"

Student comments on the statement "The online Quizlet study tool aided my self-assessment in studying histology"	Recommendations by students
• Good for identifying organs and structures.	• More general knowledge questions
• Provided collection of images with randomized order (instead of needing to go through each lab or the textbook)	• Go over vocabulary
• Very nice supplementation to the course.	• More images
• Really enjoyed it as a final preparation before quizzes and tests to know for sure that I know the material.	• More questions
• Helpful in practicing identification.	• Divide them into each topic and give multiple chapters to study
• Excellent tool.	
• Good resource	

10.4 Discussion

10.4.1 Introduction

The current study demonstrated that the cohort of preclinical first-year medical students at a US medical school who used the online game-based learning platform Quizlet as a supplementary resource to review histological image identification reported flashcards as the most popular study tool. The study demonstrated that in the duration of 4 years the student use of flashcards for all the Quizlet study sets was higher than the combined use of all other study tools: Learn, Test, Match, Gravity, and Speller. There was an increase in the use of Quizlet study sets each year, although, there was a decrease in the use of Quizlet study sets within the same year. Additionally, students reported an overall higher satisfaction with the use of Quizlet as a supplementary study tool to review histological image identifications.

10.4.2 Use of Game-Based Study Tools in Medical School

A number of studies reveal the use of supplementary learning resources in medical school Anki (https://apps.ankiweb.net), Firecraker (2015), Study Blue, 2011 (Chegg 2003), ALERT STUDENT platform (Taveira-Gomes et al. 2015). Many studies have shown that interactive instructional techniques can increase student interest, cognitive processing, and curricular integration (Bills 1997; Leong et al. 2003; Gould et al. 2008; Khalil et al. 2010). The current study found that the year-to-year use of Quizlet study tools to review image-based content for the histology course was increased by almost 50% ($M = 445$ in 2018 compared to $M = 849$ in 2021). This increase can be attributed to recommendations by senior-year students. Although authors do not have data on prior exposure of students to online game-based tools in undergraduate college, it is highly likely that students who might have previously used a game-based study tool would tend to use similar study tools in future for their learning purposes (Erhel and Jamet 2013). Within each year, there was a decline in usage of Quizlet, and that might be related to familiarity with the course content. As the course progressed students became familiar with the learning resources that they may prefer over Quizlet.

10.4.3 Flashcards Versus Other Game-Based Study Tools

A few examples of digital FCs include Anki, Cram, Open cards, Osmosis, and Quizlets (Hart-Matyas et al. 2019). Flashcards were reported to be commonly used in undergraduate colleges (Kornell and Bjork 2008) and allied health professional schools (Al-Rawi et al. 2015; McAndrew et al. 2016; Wanda et al. 2016). A couple of publications reported on the use of

flashcards as a study tool in medical schools (Allen et al. 2008; Taveira-Gomes et al. 2015). None of these studies compared the use of flashcards to other study tools. The current study compared student usage of flashcards to other study tools and reported that the study tool Flashcards were used significantly higher ($p < 0.0001$ using chi-square) and was followed by other study tools Learn, Test, Match, Gravity, and Speller. The present study is unique in comparing the use of flashcards to other study tools while the previously published studies reported on electronic FCs as a singular study tool.

10.4.4 Flashcard Use and Popularity in Higher Education and Professional Training

Traditional paper-based flashcards are popular in undergraduate colleges (Golding et al. 2012). The use of digital flashcards was reported in a number of training specialties; examples include a dental hygiene school to study oral pathology (Al-Rawi et al. 2015), graduate school to study molecular and cell biology (Taveira-Gomes et al. 2015), degree courses like pharmacy school to study brand and generic drug names (Whitman et al. 2019) and medical school to study clinical nephrology and psychiatry (Allen et al. 2008; Schmidmaier et al. 2011; Deng et al. 2015) and recently digital flashcards were reported to be used in postgraduate medical training like OBGYN (Tsai et al. 2021) and Orthopedics (Lambers and Talia 2021).

FCs work best with questions that require lower-order thinking skills, such as memorization of specific facts (Anderson and Krathwohl 2001; Schmidmaier et al. 2011). O'Hanlon and Laynor (2019) published a commentary on a new generation of online study resources and mentioned sites like SketchyMedical and Picnomic that use visual learning mnemonics (O'Hanlon and Laynor 2019). None of these publications reported on the use of flashcards for visual image-based learning including histology in medical school training. The current study reveals FCs as the most popular Quizlet study tool.

The popularity of flashcards is supported and attributed to the following features of flashcards: Self-testing (Wissman et al. 2012; Abramson et al. 2002), learning by doing (Bryson 2012), and spaced repetition (Al-Rawi et al. 2015; Deng et al. 2015). It is found that self-testing and retesting of the learned content at regular intervals help to monitor learning. Wissman et al. (2012) surveyed a large cohort of undergraduate students ($n = 374$) to find out students self-testing behaviors in terms of the amount of practice using flashcards and retesting by using flashcards (Wissman et al. 2012). The survey concluded that students understood that the amount of practice was relevant to learning but failed to understand the importance of practicing with longer lag periods (Wissman et al. 2012). In a study by Kornell and Son (2009), the authors asked learners why they chose to self-test during study (Kornell and Son 2009). Sixty-six percent of learners reported self-testing to determine how well they knew the information, whereas 20% said because they learn more when they restudy. The ability of resources to provide in-built spaced repetition and interactivity is crucial for self-testing and quizzing. Another study on repetitive testing and repetitive studying revealed that repetitive testing promoted better recall than repetitive studying after 1 week ($p < 0.001$) (Schmidmaier et al. 2011). Similar findings were reported in another study wherein the testing effect played an important role in memory retention. The study concluded that after an initial contact with the material, it is more beneficial to test rather than re-study the material (Karpicke and Roediger 2008; Taveira-Gomes et al. 2015). Bryson (2012) in his commentary listed different websites that supported the making of flashcards to learn anatomy and physiology and, argued that the process of creating own flashcard is an active learning process like taking lecture notes or drawing concept maps and can immensely benefit the learner (Bryson 2012). Space repetition is another study technique that supports the active recall of the content. Flashcards support spaced repetition by allowing to review and recall information at optimal spacing intervals until the information is learned sufficiently to recall (Al-Rawi et al. 2015;

Deng et al. 2015). In a study that surveyed dental hygiene students and predoctoral dental students toward their attitudes on the use of an electronic flashcard system called Anki to study case-based questions concluded that 25% of students from dental college and 33% of students' dental hygiene who took advantage of automated spaced repetition were most benefitted (Al-Rawi et al. 2015).

10.4.5 The Learner Experiences

Overall, students were satisfied with the use of Quizlet as a supplementary learning resource which is consistent with another study in a degree pharmacy college that investigated the student experience of the Quizlet study tool (Whitman et al. 2019). Perception scores suggest strong agreement to the statement "The online Quizlet study tool aided my self-assessment in studying histology." The student comments strongly suggest that the study tools within Quizlet were well received, and students interacted with the resource to gain learning engagement.

10.4.6 Future Works

Further studies need to investigate the use of Quizlet to study image-based content and its impact on student performance in terms of knowledge gain both short term and long term. Another interesting study might be to design a control and experimental group to find out if learning outcome differs between students who use the Quizlet platform compared to those who do not.

10.4.7 Conclusion

The online image-based study tools allowed students to enhance learning by repetition and recapitulation which was critical for formative assessments. The data presented indicates a strong student preference for flashcards as a tool to learn and study visual content. The study highlights the need for faculty to use evidence-based approaches to design study tools that promote self-testing in a self-paced manner. We found that overall, Quizlet is a well-received modality for learning image recognition. We recommend that medical educators incorporate flashcards when designing online study tools.

Website resources for creating and generating tests:

Easy TestMaker (easytestmaker.com)
Help teaching (www.helpteaching.com)
Brainscape (https://www.brainscape.com/packs/histology-images-1313066?origin=genome)
Iowa Virtual Slidebox (http://www.path.uiowa.edu/virtualslidebox/)
Quizlet https://quizlet.com/en-gb/help
Anki (https://apps.ankiweb.net)

References

Abramson CI, Robinson EG, Rice J et al (2002) An easy-to-use word processing program for creating concept cards in psychology courses: a method for teachers. Psychol Rep 90(3 Pt 1):968–974

Allen EB, Walls RT, Reilly FD (2008) Effects of interactive instructional techniques in a web-based peripheral nervous system component for human anatomy. Med Teach 30(1):40–47

Al-Rawi W, Easterling L, Edwards PC (2015) Development of a mobile device optimized cross platform-compatible oral pathology and radiology spaced repetition system for dental education. J Dent Educ 79(4):439–447

Anderson LW, Krathwohl DR (2001) A taxonomy for learning, teaching and assessing: a revision of Bloom's taxonomy of educational objectives. Longman, New York

Back DA, Behringer F, Haberstroh N et al (2016) Learning management system and e-learning tools: an experience of medical students' usage and expectations. Int J Med Educ 7:267–273

Bell LTO, Evans DJR (2014) Art, anatomy, and medicine: is there a place for art in medical education? Anat Sci Educ 7(5):370–378

Betrancourt M (2005) The animation and interactivity principles in multimedia learning. In: Mayer R (ed) The Cambridge handbook of multimedia learning. Cambridge University Press, New York, NY, pp 287–296

Bills CG (1997) Effects of structure and interactivity on internet-based instruction. Report no. Report Number|, Date. Place Published|: Institution|

Brelje TC, Sorenson RL (2014) Atlas of human histology: a guide to microscopic structure of cells, tissues and organs. http://histologyguide.com/index/index-A.html. Accessed 24 Feb

Bringman-Rodenbarger L, Hortsch M (2020) How students choose E-learning resources: the importance of ease, familiarity, and convenience. FASEB Bioadv 2(5):286–295

Bryson D (2012) Using flashcards to support your learning. J Vis Commun Med 35(1):25–29

Campos-Sanchez A, Lopez-Nunez JA, Scionti G et al (2014) Developing an audiovisual notebook as a self-learning tool in histology: perceptions of teachers and students. Anat Sci Educ 7(3):209–218

Chariker JH, Naaz F, Pani JR (2011) Computer-based learning of neuroanatomy: a longitudinal study of learning, transfer, and retention. J Educ Psychol 103(1):19–31

Chegg I (2003) Study blue. https://www.chegg.com/flashcards?referrer=https://www.studyblue.com. Accessed 12 Nov

Chen W, Allen C (2017) Concept mapping: providing assessment of, for, and as learning. Med Sci Educ 27(2):149–153

Demirdover CYM, Vayvada H, Atabey A, Eylul A (2008) Comparison of learning with concept maps and classical methods among medical students. In: Cañas AJ, Åhlberg M, Novak JD (eds) Concept mapping: connecting educators

Deng F, Gluckstein JA, Larsen DP (2015) Student-directed retrieval practice is a predictor of medical licensing examination performance. Perspect Med Educ 4(6):308–313

Ebbinghaus H (1913) Memory: a contribution to experimental psychology. 1885. Teachers College, New York

Erhel S, Jamet E (2013) Digital game-based learning: impact of instructions and feedback on motivation and learning effectiveness. Comput Educ 67:156–167

Firecracker L (2015) Firecracker | learn faster, remember everything. https://www.firecracker.me/. Accessed 7 Nov

Friedman RB (1996) Top ten reasons the world wide web may fail to change medical education. Acad Med 71(9):979–981

García M, Victory N, Navarro-Sempere A et al (2019) Students' views on difficulties in learning histology. Anat Sci Educ 12(5):541–549

Gheysens K, Lebeau R, Glendinning D (2017) Teaching spinal cord neuroanatomy through drawing: an interactive, step-wise module. MedEdPORTAL 13:10592

Golding JM, Wasarhaley NE, Fletcher B (2012) The use of flashcards in an introduction to psychology class. Teach Psychol 39(3):199–202

Gould DJ, Terrell MA, Fleming J (2008) A usability study of users' perceptions toward a multimedia computer-assisted learning tool for neuroanatomy. Anat Sci Educ 1(4):175–183

Greene SJ (2018) The use and effectiveness of interactive progressive drawing in anatomy education. Anat Sci Educ 11(5):445–460

Hafferty FW (1998) Beyond curriculum reform: confronting medicine's hidden curriculum. Acad Med 73(4):403–407

Hart-Matyas M, Taylor A, Lee HJ et al (2019) Twelve tips for medical students to establish a collaborative flashcard project. Med Teach 41(5):505–509

Hoffman HM, Irwin AE, Ligon RG (1992) PathPics: an image-based instructional program used in the pathology and histology curriculum and transmitted over a wide area network. Proc Annu Symp Comput Appl Med Care 1992(01/01):796–797

Holland J, Clarke E, Glynn M (2016) Out of sight, out of mind: do repeating students overlook online course components? Anat Sci Educ 9(6):555–564

Hortsch M (2013) Virtual biology: teaching histology in the age of Facebook. FASEB J 27(2):411–413

Jape D, Zhou J, Bullock S (2022) A spaced-repetition approach to enhance medical student learning and engagement in medical pharmacology. BMC Med Educ 22(1):337

Javaid MA, Chakraborty S, Cryan JF et al (2018) Understanding neurophobia: reasons behind impaired understanding and learning of neuroanatomy in cross-disciplinary healthcare students. Anat Sci Educ 11(1): 81–93

Jurjus RA, Lee J, Ahle S et al (2014) Anatomical knowledge retention in third-year medical students prior to obstetrics and gynecology and surgery rotations. Anat Sci Educ 7(6):461–468

Jurjus RA, Brown K, Goldman E et al (2016) Curricular response to increase recall and transfer of anatomical knowledge into the obstetrics/gynecology clerkship. Anat Sci Educ 9(4):337–343

Karpicke JD, Blunt JR (2011) Retrieval practice produces more learning than elaborative studying with concept mapping. Science 331(6018):772–775

Karpicke JD, Roediger HL (2008) The critical importance of retrieval for learning. Science 319(5865):966–968

Kerfoot BP, DeWolf WC, Masser BA et al (2007) Spaced education improves the retention of clinical knowledge by medical students: a randomised controlled trial. Med Educ 41(1):23–31

Khalil MK, Nelson LD, Kibble JD (2010) The use of self-learning modules to facilitate learning of basic science concepts in an integrated medical curriculum. Anat Sci Educ 3(5):219–226

Kharbach M (2022) Educastional technology and mobile learning. https://www.educatorstechnology.com/2014/02/10-useful-web-tools-for-creating-online.html. Accessed 6 Nov

Kirschner PA (2002) Cognitive load theory: implications of cognitive load theory on the design of learning. Learn Instr 12(1):1–10

Kornell N, Bjork RA (2008) Optimising self-regulated study: the benefits - and costs - of dropping flashcards. Memory 16(2):125–136

Kornell N, Son LK (2009) Learners' choices and beliefs about self-testing. Memory 17(5):493–501

Lambers A, Talia AJ (2021) Spaced repetition learning as a tool for orthopedic surgical education: a prospective cohort study on a training examination. J Surg Educ 78(1):134–139

Leong SL, Baldwin CD, Adelman AM (2003) Integrating web-based computer cases into a required clerkship: development and evaluation. Acad Med 78(3): 295–301

Lisa L, Oana R (2022) University of Colorado: virtual histology Lab. http://leeshistology.com/slides/human/general/neural/31#!/lat=-130&lng=-99.5&zoom=0

Lu M, Farhat JH, Beck Dallaghan GL (2021) Enhanced learning and retention of medical knowledge using the Mobile flash card application Anki. Med Sci Educ 31(6):1975–1981

Luo L, Kiewra KA, Samuelson L (2016) Revising lecture notes: how revision, pauses, and partners affect note taking and achievement. Instr Sci 44(1):45–67

McAndrew M, Morrow CS, Atiyeh L et al (2016) Dental student study strategies: are self-testing and scheduling related to academic performance? J Dent Educ 80(5): 542–552

McLean M (2001) Web pages: an effective method of providing CAI resource material in histology. Med Teach 23(3):263–269

Muirhead B (2006) Creating concept maps: integrating constructivism principles into online classes. Int J Instruct Technol Distance Learn 3(1):17–30

O'Hanlon R, Laynor G (2019) Responding to a new generation of proprietary study resources in medical education. J Med Libr Assoc 107(2):251–257

Patel SG, Rosenbaum BP, Chark DW et al (2006) Design and implementation of a web-based, database-driven histology atlas: technology at work. Anat Rec B New Anat 289(5):176–183

Reilly FD (2011) Outcomes from building system courseware for teaching and testing in a discipline-based human structure curriculum. Anat Sci Educ 4(4): 190–194

Routt E, Mansouri Y, de Moll EH et al (2015) Teaching the simple suture to medical students for long-term retention of skill. JAMA Dermatol 151(7):761–765

Schmidmaier R, Ebersbach R, Schiller M et al (2011) Using electronic flashcards to promote learning in medical students: retesting versus restudying. Med Educ 45(11):1101–1110

Shapiro L, Bell K, Dhas K et al (2020) Focused multisensory anatomy observation and drawing for enhancing social learning and three-dimensional spatial understanding. Anat Sci Educ 13(4):488–503

Sims R (1997) Interactivity: a forgotten art? Comput Hum Behav 13(2):157–180

Soma L (2016) Interactive tutorial of normal lymph node histology for pathology and laboratory medicine residents and medical students. MedEdPORTAL 12:10513

Sun M, Tsai S, Engle DL et al (2021) Spaced repetition flashcards for teaching medical students psychiatry. Med Sci Educ 31(3):1125–1131

Sweller J (1994) Cognitive load theory, learning difficulty, and instructional design. Learn Instr 4(4):295–312

Takizawa PA (2011) Histology @Yale. Available at: http://medcell.org/histology/histology.php

Taveira-Gomes T, Prado-Costa R, Severo M et al (2015) Characterization of medical students recall of factual knowledge using learning objects and repeated testing in a novel e-learning system. BMC Med Educ 15:4

Thomas L, Bennett S, Lockyer L (2016) Using concept maps and goal-setting to support the development of self-regulated learning in a problem-based learning curriculum. Med Teach 38:930

Trelease RB (2016) From chalkboard, slides, and paper to e-learning: how computing technologies have transformed anatomical sciences education. Anat Sci Educ 9(6):583–602

Tsai S, Sun M, Asbury ML et al (2021) Novel spaced repetition flashcard system for the in-training examination for obstetrics and gynecology. Med Sci Educ 31(4):1393–1399

Vogelsang M, Rockenbauch K, Wrigge H et al (2018) Medical education for "generation Z": everything online?! - An analysis of internet-based media use by teachers in medicine. GMS J Med Educ 35(2):Doc21

Wanda D, Fowler C, Wilson V (2016) Using flash cards to engage Indonesian nursing students in reflection on their practice. Nurse Educ Toda 38:132–137

Whitman AC, Tanzer K, Nemec EC 2nd (2019) Gamifying the memorization of brand/generic drug names. Curr Pharm Teach Learn 11(3):287–291

Wissman KT, Rawson KA, Pyc MA (2012) How and when do students use flashcards? Memory 20(6): 568–579